UNITED STATES DEPARTMENT OF THE INTERIOR

GEOLOGICAL SURVEY

THE MORGAN HILL, CALIFORNIA EARTHQUAKE OF APRIL 24, 1984 (A PRELIMINARY REPORT)

VOLUME I

Compiled by

Seena N. Hoose

Open-File Report 84-498 A

UNITED STATES DEPARTMENT OF THE INTERIOR

GEOLOGICAL SURVEY

THE MORGAN HILL, CALIFORNIA EARTHQUAKE OF APRIL 24, 1984 (A PRELIMINARY REPORT)

VOLUME I

Compiled by

Seena N. Hoose

Open-File Report 84-498

This report is preliminary and has not been reviewed for conformity with U.S. Geological Survey editorial standards and stratigraphic nomenclature. Any use of trade names is for descriptive purposes only and does not imply endorsement by the USGS.

VOLUME I

CONTENTS

THE 1984 MORGAN HILL, CALIFORNIA, EARTHQUAKE

W. H. Bakun, M. M. Clark, R. Cockerham, W. L. Ellsworth, A. G. Lindh, W. H. Prescott, A. F. Shakal⁺, and P. Spudich

U.S. Geological Survey
345 Middlefield Rd. ms-977
Menlo Park, CA 94025

ABSTRACT

The Morgan Hill, California, earthquake (magnitude 6.1) of 24 April 1984 ruptured a 30-km-long segment of the Calaveras fault zone to the east of San Jose, California. Although it was recognized in 1980 that a magnitude 6 earthquake occurred on this segment in 1911 and that a repeat of this event might reasonably be expected, no short-term precursors were noted so that the time of the earthquake was not predicted. Unilateral rupture propagation toward the southsoutheast and an energetic late source of seismic radiation located near the southeast end of the rupture zone contributed to the highly focused pattern of strong motion, including an exceptionally large horizontal acceleration of 1.29g at a site on a dam abutment near the southeast end of the rupture zone.

INTRODUCTION

On April 24, 1984 at 21:15:18.8 UTC, a moderate-size[1] earthquake occurred on the Calaveras fault to the east of San Jose, CA (Fig. 1). The earthquake was felt throughout central California[2], with damage estimated at $7.5 million[3]. Because of the concentrated damage near the south end of Anderson Reservoir and the town of Morgan Hill, the April 24 event has been called the Morgan Hill earthquake.

The epicenter (37° 19.02'N; 121° 40.89'W) of the main shock was located on the Calaveras fault zone 5 km westsouthwest of Mt. Hamilton, and about 65 km northwest of the junction of the Calaveras and San Andreas faults. Nearly all of the aftershocks locate on the 26-km-long section of the Calaveras fault zone southeast of the epicenter of the main shock, with concentrations of aftershocks near San Felipe Valley and Anderson Reservoir (Fig. 2). We use the spatial extent of the aftershocks (Figs. 1 and 2b) to define the rupture zone of the Morgan Hill earthquake, although rupture during the main shock probably did not extend over the entire length. This distribution of the aftershocks suggests that the source mechanism of the earthquake can be described by unilateral rupture propagation southsoutheast from the main shock epicenter to the south end of Anderson Reservoir.

As yet, no unambiguous surface fault rupture has been found. Prominent discontinuous post-earthquake surface cracks in the fault zone near the south end of Anderson Reservoir may be the result of slumping during the strong shaking rather than an expression of fault slip (Prescott, King, and Gu,

⁺ Calif. Div. of Mines and Geology, Sacramento, Ca.

1984). No coseismic fault slip was observed at the small-aperture Grant Ranch geodetic network located in Halls Valley 5 km northwest of the main shock epicenter. The nearest creepmeter, at Shore Road (Fig. 1) recorded 12.9 m of surface slip in the 18 hours following the Morgan Hill earthquake[4].

There are, as yet, no identified precursors that might have permitted a prediction of the time of the 1984 Morgan Hill earthquake[5]. The rupture zone lies within the dense network of seismographic stations operated by the U.S. Geological Survey in central California so that all earthquakes there with magnitude $\geq$ 1.5 are recorded and located. Only two foreshocks, both having magnitude $\leq$ 1.0, were observed[6]. Significant activity did occur near the two ends of the rupture zone in the 16 months before the Morgan Hill earthquake (Fig. 2c); the pattern of precursory seismicity near the ends of the rupture is consistent with seismicity observed before large earthquakes on plate boundaries (Kelleher, J., and Savino, J., 1975) and also before M_L 4-6 earthquakes on the San Andreas fault system (Bakun, W.H., 1980; Bakun, W.H., and others, 1980). The 1979 Coyote Lake earthquake (magnitude 5.9) occurred on the section of the Calaveras fault immediately to the southeast of the rupture zone (Bakun, W.H., 1980 and Reasenberg, P., and Ellsworth, W.L., 1982) and a number of magnitude 3-4 earthquakes have occurred in the last 6 years immediately to the northwest of the rupture zone[7] (Bakun, W. H., 1980). Thus, seismicity in recent years has outlined the rupture zone as a section of the Calaveras fault where cumulative seismic slip has lagged.

The rupture zone of the Morgan Hill earthquake also lies within a dense geodetic network, so that displacements associated with the earthquake are relatively well determined. The observed baselines range from 12 to 43 km, and the coseismic changes average a few cm (Prescott, King, and Gu, 1984). Using a 25-km-long rupture length and the 4 to 10 km depth range of the aftershocks as the rupture width, the observed line length changes are consistent with a constant right-lateral displacement of 42(±4) cm over a 25x6 km^2 area[8].

The 32-km-long Loma Prieta-Mt. Hamilton line (Fig. 1) has been measured about once a month since late 1981. The length was measured both 8 days and 1 day before the earthquake (Fig. 1a); these two measurements are within 1.7 and 3.9 mm respectively of the average of the previous four measurements, all made in 1984. Because the standard deviation of any single measurement is 7 mm, these changes are not significant (Prescott, King and Gu, 1984). These observations limit the amount of any preearthquake slip that might have occurred the week before the earthquake to less than 7 cm if the slip occurred over the entire rupture area. A survey of the Grant Ranch geodetic network in Halls Valley (Fig. 1) made 2 weeks before the earthquake also showed no anomalous deformation.

The length of the Llagas-Sheep geodetic line increased markedly in the 4-1/2 years between the 1979 Coyote Lake and the 1984 Morgan Hill earthquakes (Fig. 1b). Significant post-seismic slip occurred along the 20-km-long section of the Calaveras fault to the south of Coyote Lake after the 1979 earthquake (M. Lisowski and N.E. King, unpublished manuscript); this afterslip probably accounts for all of the accelerated extension of the Llagas-Sheep geodetic line. During this same time period, the M 3-4.5 shocks (Fig. 2c) near Halls Valley and Coyote Lake may have increased the shear stress on this fault segment.

A remarkable set of strong-ground motion recordings was obtained for the Morgan Hill earthquake. Ground accelerations were generally larger south of the rupture zone than to the north[9]. Severe damage was limited to the vicinity of Morgan Hill, and the largest horizontal accelerations were recorded near there as well (Fig. 3). These observations are consistent with pronounced focusing of seismic energy to the southeast of the rupture zone caused by the predominantly unilateral southeast rupture expansion. A large, late pulse on some of the strong motion records, such as the pulse 11 sec after trigger on the HVY accelerogram, shows the existence of an energetic source of seismic radiation (Fig. 3) near the southeast end of the rupture zone. The timing of the S waves from this source is consistent with a location[10] near Anderson Reservoir (Fig 2b) that is noticeably deficient in located aftershocks. While this location suggests a minimum rupture length of 16 km, it is not yet clear how far the rupture travelled or how the pulses from the second source were generated. Both deceleration of rupture (Savage, J.C., 1965) and the breaking of a region of concentrated stress are possible causes, but it is difficult to distinguish between the two based on ground motion data (Madariaga, R., 1983; Spudich, P., and Frazer, L.N., 1984). Whatever the cause, the location is coincident with geometric obstructions in the Calaveras fault zone at the southeast end of Anderson Lake[11].

The features of the Morgan Hill earthquake appear to support the hypothesis that the active faults in the San Andreas fault system are segmented by mapped complexities (offsets or bends) that control the dynamics of earthquakes. This hypothesis provides a potentially powerful tool for evaluating future earthquake behavior and seismic shaking (Bakun, W.H., 1980; Bakun, W.H. and others, 1980; Lindh, A.G. and Boore, D.M., 1981). Fault complexities mark the places where stress might be concentrated and earthquakes start, so that earthquake precursors should be sought near these places. Also, the probable size of future earthquakes might be estimated by the distance between adjacent geometric complexities. Furthermore, the nature of the complexity might be used to identify those places on the fault zone, like the southeast end of Anderson Reservoir, that are likely to generate strong ground motions.

The 1979 Coyote Lake earthquake and the 1984 Morgan Hill earthquakes apparently were repeats of earthquakes in 1897 (Reasenberg, P., and Ellsworth, W.L., 1982) and in 1911 (Bufe, C.G., Bakun, W.H., McEvilly, T.V., 1979), respectively, implying recurrence intervals of about 75 years. Recent studies (Lindh, A.G. and Boore, D.M., 1981; Bakun, W.H. and McEvilly, T.V., 1984) of the Parkfield section of the San Andreas fault suggest that the seismicity on a fault segment bounded by geometric complexities can be described by characteristic earthquakes that repeat with a predictable recurrence time. This support for the concepts of characteristic earthquakes and predictable recurrence intervals adds credence to long-term forecasts of earthquake potential (Lindh, A.G., 1983) and represents progress toward the goal of reliable earthquake prediction.

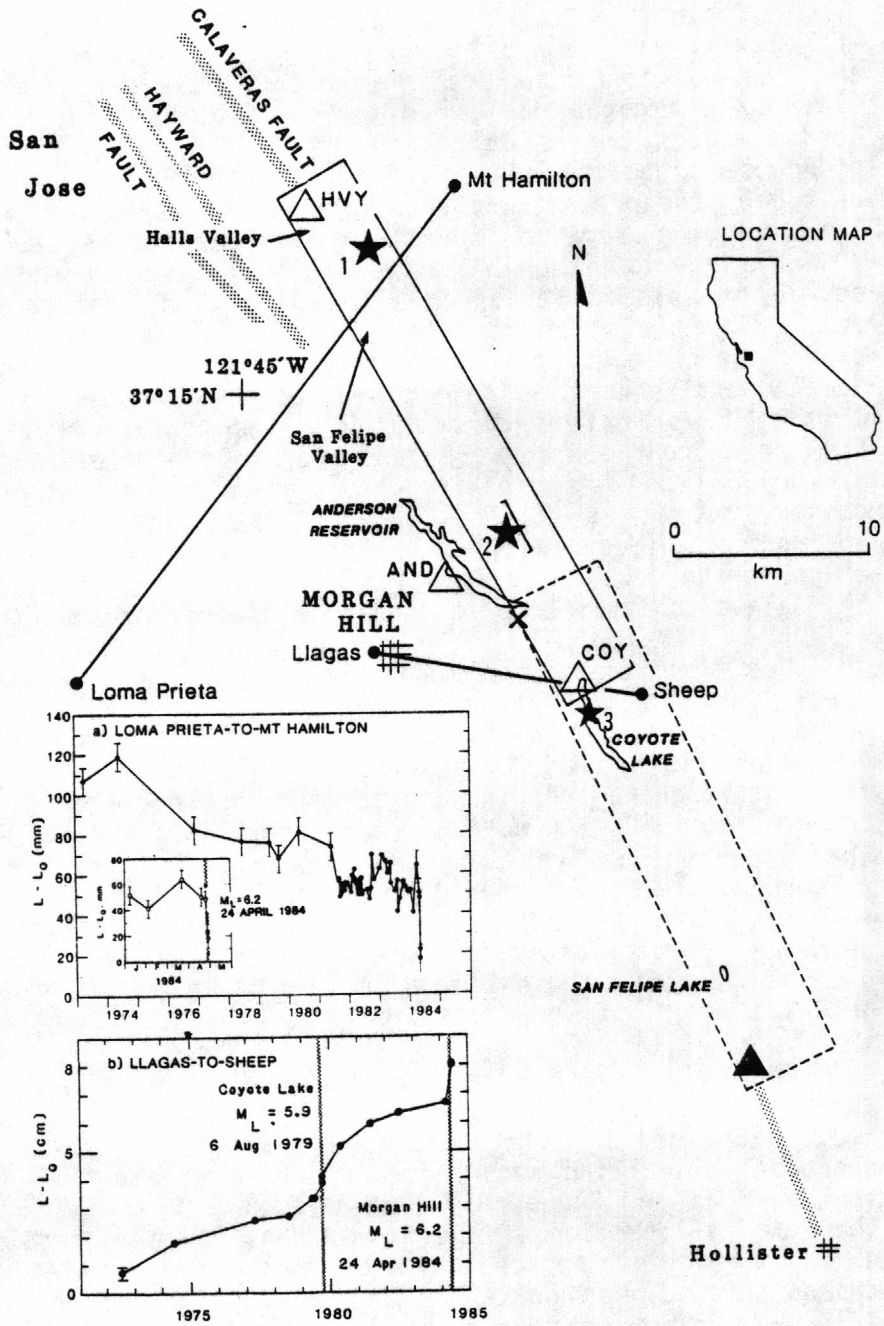

Figure 1. Map showing the Calaveras and Hayward fault zones (stippled bands) outside the rupture zone of the 1984 Morgan Hill earthquake (solid box) and the aftershock zone of the 1979 Coyote Lake earthquake (Reasenberg, P. and Ellsworth, W. L., 1982) (dashed box) relative to the locations of selected geophysical instrumentation. Stars are epicenters: 1, main shock; 2, delayed source; 3, 1979 Coyote Lake main shock. Open triangles are strong-motion accelerographs: Halls Valley (HVY); Anderson Dam-downstream (AND); Coyote Dam abutment (COY). Solid triangle is the Shore Road creepmeter. X is the locus of severe damage, in the unincorporated Jackson Oaks area of Morgan Hill. (a) The length of the line Loma Prieta-Mt. Hamilton as a function of time. Recent measurements are shown at an expanded time scale in the insert. Error bars are ±1 σ. (b) The length of the line Llagas-Sheep.

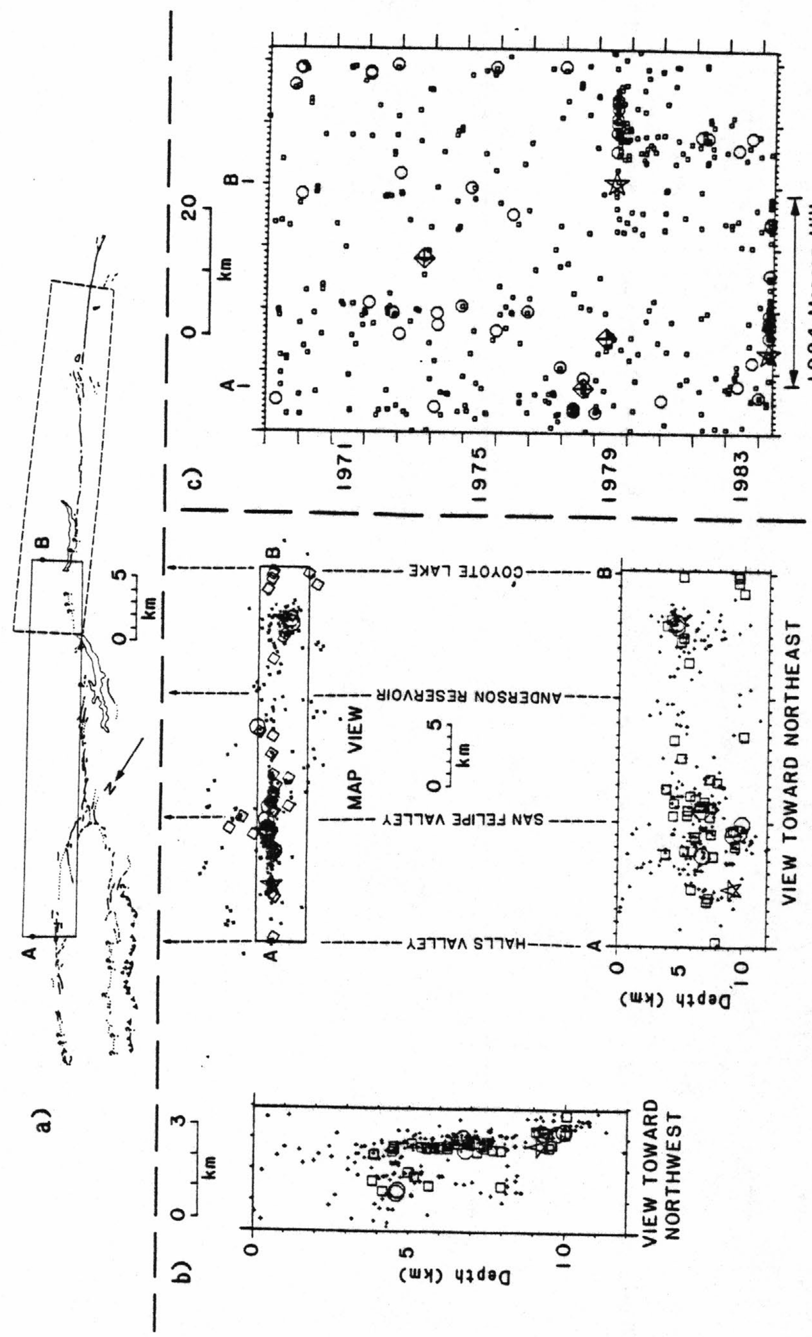

Figure 2. (a) Traces of the Calaveras fault (Herd, D. G., unpublished map) relative to the 1984 Morgan Hill and 1979 Coyote Lake earthquake rupture zones (Fig. 1) (b) Map and cross sections of seismicity (April 24, 1984 2115 UTC to May 11 0000UTC) along the 1984 Morgan Hill earthquake rupture zone. Only epicenters within the box (map view) are shown on the cross sections. The star is the hypocenter of the main shock. Hypocenter locations were obtained using a regional velocity model (Ellsworth, W. L. and Marks, S. M., 1980); displacement of epicenters off the fault traces probably reflects crustal velocities near the rupture zone not accounted for in the model. (c) Space-time plot of seismicity ($M_L \geq 2$) along the Calaveras fault zone. Symbol type is proportional to event magnitude: +, □, ○, ⊕, ★ for magnitude 1, 2, 3, 4, 5 and larger, respectively.

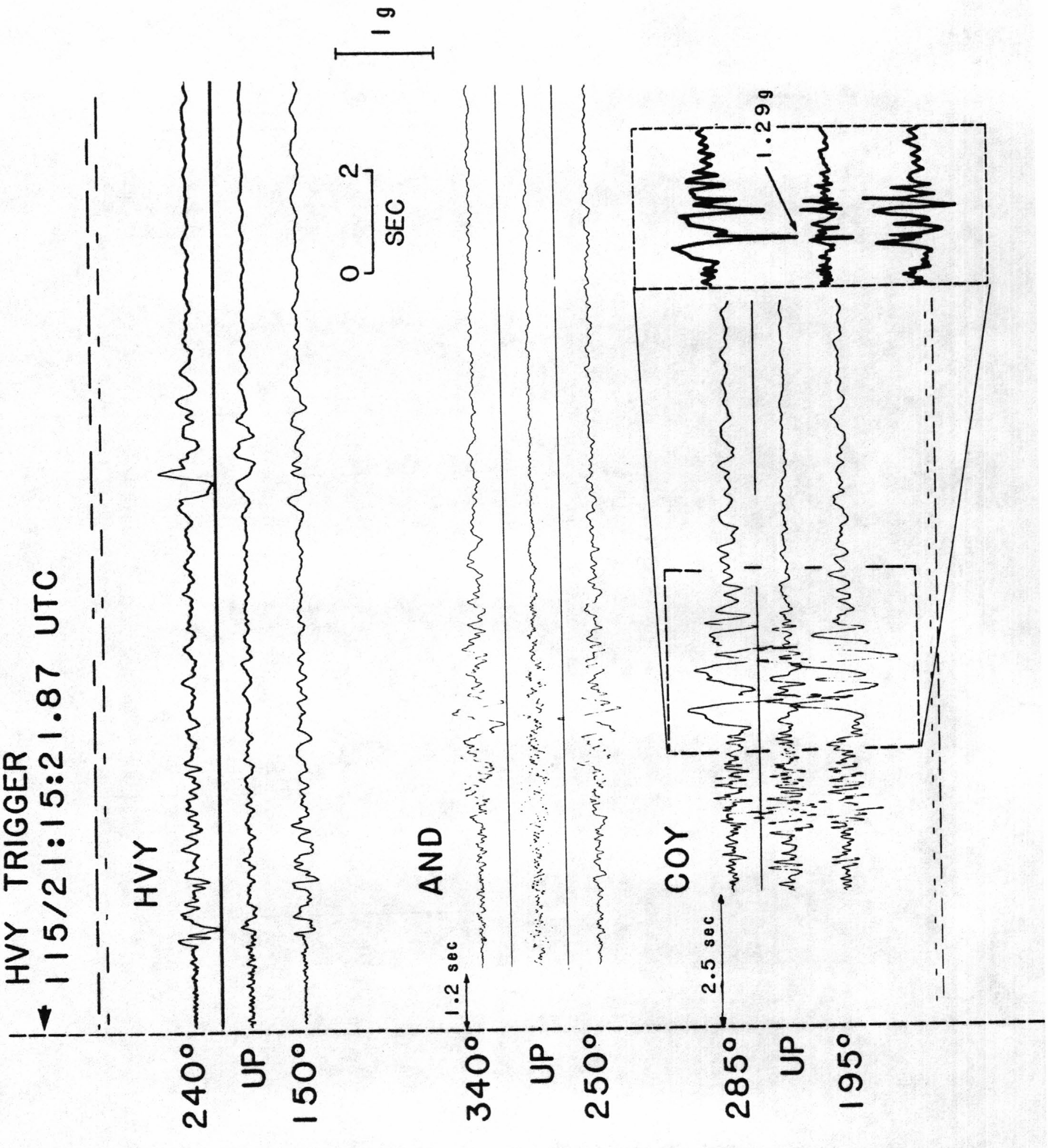

Figure 3. Strong-motion accelerograms recorded at Halls Valley (HVY), Anderson Dam-downstream (AND), and Coyote Dam abutment (COY). Traces are aligned on a common absolute time base. Dashed vertical line at the left marks the trigger time of the HVY recorder. Delays in trigger start times at the other sites are indicated. Up on the records corresponds to ground motion directions indicated at the left. A tracing of the COY accelerograms near the 1.29g peak acceleration toward 105° is shown in the inset. The straight horizontal lines between accelerogram traces are reference marks.

FOOTNOTES

1. National Earthquake Information Service in Golden, Co. reported a surface wave magnitude M_S = 6.1 and a body-wave magnitude m_b = 5.7. The moment magnitude (Hanks, T.C. and Kanamori, H., 1979) using a geodetic moment of 1.9 x 10^{25} dyne-cm was 6.2 [8]. A preliminary local magnitude M_L of 6.2 was obtained by the Univ. of Calif., Berkeley, Seismographic Station from seismographs located north and northwest of the rupture zone; M_L from seismograms written in southern California is about 6.4-6.5. The relatively-low m_b of 5.7 reflects the size of the initial source; the larger M_S, moment magnitude, and M_L estimates reflects the extended source, including the energetic source near the southeast end of the rupture zone[10].

2. High-rise buildings in San Francisco, 75 km northwest of the epicenter, although strongly shaken, did not suffer structural damage. Transient distortion during the shaking did, however, break fasteners and soldered joints in copper sheets that covered the steel-frame cupola atop the dome of San Francisco City Hall (N. M. Karasick, San Francisco City Architect, oral communication, 1984).

3. Damage of $7.0 million to the private property and $0.5 million to local government facilities, according to preliminary damage assessment by the Calif. Office of Emergency Services.

4. The afterslip at Shore Road is the largest creep event recorded in the 13 yr history at this site. For comparison, slip at Shore Road in the 24 hour following the 1979 Coyote Lake earthquake was 8.9 mm (S. Schulz and B. D. Brown, personal communication, 1984; Schulz, 1984).

5. Although the time of the earthquake was not predicted, both its magnitude and location were anticipated in 1980 (Bakun, W.H., 1980). Also, an increase in the number of magnitude 6-7 shocks in the San Francisco Bay area was anticipated on the basis of long-term cycles of strain accumulation and release, (Ellsworth, W. L., Lindh, A. G., Prescott, W. H. and Herd, D. G., 1981).

6. Two small foreshocks on April 24 at 03:41:37.0 UTC (magnitude 0.7) and 18:11:37.7 UTC (magnitude 0.4), both located at the main shock epicenter, have been identified. For comparison, more than 150 earthquakes (magnitude $\geq$ 1.0) occurred within the rupture zone in the preceding 12 months.

7. Earthquakes near Halls Valley since 1979 include the events on 15 Jan 1981 (M_L 4.8) and on 23 Oct 1983 (M_L 3.8).

8. The geodetic moment is 1.9 x 10^{25} dyne-cm (Prescott, King, and Gu, 1984). For comparison, the geodetic moment for the 1979 Coyote Lake earthquake was 1.6x10^{25} dyne-cm.

9. For example, peak horizontal accelerations were 5-8 times higher to the southeast of the rupture zone than to the northwest at distances of 25-50 km.

10. The inferred time of this source is 5 seconds after the main shock origin time. It is located between 16 and 20 km southeast of the main shock epicenter. Assuming this source is part of continuous rupture from the main shock epicenter, the minimum average rupture velocity is 80 to 90 % of the shear-wave velocity β; a rupture velocity greater than β cannot be ruled out at this time. These calculations use details of the local velocity structure [Blümling, P., Mooney, W. D., and Lee, W. H. K., (in press)].

11. Available maps [Radbruch-Hall, D.H., *U.S. Geological Survey, Miscellaneous Geological Investigations Map I-813* (1974); Dibblee, T. W. Jr., Preliminary geologic maps of the Lick Observatory, Gilroy, Morgan Hill, and Mount Sizer quadrangles, Santa Clara Co., Ca., *U.S. Geological Survey Open-File Reports 72-90* (1972) and *73-59*, (1973); Herd, D. G., unpublished map] show this complexity either as a major left step or bend. Investigations in progress should clarify the character and dimension of this complexity.

ACKNOWLEDGEMENTS

We thank R. Archuleta, T. C. Hanks, W. Thatcher, A. McGarr, R. A. Page, J. C. Savage, W. Thatcher, and R. E. Wallace for their critical comments on the manuscript.

REFERENCES

Bakun, W. H., 1980, Seismic activity on the southern Calaveras fault in central California: *Bulletin, Seismological Society of America*, v. 70, p. 1181-1197.

Bakun, W. H., Stewart, R. M., Bufe, C. G., and Marks, S. M., 1980, Implication of seismicity for failure of a section of the San Andreas fault: *Bulletin, Seismological Society of America*, v. 70, p. 185-201.

Bakun, W. H. and McEvilly, T. V., 1984, Recurrence models and Parkfield, California earthquakes: *Journal Geophysical Research*, v. 89, p. 3051-3058.

Blümling, P., Mooney, W. D., Lee, W. H. K., Crustal structure of the southern Calaveras fault zone, central California, from seismic refraction investigations: *Bulletin, Seismological Society of America* (in press).

Bufe, C. G., Bakun, W. H., McEvilly, T. V., 1979, Historic seismic activity and the 1979 Coyote Lake earthquake: *EOS, Transactions, American Geophysical Union*, v. 60, p. 891.

Ellsworth, W. L. and Marks, S. M., 1980, Seismicity of the Livermore Valley, California region 1969-1979: *U.S. Geological Survey Open-File Report 80-515*, 42 p.

Ellsworth, W. L., Lindh, A. G., Prescott, W. H., and Herd, D. G., 1981, The 1906 San Francisco earthquake and the seismic cycle: Earthquake Prediction - An International Review, Maurice Ewing Series 4, ed. by Simpson, D. W., and Richard P.G.: *American Geophysical Union*, Washington, D.C., p. 126-140.

Hanks, T. C. and Kanamori, H., 1979, A moment magnitude scale: *Journal Geophysical Research*, v. 84, p. 2348-2350.

Kelleher, J. and Savino, J., 1975, Distribution of seismicity before large strike slip and thrust-type earthquakes: *Journal Geophysical Research*, v. 80, p. 260-275.

Lindh, A. G., 1983, Preliminary assessment of long-term probabilities for large earthquakes along selected fault segments of the San Andreas fault system in California: *U.S. Geological Survey Open-File Report 83-63*.

Lindh, A. G. and Boore, D. M., 1981, Control of rupture by fault geometry during the 1966 Parkfield earthquake: *Bulletin, Seismological Society of America*, v. 71, p. 95-116.

Madariaga, R., 1983, High frequency radiation from dynamic earthquake fault models: *Ann. Geophys.* 1, p. 17-23.

Prescott, W. H., King, N. E., Gu, G., 1984, Preseismic and coseismic deformation associated with the 1984 Morgan Hill, Calif., earthquake: *U.S. Geological Survey Open-File Report No. 84-498* the Morgan Hill, California, Earthquake of April 24, 1984 (A Preliminary Report), p. 50-59.

Reasenberg, P. and Ellsworth, W. L., 1982, Aftershocks of the Coyote Lake, California, earthquake of August 6, 1979: A detailed study: *Journal, Geophysical Research*, v. 87, p. 10637-19655.

Savage, J. C., 1965, The stopping phase on seismograms: *Bulletin, Seismological Society of America*, v. 55, p. 47-58.

Schulz, S. S., 1984, Response of USGS creepmeters near Hollister to the April 24, 1984, Morgan Hill earthquake: *U.S. Geological Survey Open-File Report No. 84-498*, p. 64-72.

Spudich, P. and Frazer, L. N., 1984, Use of ray theory to calculate high frequency radiation from earthquake sources having spatially variable rupture velocity and stress drop: *Bulletin, Seismological Society of America*, in press.

LOCATION, FOCAL MECHANISM, AND MAGNITUDE OF THE MORGAN HILL EARTHQUAKE DERIVED FROM CALNET RECORDS

Jerry Eaton

U.S. Geological Survey
345 Middlefield Rd, ms-977
Menlo Park, CA 94025

Seismograms of the mainshock were played back from magnetic tape for both the northern and southern California networks. P-wave onset times and first motion directions as well as maximum amplitudes and associated periods were read from paper playbacks. The hypocenter was calculated from several different crustal models (with associated stations delays) and first motion plots were made for each solution. Magnitudes based on peak amplitudes were calculated from available unclipped records.

The epicentral region of the April 24 earthquake is geologically complex, and its crustal velocity structure is poorly understood. The complexity of the region is illustrated by a map of Pn timeterm-differences (Fig 1) which shows several marked basins (large delays) superposed on a regional trend of increasing values from west to east across the Coast Ranges (Eaton, cir. 1980). The band of persistent microearthquakes located by standard Calnet procedures, which apparently is associated with the Calaveras fault, is offset several kilometers east of the fault zone mapped at the surface. This offset is probably an artifact of the crustal model and station delays, but substantially higher velocities at mid-crustal depths (6 to 12 km) east of the fault than west of it would be required to move the microearthquake hypocenters onto the fault.

Hypocentral solutions of the April 24 main shock based on three different crustal model-station delay sets (Fig. 2) all lie east of the principal mapped strands of the Calaveras fault shown by Radbruch-Hall (1974). First motion plots for all three solutions are almost identical as to the strikes and dips of the nodal planes, but they differ in the number and degree-of-misfit of discordant observations. The three crustal models were: (a) the standard Calnet model and station delay set, (b) a model and station delays developed by Ellsworth and Marks (1980) by inversion of explosion and local earthquake arrival times in the East Bay region, (c) station delays derived from the Pn timeterm-difference map by subtracting the regional trend (0.0 near the coast to +1.0 at the edge of the Great Valley) from individual station values, and a crustal model developed from the standard Calnet model by an iterative process in which layer velocities and depths were modified to minimize the rms of onset time residuals and to permit separation of compressional and dilatational first motions into different fields. The crustal models are listed in table 1 and the corresponding station delay sets for stations at epicentral distances less than 35 km (stations beyond 35 km are not used in the solution) are listed in table 2. In Fig 2 the hypocenters are labelled A, B, and C according to the the crustal models used to obtain them.

First motion plots for the three models are shown in Fig 3 (A, B, C corresponding to the respective models). Nodal planes in all three solutions are very similar. Solutions B and C are preferred to A because they have fewer discordant points, but there is little basis for choosing between B and

C. In all three solutions the stations nearest the epicenter, CCO and CMH, are seriously discordant and suggest that the epicenters are too far east. Accordingly, a trial hypocenter for another first motion plot was obtained by "moving" hypocenter C 2.6 km toward the southwest to D (about 1 km southwest of the principal trace of the fault shown by Radbruch-Hall (1974). The nodal planes of the first motion plot for this trial hypocenter are the same as those for solution C, and the plotted points for CCO and CMH have moved much closer to concordant sectors of the plot. An additional shift of several tenths of a kilometer toward the southwest would be required to move CCO and CMH into appropriate fields.

An alternate explanation of the discordant points CCO and CMH is that the average crustal velocity just east of the fault is several tenths km/sec higher than just west of the fault and that the first arrivals at those stations left the focus along paths east of the fault and were then refracted across the fault. For a focal depth of 9 km a fairly modest velocity contrast brings refracted waves to the surface as first arrivals considerably west of the fault: for $V_e = 5.7$ and $V_w = 5.5$ refracted waves from east of the fault would be first arrivals up to 2.5 km west of the fault.

This brief analysis suggests the range of uncertainty in the location of the earthquake, but it does not resolve the uncertainty. Hypocenter solution C and first motion plot C are tentatively adopted for the April 24 earthquake, with the caution that some evidence supports a location 2 km or more toward the southwest. In fact, it is likely that the April 24 earthquake and its aftershocks as well as the persistent microearthquakes located by Calnet in this region lie beneath the surface expression of the Calaveras fault.

Three low-gain horizontal component seismometers in northern California and ten low gain vertical component seismometers in southern California produced records from which maximum amplitudes and associated periods could be measured. The distance and azimuth of each station from the epicenter as well as the magnitude computed for it are shown in Table 3. The average of the three northern California stations is 6.17. The ten values from southern California average 6.74, substantially larger than the northern California average. A correction of +0.25 unit is added to magnitudes computed from a vertical component instead of a horizontal component seismometer to compensate for the average ratio of horizontal to vertical maximum amplitudes. This correction was determined from a limited number of recordings of small to moderate earthquakes recorded at distances less than 200 km in central California, and it may be inappropriate for larger earthquakes recorded at much greater distances.

We should also note the rather narrow range in azimuth of the stations reporting magnitudes in northern California (328 degrees to 353 degrees) and southern California (125 degrees to 134 degrees). The difference in northern and southern California magnitudes may arise from a strong azimuthal variation in energy radiated by the earthquake.

Allowing for the uncertainty in the magnitude correction applied to the vertical component seismometers we have:

Northern California	M 6.2
Southern California	M 6.5 to 6.7

Summary of results on the Morgan Hill Quake:

Hypocenter (C)	Origin	84 04 24 21 15 18.74
	Latitude	37 18.56'N
	Longitude	121 40.74'W
	Depth	8.7 km
	Magnitude	6.2 (6.5-6.7 So Ca)
	Fault Plane	Strike N 33 W Dip 84 SW
	Aux Plane	Strike N 57 E Dip 86 NW
	Movement	Right lateral strike slip

TABLE 1 CRUSTAL MODELS

A		B		C	
Velocity	Depth	Velocity	Depth	Velocity	Depth
4.00	0.00	3.40	0.00	3.50	0.00
5.90	3.50	4.70	1.00	5.20	1.00
6.80	15.00	5.20	3.00	5.50	3.00
8.05	25.00	5.60	5.00	5.70	7.00
		5.70	7.00	6.10	9.00
		5.80	9.00	6.50	15.00
		6.00	11.00	8.00	28.00
		6.80	13.00		
		8.00	28.00		

TABLE 2 STATION CORRECTIONS

Station	A	B	C
CCO	+.31	+.13	+.50
CMH	+.16	+.02	+.20
CSC	+.27	+.43	+.50
CAO	-.01	-.29	0.00
JST	-.10	-.15	+.30
CAD	-.09	-.04	+.10
CML	0.00	-.09	-.10
CAL	-.01	-.11	0.00
CMM	0.00	-.26	-.10
JCB	-.07	-.29	+.10
JAL	-.11	-.22	0.00
HSP	0.00	-.37	-.10
JHL	-.15	-.27	0.00
CDV	0.00	-.18	+.10
JSS	-.09	-.13	+.10
CMJ	-.10	+.04	0.00
JRR	-.20	-.38	+.10
JLX	-.07	-.31	+.10
CMR	-.06	-.02	-.10
HGS	-.07	-.56	-.10
JEC	-.04	-.25	+.50
CMP	0.00	-.58	-.10
HGW	-.24	-.39	-.20
COS	0.00	-.31	0.00
JSG	+.15	-.01	+.50
CVA	0.00	0.00	-.10
CMN	-.10	0.00	-.10

TABLE 3 MAGNITUDE DETERMINATIONS FOR THE APRIL 24 EARTHQUAKE

Station	Distance	Azimuth	Magnitude	
LTCN	324 km	353 deg	6.2	
KMPN	405	328	6.0	6.17 av. No. Cal.
KMPE	405	328	6.3	
RLBZ	459	131	6.7	
RBRZ	481	132	6.6	
RGAZ	525	134	6.4	
RBIZ	548	127	7.0	
RRFZ	571	129	7.0	6.74 av. So. Cal.
RPBZ	590	133	6.5	(-0.0 to -0.25)
DCUZ	607	125	6.8	6.5 to 6.7
REWZ	609	128	6.9	
ECYZ	656	132	6.8	
ICWZ	663	127	6.7	

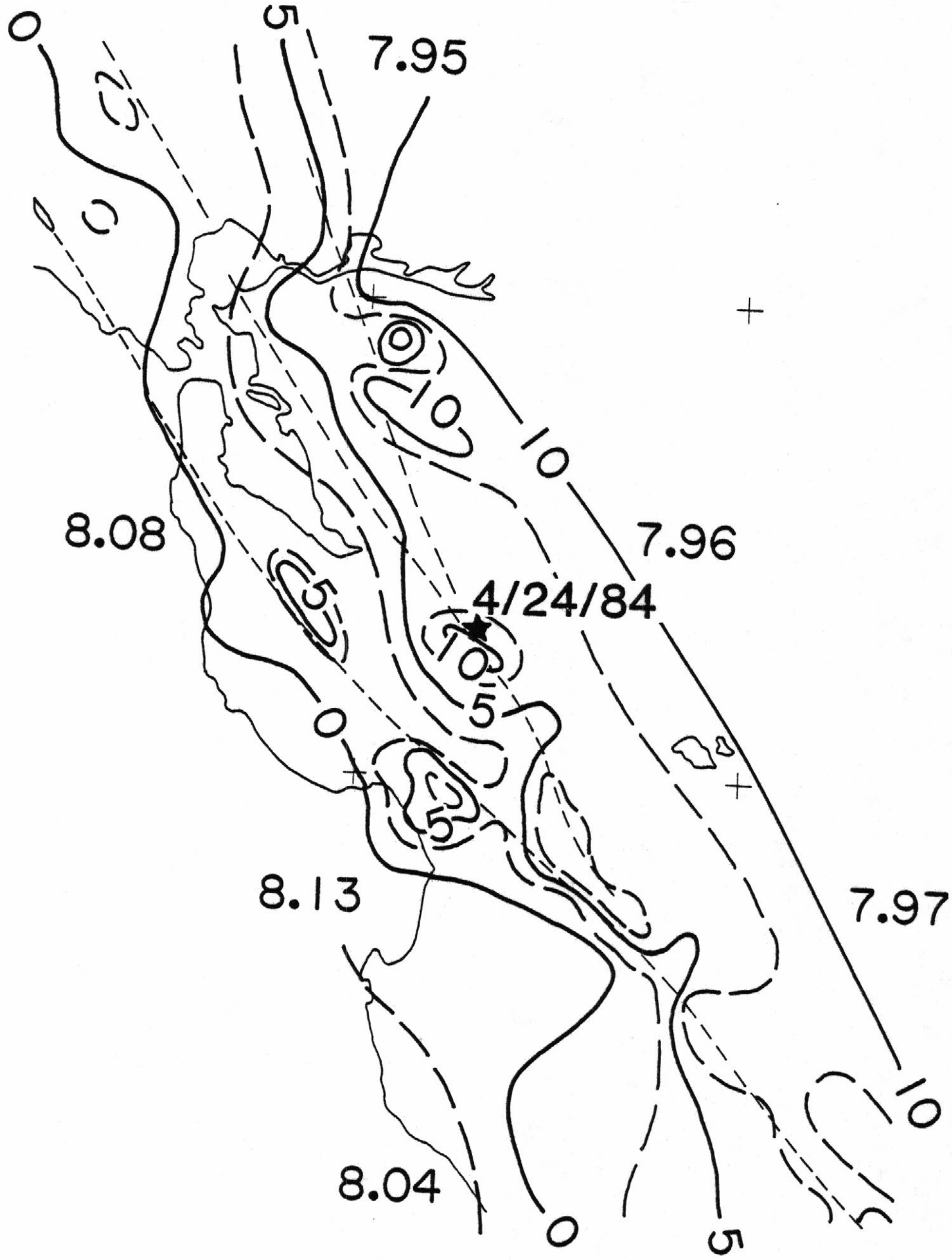

Figure 1. Pn timeterm-difference map for the Calaveras fault region. The boldest numbers are Pn velocities in kilometers per second. Pn traveltime-difference contour values are in tenths of seconds. The April 24 epicenter lies within a prominent "basin" marked by large positive Pn timeterm-differnce values.

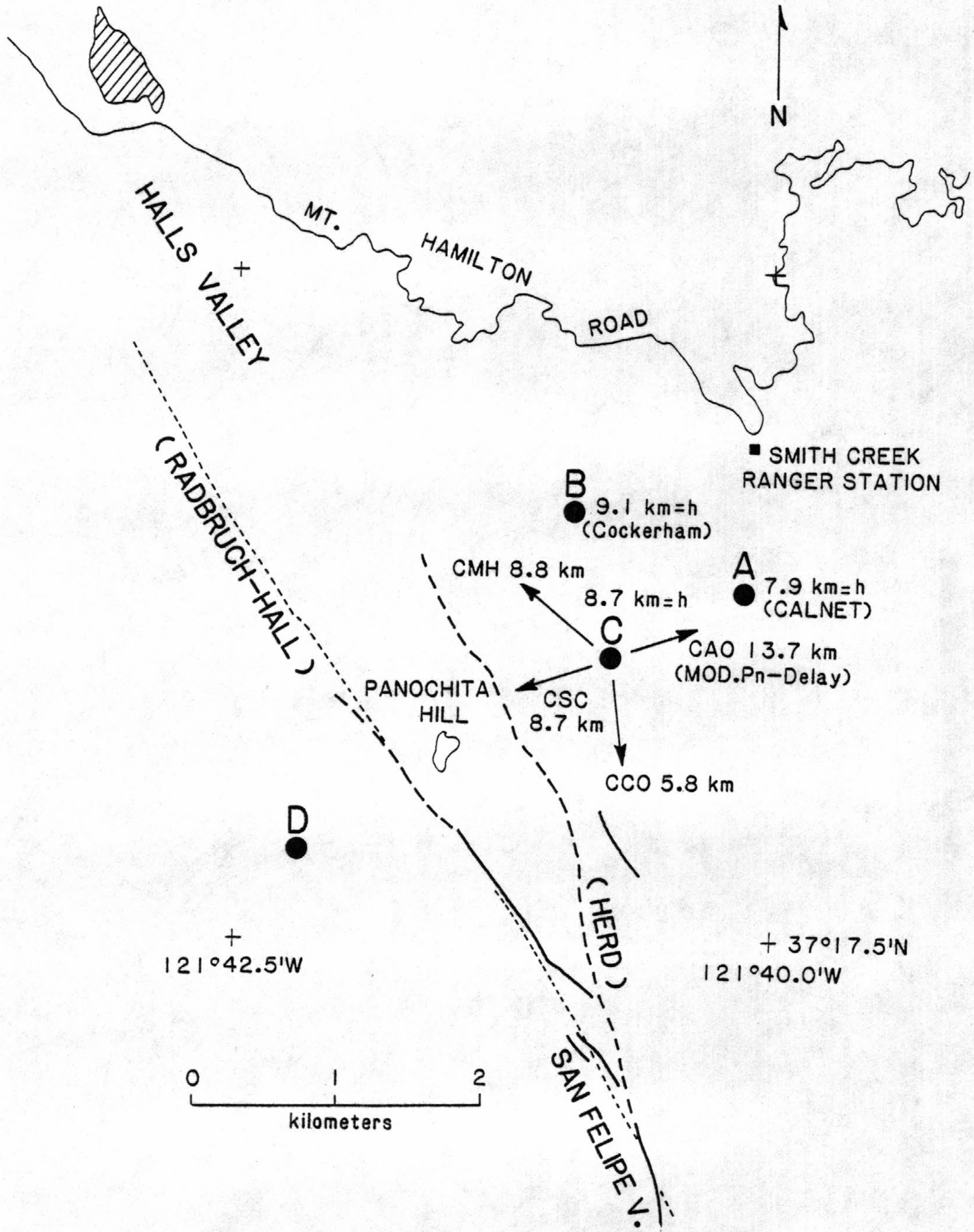

Figure 2. Sketch map of the epicentral region of the April 24 earthquake. Epicenter designations correspond to the model used to determine them. Directions and distances to the nearest stations are indicated for epicenter C.

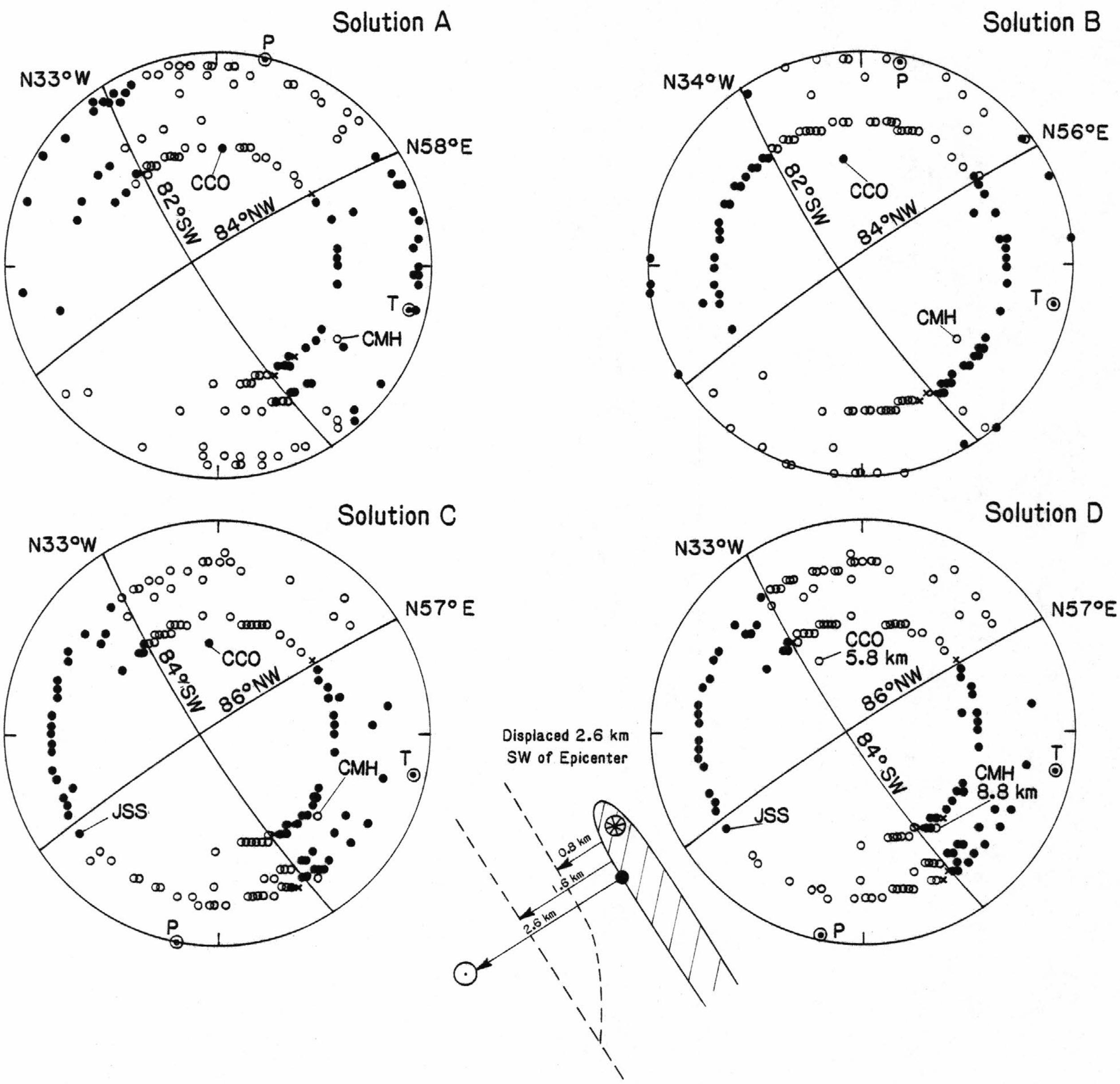

Figure 3. First motion plots for different hypocentral solutions of the April 24 earthquake. Letters designating solutions correspond to those in Fig. 2. Dilatational and compressional first motions are marked by open and closed circles, respectively. Conflicting first motions are indicated by X's.

REFERENCES

Eaton, J. P., (Ca. 1980), Unpublished Pn timeterm difference map for central California based on the analysis of Pn traveltime data from about 50 earthquakes between 1978 and 1980.

Ellsworth, W. L., and Marks, S. M., 1980, Seismicity of the Livermore Valley, California Region 1969-1979. *U.S. Geological Survey Open-File Report 80-515.*

Radbruch-Hall, Dorothy H., 1974, Map showing recently active breaks along the Hayward fracture zone and the southern part of the Calaveras fault zone, California. *U.S. Geological Survey Miscellaneous Investigations Series Map I-813.*

STRONG-MOTION RESULTS FROM THE MAIN SHOCK OF APRIL 24, 1984

*A.G. Brady, R.L. Porcella, G.N. Bycroft, E.C. Etheredge, P.N. Mork, B. Silverstein, and A.F. Shakal**

U.S. Geological Survey
345 Middlefield Rd. ms-977
Menlo Park, CA 94025

* California Division of Mines and Geology

The permanent accelerograph networks of both the U.S. Geological Survey (USGS) and the California Division of Mines and Geology (CDMG) have provided an important set of strong-motion records from the main shock of the Morgan Hill earthquake. Accompanying contributions provide details of the event. Altogether about 75 stations were triggered amongst the combined networks, at epicentral distances ranging from about 4 km (Hall's Valley, a CDMG-maintained station) to more than 100 km.

Figure 1 shows the locations of accelerograph stations in both networks at the time of the April 24, 1984 main shock. The triangle symbols are replaced by squares for a triggered station, and by circles for a non-triggered station. Remaining triangles indicate the station had not been visited when the figure was prepared. The list in Table 1 summarizes the data for the USGS-maintained stations. A comparable list for CDMG-maintained stations is provided in Shakal and others (1984). The maximum acceleration for each component scaled from the original records is listed, together with the duration in seconds for which the acceleration reached amplitudes greater than 0.1 g. Copies of USGS film records from Anderson Dam, Hollister Differential Array and City Hall Annex, San Jose Interchange, and San Justo Damsite are shown in Figure 2.

Table 1 contains information on both 70-mm film records and digital records (Kinemetrics' DSA-1). The entry "Hollister Differential Array" refers to a film recorder included within the Hollister Digital Differential Array. The array provided four digital records in addition to the listed film recorder. Also, a set of 3 digital records was obtained from various locations on a span of the San Jose Freeway Interchange (US-101, I-680, I-280). The details entered in Table 1 for this station are from the film recorder, located within the bridge box girder, but close to the abutment. The Palo Alto Veteran's Administration Hospital has two digital recorders located in separate buildings.

Digitizing and processing of film records has been carried out for the following stations: Anderson Dam (crest and downstream), Hollister Differential Array, Hollister City Hall Annex, San Justo Damsite (right and left abutments), and the San Jose Freeway Interchange.

Processing for corrected ground motions from the digital records at the Hollister Differential Digital Array (see Figure 3) are included. The individual stations in the array are arranged along the two legs of a V; four stations along a 2000' length, and two more along a 1000' length at 33° to the first. The array is located at Hollister Airport, 4 km north of Hollister City Hall. At the present time, only stations 1, 3, 4, and 5 have been processed. Malfunctions on the other two recorders may limit their usefulness.

Processing

All the records (7 film, 4 digital) have been processed according to the descriptions in AGRAM (Converse 1983). Briefly, the steps are as follows:

1. Digitizing of the film records at a commercial digitizing firm (IOM TOWILL in Santa Clara, California) on a trace-following, computer-controlled laser scanner. Unequal time spacing, at an average of 600 samples per second, is used.
2. Butting the separately-digitized, 10-s frames together, using specially inserted vertical lines; each vertical line is digitized twice, once in each adjacent frame.
3. Preparation of uncorrected data by subtracting out the reference traces, using the time marks for the X-coordinates, and subtracting the average value. Plots of the uncorrected data are contained in the Appendix.
4. The data from both film and digital recordings are then passed through a correction algorithm that applies a high frequency filter (50 Hz), instrument corrections, and decimation to 200 sps. A low-frequency high-pass Butterworth filter (0.25 s, order 8) removes all periods longer than 4 s from the data. These parameters were chosen after consideration of: (a) the strong-motion duration of the records, (b) any distortion during pre-event memory on the digitals, (c) displacements calculated at Anderson Dam, and (d) displacements of adjacent film and digital recordings at the Hollister Differential Array. Plots of the corrected acceleration, velocity, and displacements for the three components of each recording are contained in the Appendix.
5. Response spectra are calculated for periods up to 4 s. The Appendix contains the linear plots of relative velocity response spectra, and the log-log tripartite plots of pseudo-velocity response.
6. Fourier amplitude spectra, calculated by FFT, are presented in the Appendix on linear axes and log-log axes.
7. All the computer plots in the appendix were prepared before the name of the earthquake was finally decided. For Mt. Hamilton Earthquake, read Morgan Hill, California, Earthquake.

The digital data from which these plots are produced are available on tape from NGDC, NOAA, Mail Stop E/GC11, 325 Broadway, Boulder, Colorado 80303.

REFERENCES

Shakal, A. F., Sherburne, R. W., and Parke, D. L., (1984). CDMG Strong-motion records from the Morgan Hill, California, earthquake of 24 April, 1984.

Converse, A. M., (1983), AGRAM: A series of computer programs for porcessing digitized strong-motion accelerograms. *U.S. Geological Survey Open-File Report 83-276*.

Table 1. USGS strong-motion data from the April 24 main shock

No.	Station Name	Coordinates (Epi. Dist.)	Component Direction (deg)	Maximum Accel. (g)	Strong (>0.1g.) Duration (sec)
1652	Anderson Dam	37.165N	340	0.301	4.0
	Downstream	121.631W	Up	.201	5.2
		(16 km)	250	.409	4.4
1652	Anderson Dam	37.166N	340	0.386	8.7
	Crest	121.631W	Up	.202	3.3
		(16 km)	250	.634	7.9
1575	Hollister	36.85N	180	0.078	-
	City Hall Annex	121.40W	Up	.425	-
		(55 km)	090	.077	-
1656	Hollister	36.888N	255	0.094	-
	Diff. Array	121.413W	Up	.222	2.0
		(51 km)	165	.089	-
1655	San Justo Damsite	36.827N	360	0.059	-
	Rt. Abut. (Dike)	121.445W	Up	.060	-
		(55 km)	270	.076	-
1655	San Justo Damsite	36.815N	360	0.074	-
	Left Abutment	121.447W	Up	.034	-
		(56 km)	270	.038	-
1571	San Jose Interchng	37.340N	322	0.123	4-peaks
	Fwy 101/680/280	121.851W	Up	.082	-
		(12 km)	232	.083	-
1227	Palo Alto VA	37.40N	302	0.022	-
	Basement	122.14W	Up	.018	-
		(37 km)	212	.022	-
1277	Palo Alto VA	37.40N	302	0.084	-
	Roof (7th level)	122.14W	Up	.034	-
		(37 km)	212	.089	-
1226	Livermore VA 37.62N		128	0.022	-
	Basement	121.76W	Up	.011	-
		(41 km)	038	.016	-
1226	Livermore VA	37.62N	128	0.027	-
	Roof (Bldg. 62)	121.76W	Up	.016	-
		(41 km)	038	.047	-
1610	Stanford Univ.	37.429N	015	.027	-
	Quad	122.169W	Up	.022	-
		(41 km)	285	.023	-

Table 1.--continued

No.	Station Name	Coordinates (Epi. Dist.)	Component Direction (deg)	Maximum Accel. (g)	Strong (>0.1g.) Duration (sec)
1602	Stanford Univ.	37.417N	360	.027	-
	SLAC Survey Hill	122.198W	Up	.020	-
		(42 km)	270	.016	-
1601	Stanford Univ.	37.419N	360	.031	-
	SLAC Test Lab.	122.205W	Up	.022	-
		(43 km)	270	.032	-
1481	Bear Valley Stn 12	36.658N	310	.057	-
	Williams Ranch	121.249	Up	.140	0.6
		(82 km)	220	.044	-
1479	Bear Valley Stn 10	36.532N	310	.021	-
	Webb Residence	121.143W	Up	.011	-
		(99 km)	220	.027	-
1475	Bear Valley Stn 6	36.504N	310	.024	-
	James Ranch	121.101W	Up	.005	-
		(103 km)	220	.016	-
1343	Bear Valley Stn 2	36.636N	130	.016	-
	Stone Canyon	121.234W	Up	.019	-
	West	(85 km)	040	.011	-
1210	Bear Valley Stn 1	36.573N	310	.010	-
	Fire Station	121.184W	Up	.010	-
		(93 km)	220	.015	-
1474	Bear Valley Stn 5	36.673N	310	.015	-
	Callens Ranch	121.195W	Up	.022	-
		(83 km)	220	.015	-
1483	Bear Valley Stn 14	36.569N	310	.021	-
	Upper Butts Road	121.043W	Up	.010	-
		(100km)	220	.028	-
1657	Hollister	36.81N	118	.078	-
	Damler Residence	121.41W	Up	.076	-
		(60 km)	028	.060	-
1032	Hollister	37.76	360	.026	-
	SAGO Vault	121.45W	Up	.026	-
		(54 km)	270	.010	-
1446	San Francisco	37.79N	135	.011	-
	Standard Oil	122.40W	Up	.005	-
	Bldg. Basement	(83km)	045	.011	-

Table 1. continued

No.	Station Name	Coordinates (Epi. Dist.)	Component Direction (deg)	Maximum Accel. (g)	Strong (>0.1g.) Duration (sec)
1239	San Francisco	37.80N	261	.011	-
	Transamerica	122.40W	Up	.005	-
	Tower Basement	(83 km)	171	.016	-
	24th Floor		261	.021	-
			Up	.021	-
			171	.027	-
	49th Floor		261	.047	-
			Up	.032	-
			171	.037	-
	58th Level		261	.097	1-peak
			Up	.035	-
			171	.083	-

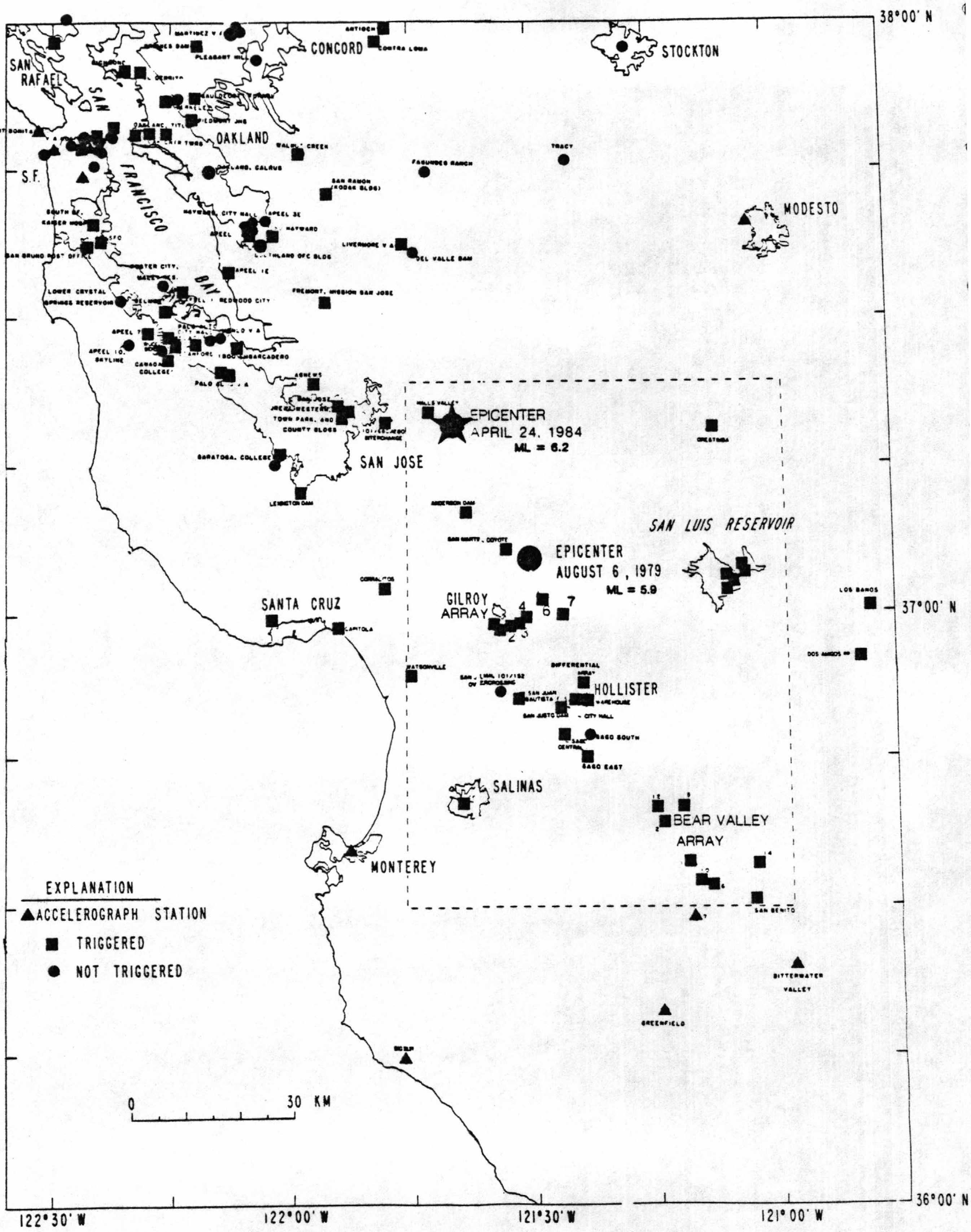

Figure 1. - Locations of accelerograph stations during the April 24 main shock.

Figure 2. - Strong-motion records from the April 24 main shock.

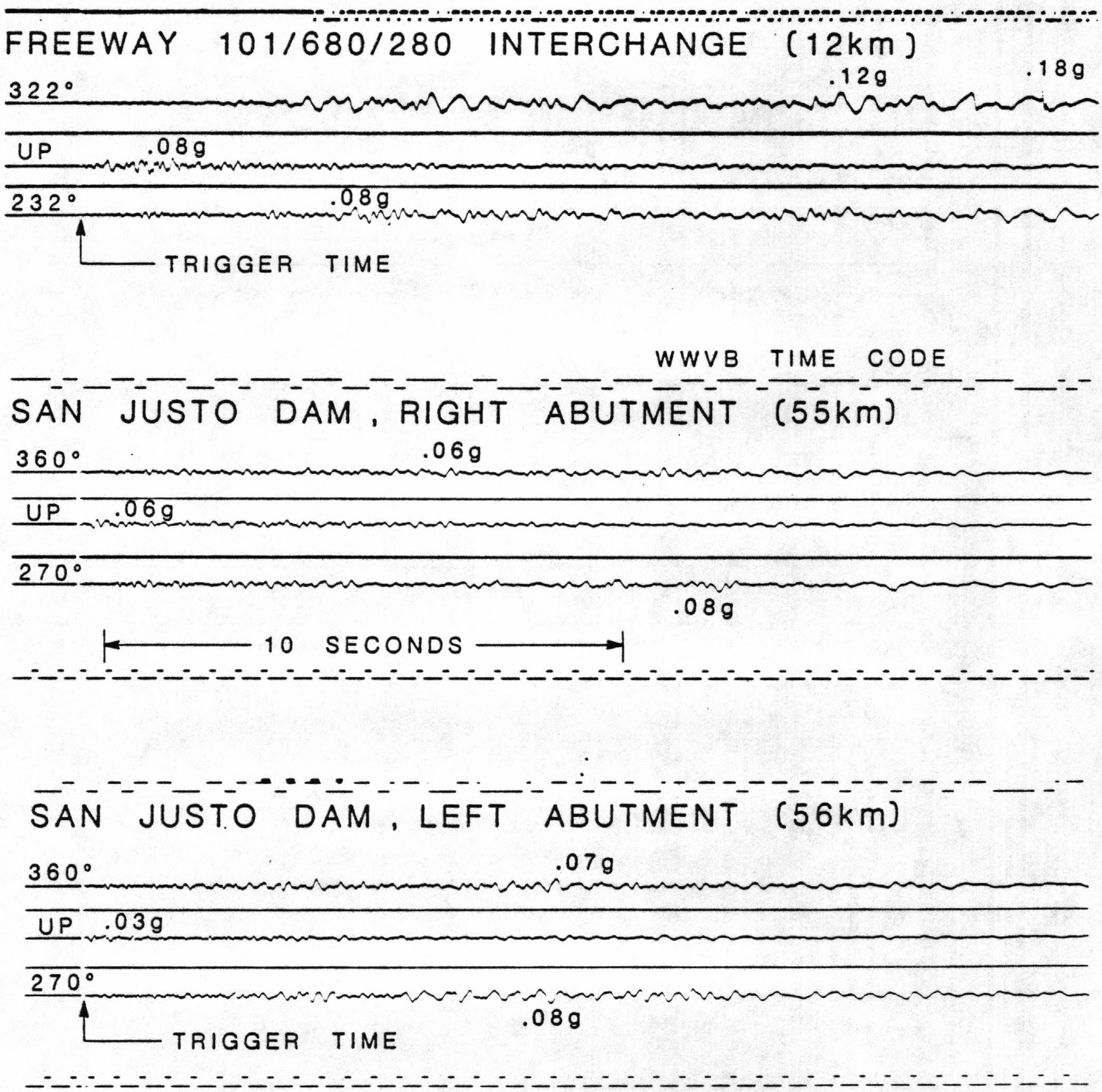

Figure 2. - continued.

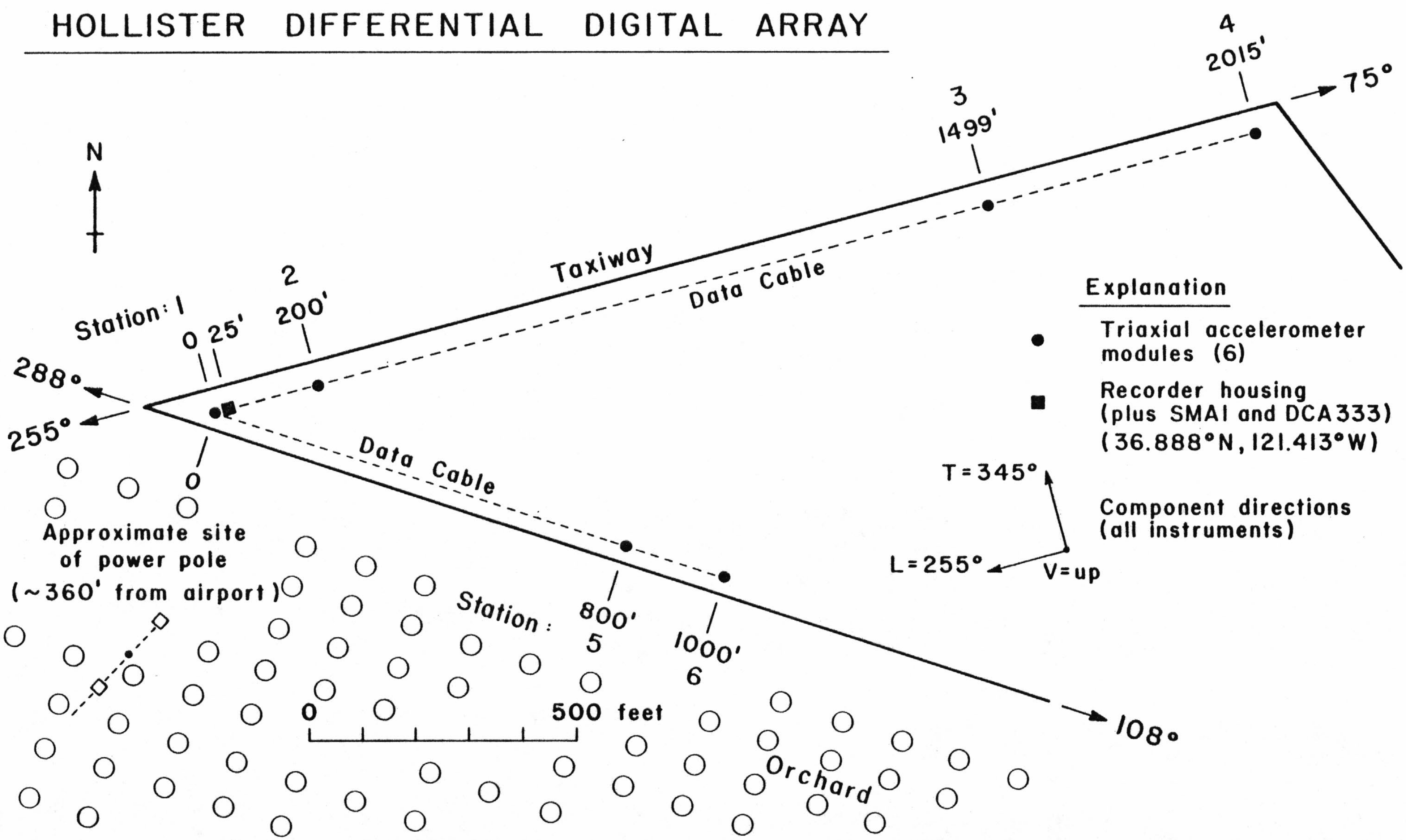

Figure 3.- Locations of accelerograph stations in the Hollister Differential Digital Array.

SOURCE PARAMETERS FOR TWO AFTERSHOCKS OF THE MORGAN HILL EARTHQUAKE

Ralph J. Archuleta, John Watson, Jon B. Fletcher
and
Eugene Sembera

U.S. Geological Survey
345 Middlefield Rd. ms-977
Menlo Park, CA 94025

In this report we present a tabulation of near-source digital seismograms for selected aftershocks of the 24 April, 1984, Morgan Hill, California, earthquake. For two of the larger aftershocks we derive estimates of their source parameters: seismic moment, corner frequency, source radius and stress drop.

Field Procedures

Within hours of the mainshock we began the deployment of GEOS (Borcherdt, and others, 1979) recorders with three-component force balanced accelerometers and three-component velocity transducers into the region near the epicenter and along the assumed rupture zone of the Calaveras fault (Figure 1). Because of the dense coverage of this area with standard USGS CALNET seismometers, the location of the aftershocks was not a primary concern. Our principal motivation was recording on scale all large aftershocks (M > 3.0) with a special emphasis on possible aftershocks M > 5.0. Thus we placed most of our instruments in the immediate vicinity of the Calaveras fault trace. Although many of the aftershocks (Figure 1) appear to lie east of the Calaveras fault (locations are taken from the USGS CALNET, R. Cockerham, pers. comm.), this is probably an artificial result of the location programs which do not properly account for the differences in velocity structure east and west of the fault.

In the first eight hours following the mainshock, six GEOS recorders were placed in the region. On the following day seven more were added. During the aftershock period the number of GEOS recorders in the field has varied between 9 and 13. The coordinates of the recorders and their days of operation are given in Table 2.

Instrumentation

The GEOS instrument is a microprocessor-based digital recorder. It is capable of sampling at 1200 samples/second with a 16 bit analog to digital converter. For each of the six components of particle acceleration and velocity the sampling rate is 200 samples/second. Variable gain settings, up to 60 db, coupled with different types of sensors allow one to record on scale a wide range of seismic events. For aftershocks we set the GEOS recorders in a trigger mode that is based on the ratio of the short term average (STA) signal to the long term average (LTA) signal. The gains were deliberately set low to insure against clipping for events with accelerations less than 1 g. The velocity transducers and force balanced accelerometer had natural periods of 2 Hz and 50 Hz, respectively. The horizontal components were oriented 0° and 90°, measured clockwise from north, for both sensors.

Data

As of May 30, we have recorded more than 126 aftershocks on four or more stations (Table 1). The three letter station codes appear in the first row while the origin times of the events appear in the first column. The first 3 digits represent Julian day; the next two repressent hour, and the next two are minutes. If a station records a particular event a single letter appears in the table. The letter is an indication of the trigger time in seconds after origin time and is used for file identification on our computer.

For the 1181648 and 1241307 events we have computed source parameters following Brune (1970, 1971). In figures 2 through 11 we show the three components of particle velocity and their respective displacement spectrum from which we determined a long period level Ω_0 and corner frequency f_c for event 1181648. In figures 12 through 16 we show similar plots for event 1241307. The spectral parameters and derived seismic parameters are listed for each event in Tables 3 and 4. An average value of the source parameters is obtained using the method outlined in Archuleta and others (1982). Hypocentral distances are based on depths of 9.97 km and 9.76 km for events 1181648 and 1241307, respectively. In our calculations of the source parameters, we have used a density of 2.8 gm/cm^3, shear wave velocity of 3.3 km/s and P-wave velocity of 5.8 km/s. With these physical constants we find the following:

P-wave

	1181648	1241307
Seismic moment:	3.0×10^{21} dyne-cm	1.2×10^{22} dyne-cm
Source radius:	0.19 km	0.35 km
Stress drop:	191 bars	122 bars

S-wave

	1181648	1241307
Seismic moment:	9.9×10^{21} dyne-cm	6.2×10^{22} dyne-cm
Source radius:	0.30 km	0.57 km
Stress drop:	161 bars	146 bars

For both events the seismic moment and the source radius determined by the P-wave spectra is significantly smaller than those derived from the S-wave spectra. Although we are very close to the source, it is clear from the curvature of the spectrum that attenuation is influencing the ground motion. We have not considered any attenuation for these preliminary calculations. The net effect of whole path attenuation would be to produce lower corner frequencies and consequently lower stress drops (Archuleta and others, 1982). These earthquakes were assigned coda magnitudes of 3.1 and 3.7 by the USGS Real Time Processor used to locate the events. However, if we apply the results of Bakun (1984) $\log M_0 = 1.2\ M_D + 17.0$ for central California earthquakes, we find M_D's of 4.2 and 4.8 for events 1181648 and 1241307, respectively. Further analysis on a larger number of the aftershocks may show that these two events are the exceptions, rather than the rule.

Acknowledgements

We wish to thank Chris Dietel and Cohen Criley for their assistance in maintaining the instruments. We also want to thank Rob Cockerham for providing us with locations for the aftershocks.

REFERENCES

Archuleta, R.J., E. Cranswick, C. Mueller, and P. Spudich (1982). Source parameters of the 1980 Mammoth Lakes, California, earthquake sequence: *Journal Geophysical Research*, v. 87, 4595-4607.

Bakun, W.H. (1984). Seismic moments, local magnitudes and coda-duration magnitudes for earthquakes in central California: *Bulletin, Seismological Society of America*, v. 79, 439-458.

Borcherdt, R.B., Fletcher, J.B., G. Jensen, G. Maxwell, E. Cranswick, J. Van-Schaack, R.E. Warrick, A General Earthquake Observation System (GEOS), submitted to *Bulletin, Seismological Society of America*.

Brune, J.N. (1970). Tectonic stress and the spectra of seismic shear waves from earthquakes, *Journal Geophysical Research*, v. 75, 4997-5009. (Correction, 1971: *Journal Geophysical Research*, v. 76, 5002.

TABLE 1
AFTERSHOCKS OF THE MORGANHILL EARTHQUAKE
(recorded by 4 or more GEOS)

ORIG.TIME	M(CODA)	AMS	BBL	COE	DFL	GRT	LAS	LON	NBR	OCR	PHR	RBH	RST	SFL	SFR	UTS
1160416	2.7			R		R	R				R		C			
1160435	1.7			G			G				G		G			
1160518	2.4			P			P				Q	P	P			P
1160733	1.7			K			K					K	K			K
1160744	1.7			S							S		S			T
1161204	1.8			I			I						I			I
1161414	2.0					Q	P				P		Q			P
1161837	1.7					K	K				K		K			L
1162026	2.4					T	S				T		S		T	T
1162102	2.0			F		G	F				G				G	G
1162214	1.6			H			H					H			H	I
1162256	1.8			M			M				M	M	M		M	M
1170042	* 3.1	I	J	J		K	J			I	J	J	J		J	J
1170050	2.6	A	A	A		A	A			A	A	A	A		A	A
1170111	1.5		N				N					N	N		N	
1170214	1.8	S	R			S	R			S		R	R		S	S
1170227	1.8						P					P	P		P	P
1170329	2.0	H	H				H			H		H	I		I	H
1170410												Q	Q		Q	Q
1170515	2.1		C			D				D		B	B		B	D
1170629	3.3	R	S			S				R	S	R	S		S	R
1170659	2.4	G	G			G				G	G	G	G		G	
1170752	2.6	B	A			B				A	A	B	A		B	A
1171532	1.9		T								A	T	T			T
1171535	2.4	J	I			I					I	I	I			
1171600		T	T			T		T			T	T	T			T
1172059	2.3	H	H			H					H	G				H
1180312	2.2	S		S	S	S	S				S	S	S	S	S	S
1180410	* 3.0	I		I	I	J	I				I	I	I	I	I	J
1180721	1.4			K	K								K	K	K	
1180725	2.2	H		I	I							I		H	I	I
1180748	1.0				H								H	I	H	
1180910	2.0			T	T								T	T	T	T
1181024	1.3			I	I							I		I	I	
1181048	1.1				S							S	S	S	S	
1181108	1.2				C							D	C	D	D	
1181319	2.7	C		C	C							C	E		D	C
1181605	1.8			M	M	M						M	M		M	M
1181648	* 3.1	L		L	L	L					L	L	L	M	L	L
1181752	1.4			C	C							C		C	C	
1181903	1.2				E							F	E	F	F	
1181955	1.7	C										D		C	D	C
1190000	1.6			C			D					C	C	C	C	
1190004	1.0				K							K	K	K		
1190116	1.5			T	T		T					T		S	T	T
1190143	1.2				P							Q	P	Q	Q	
1190354	1.3				D							E	E	E	E	
1190443	1.3			I	I								I		I	
1190718	2.6	F		G	G	H	G	G					H	G	G	
1190826	2.2			K	K	K	K						K	K	K	
1190838	1.9			Q			Q						Q	Q	Q	

ORIG.TIME	M(CODA)	AMS	BBL	COE	DFL	GRT	LAS	LON	NBR	OCR	PHR	RBH	RST	SFL	SFR	UTS
1191115	1.4				N								O	N	N	
1191130	1.7			N	M		M							M	N	N
1191451	1.6			A	A		A						A		A	A
1191543	1.9	D		D	D		D						D		D	D
1191612	1.9			O			O						O		O	
1191748	1.1			P	O							P			P	
1191752	1.2			C	C							C			C	
1191853	1.9			Q	Q	Q	Q					Q	Q		Q	Q
1192033	1.3			A	T							A	T		A	
1192108	1.3			K	J							K	K		K	
1200103	0.6			M	M							M	L			
1200143	1.9	C		B	B	C		C			B	C	B			C
1200601	1.5			A	A							A	A			A
1201920	1.7			H	H	I	H				H	H	H		I	
1202358	2.6	G		H	H	H	H	G			H	H	H		H	H
1210053	1.6					B						B	B		B	
1210113	1.9			I	H		H					I	H		I	H
1210312	1.2				I							I	I		I	
1210352	1.6				N						O	O	O		O	
1211128	1.0			D	D							D	D		D	
1211446	1.4			A	A							A	A		A	
1220220	2.3			A	A	B	B					B	A		B	A
1220400	2.4			D	C	D	D					D	D		D	D
1221518	2.6	P		O	O	P	O					P				P
1222323	2.6	D		D	D	D	D	D				D			D	
1230444	2.7			H	H	H	H	H				H			H	
1231918	1.9			D	C							D			D	
1230401	2.3			Q	P	Q						Q				
1241050	1.8			H	H	H						H				
1241302	2.0	R		R	Q	R						R				
1241307	3.7	E		E	D	D						E				
1251842	2.7			T	T	T	T					T				
1260331	2.2			S	S	S	S					S	S			
1260352	1.9			D	D	E	D					E	D			
1260550	2.7			F	F		F					F				
1260632	1.7			Q	Q	Q	R					R	Q			
1261142	1.9				B		B					B	B			
1261501	1.8			I	I		I						I			
1262330	1.7				K	K	L				K	K	K			
1271129	2.5			C	C	C	D				D		C			
1281427	2.6			G	G	G							G			
1291334	1.9			C	C		C						C			
1310110	2.1			N	N		N		N	N						
1310307	2.3			E	E		E		E							
1320025	2.1			R	R	S	S		S							
1320044	1.5			E	E		F			E						
1320308				J	J				I	J						
1320431		J		K	K		K		J	K						
1322326	2.3			B	B	C	C		C							
1362252	2.2			J	J	I	J									
1370745	1.9				M	M	N		N							
1371709					J	J	K		K							
1380843	3.0	B			A	B	B	B	B	B						
1381557	2.1				P	P	Q		P							

ORIG.TIME	M(CODA)	AMS	BBL	COE	DFL	GRT	LAS	LON	NBR	OCR	PHR	RBH	RST	SFL	SFR	UTS
1390207	2.0					I	I		I	I						
1391417	2.8	F				F	E		F	E						
1391930	2.4				I	I	I		I							
1401649	2.8			R	R	Q	R		R							
1410016	1.6			G	G	G	H		H							
1430254	2.4			E	E	E	F		E	F						
1441835	1.7			T	T	T	T									
1442141	2.3				K	K	K		K	K						
1482023	1.8			P	P	P	P									
1502132	2.3			G	G	H			G	G						
1510328				F	E	F			F	F						
1511238				D	D	D			D	D						

TABLE 2

LOCATION AND DAYS OF OPERATION FOR EACH GEOS STATION

STATION	LATITUDE		LONGITUDE		OPERATING INTERVALS
AMS	37	9.63	121	36.92	117-140
BBL	37	18.46	121	39.41	116-117
COE	37	15.82	121	40.45	116-157
DFL	37	17.36	121	37.76	118-156
GRT	37	19.91	121	43.11	116-154
LAS	37	14.85	121	40.41	116-150
LON	37	11.43	121	37.24	116-129, 135-143, 153-156
NBR	37	10.17	121	38.76	130-152
OCR	37	12.67	121	38.19	116-118, 129-157
PHR	37	18.88	121	41.67	116-127
RBH	37	14.10	121	41.15	116-127
RST	37	19.00	121	40.13	116-129
SFL	37	15.54	121	34.86	116-119
SFR	37	16.95	121	44.32	116-128
UTS	37	12.72	121	39.74	116-152

Latitude and longitude are measured in degrees and minutes north and west respectively.

Operating intervals are Julian days--Julian day 116 is equivalent to April 24

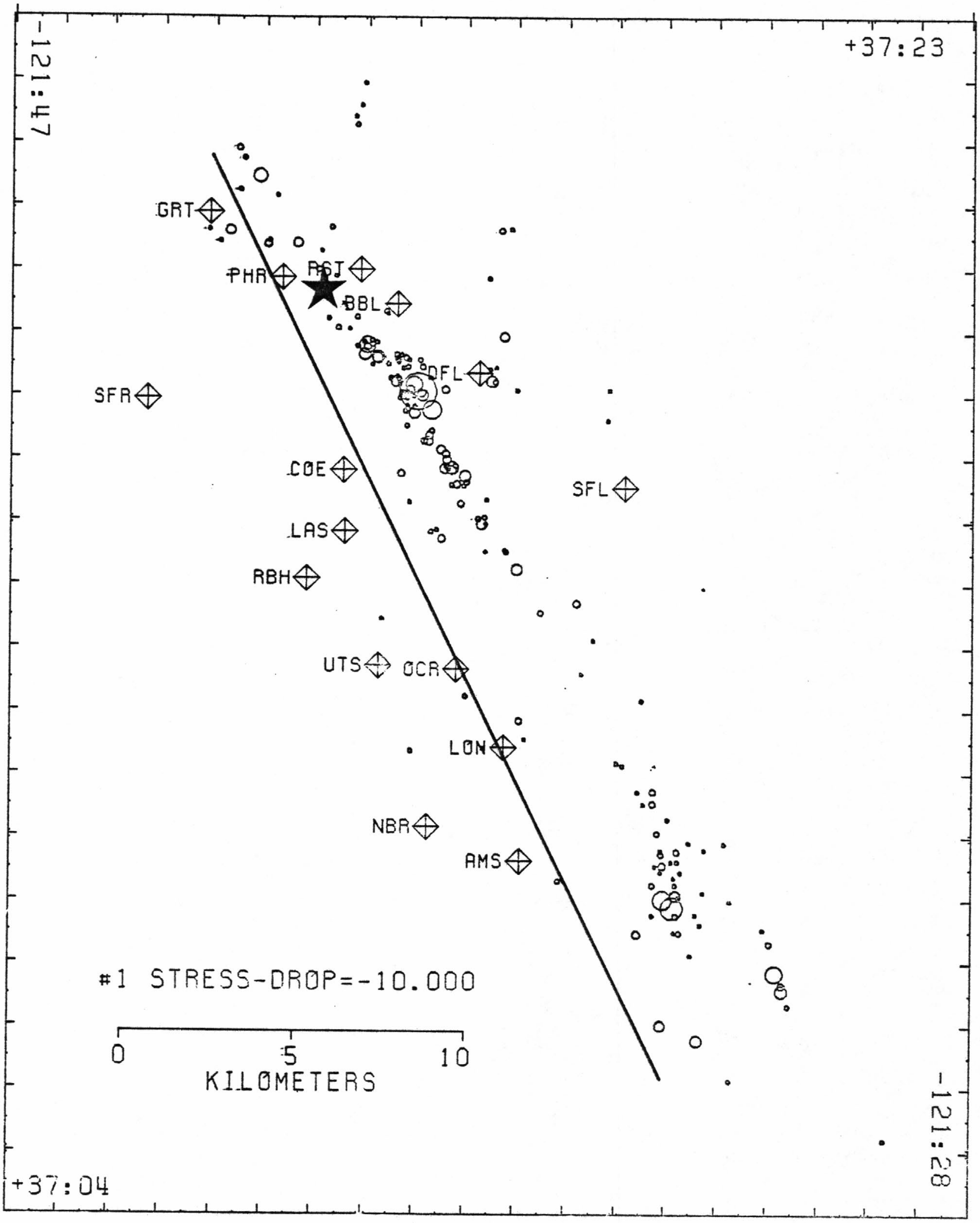

Figure 1. A map view of the source region showing the locations of the GEOS recorders, aftershocks M $\geq$ 1.5 recorded by one or more GEOS and the approximate location of the surface trace of the Calaveras fault. A large star indicates the mainshock epicenter.

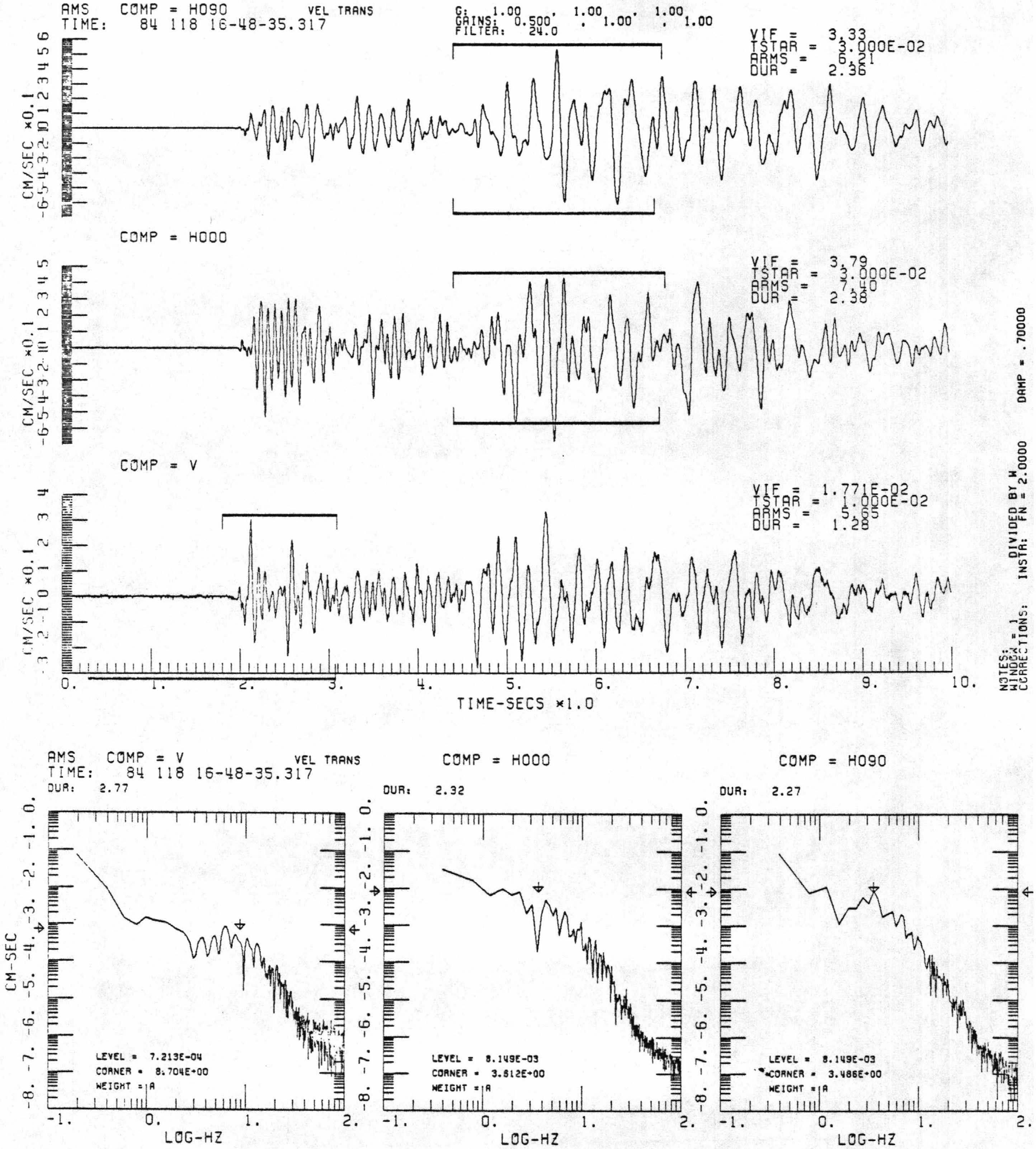

Figures 2-10. For event 1181648 (April 27, 16 hr 48 min), the 3 components of particle velocity for stations AMS, COE, DFL, GRT, PHR, RBH, RST, SFR, and UTS are shown. The lower heavy line associated with each trace shows the time window of the signal used to determine the displacement spectrum which is plotted at the bottom. From the spectrum of each component we have selected a corner frequency and a long period level. These spectral parameters and derived source parameters are listed in Table 3.

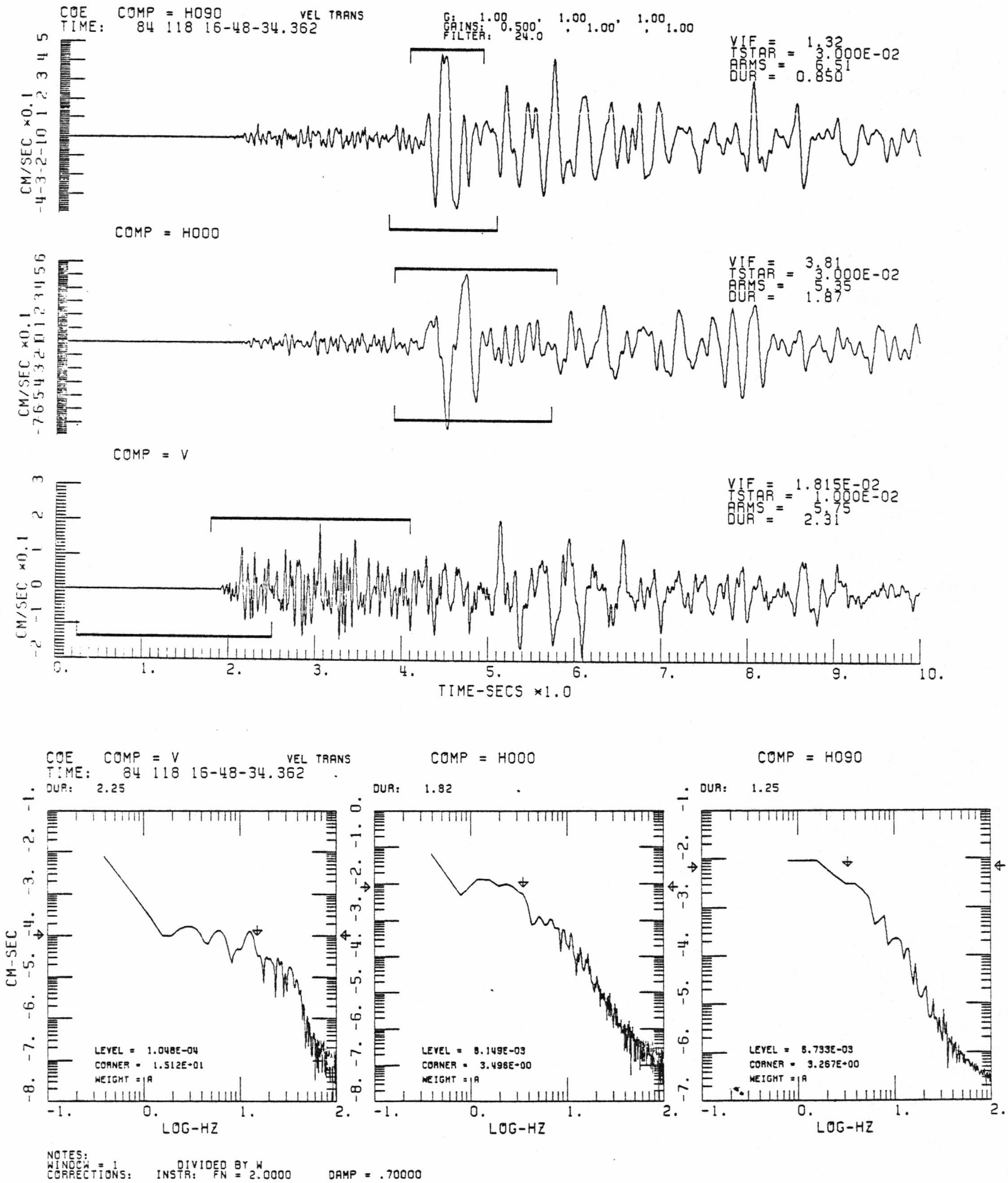
COE COMP = H090 VEL TRANS
TIME: 84 118 16-48-34.362
G: 1.00, 1.00, 1.00
GAINS: 0.500, 1.00, 1.00, 1.00
FILTER: 24.0
VIF = 1.32
TSTAR = 3.000E-02
ARMS = 6.51
DUR = 0.850
CM/SEC ×0.1
COMP = H000
VIF = 3.81
TSTAR = 3.000E-02
ARMS = 5.35
DUR = 1.87
COMP = V
VIF = 1.815E-02
TSTAR = 1.000E-02
ARMS = 5.75
DUR = 2.31
TIME-SECS ×1.0
COE COMP = V VEL TRANS
TIME: 84 118 16-48-34.362
DUR: 2.25
LEVEL = 1.048E-04
CORNER = 1.512E+01
WEIGHT = |A
CM-SEC
LOG-HZ
COMP = H000
DUR: 1.82
LEVEL = 8.149E-03
CORNER = 3.496E+00
WEIGHT = |A
COMP = H090
DUR: 1.25
LEVEL = 6.733E-03
CORNER = 3.267E+00
WEIGHT = |A
NOTES:
WINDOW = 1 DIVIDED BY W
CORRECTIONS: INSTR: FN = 2.0000 DAMP = .70000

Figure 3.

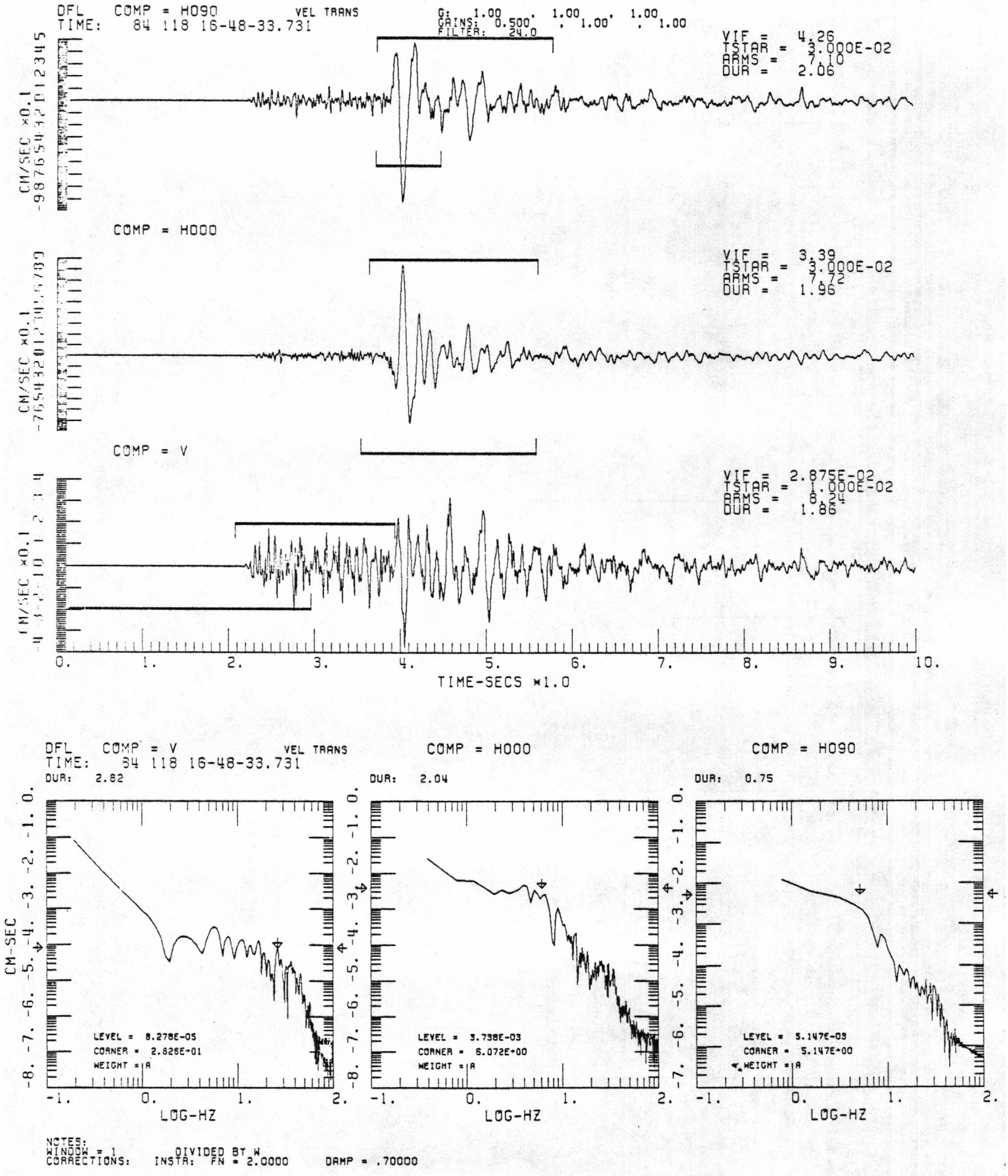
DFL COMP = H090 VEL TRANS
TIME: 84 118 16-48-33.731
VIF = 4.26
TSTAR = 3.000E-02
ARMS = 7.10
DUR = 2.06
COMP = H000
VIF = 3.39
TSTAR = 3.000E-02
ARMS = 7.72
DUR = 1.96
COMP = V
VIF = 2.875E-02
TSTAR = 1.000E-02
ARMS = 8.24
DUR = 1.86
CM/SEC ×0.1
TIME-SECS ×1.0
DFL COMP = V VEL TRANS
TIME: 84 118 16-48-33.731
DUR: 2.82
LEVEL = 8.278E-05
CORNER = 2.826E+01
WEIGHT = A
COMP = H000
DUR: 2.04
LEVEL = 3.738E-03
CORNER = 6.072E+00
WEIGHT = A
COMP = H090
DUR: 0.75
LEVEL = 5.147E-03
CORNER = 5.147E+00
WEIGHT = A
CM-SEC
LOG-HZ
NOTES:
WINDOW = 1 DIVIDED BY W
CORRECTIONS: INSTR: FN = 2.0000 DAMP = .70000

Figure 4.

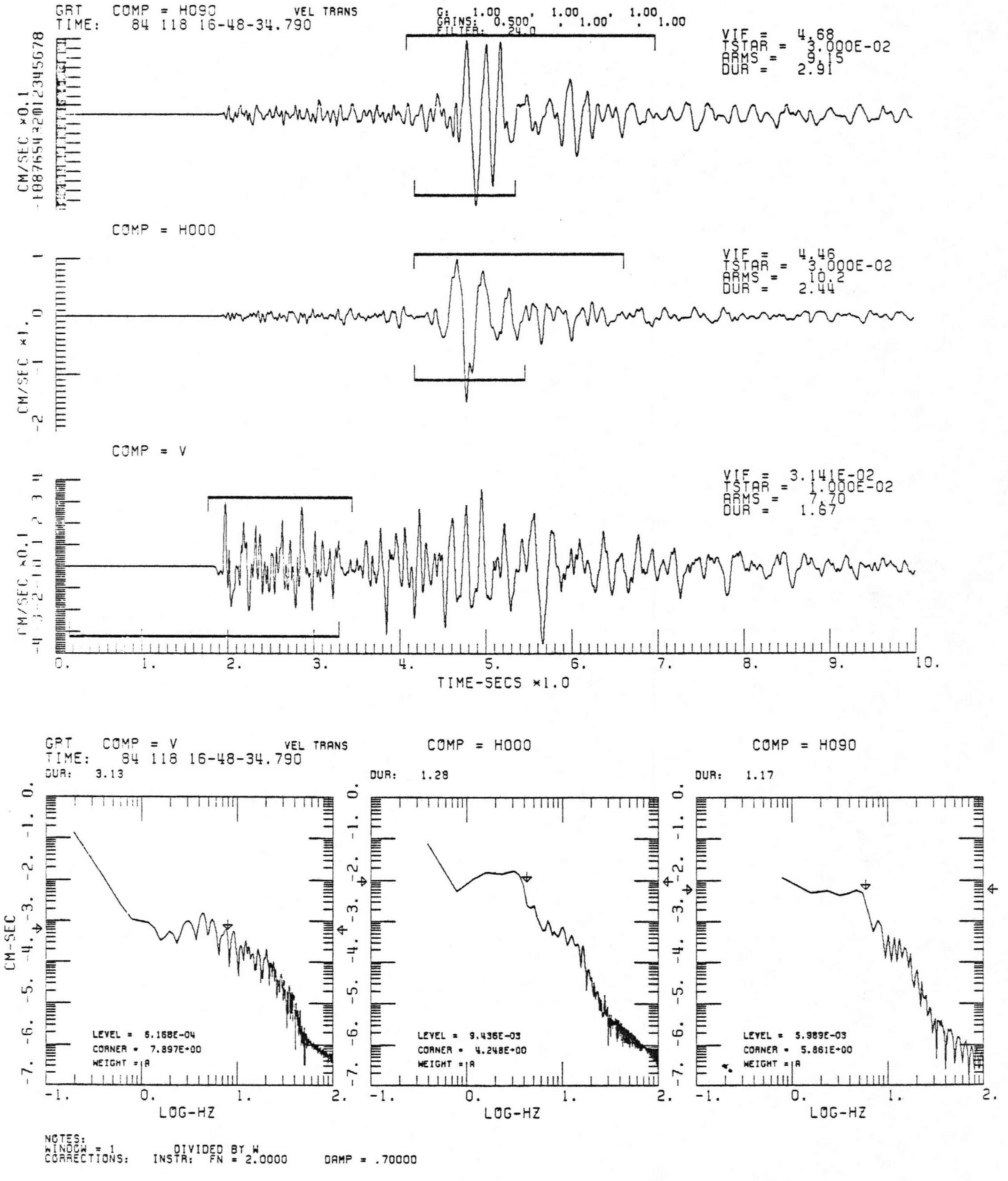
GRT COMP = H090 VEL TRANS
TIME: 84 118 16-48-34.790
VIF = 4.68
TSTAR = 3.000E-02
ARMS = 9.15
DUR = 2.91
COMP = H000
VIF = 4.46
TSTAR = 3.000E-02
ARMS = 10.2
DUR = 2.44
COMP = V
VIF = 3.141E-02
TSTAR = 1.000E-02
ARMS = 7.70
DUR = 1.67
TIME-SECS *1.0
GRT COMP = V VEL TRANS
TIME: 84 118 16-48-34.790
DUR: 3.13
LEVEL = 6.168E-04
CORNER = 7.897E+00
WEIGHT = A
COMP = H000
DUR: 1.28
LEVEL = 9.436E-03
CORNER = 4.248E+00
WEIGHT = A
COMP = H090
DUR: 1.17
LEVEL = 5.989E-03
CORNER = 5.861E+00
WEIGHT = A
CM-SEC
LOG-HZ
NOTES:
WINDOW = 1 DIVIDED BY W
CORRECTIONS: INSTR: FN = 2.0000 DAMP = .70000

Figure 5.

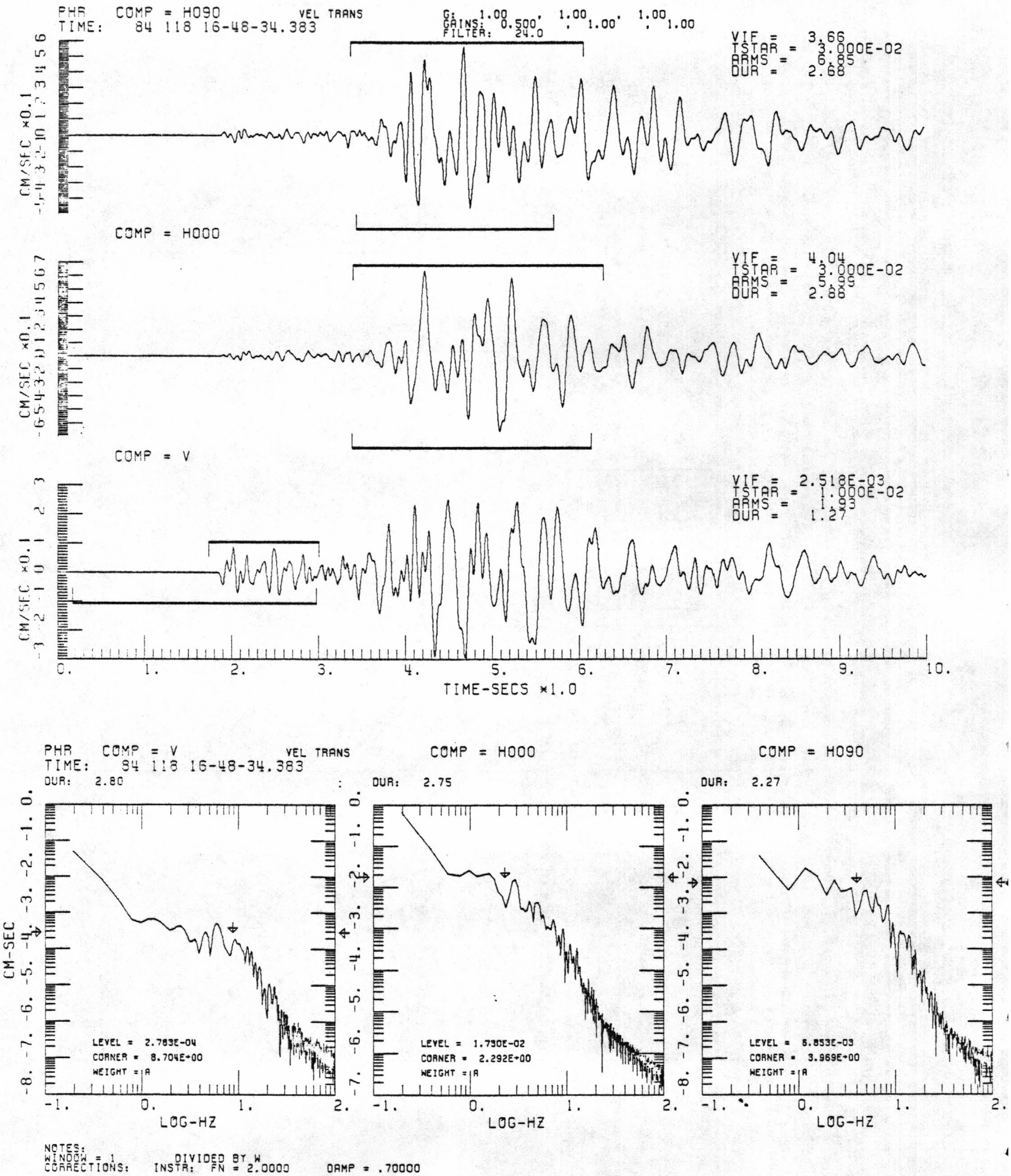

PHR COMP = H090 VEL TRANS
TIME: 84 118 16-48-34.383
G: 1.00, 1.00, 1.00
GAINS: 0.500, 1.00, 1.00
FILTER: 24.0
VIF = 3.66
TSTAR = 3.000E-02
ARMS = 6.85
DUR = 2.68
CM/SEC ×0.1
COMP = H000
VIF = 4.04
TSTAR = 3.000E-02
ARMS = 5.99
DUR = 2.86
COMP = V
VIF = 2.518E-03
TSTAR = 1.000E-02
ARMS = 1.93
DUR = 1.27
TIME-SECS ×1.0
PHR COMP = V VEL TRANS
TIME: 84 118 16-48-34.383
DUR: 2.80
COMP = H000
DUR: 2.75
COMP = H090
DUR: 2.27
CM-SEC
LEVEL = 2.783E-04
CORNER = 8.704E+00
WEIGHT = A
LEVEL = 1.730E-02
CORNER = 2.292E+00
WEIGHT = A
LEVEL = 5.853E-03
CORNER = 3.969E+00
WEIGHT = A
LOG-HZ
NOTES:
WINDOW = 1 DIVIDED BY W
CORRECTIONS: INSTR: FN = 2.0000 DAMP = .70000

Figure 6.

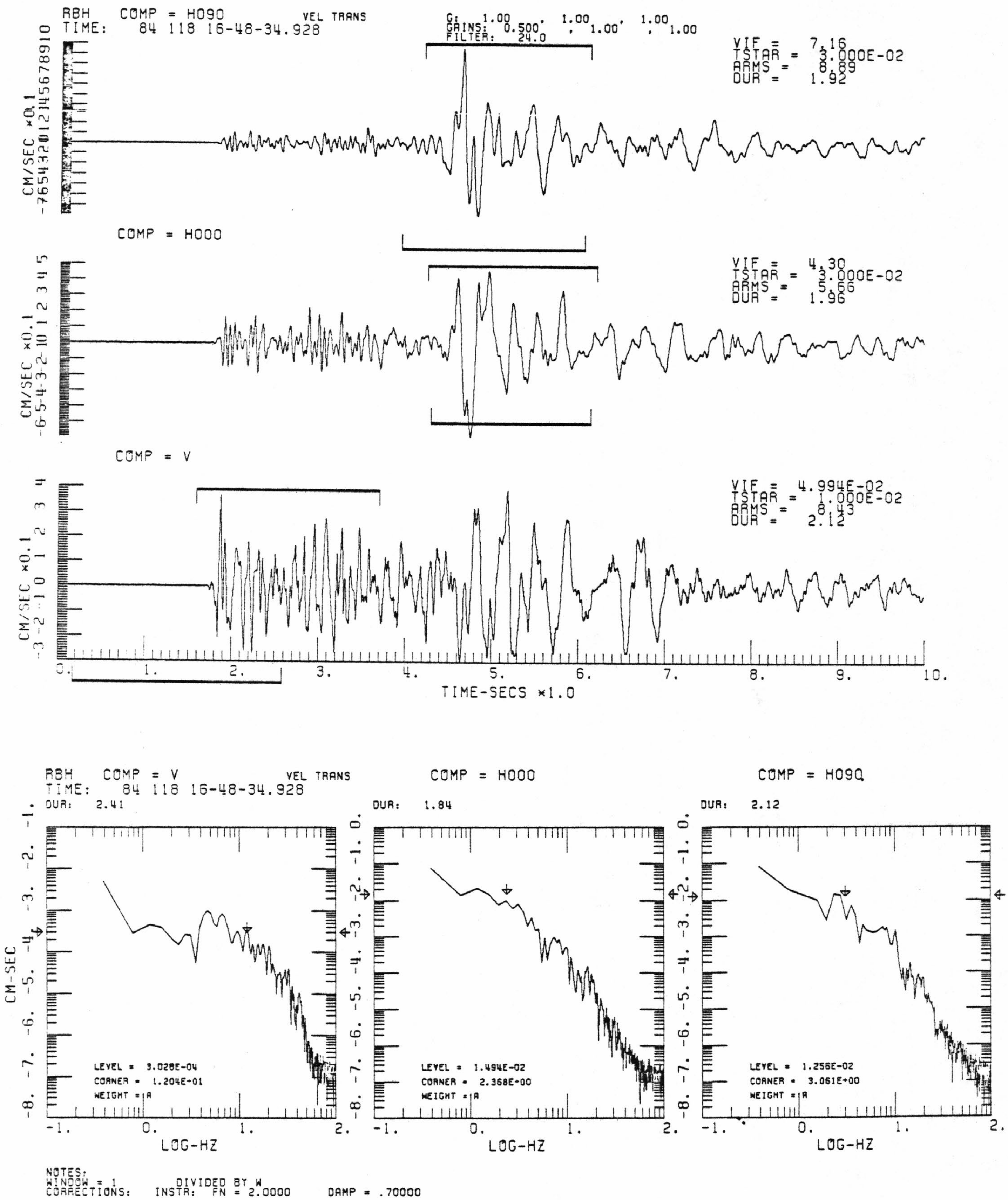
RBH COMP = H090 VEL TRANS
TIME: 84 118 16-48-34.928
G: 1.00 , 1.00 , 1.00
GAINS: 0.500 , 1.00 , 1.00
FILTER: 24.0
VIF = 7.16
TSTAR = 3.000E-02
ARMS = 8.89
DUR = 1.92
CM/SEC ×0.1
COMP = H000
VIF = 4.30
TSTAR = 3.000E-02
ARMS = 5.66
DUR = 1.96
COMP = V
VIF = 4.994E-02
TSTAR = 1.000E-02
ARMS = 8.43
DUR = 2.12
TIME-SECS ×1.0
RBH COMP = V VEL TRANS
TIME: 84 118 16-48-34.928
DUR: 2.41
COMP = H000
DUR: 1.84
COMP = H090
DUR: 2.12
CM-SEC
LEVEL = 3.028E-04
CORNER = 1.204E+01
WEIGHT = A
LEVEL = 1.494E-02
CORNER = 2.368E+00
WEIGHT = A
LEVEL = 1.256E-02
CORNER = 3.061E+00
WEIGHT = A
LOG-HZ
NOTES:
WINDOW = 1 DIVIDED BY W
CORRECTIONS: INSTR: FN = 2.0000 DAMP = .70000

Figure 7.

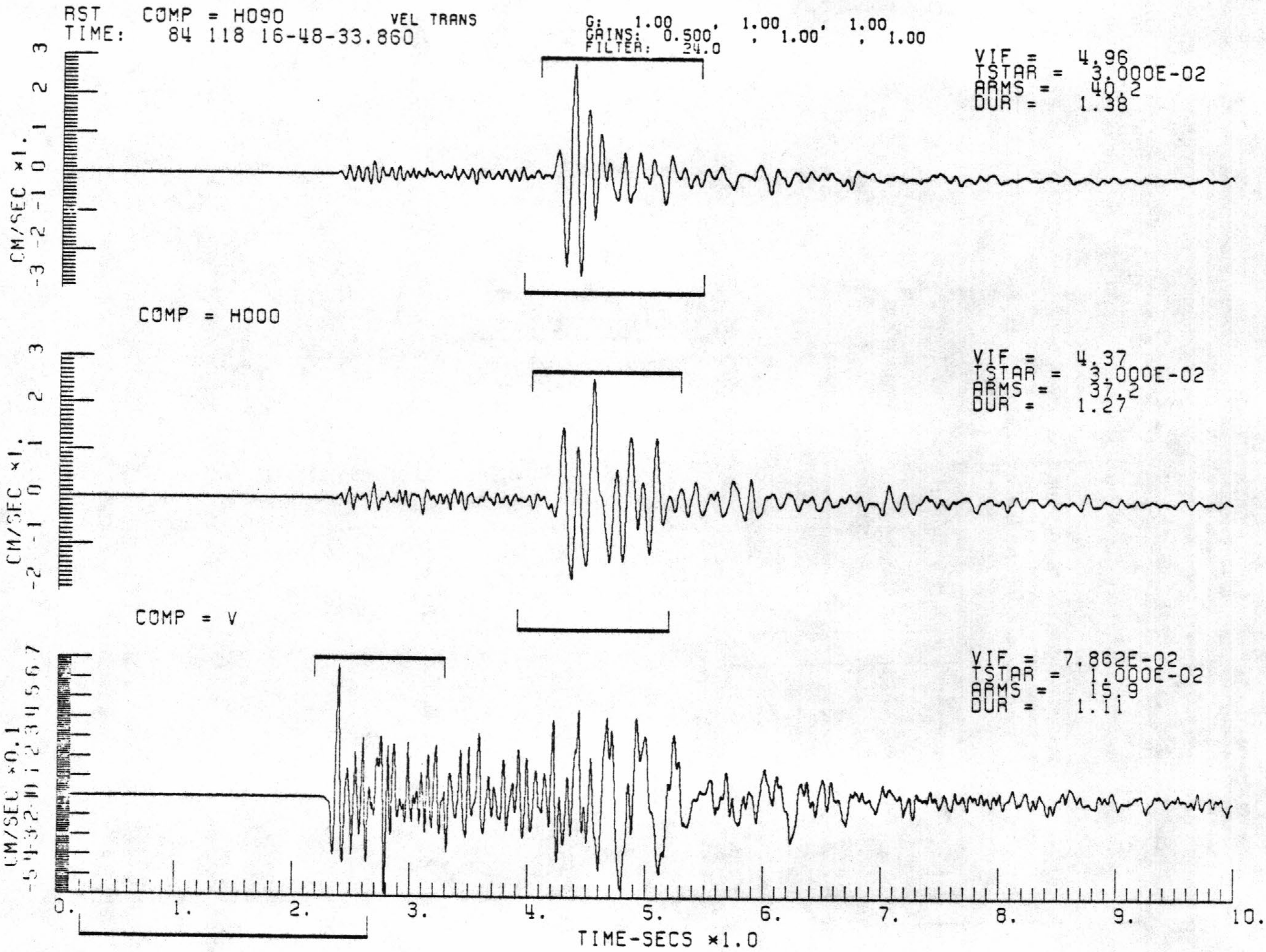
RST COMP = H090 VEL TRANS
TIME: 84 118 16-48-33.860
G: 1.00, 1.00, 1.00
GAINS: 0.500, 1.00, 1.00
FILTER: 24.0
VIF = 4.96
TSTAR = 3.000E-02
ARMS = 40.2
DUR = 1.38
CM/SEC ×1.
COMP = H000
VIF = 4.37
TSTAR = 3.000E-02
ARMS = 37.2
DUR = 1.27
COMP = V
VIF = 7.862E-02
TSTAR = 1.000E-02
ARMS = 15.9
DUR = 1.11
CM/SEC ×0.1
TIME-SECS ×1.0

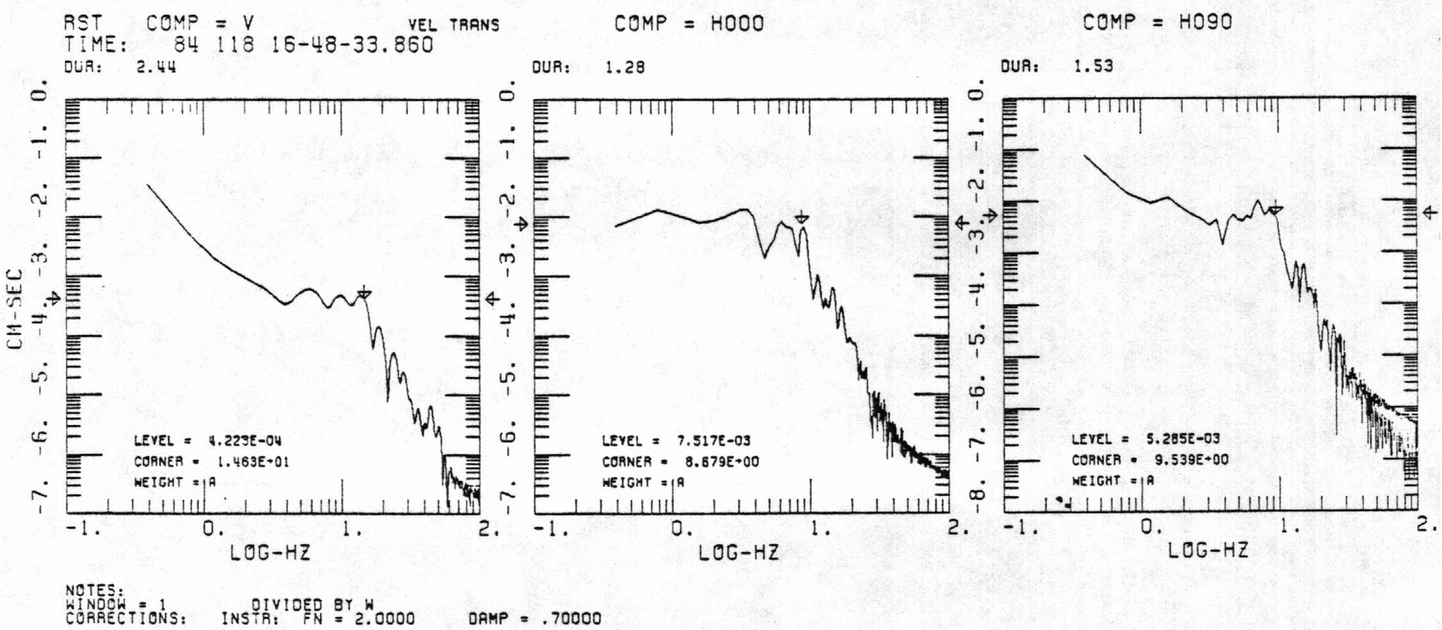
RST COMP = V VEL TRANS
TIME: 84 118 16-48-33.860
DUR: 2.44
LEVEL = 4.223E-04
CORNER = 1.463E+01
WEIGHT = A
COMP = H000
DUR: 1.28
LEVEL = 7.517E-03
CORNER = 8.679E+00
WEIGHT = A
COMP = H090
DUR: 1.53
LEVEL = 5.285E-03
CORNER = 9.539E+00
WEIGHT = A
CM-SEC
LOG-HZ
NOTES:
WINDOW = 1 DIVIDED BY W
CORRECTIONS: INSTR: FN = 2.0000 DAMP = .70000

Figure 8.

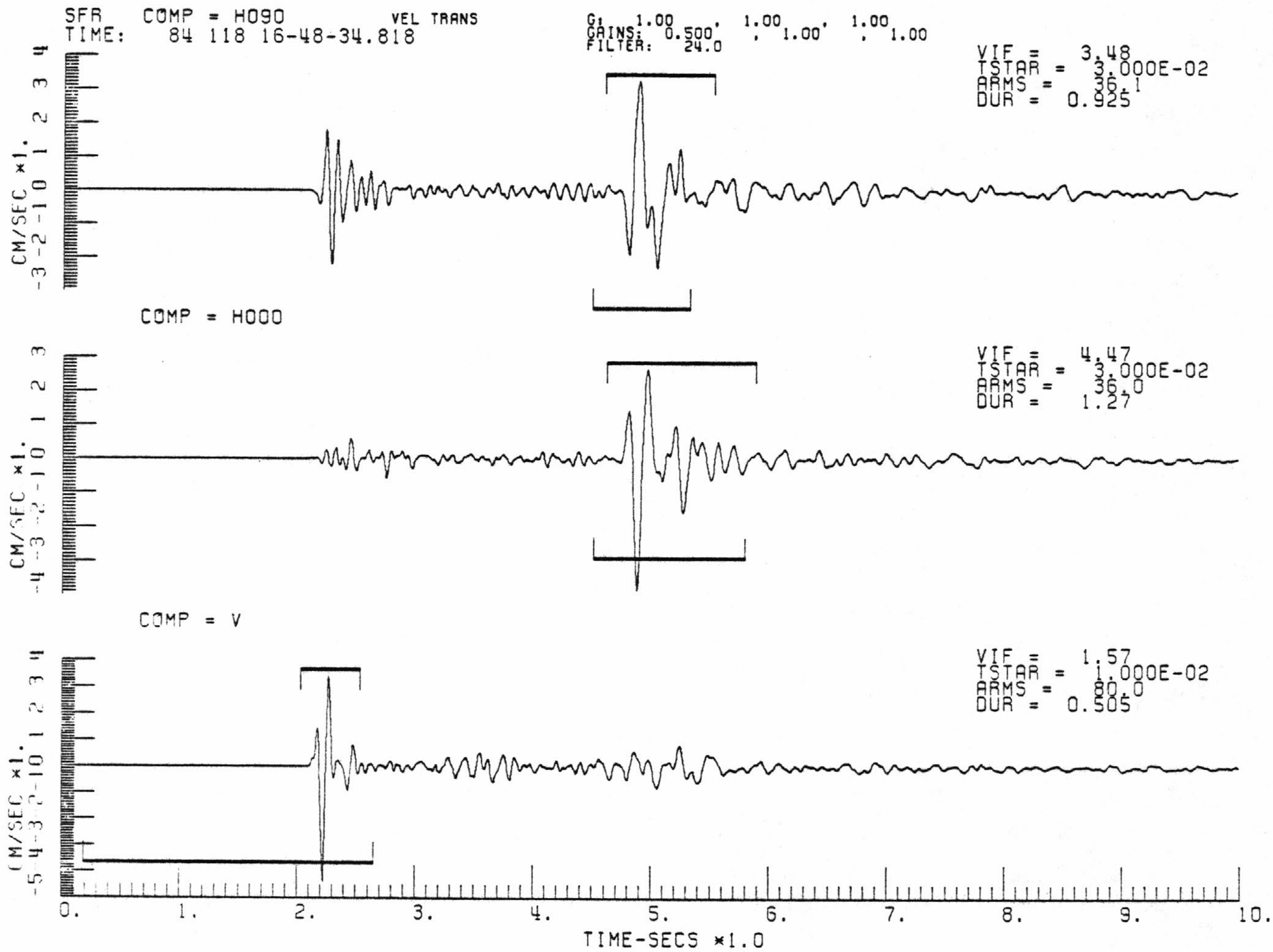
SFR COMP = H090 VEL TRANS
TIME: 84 118 16-48-34.818
G: 1.00, 1.00, 1.00
GAINS: 0.500, 1.00, 1.00
FILTER: 24.0
VIF = 3.48
TSTAR = 3.000E-02
ARMS = 36.1
DUR = 0.925
COMP = H000
VIF = 4.47
TSTAR = 3.000E-02
ARMS = 36.0
DUR = 1.27
COMP = V
VIF = 1.57
TSTAR = 1.000E-02
ARMS = 80.0
DUR = 0.505
CM/SEC ×1.
TIME-SECS ×1.0

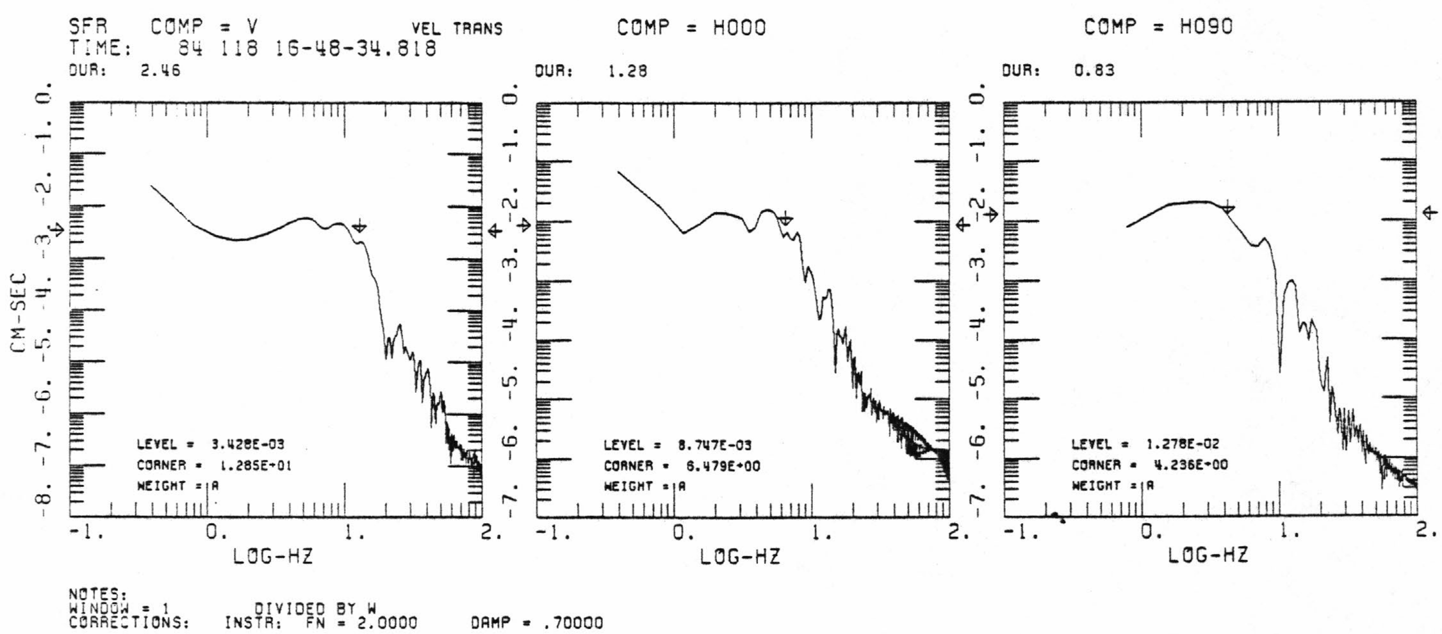
SFR COMP = V VEL TRANS
TIME: 84 118 16-48-34.818
DUR: 2.46
LEVEL = 3.428E-03
CORNER = 1.285E+01
WEIGHT = A
COMP = H000
DUR: 1.28
LEVEL = 8.747E-03
CORNER = 6.479E+00
WEIGHT = A
COMP = H090
DUR: 0.83
LEVEL = 1.278E-02
CORNER = 4.236E+00
WEIGHT = A
CM-SEC
LOG-HZ
NOTES:
WINDOW = 1 DIVIDED BY W
CORRECTIONS: INSTR: FN = 2.0000 DAMP = .70000

Figure 9.

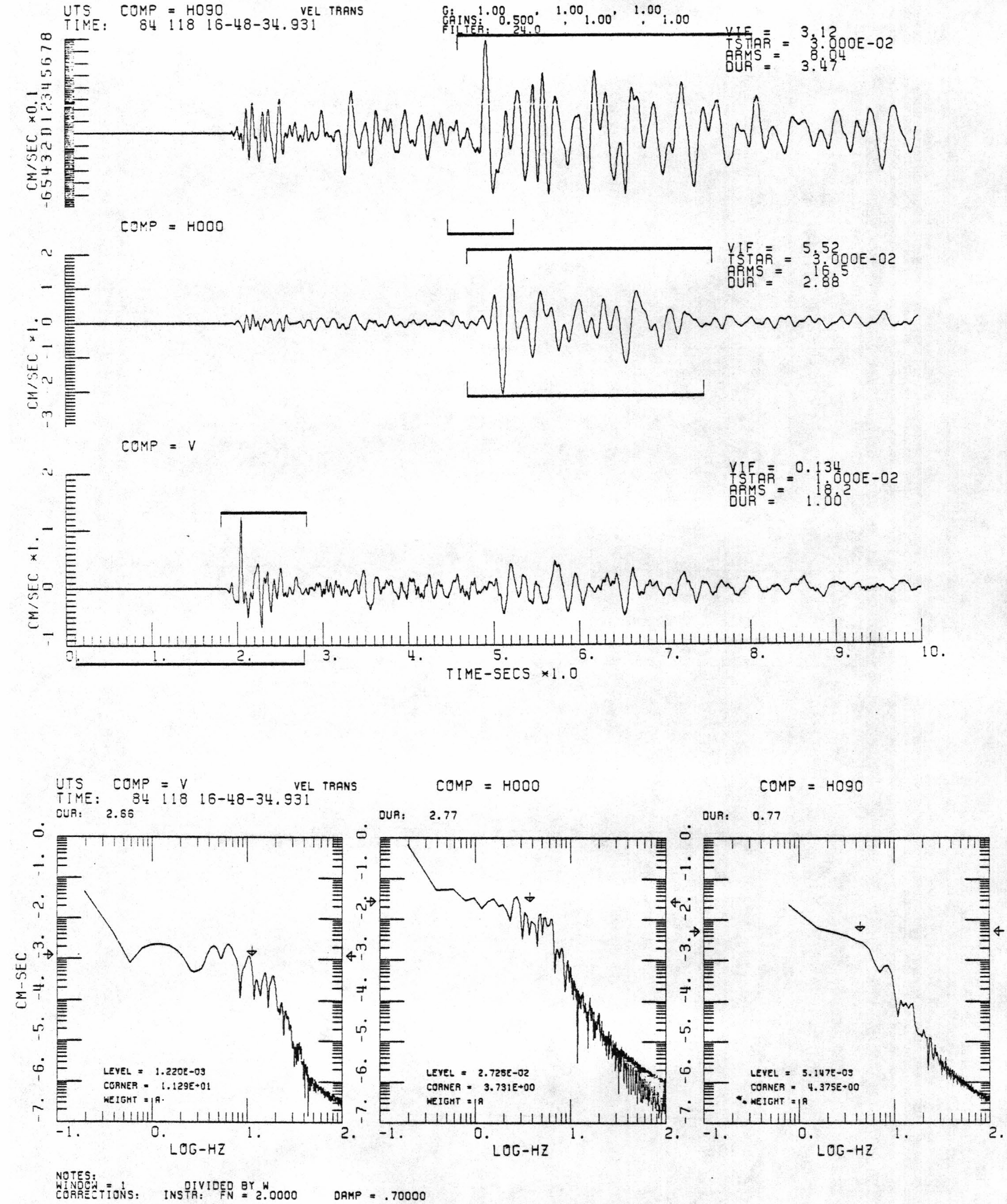

UTS COMP = H090 VEL TRANS
TIME: 84 118 16-48-34.931
G: 1.00 1.00 1.00
GAINS: 0.500 1.00 1.00
FILTER: 24.0
VIF = 3.12
TSTAR = 3.000E-02
ARMS = 8.04
DUR = 3.47
CM/SEC ×0.1
COMP = H000
VIF = 5.52
TSTAR = 3.000E-02
ARMS = 16.5
DUR = 2.88
CM/SEC ×1.
COMP = V
VIF = 0.134
TSTAR = 1.000E-02
ARMS = 18.2
DUR = 1.00
CM/SEC ×1.
TIME-SECS ×1.0
UTS COMP = V VEL TRANS
TIME: 84 118 16-48-34.931
DUR: 2.66
LEVEL = 1.220E-03
CORNER = 1.129E+01
WEIGHT = A
COMP = H000
DUR: 2.77
LEVEL = 2.726E-02
CORNER = 3.731E+00
WEIGHT = A
COMP = H090
DUR: 0.77
LEVEL = 5.147E-03
CORNER = 4.375E+00
WEIGHT = A
CM-SEC
LOG-HZ
NOTES:
WINDOW = 1 DIVIDED BY W
CORRECTIONS: INSTR: FN = 2.0000 DAMP = .70000

Figure 10.

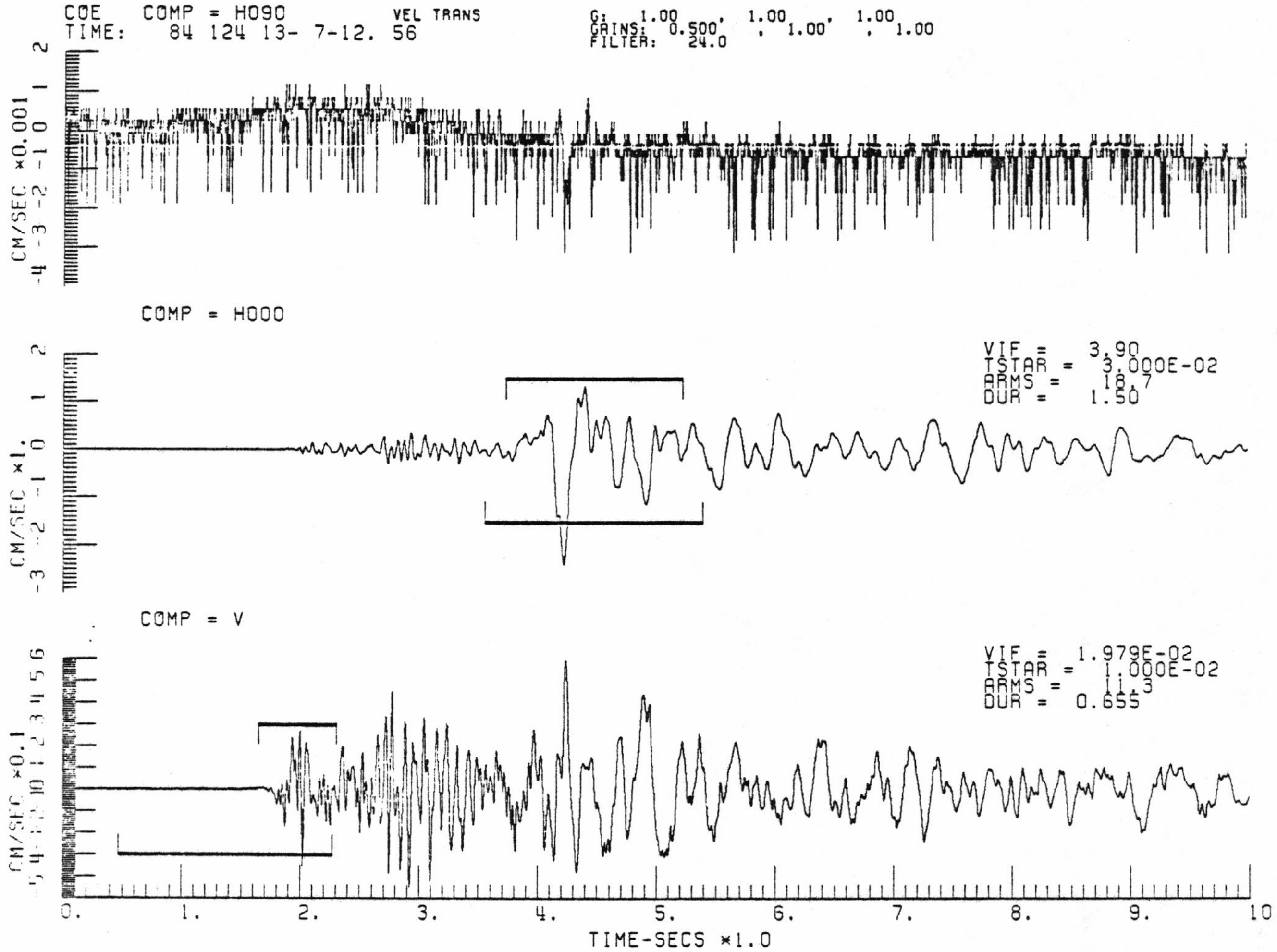

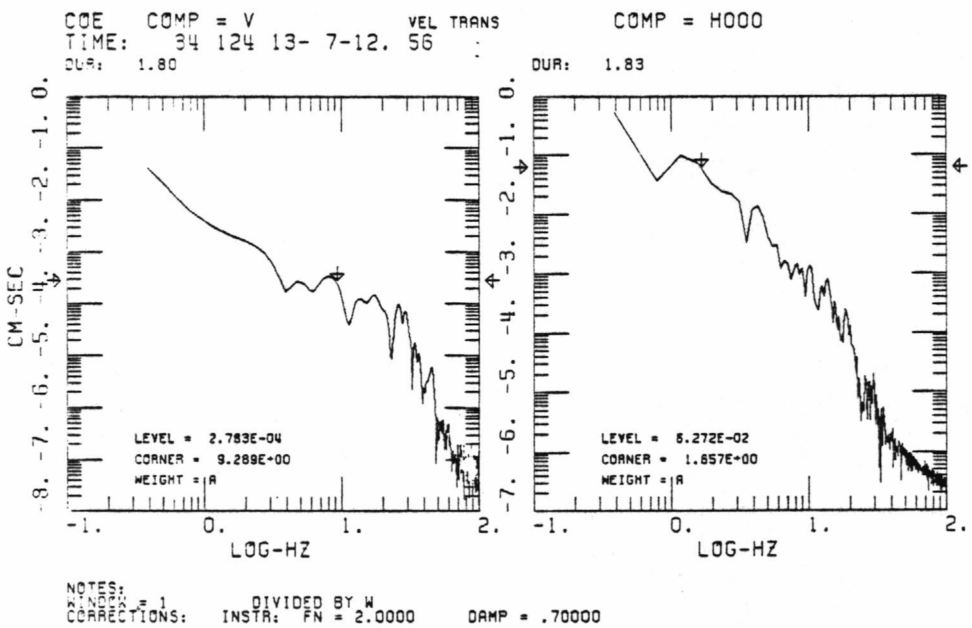

Figures 11-15. Event 1241307 particle velocities and spectra. Same description as for Figures 2-11, except that stations are COE, DFL, GRT, RBH, and UTS. Spectral parameters and derived source parameters are listed in Table 4.

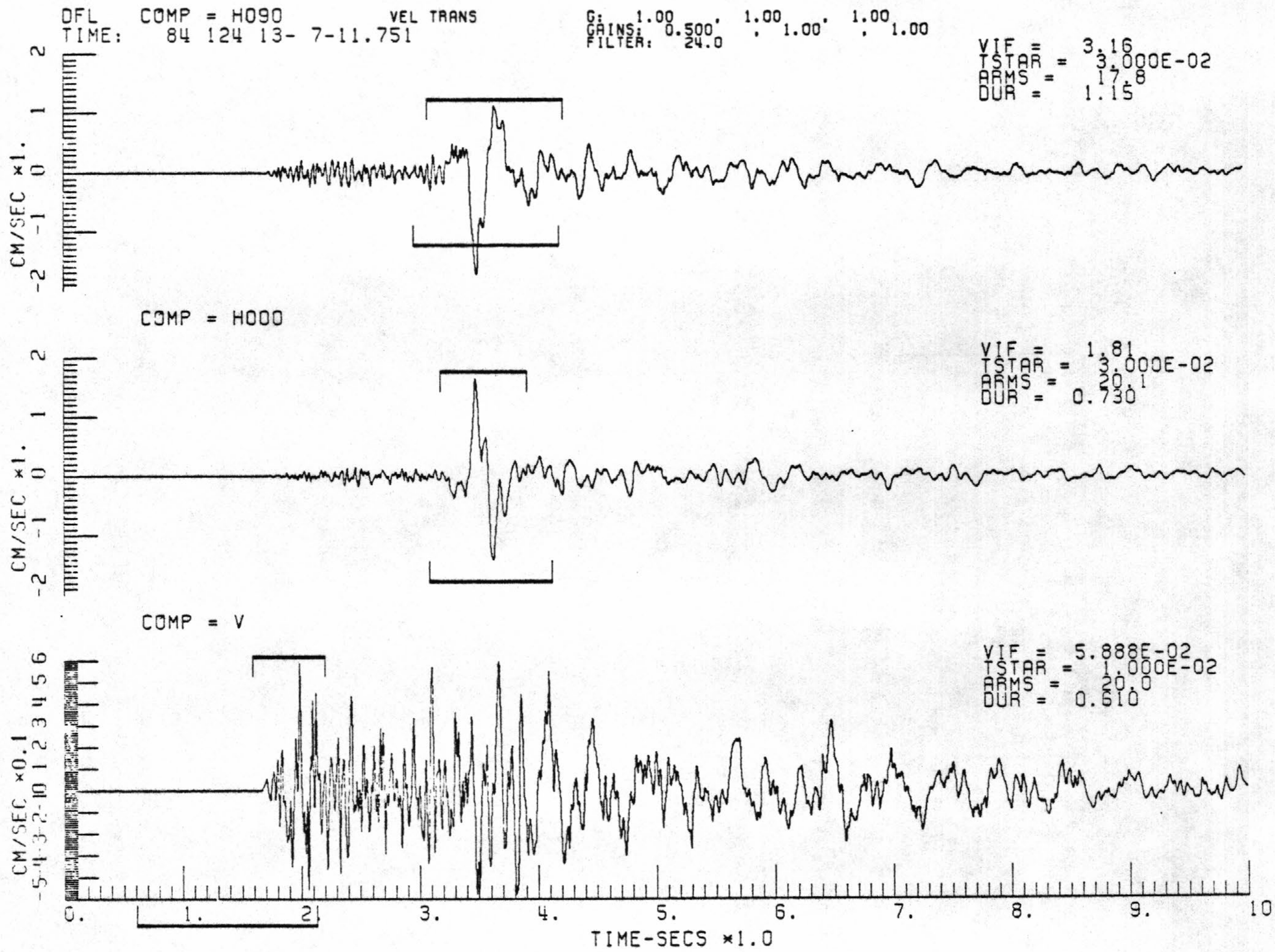
DFL COMP = H090 VEL TRANS
TIME: 84 124 13- 7-11.751
G: 1.00 , 1.00 , 1.00
GAINS: 0.500 , 1.00 , 1.00
FILTER: 24.0
VIF = 3.16
TSTAR = 3.000E-02
ARMS = 17.8
DUR = 1.15
CM/SEC ×1.
COMP = H000
VIF = 1.81
TSTAR = 3.000E-02
ARMS = 20.1
DUR = 0.730
COMP = V
VIF = 5.888E-02
TSTAR = 1.000E-02
ARMS = 20.0
DUR = 0.610
CM/SEC ×0.1
TIME-SECS ×1.0

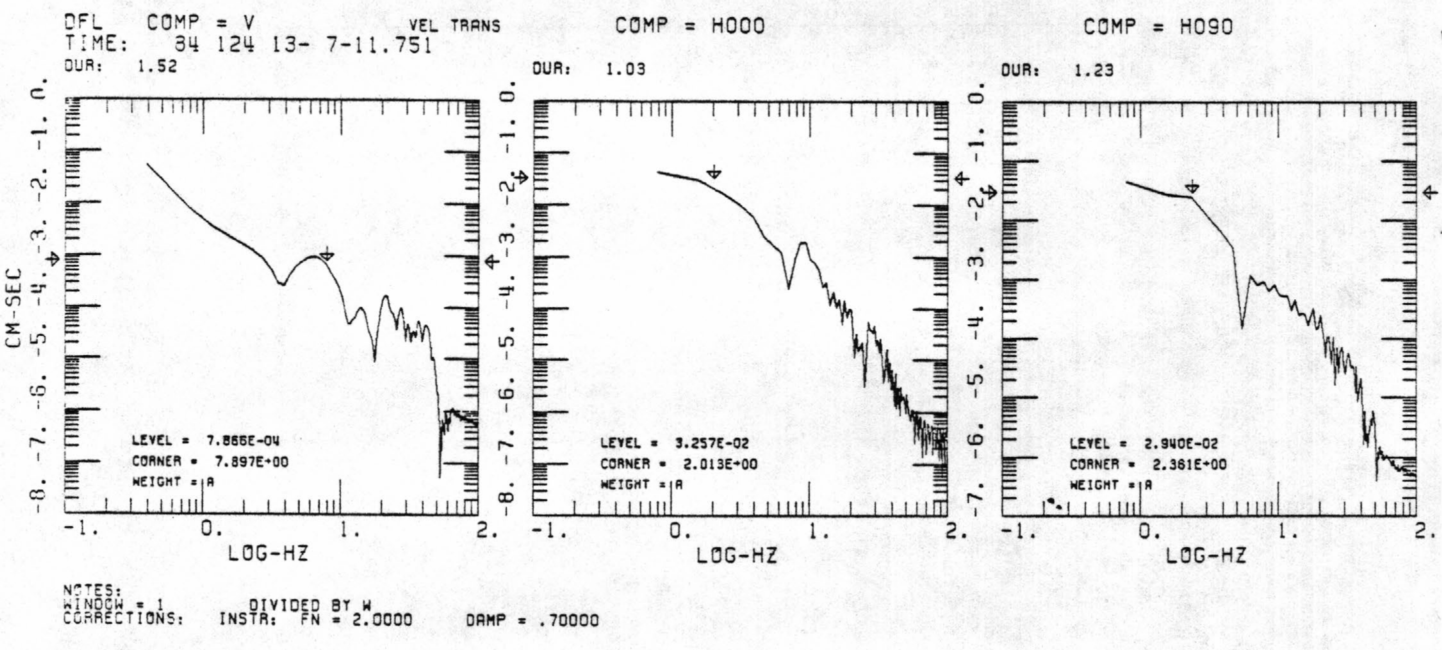
DFL COMP = V VEL TRANS
TIME: 84 124 13- 7-11.751
DUR: 1.52
COMP = H000
DUR: 1.03
COMP = H090
DUR: 1.23
CM-SEC
LEVEL = 7.866E-04
CORNER = 7.897E+00
WEIGHT = A
LEVEL = 3.257E-02
CORNER = 2.013E+00
WEIGHT = A
LEVEL = 2.940E-02
CORNER = 2.361E+00
WEIGHT = A
LOG-HZ
NOTES:
WINDOW = 1 DIVIDED BY W
CORRECTIONS: INSTR: FN = 2.0000 DAMP = .70000

Figure 12.

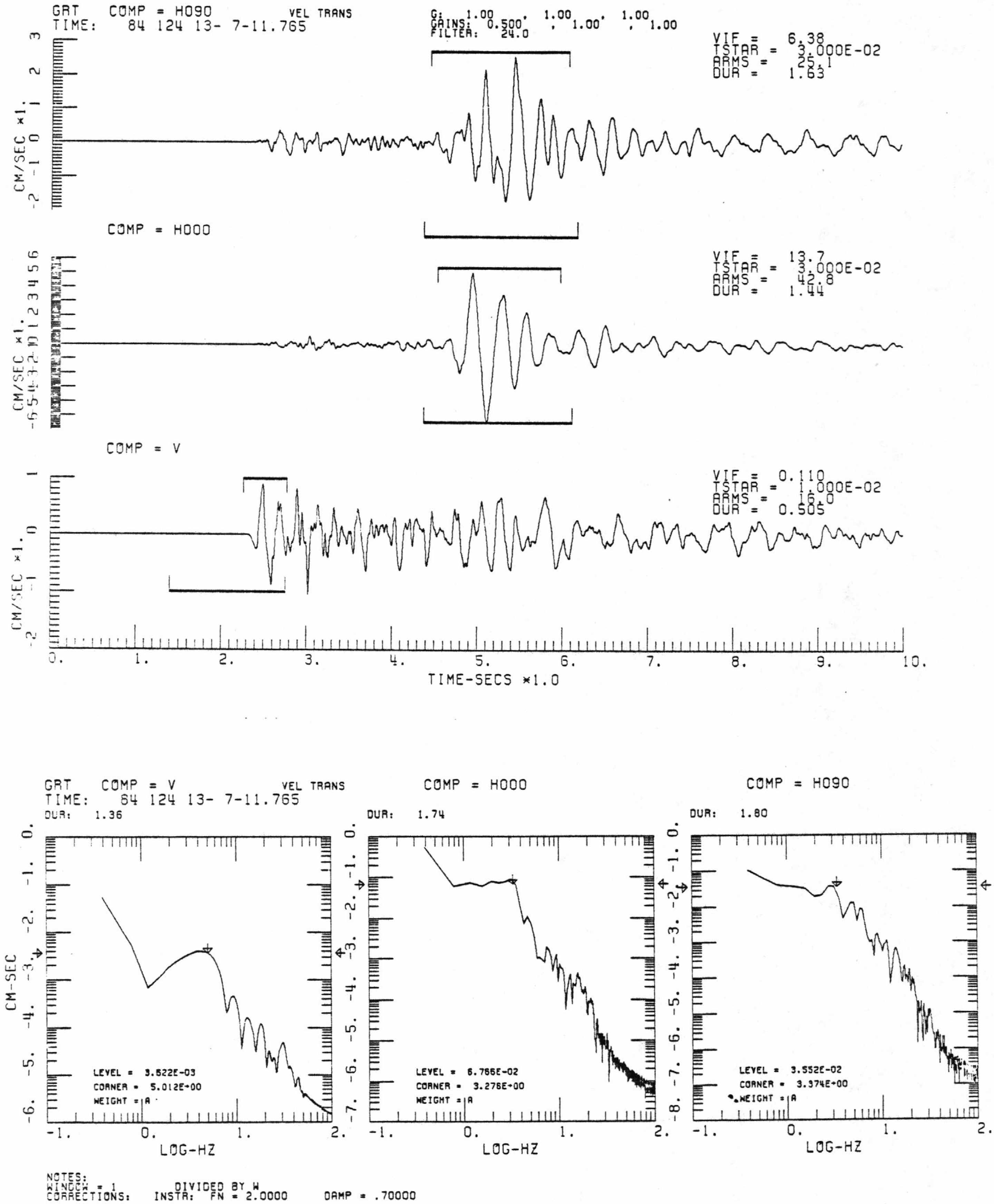
GRT COMP = H090 VEL TRANS
TIME: 84 124 13- 7-11.765
G: 1.00, 1.00, 1.00
GAINS: 0.500, 1.00, 1.00
FILTER: 24.0
VIF = 6.38
TSTAR = 3.000E-02
ARMS = 25.1
DUR = 1.63
CM/SEC ×1.
COMP = H000
VIF = 13.7
TSTAR = 3.000E-02
ARMS = 42.8
DUR = 1.44
COMP = V
VIF = 0.110
TSTAR = 1.000E-02
ARMS = 16.0
DUR = 0.505
TIME-SECS ×1.0
GRT COMP = V VEL TRANS
TIME: 84 124 13- 7-11.765
DUR: 1.36
CM-SEC
LEVEL = 3.622E-03
CORNER = 5.012E+00
WEIGHT = A
LOG-HZ
COMP = H000
DUR: 1.74
LEVEL = 6.766E-02
CORNER = 3.276E+00
WEIGHT = A
LOG-HZ
COMP = H090
DUR: 1.80
LEVEL = 3.552E-02
CORNER = 3.374E+00
WEIGHT = A
LOG-HZ
NOTES:
WINDOW = 1 DIVIDED BY W
CORRECTIONS: INSTR: FN = 2.0000 DAMP = .70000

Figure 13.

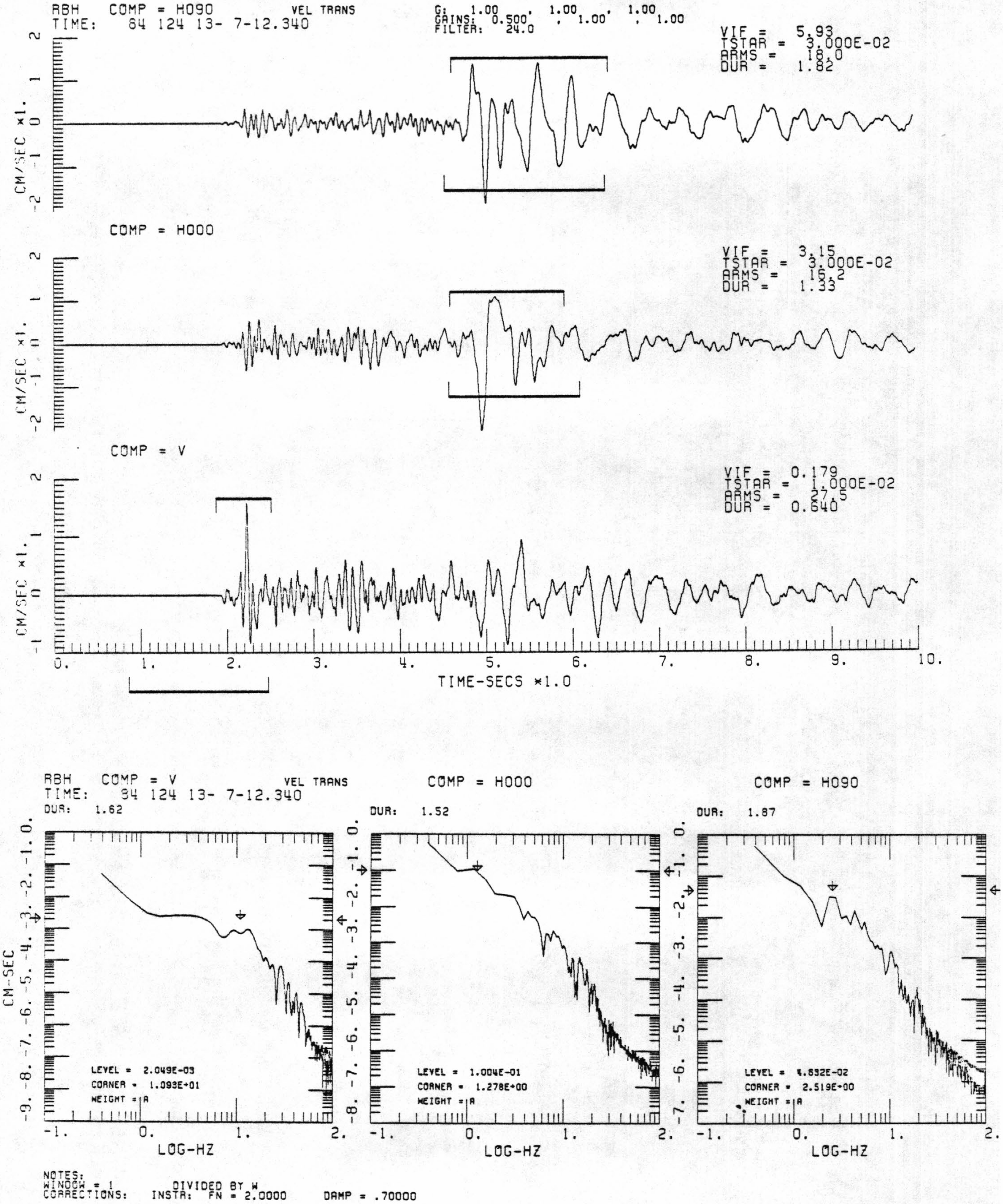
RBH COMP = H090 VEL TRANS
TIME: 84 124 13- 7-12.340
G: 1.00 , 1.00 , 1.00
GAINS: 0.500 , 1.00 , 1.00
FILTER: 24.0
VIF = 5.93
TSTAR = 3.000E-02
ARMS = 18.0
DUR = 1.82
COMP = H000
VIF = 3.15
TSTAR = 3.000E-02
ARMS = 16.2
DUR = 1.33
COMP = V
VIF = 0.179
TSTAR = 1.000E-02
ARMS = 27.5
DUR = 0.640
CM/SEC ×1.
TIME-SECS ×1.0
RBH COMP = V VEL TRANS
TIME: 84 124 13- 7-12.340
DUR: 1.62
LEVEL = 2.049E-03
CORNER = 1.093E+01
WEIGHT = A
COMP = H000
DUR: 1.52
LEVEL = 1.004E-01
CORNER = 1.278E+00
WEIGHT = A
COMP = H090
DUR: 1.87
LEVEL = 4.632E-02
CORNER = 2.519E+00
WEIGHT = A
CM-SEC
LOG-HZ
NOTES:
WINDOW = 1 DIVIDED BY W
CORRECTIONS: INSTR: FN = 2.0000 DAMP = .70000

Figure 14.

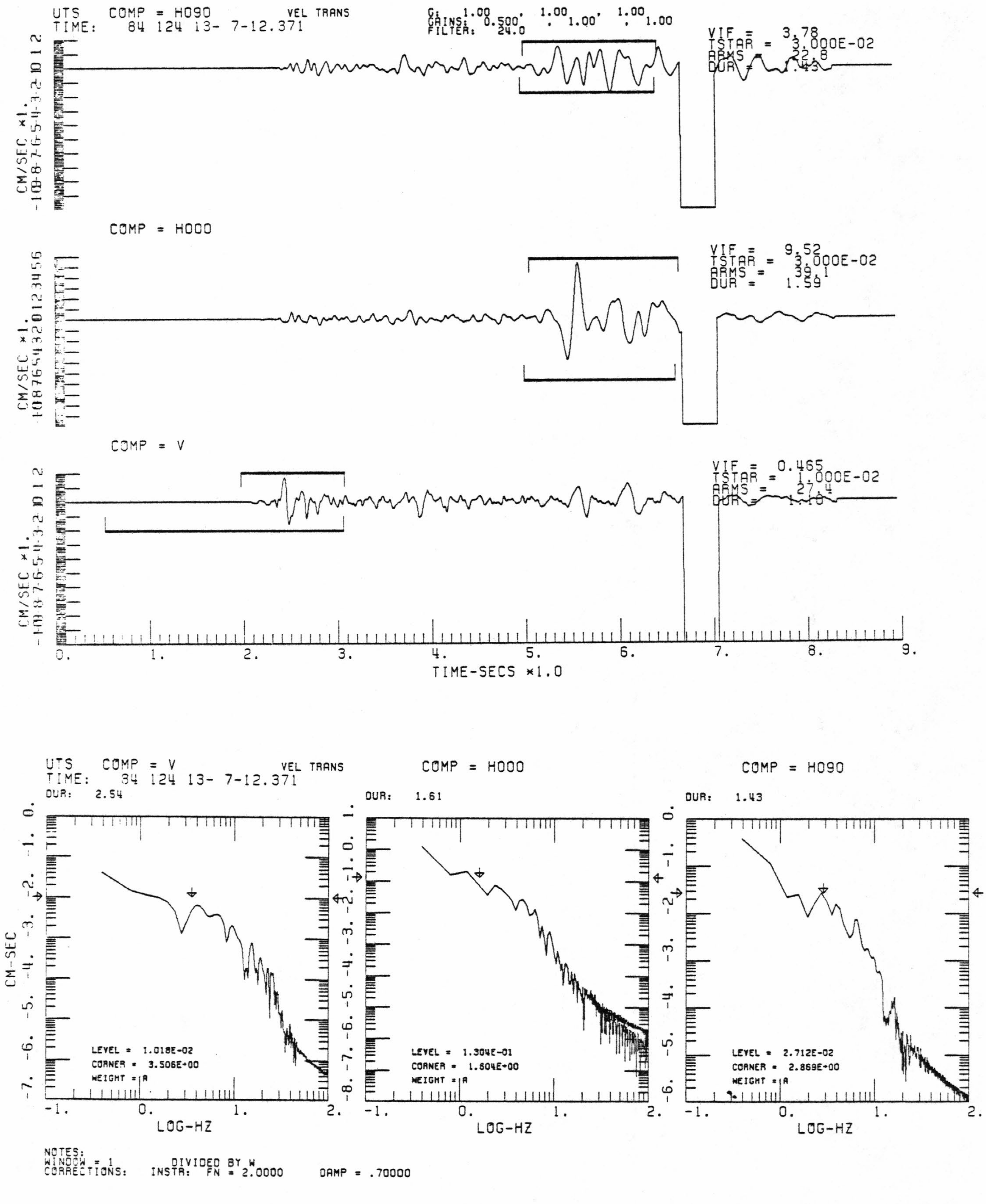
UTS COMP = H090 VEL TRANS
TIME: 84 124 13- 7-12.371
G: 1.00, 1.00, 1.00
GAINS: 0.500, 1.00, 1.00
FILTER: 24.0
VIF = 3.78
TSTAR = 3.000E-02
ARMS = 22.8
DUR = 1.43
COMP = H000
VIF = 9.52
TSTAR = 3.000E-02
ARMS = 39.1
DUR = 1.59
COMP = V
VIF = 0.465
TSTAR = 1.000E-02
ARMS = 27.4
CM/SEC ×1.
TIME-SECS ×1.0
UTS COMP = V VEL TRANS
TIME: 84 124 13- 7-12.371
DUR: 2.54
COMP = H000
DUR: 1.61
COMP = H090
DUR: 1.43
CM-SEC
LOG-HZ
LEVEL = 1.018E-02
CORNER = 3.506E+00
WEIGHT = A
LEVEL = 1.304E-01
CORNER = 1.604E+00
WEIGHT = A
LEVEL = 2.712E-02
CORNER = 2.869E+00
WEIGHT = A
NOTES:
WINDOW = 1 DIVIDED BY W
CORRECTIONS: INSTR: FN = 2.0000 DAMP = .70000

Figure 15.

Table 3

Source Parameters for Event 1181648

Station	R km	Z $\log X_0(p)$ cm-s	H000 $\log X_0(s)$ cm-s	H090 $\log X_0(s)$ cm-s	H avg $\log X_0(s)$ cm-s	Z f_c (p) Hz	H000 f_c (s) Hz	H090 f_c (s) Hz	H avg f_c (s) Hz	Z $\log M_0$ (p) dyne-cm x 10^{21}	H avg $\log M_0$ (s) dyn-cm x 10^{21}	Z r(p) km	H avg r(s) km
COE	10.3	-4.00	-2.092	-2.174	-2.133	15.1	3.5	3.3	3.4	20.770	21.903	.14	.42
DFL	10.2	-4.081	-2.432	-2.292	-2.362	26.3	6.1	5.1	5.6	20.688	21.670	.08	.22
GRT	13.3	-3.208	-2.027	-2.229	-2.128	7.9	4.2	5.9	5.0	21.673	22.019	.27	.24
PHR	11.6	-3.553	-1.770	-2.167	-1.969	8.7	2.3	4.0	3.1	21.269	22.118	.25	.39
RBH	11.8	-3.523	-1.824	-1.886	-1.855	12.0	2.4	3.1	2.7	21.306	22.240	.18	.45
RST	11.4	-3.377	-2.125	-2.277	-2.201	14.6	8.7	9.5	9.1	21.437	21.879	.15	.13
SFR	13.0	-2.469	-2.770	-1.886	-2.328	12.8	6.5	4.2	5.4	22.402	21.809	.17	.23
UTS	12.6	-2.921	-1.569	-2.292	-1.931	11.3	3.7	4.4	4.0	21.937	22.192	.19	.31
AMS	16.8	-3.143	-2.092	-2.092	-2.092	8.7	3.6	3.5	3.5	21.840	22.156	.25	.35
			<-2.111> ± .172					<4.6> ± 2.0		<21.480>	<21.998>	<.19>	<.30>
										± .552	± .194	± .06	± .11

Table 4

Source Parameters for Event 1241307

Station	R km	Z log $X_o(p)$ cm-s	H000 log $X_o(s)$ cm-s	H090 log $X_o(s)$ cm-s	H avg log $X_o(s)$ cm-s	Z $f_c(p)$ Hz	H000 $f_c(s)$ Hz	H090 $f_c(s)$ Hz	H avg $f_c(s)$ Hz	Z log $M_o(p)$ dyn-cm	H avg log M_o (s) dyn-cm	Z r(p) km	H avg r(s) km
COE	10.1	-3.553	-1.201	--	-1.201	9.3	1.6	--	1.6	21.208	22.826	.23	.76
DFL	10.2	-3.102	-1.481	1.538	-1.510	7.9	2.0	2.4	2.2	21.664	22.522	.27	.56
GRT	14.0	-2.444	-1.167	-1.444	-1.306	5.0	3.3	3.4	3.3	22.459	22.717	.43	.37
RBH	12.7	-2.699	-1.000	-1.337	-1.169	11.0	1.3	2.5	1.9	22.162	22.958	.20	.64
UTS	14.3	-2.000	-.886	-1.569	-1.227	3.5	1.6	2.9	2.3	22.912	22.951	.61	.53
											<22.081>	<22.795>	<.35>
<.57>													
											± .666	± .182	± .17
± .14													

PRESEISMIC AND COSEISMIC DEFORMATION ASSOCIATED WITH THE 1984 MORGAN HILL, CALIFORNIA, EARTHQUAKE

William H. Prescott, Nancy E. King, and Gu Guohua

U.S. Geological Survey
345 Middlefield Road, MS/977
Menlo Park, California 94025

ABSTRACT

The Morgan Hill earthquake of 24 April 1984 occurred in the middle of net-work of geodetic lines. Lines within 5 km of the epicenter were measured 2 weeks, 8 days and 1 day prior to the earthquake. None of the preearthquake measurements is unusual. Dislocation modeling of the rupture surface suggests that less than 70 mm of preseismic slip could have occurred on the rupture surface prior to the earthquake. A small aperture geodetic network located 5 km northwest of the epicenter was observed 2 weeks prior to the event. It indicated no detectable preseismic surface slip had occurred. The geodetic data suggest that the event involved about 420 mm of slip on a surface defined by the aftershocks producing a moment of 1.9 x 10^{25} dyne-cm. Slip on the fault near the surface in Hall's Valley during the event was at most about 8 mm and may have been zero. As of the first week in June postseismic slip has amounted to about half of the coseismic slip.

INTRODUCTION

The Hall's Valley earthquake of 24 April 1984 occurred in the middle of a dense frequently monitored geodetic network. The NW end of the aftershock was located 5 km from one station of a large scale geodetic network (average line lengths of greater than 20 km) and also less than 5 km from a small aperture geodetic network (typical line lengths of about 5 km). All of these lines had been measured many times prior to the earthquake. One of the longer lines to the station nearest the epicenter is part of an experiment specifically designed to search for precursors prior to earthquakes. It has been measured monthly for several years. This line was measured 8 days prior to the earthquake and again on the day preceding the earthquake. The small aperture network had been measured just two weeks prior to the event. Consequently this earthquake, a magnitude 6.2 event (Eaton, pers. comm.), provided a unique opportunity to look for evidence of preseismic slip or other geodetic anomalies. In addition all of these lines have been remeasured since the earthquake, and place constraints on the coseismic slip. All distances were measured either with a geodolite using techniques described by Savage and Prescott (1973) or with an HP 3800 series instrument using techniques described by Lisowski and Prescott (1980).

PRESEISMIC DATA

The earthquake epicenter is located about 20 km east of San Jose, California (Figure 1) in Hall's Valley at the foot of Mt. Hamilton. Mt. Hamilton is one of four stations in a network that the U.S. Geological Survey has measured nearly every month since September 1981. Prior to the earthquake none of the lines had shown any unusual variation in length. In particular, the observations made during the months, weeks, and days prior to the earthquake do not stand out at all. The most interesting line is the line from Loma Prieta to Mt. Hamilton. This line was measured 8 days before the earthquake and again on the day preceding the earthquake (Figure 2). These two measurements are within 1.7 and 3.9 mm respectively of the average of the previous four measurements (all those made this year). Since the standard deviation of a single measurement of this line is 7 mm, it is clear that these measurements were not in any way anomalous. The Loma Prieta to Mt. Hamilton line crosses the Calaveras fault at an angle of 65°. Such a high angle is less than ideal for detecting strike slip movement on the Calaveras fault, but it does have the advantage of also being somewhat sensitive to motion normal to the fault. Thus, if a precursory episode of either right-lateral strike slip or of normal dilatation (dilantancy) occurred more than 24 hours prior to the earthquake, and if it was of sufficient magnitude, it would have been detected. The qualification, "of sufficient magnitude", is an important one. The question of how large a precursory slip event could have occurred without producing a detectable change in the line Loma Prieta to Mt. Hamilton is best answered in the context of the models for the coseismic slip, and will be covered in the discussion at the end.

The only other line with a long history of frequent observations, that has any bearing on this earthquake is the line Loma Prieta to Allison (Figure 1). This line has also been measured monthly since 1981, however, it was not measured in the week prior to the earthquake. Station Allison is located between the Calaveras and Hayward faults and is more distant from the epicenter of the Hall's Valley earthquake than Mt. Hamilton. No significant changes in the line length were observed prior to the earthquake.

The Grant Ranch network is a collection of short lines located in Hall's Valley (Figure 1). This network has been surveyed occasionally since 1977. In the interests of brevity, only the data for the fault crossing lines of the network are shown in Figure 3. Changes in the length of the lines Barn to Halls and Halls to Pueblo, suggest that some surface fault slip (creep) has been occurring on the northeastern side of the network. The line Barn to Yerba is more ambiguous, but may indicate that additional slip is occurring along the fault strand southeast of station Barn. Assuming rigid block motion the average slip rate across the network over the 7 years of observation has been 10.2 ± 0.9 mm/a. The last survey prior to the earthquake was made 2 weeks before the event. There is no evidence of any unusual change in the lengths of these lines prior to the earthquake. The length of the lines and the location of the stations are such that the net is only affected by fault slip occurring at the surface, whereas the longer lines are also sensitive to slip at depth.

COSEISMIC DATA

Since the earthquake, all of the lines in the area have been reobserved. Some of the Grant Ranch lines were remeasured on the afternoon of the earthquake. The rest of the Grant Ranch network was measured on the 25th of May and a few lines were repeated on the 26th. The line Hamilton to Loma Prieta was observed on both the 25th and 26th. The line Hamilton to Llagas was observed on both the 26th and 27th. The remaining lines have each been measured once since the earthquake (Figure 4). The observed changes are summarized in the Table 1. For lines that had been measured within a month prior to the earthquake, the 'before' length is the last measurement prior to the earthquake. For lines measured earlier the 'before' length was calculated by extrapolating a least-square-linear-fit forward to 24 April 1984 the day of the Morgan Hill earthquake. The 'after' length is the mean of all the measurements made after the earthquake. There are significant changes in many of the lines in the area, but most of the changes are modest; the largest is 56 mm.

The observed changes in the lengths of these lines place constraints on the amount of slip that occurred during the main shock. In modeling these changes we assumed that the rupture plane of the mainshock was defined by the distribution of aftershocks. Aftershocks during the week following the event defined a surface extending southeast from the main shock hypocenter for about 25 km; the aftershocks were distributed between 4 and 10 km (Cockerham, pers. comm.). Following the formulation of Chinnery (1961) we assumed a uniform dislocation on a rectangular, vertical strike slip fault surface embedded in an infinite elastic half space. Using a least-squares process the amount of slip that best fit the observed coseismic line length changes was determined to be 420 ± 40 mm. Although the slip appears very well determined, it should be recognized that the error estimate is conditioned on the assumption that there is no uncertainty in the dislocation geometry. Altering the geometry produces changes much greater than might be suggested by the 40 mm uncertainty quoted above. In general the solution was insensitive to the length of the dislocation as long as the northwest end was fixed at the main shock hypocenter. Decreasing the depth, while maintaining a constant dislocation width, caused the estimated slip to decrease by about 140 mm per km of decrease in depth. The geodetic data are not adequate to constrain the geometry of the slip surface by themselves. In part this is due to an inherent difficulty in placing constraints on slip at depth from measurements made at the surface, and in part, the difficulty stems from the small size of the observed changes. The line length changes imply a geodetic moment of 1.9×10^{25} dyne-cm. For comparison the Coyote Lake earthquake of 1979, that occurred on the next section to the southeast had a geodetic moment of 1.6×10^{25} dyne-cm (King and others, 1981).

Coseismic changes in the Grant Ranch network were very small. There was no change in the Barn to Halls line, indicating that no slip occurred at the surface on the northeastern side of the network. The two lines crossing the southwestern side at low angle changed slightly, -8 mm and +5 mm. These changes were in a direction consistent with right-lateral slip, but are only marginally above even a one sigma noise level. If coseismic slip occurred at the surface in Hall's Valley, it was at most about 8.5 mm, and occurred on the southwest side of station Barn. In contrast the slip during the 7 years preceding the earthquake appears to be concentrated on the northeast side of station Barn. The absence of coseismic slip at Grant Ranch is consistent with the observations that Grant Ranch is located slightly northwest of the epicenter of the main shock, that the rupture appears to have propagated to the southeast, and that no evidence of surface rupture has been detected anywhere along the aftershock zone.

DISCUSSION

One question of interest is how large a precursory slip event could have occurred and where could it have occurred without producing a detectable line length anomally. Although the line Hamilton to Llagas is most ideally situated for detecting slip on the coseismic rupture surface, it had not been surveyed during the two months preceding the earthquake. Data for the line Hamilton to Loma Prieta gives us much better temporal resolution at the expense of spatial resolution. The calculated slip listed in the next to the last column of Table 1 allows us to calculate how much slip could have occurred prior to the event without causing a detectable change in the length of the line Hamilton to Loma Prieta. The dislocation model indicates that 420 mm of slip on the aftershock surface would produce a 30 mm change in the length of the line Hamilton to Loma Prieta (Table 1). Both measurements before the earthquake were within 5 mm of the mean of the preceding measurements. 5 mm change in the line Hamilton to Loma Prieta would be produced by only 70 mm of fault slip on the rupture plane. We conclude that if any anomaly occurred it had to have a magnitude of less than 70 mm. This argument assumes that the precursory slip, if any, occurred on the same plane as the 24 April earthquake. Other scenarios are possible. Since the epicenter was located at the northwestern end of the aftershock zone, it is conceivable that precursory slip might occur along the section of the Calaveras fault located to the northwest of the aftershock zone (Figure 1). Because Hamilton is located so close to the end of the aftershock zone, the Hamilton to Loma Prieta line would be nearly as sensitive to slip on this fault section as it is to slip on the aftershock zone. Thus again an upper limit to the size of a possible undetected precursory slip event is about 70 mm. In fact precursory slip on the next section to the northwest is even less likely since another of the monitor lines from Loma Prieta, to Allison, would be expected to be sensitive to slip along that section. This line was measured one month before the earthquake. We conclude that if any buried preslip occurred it must of been of less than 70 mm. Or it must have involved a portion of the fault surface smaller than the aftershock surface. To be detectable in amounts as small as 70 mm, the preslip would have to involve a substantial portion of the fault plane. One could justifiably argue that much greater amounts of slip could have occurred on much smaller portions of the fault surface without being detected.

The small aperture network located in Hall's Valley places a further constraint on the possible occurrence of slip prior to this earthquake. The Grant Ranch network is located within 5 km of the epicenter and was measured 2 weeks before the event. No anomalous deformation was observed. This network is insenitive to slip at depth because of its small scale, but it is quite sensitive to surface slip. The observations tell us that no significant amount of accelerated creep preceded the earthquake; at least not NW the epicenter, not 2 weeks before the earthquake, and not exceeding about 20 mm.

As of early June 1984 postseismic slip following the earthquake has amounted to about 50% of the coseismic slip. If the earthquake follows the pattern of the 1979 Coyote Lake event (Reasenberg and Ellsworth, 1982) we can expect that in the next few months additional slip will occur. During the Coyote Lake earthquake, the coseismic slip was similarly small, but postseismic slip amounting to nearly 100 mm occurred in the 4 months following the earthquake (Lisowski and King, unpub. ms.).

ACKNOWLEDGEMENTS

This paper has benefitted from the comments of P. Segall and A. Lindh.

Table 1. Change in line lengths at the time of the Hall's Valley Earth-quake. For lines that were measured more than a month prior to the earthquake, the before length is calculated by extrapolating the earlier observa-tions to the time of the earthquake.

Station Names		Before (M)	After (M)	Diff. (mm)	Model (mm)	Std. Dev. (mm)
Allison	Hamilton	26696.0857	.0995	14.2	19.6	6.1
Allison	Loma Prieta	43129.1733	.1896	16.3	-4.9	9.1
American	Hamilton	20649.1734	.1845	11.1	2.8	5.1
Gilroy	Llagas	17601.1574	.1476	-9.8	11.4	4.6
Hamilton	Llagas	23178.1347	.0788	-55.9	-58.5	5.5
Hamilton	Loma Prieta	31227.9758	.9501	-25.7	-31.3	6.9
Hamilton	Sheep	27435.0842	.0610	-23.2	-20.3	6.2
Hamilton	Mt. Stake	20897.4510	.4526	1.6	6.2	5.1
Hamilton	Mocho	16914.6944	.7146	20.2	16.0	4.5
Hamilton	Mt. Oso	30082.4161	.4422	26.1	18.1	6.7
Hamilton	Rose	20143.6586	.6847	26.1	22.0	5.0
Llagas	Loma Prieta	15940.5697	.5929	23.2	4.2	4.4
Llagas	Sheep	13539.0145	.0411	26.6	19.1	4.0

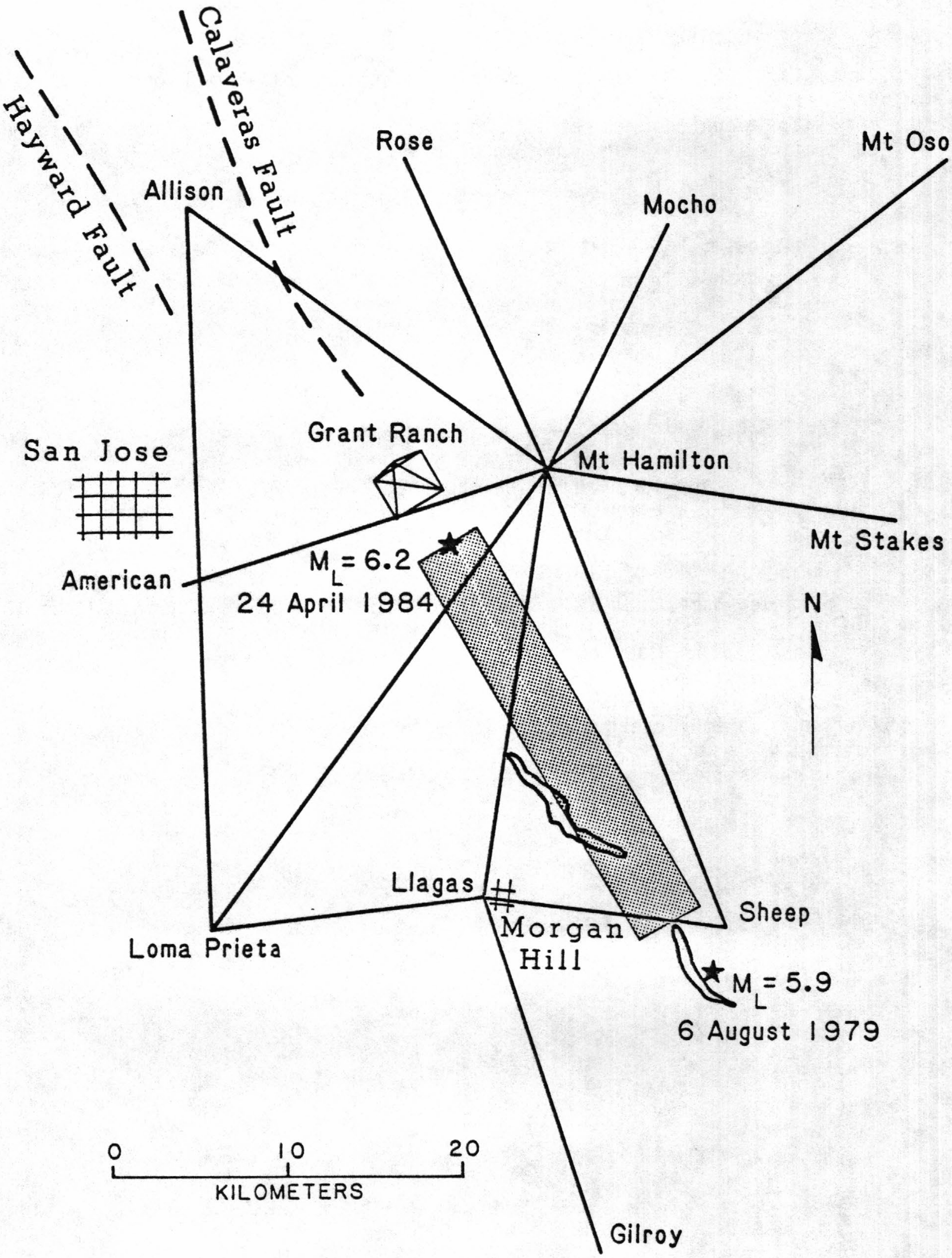

Figure 1. Map of the area covered by the geodetic network. Box contains aftershocks located during the first week following the earthquake (Cockerham, pers. comm.).

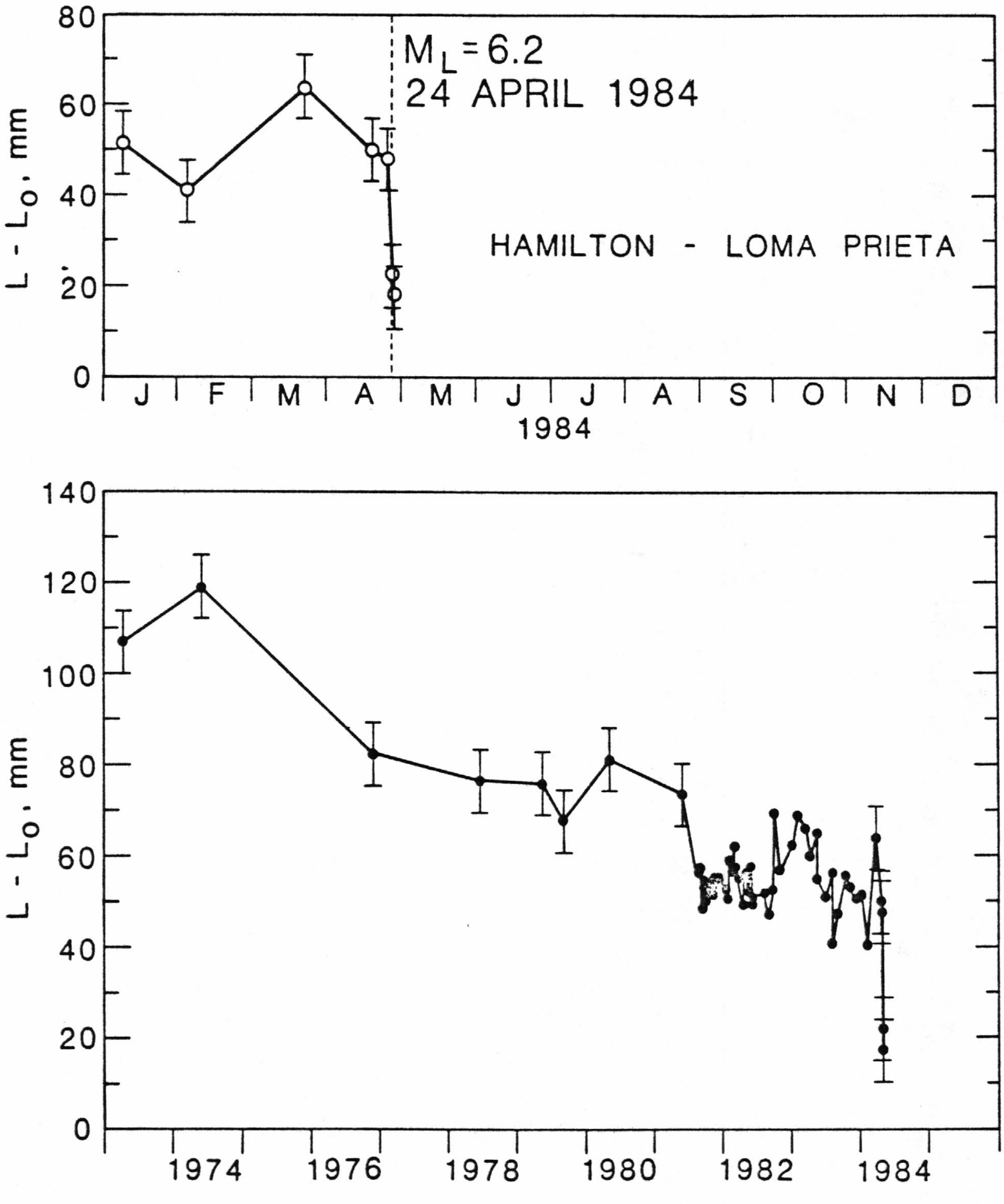

Figure 2. Plot of the length of the line Hamilton to Loma Prieta as a function of time. The last year's measurements are also shown on an expanded time scale. Error bars indicate plus and minus one standard deviation.

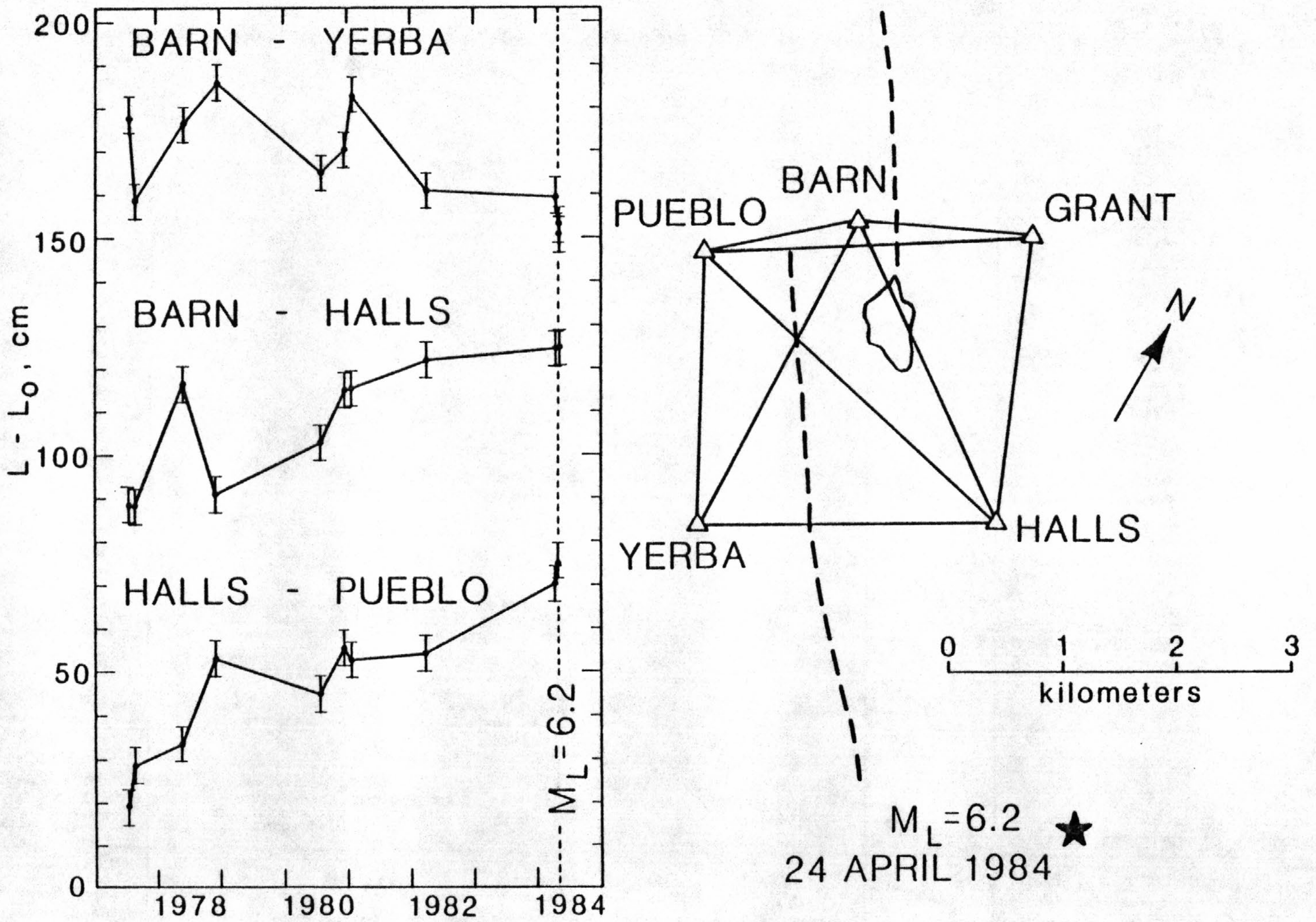

Figure 3. Plot of the length of low angle fault crossing lines in the Grant Ranch network. Error bars indicate plus and minus one standard deviation.

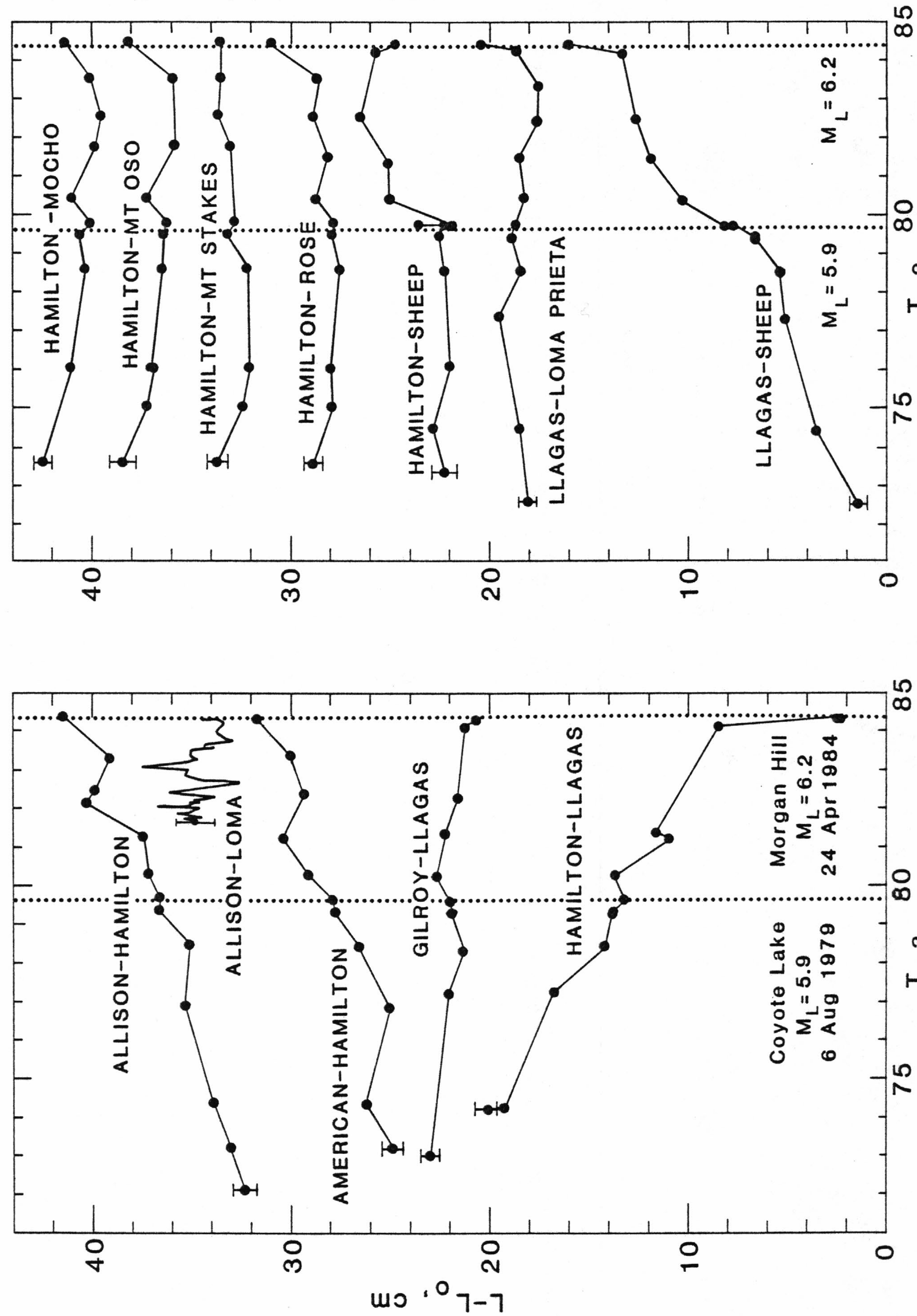

Figure 4. Plot of line length as a function of time. Error bars indicate plus and minus one standard deviation.

REFERENCES

Chinnery, M., 1961, Deformation of the ground around surface faults, *Bulletin, Seismological Society of America*, v. 51, p. 355-372.

King, N.E., J.C. Savage, M. Lisowski, and W.H. Prescott, 1981, Preseismic and coseismic deformation associated with the Coyote Lake, California earthquake, *Journal Geophysical Research*, v. 86, p. 892-898.

Lisowski, M. and W.H. Prescott, 1981, Short range distance measurements along the San Andreas fault system in California, 1975-1979, *Bulletin, Seismological Society of America*, v. 71(5), p. 1607-1624.

Prescott, W.H., M. Lisowski, and J.C. Savage, 1981, Geodetic measurements of crustal deformation on the San Andreas, Hayward and Calaveras Faults near San Francisco, California, *Journal Geophysical Research*, v. 86, p. 10853-10869.

Reasenberg, P. and W.L. Ellsworth, 1982, Aftershocks of the Coyote Lake, California, Earthquake of August 6, 1979: A detailed study, *Journal Geophysical Research*, v. 87, p. 10637-10655.

Savage, J.C. and W.H. Prescott, 1973, Precision of Geodolite distance measurements for determining fault movement, *Journal Geophysical Research*, v. 78, p. 6001-6008.

ALINEMENT ARRAY MEASUREMENT FOLLOWING THE 24 APRIL 1984 MORGAN HILL EARTHQUAKE

Beth D. Brown

U.S. Geological Survey
345 Middlefield Rd., ms-977
Menlo Park, California 94025

On April 24, 1984, the Morgan Hill earthquake (M_L = 6.2) occurred 22 km southeast of San Jose, California. Bakun et al. (1984) locate the epicenter 5 km westsouthwest of Mt. Hamilton on the Calaveras fault, with nearly all aftershocks located on a 26 km-long section southeast of the epicenter and concentrating near San Felipe Valley and Anderson Reservoir. On April 26, 1984, an alinement array, (San Felipe Ranch - SFR4) was installed in the San Felipe Valley 4 km south of the epicenter (see Figure 1 in Bakun et al., 1984) to measure any afterslip that might occur. The array spans both fault traces identified by Radbruch-Hall (1974) and D. G. Herd (unpublished map). The array location, at the north end of the San Felipe Valley, is shown on Figure 1 and is diagrammed on Figure 2. Slip along one or both traces would be reflected by a change in angle ϕ (see Figure 2), as determined by remeasurement of the targets. Calculation of slip follows the formula below:

$$s = \frac{(\tan\Delta)d}{h}$$

where s = slip
Δ = change in angle ϕ
d = distance from theodolite to end target
h = correction factor = cos (difference from 90° of the theodolite to end target trend and the fault trend)

The measurements primarily followed the surveying procedure as described by Burford and Harsh (1980) with additional techniques from Galehouse et al. (1982).

An initial measurement of the San Felipe Ranch array was completed on April 26, 1984. A remeasurement on April 28 indicated left-lateral movement of 1.81 ± 0.8 mm. Further remeasurements on May 3 and May 30 showed right-lateral movement of 0.5 ± 0.6 mm and 0.4 ± 1.0 mm respectively. Therefore, three remeasurements of the array indicate no appreciable movement in excess of our error limits. The San Felipe site will continue to be monitored. Additional deflection monuments will be installed to delineate the actual fault traces as soon as possible.

In conclusion, although the alinement array is located well within the aftershock zone, no evidence of afterslip associated with the Morgan Hill earthquake has been found as of the 30th of May within the zone covered by the San Felipe alinement array.

REFERENCES

Bakun, W. H., M. M. Clark, R. Cockerham, W. L. Ellsworth, A. G. Lindh, W. H. Prescott, A. F. Shakal, and P. Spudich, 1984, The 1984 Morgan Hill, California, earthquake: A Preliminary Report: in *U.S. Geological Survey Open-File Report 84-498*, p. 1-9.

Burford, R. O., and P. W. Harsh, 1980, Slip on the San Andreas fault in central California from alinement array surveys, *Bulletin Seismological Society of America*, v. 70, p. 1233-1261.

Galehouse, J. S., B. D. Brown, B. Pierce, and J. J. Thordsen, 1982, Changes in movement rates on certain East Bay faults: in Proceedings - Conference on Earthquake Hazards in the Eastern San Francisco Bay Area; Hart, E. W., Hirschfeld, S. E., and Schulz, S. S., editors; *Special Publication 62, Calif. Div. Mines and Geology*, p. 239-250.

Radbruch-Hall, D. H., 1974, Map showing recently active breaks along the Hayward fault zone and the southern part of the Calaveras fault zone, California: *U.S. Geological Survey Miscellaneous Investigation Series Map I-813*, 2 sheets, scale 1:24,000.

ACKNOWLEDGEMENTS

I would like to thank Brett Baker and Kate Breckenridge who assisted with the field measurements.

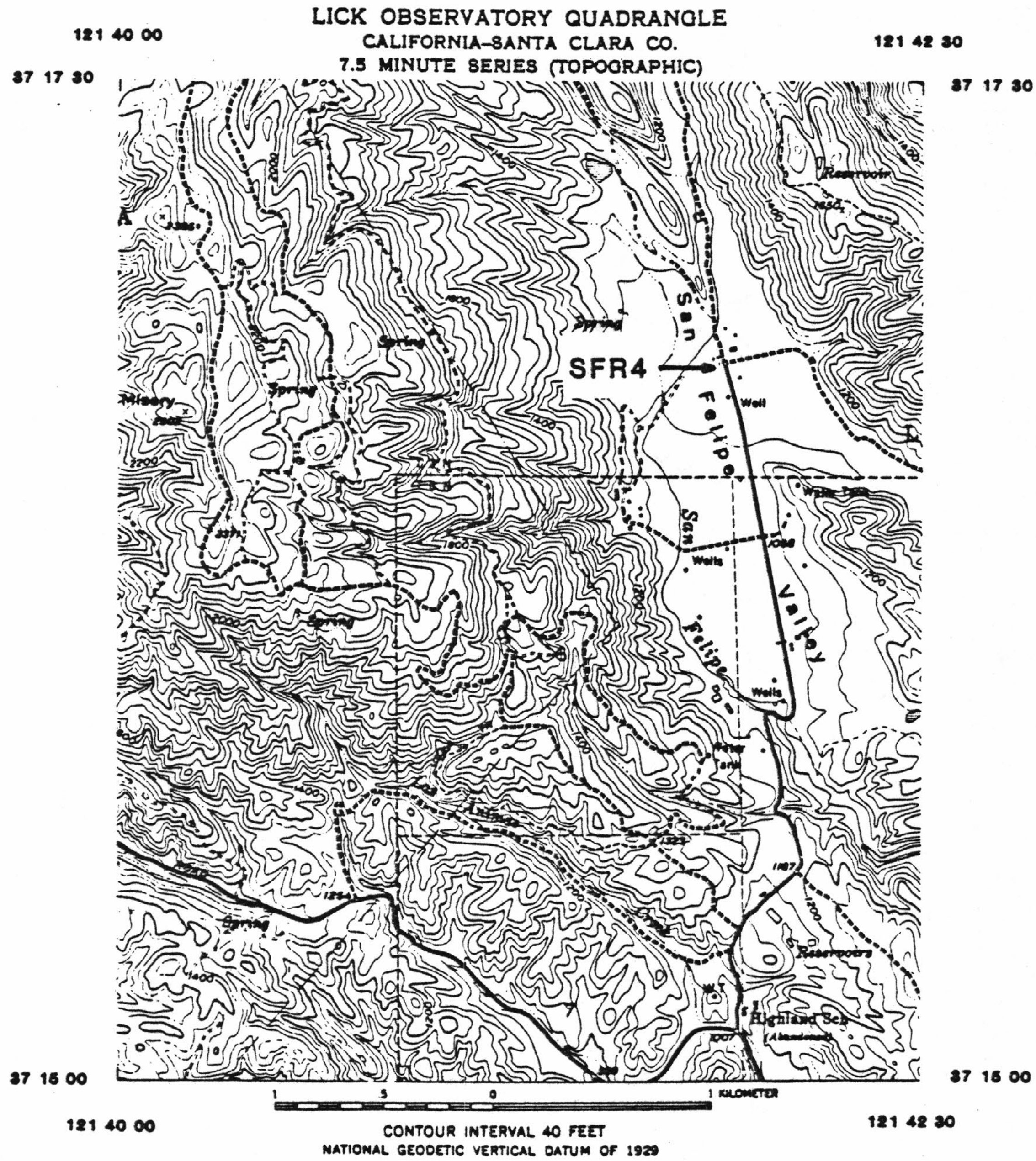

FIGURE 1. LOCATION MAP–USGS SAN FELIPE RANCH ALINEMENT ARRAY

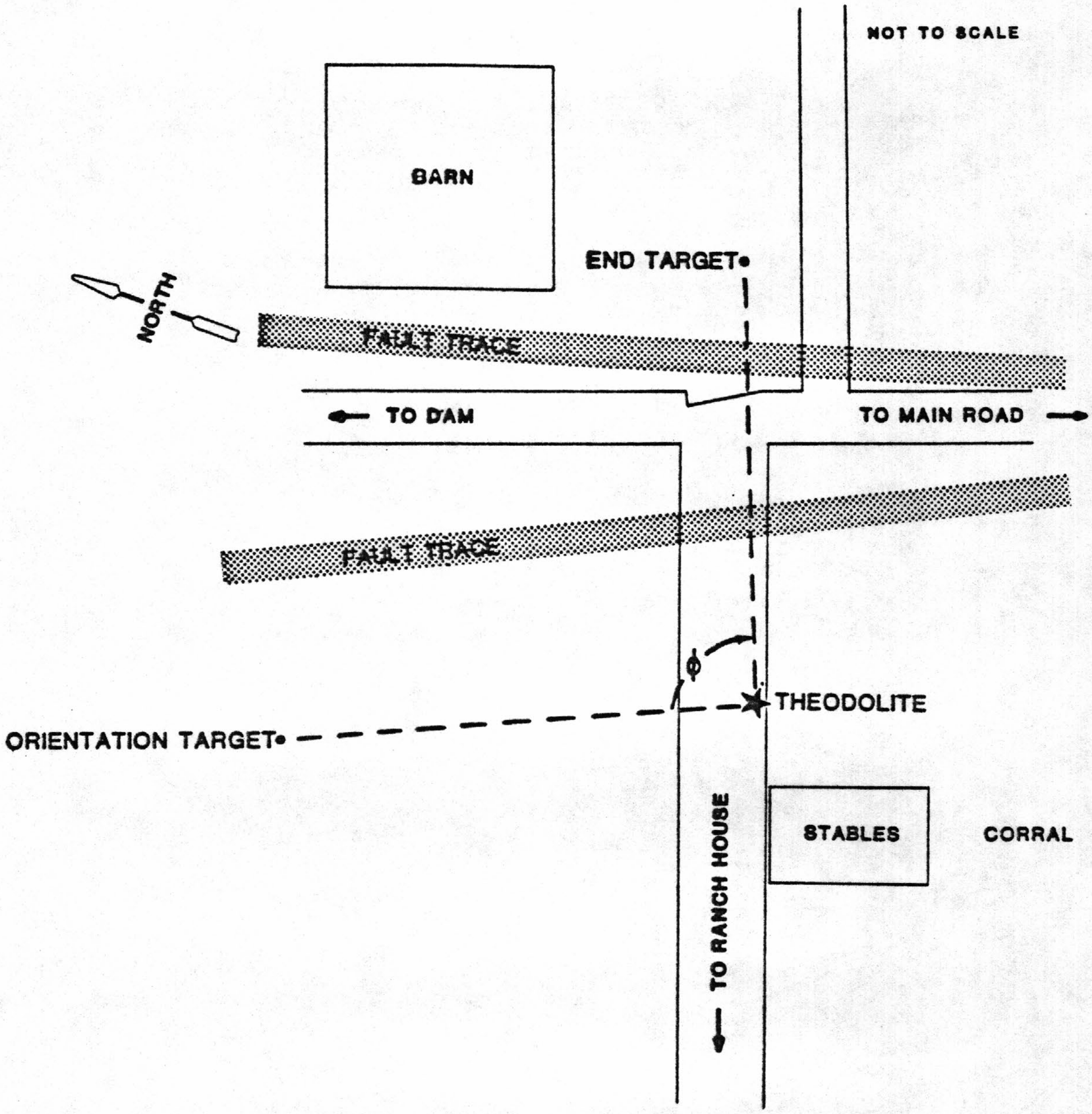

FIGURE 2. SAN FELIPE RANCH ALINEMENT ARRAY DIAGRAM

RESPONSE OF USGS CREEPMETERS NEAR HOLLISTER TO THE APRIL 24, 1984, MORGAN HILL EARTHQUAKE

Sandra S. Schulz

U.S. Geological Survey
345 Middlefield Road ms-977
Menlo Park, CA 94025

ABSTRACT

The Morgan Hill earthquake (M_L 6.2) on April 24, 1984, along the Calaveras fault produced 12.9 mm of afterslip with associated ground breakage at USGS creepmeter SHR1, 50 km southeast on the same fault. No other surface evidence of afterslip was found on recognized traces of the Calaveras fault from SHR1 10 km southeast to Hollister. In downtown Hollister, three creep-meters showed only normal activity since January, 1984. Surface inspection and instrument readings indicate that the afterslip at SHR1 did not propagate as far as Hollister. The April 24 earthquake also produced coseismic steps on USGS creepmeters along 200 km of the San Andreas fault.

The USGS creepmeter network monitoring the Calaveras fault near Hollister has its northern terminus at station SHR1 (Shore Road), 50 km southeast of the April 24, 1984, Morgan Hill earthquake epicenter (Figure 1). The earthquake (M_L 6.2) produced a coseismic right-lateral step of 0.11 mm at SHR1, followed by onset of a single afterslip event that reached 12.9 mm after 18 hours (Figure 2). Previously, no single creep event greater than 9 mm had been recorded at SHR1 since installation in 1971. SHR1 did not record coseismic steps during two magnitude 3+ aftershocks on May 3, 1984. (See W. H. Bakun and others, this volume, for location of SHR1 with respect to rupture zone).

The creep rate at SHR1 averages 9-12 mm per year (Schulz and others, 1982), and tension cracks across Shore Road are common. The present cracks have been forming since repaving in 1982, and it was not clear if the April 24 afterslip widened them (Figure 3). However, a fresh crack 1 meter long and 0.5 cm wide at its center was observed April 25 in the southeast dirt shoulder of Shore Road (Figure 4), and hairline cracks extended from the northwest dirt shoulder into the pavement (Figure 5).

A search on April 25 along the known creeping trace of the Calaveras fault between Shore Road and Hollister produced no further surface evidence of afterslip. However, the fault geometry appears to change in this area (Slater and Burford, 1979), and it is possible not all potential moving traces have been located.

An active trace of the fault has been identified on Wright Road 8.5 km southeast of SHR1 (Figure 1). A USGS creepmeter (WRT1) operating here until 1983 recorded a creep rate of 11-13 mm per year, and a San Francisco State University survey across the trace has measured a similar rate (Jon Galehouse, pers. comm., 1984). A resurvey by Jon Galehouse and Beth Brown on April 25, 1984 showed no significant change in creep rate since January, 1984 (Galehouse, this volume). Also, no surface cracks were visible in fields on either side of Wright Road or next to the previous creepmeter site.

The three USGS creepmeters in Hollister do not record on on-site recording devices called Rustraks. Dial readings on April 25 showed 1 mm of left-lateral movement (contraction) at the base of Park Hill since January 24, 1984, and less than 1 mm right-lateral movement (extension) at the two instruments in central Hollister, all normal amounts for this time of year.

Based on the San Francisco State survey at Wright Road and on the creepmeter dial readings in Hollister, it appears the large afterslip seen at SHR1 may have ended in that immediate area. If it did extend farther southeast, it may have been on a trace not now recognized.

It is interesting to compare SHR1's reaction to the Coyote Lake earthquake of August 6, 1979 (M 5.9) (Figure 1). Located 20 km southeast of that epicenter, SHR1 recorded a 4.2 mm right-lateral coseismic step and two afterslip events in the next 24 hours, for a total slip of 8.3 mm (Figure 2). The Coyote Lake earthquake ended a 3-year creep lag at SHR1 (Raleigh, 1979; Schulz and Burford, 1983). However, there was no apparent long-term creep lag at SHR1 preceding the April 24, 1984, earthquake (unpublished creep project data, 1984).

In addition to the activity at SHR1, the April 24 earthquake produced coseismic steps on creepmeters along the San Andreas fault in central California. Steps ranged in size from 0.33 mm south of Hollister to 0.10 mm at Parkfield, 200 km southeast of the epicenter.

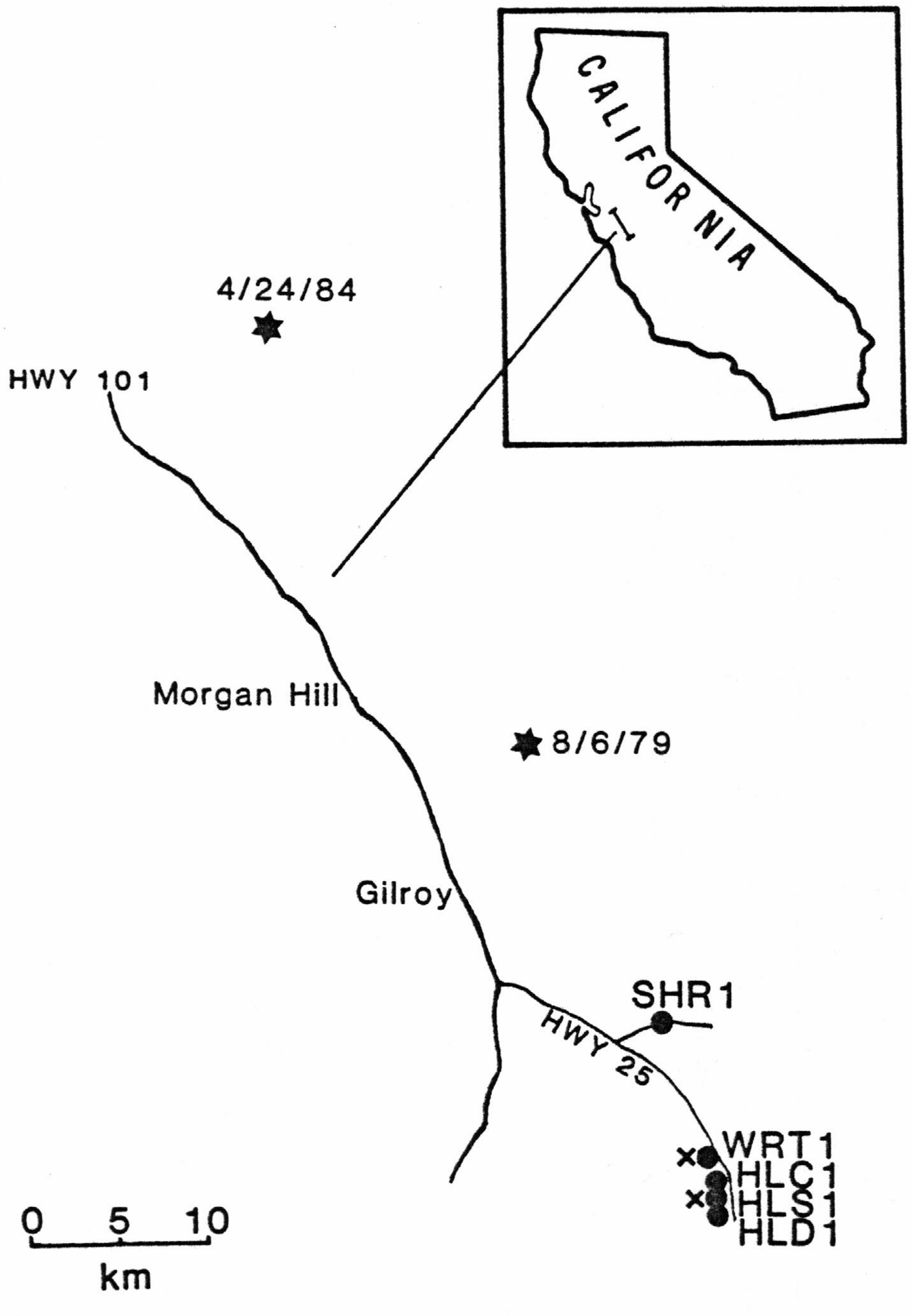

Figure 1. Map showing epicenters of April 24, 1984, Morgan Hill and August 6, 1979, Coyote Lake earthquakes (stars). Circles indicate USGS creepmeters and X's indicate San Francisco State University survey lines.

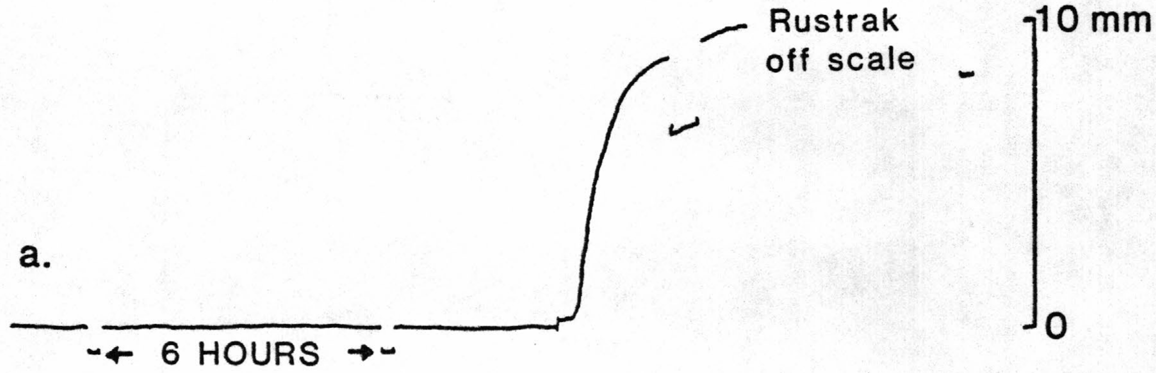

Figure 2a. Rustrak trace showing SHR1's response to April 24, 1984, Morgan Hill earthquake. A 0.11 mm coseismic step was followed within 23 minutes by 12.0 mm of afterslip over the next 18 hours. Recorder went offscale after 4 hours. See (b) below.

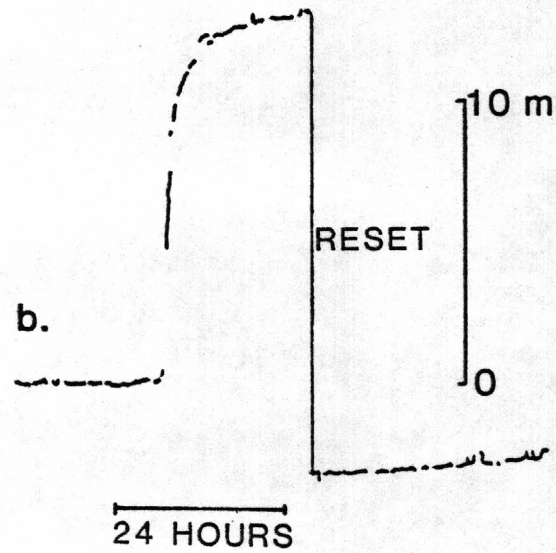

Figure 2b. Telemetry trace showing entire event (ten-minute samples). Left-lateral step was mechanical reset on April 25 to prevent instrumental range being exceeded.

Figure 2c. Rustrak trace showing SHR1's response to August 6, 1979, Coyote Lake earthquake. A 4.2 coseismic step was followed by 4.1 mm afterslip in two events over the next 24 hours.

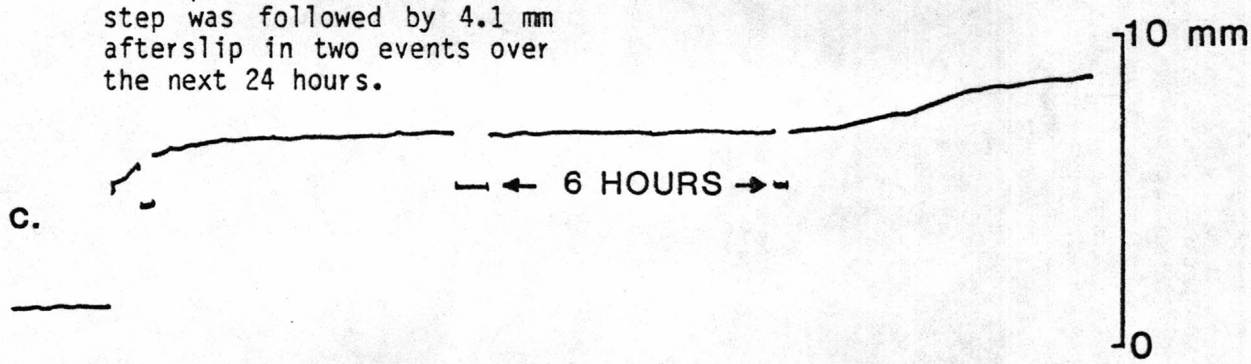

Figure 3. View northeast along trace of Calaveras fault at Shore Road 10 km northeast of Hollister. SHR1 lies in road shoulder off right side of photo, crossing the trace at an angle of 45°. Cracks in road began after repaving in 1982. Fifteen-cm white scale in lower right-hand corner indicates location of fresh crack in road shoulder apparently caused by afterslip following April 24 earthquake (see Figure 4).

Figure 4. Close-up of fresh crack 1 m long and 0.5 cm at widest opening, beside Shore Road. Scale is 15 cm long.

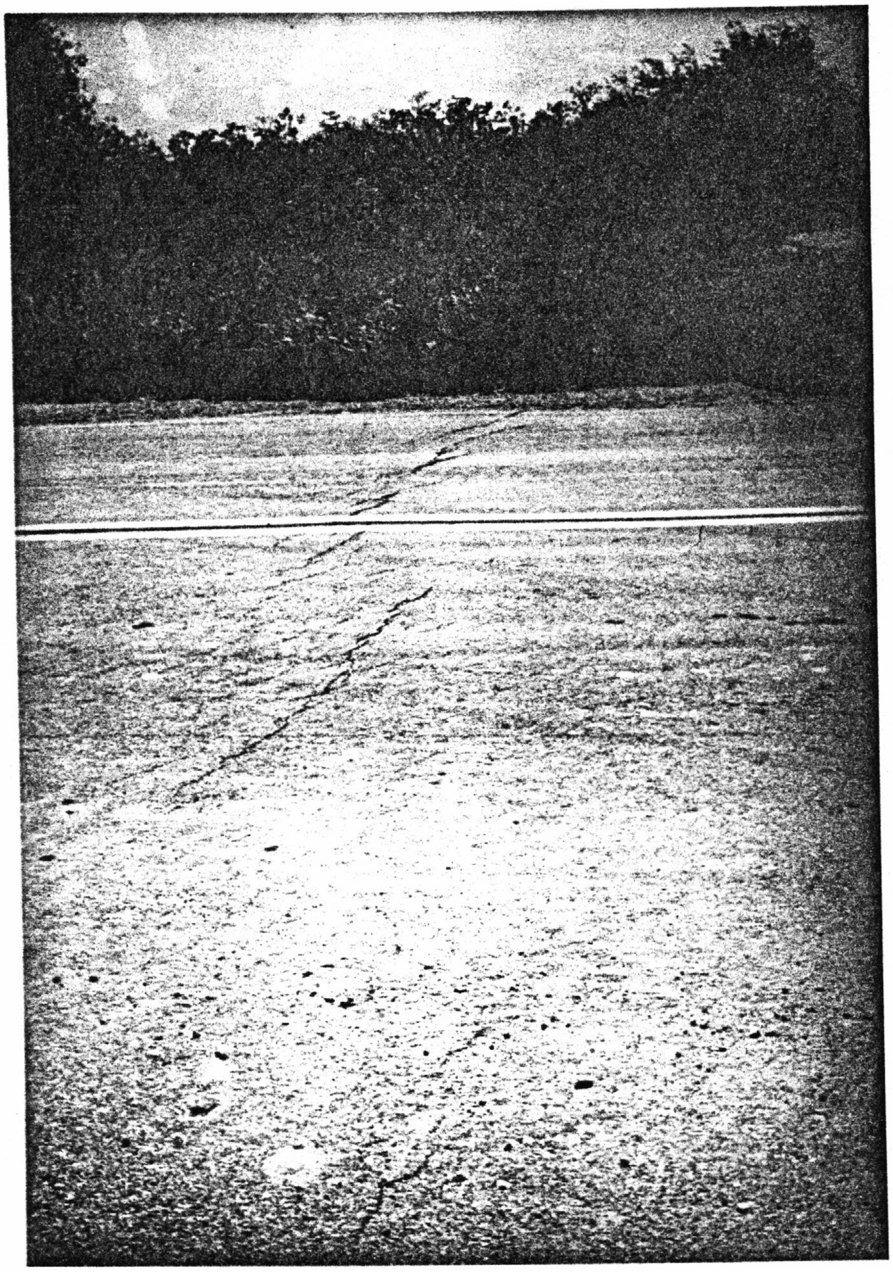

Figure 5. View southeast along Calaveras fault trace at Shore Road. SHR1 is in shoulder in left upper center of picture. Arrow indicates hairline crack extending from dirt shoulder into roadway.

REFERENCES

Bakun, W. H., M. M. Clark, R. Cockerham, W. L. Ellsworth, A. G. Lindh, W. H. Prescott, A. F. Shakal and P. Spudich, 1984, The 1984 Morgan Hill, California, Earthquake: *U.S. Geological Survey Open-File Report No.84-498*, p. 1-9.

Galehouse, J. S., 1984, Theodolite measurements following the 24 April 1984 Morgan Hill earthquake, *U.S. Geological Survey Open-File Report No. 84-498*, p. 72-75.

Galehouse, J. S. and B. D. Brown, 1984, Southeastern limit of surface displacement on the Calaveras fault associated with the 24 April 1984 Morgan Hill earthquake, *U.S. Geological Survey Open-File Report No. 84-498*, p. 85-91.

Raleigh, C. B., W. Stuart, and P. W. Harsh, 1979, Creep on the Calaveras fault near Coyote Lake (abstract), *EOS (American Geophysical Union Transactions)*, v. 60 (46), p. 890.

Schulz, Sandra, Robert O. Burford and Barbara Mavko, 1983, Influence of seismicity and rainfall on episodic creep on the San Andreas fault system in central California, *Journal Geophysical Research*, v. 88, B9, p. 7475-7484.

Schulz, Sandra S., Gerald M. Mavko, Robert O. Burford, and William D. Stuart, 1982, Long-term fault creep observations in central California, *Journal Geophysical Research*, v. 87, B8, p. 6977-6982.

Slater, L. E. and R. O. Burford, 1979, A comparison of long-baseline strain data and fault creep records obtained near Hollister, California, *Tectonophysics*, v. 52, p. 481-496.

THEODOLITE MEASUREMENTS FOLLOWING THE 24 APRIL 1984 MORGAN HILL EARTHQUAKE

Jon S. Galehouse
San Francisco State University

We have three theodolite triangulation measurement sites on the Calaveras fault (see Figure 1). One site is in San Ramon near the northwesterly terminus of the Calaveras fault, about 60 km northwest of the 24 April 1984 Morgan Hill earthquake epicenter determined by Bakun et al. (1984). Two sites are in the Hollister area about 60 km southeast of the epicenter. Our theodolite data indicate that no significant changes in creep rates occurred prior to the earthquake and no surface displacement associated with the earthquake occurred at any of our three sites.

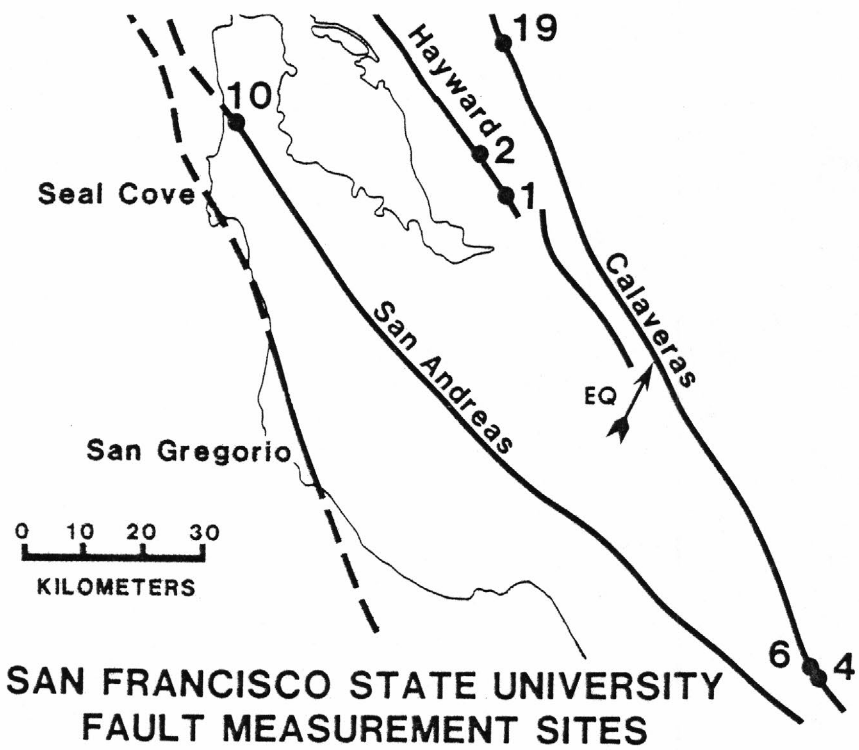

Figure 1. Map showing San Francisco State University theodolite triangulation measurement sites mentioned in the text. The EQ arrow shows the epicenter of the 24 April 1984 Morgan Hill earthquake determined by Bakun et al. (1984).

We have been monitoring our site in San Ramon (SF-19) since November 1980. The average rate of right-lateral movement has been about one millimeter per year for the past 3.5 years (see Figure 2). Our last measurement prior to the Morgan Hill earthquake was on 19 January 1984, 96 days before the 24 April event. We remeasured the site on 29 April and 3 June, 5 and 40 days following the earthquake. All three measurements were normal compared to the overall average since November 1980. No signs of surface rupture were observed at the site.

We began monitoring our site on Wright Road about 1.5 km north of Hollister (SF-06) in October 1979, about 2.5 months after the Coyote Lake earthquake. Slip along this segment of the Calaveras fault is fairly uniform, averaging about 13 millimeters per year for the past 4.6 years (see Figure 2). This is the fastest rate of movement of any of our 20 sites on ten active faults in the San Francisco Bay region. Our last measurement at Wright Road prior to the Morgan Hill earthquake was on 28 January 1984, 87 days before the event. We measured the site on 25 April, the day after the earthquake, and again on 2 June, 39 days after the quake. All three measurements were normal compared to the overall average since October 1979.

We began monitoring our site on Seventh Street in Hollister (SF-04) in September 1979, 54 days after the Coyote Lake earthquake. This site is about 2.3 km southeast of our site on Wright Road and is on a different segment of the Calaveras fault (Radbruch-Hall, 1974). Slip on Seventh Street is much more episodic than at Wright Road, with times of relatively rapid right-lateral movement alternating with times of little net movement (see Figure 2). The overall average rate of right-lateral displacement for the past 4.7 years has been about eight millimeters per year.

At the time of the Morgan Hill earthquake, the Calaveras fault at Seventh Street was in an overall phase of slight left-lateral movement that had lasted about a year (see Figure 2). Our measurement on 25 April, the day after the earthquake, was virtually the same as the last previous measurement on 28 January 1984. However, our measurement on 2 June, 39 days after the earthquake, showed right-lateral movement of about seven millimeters. This pattern of movement is not unusual for this site inasmuch as virtually the same thing occurred from mid-1981 to mid-1982. About a year of slight left-lateral movement was followed by relatively rapid right-lateral movement of about a centimeter. This change in direction and rate in 1982 occurred without being associated with any nearby earthquakes. Consequently, the change at Seventh Street shortly after the Morgan Hill earthquake was probably coincidental and not a result of the quake.

Our measurement site in Fremont (SF-01) on the Hayward fault about 38 km northwest of the Morgan Hill epicenter (see Figure 1) showed no significant change in creep rate either prior to or following the earthquake. The average rate of creep at this site has been about five millimeters per year for the past 4.7 years. Similarly, our measurement site in Union City (SF-02) on the Hayward fault about 45 km northwest of the epicenter also showed no unusual behavior. The creep rate here has been about four and one-half millimeters per year for the past 4.7 years.

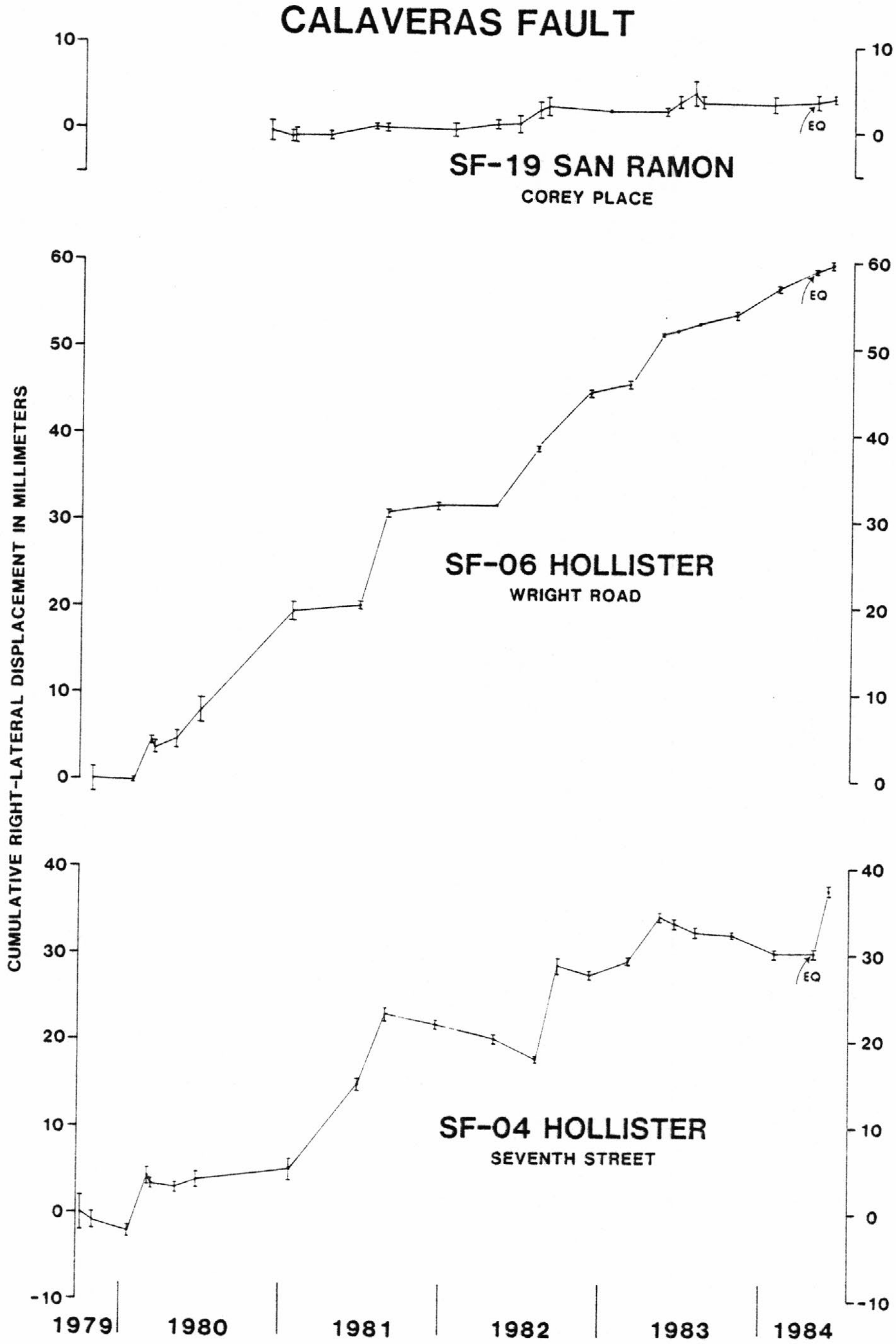

Figure 2. Data from San Francisco State University theodolite triangulation measurement sites on the Calaveras fault. An upward-sloping portion of a line indicates right-lateral slip and a downward-sloping portion indicates left-lateral slip. The error bars indicate one standard deviation on either side of the plotted points. The EQ arrows indicate the time of the Morgan Hill earthquake.

Finally, our measurement site in South San Francisco (SF-10) on the San Andreas fault about 80 km northwest of the epicenter (see Figure 1) remained virtually locked as it has been since we began measuring it 4.2 years ago.

In summary, no unusual and/or significant changes in creep rates occurred either before or after (through early June 1984) the Morgan Hill earthquake at our measurement sites on the Calaveras, Hayward, and San Andreas faults.

REFERENCES

Bakun, W. H., Clark, M. M., Cockerham, R., Ellsworth, W. L., Lindh, A. G., Prescott, W. H., Shakal, A. F., and Spudich, P., 1984, The 1984 Morgan Hill, California earthquake: a preliminary report: in *U.S. Geological Survey Open-File Report 84-498*, p. 1-9.

Radbruch-Hall, D. H., 1974, Map showing recently active breaks along the Hayward fault zone and the southern part of the Calaveras fault zone, California: *U.S. Geological Survey Miscellaneous Investigation Series Map I-813*, 2 sheets, scale 1:24,000.

MAGNETIC FIELD MEASUREMENTS NEAR THE MORGAN HILL EARTHQUAKE OF APRIL 24, 1984

R.J. Mueller and M.J.S. Johnston

U.S. Geological Survey
345 Middlefield Rd., ms-977
Menlo Park, California 94025

ABSTRACT

The epicenter of the Morgan Hill earthquake (M_L = 6.0 ± 0.3) of April 24, 1984 is located on the Calaveras fault and within an array of magnetometer stations. The magnetometer stations located along the Calaveras fault were not operational at the time of, or for the 16 month period prior to the earth-quake, but were reinstalled within hours of the main shock. Comparison of magnetic field differences after the earthquake with those 16 months prior indicate no significant variations >0.75 nT. Analysis of hourly magnetic field differences for the 12 day period following the earthquake indicate no significant variations >1.0 nT associated with the aftershock activity. A seismomagnetic model of the earthquake, using uniform magnetization, indicates the magnetometer stations along the Calaveras fault are poorly located to detect stress-generated magnetic field changes. The same model, using a distribution of magnetic material only on the west side of the fault, indicates station C1Y was located near the point of maximum expected field changes. The lack of any magnetic field changes >1.0 nT at station C1Y, requires a stress change ≤1.2 MPa for the 12 day period following the Morgan Hill earthquake.

INTRODUCTION

A moderate earthquake (M_L = 6.0 ± 0.3) occurred on the Calaveras fault at 2115 UT on April 24, 1984 at a depth of ~10 km (the Morgan Hill earthquake). The epicenter was located 15 km east of San Jose, California and 20 km north of Morgan Hill, California with aftershocks extending ~30 km to the south of the main shock. The southern end of the aftershock zone coincides with the northern end of the aftershock zone of a M_L=5.9 earthquake which occurred August 6, 1979 (the Coyote Lake earthquake).

The U.S.G.S. operates a network of magnetometer stations in central California in an effort to detect local magnetic field perturbations related to tectonically induced stress changes (Figure 1). Previous studies of magnetic field perturbations associated with earthquakes in this region are inconclusive. A 2 nT variation in the local magnetic field was observed during the 2 month period prior to a M_L=5.2 earthquake in November, 1974 (Smith and Johnston, 1976). On the other hand, no significant magnetic field variation was observed prior to or during the August, 1979 Coyote Lake earthquake (Johnston et al., 1981).

Station MTH, the nearest station in the U.S.G.S. magnetometer network, is located 2 km east of the April 24, 1984 Morgan Hill earthquake (Figure 1). Both stations MTH and COY have not been operational since January, 1983, but were reinstalled using portable on-site recording systems after the Morgan Hill earthquake. Station MTH was operational within 3 hours and station COY within 24 hours of the mainshock. In addition, station C1Y, which was established after the August, 1979 earthquake, was reoccupied and a new station EMT was established as a reference for station MTH (Figure 1). The data collected with the on-site recording systems at these four stations and data from two telemetered magnetometer stations, EUC and SAR, are examined in this report in an attempt to isolate any local magnetic field variations associated with the Morgan Hill earthquake.

DATA

The four on-site recording systems measure total magnetic field intensity at a 0.25 nT sensitivity and the data from the two telemetered stations at a 0.125 nT sensitivity. The field at all stations is synchronously sampled at a ten minute sampling interval. All stations use the E.G. & G. Geometrics, Inc. model G-816 or G-826 proton precession magnetometer. Instrumental details are described by Mueller and others, 1981.

Since no magnetometer stations were operational along the Calaveras fault at the time of or during the 16 months prior to the Morgan Hill earthquake, observation of coseismic and preseismic effects with periods <16 months is not possible. What may be observed are preseismic perturbations with periods >16 months resulting in a coseismic net field offset and postseismic local magnetic field variations related to aftershocks.

The simplest method of isolating magnetic field changes and reducing the effects of ionospheric and magnetospheric disturbances is to difference the magnetic field observations between adjacent stations. Figure 2 shows 3-day averages of differenced 10-minute magnetic field data for stations near the Morgan Hill earthquake. The top three plots include data from stations along the Calaveras fault and the bottom reference plot includes data from two stations located off the Calaveras fault. An annual cycle is apparent in the two middle plots. We suspect this is due to a temperature related response at station COY, though we have no good evidence for this. Thermal testing of the electronic equipment at station COY when it was operational indicate no response to temperature over a range from 5 °C to 30 °C. The arrows in Figure 2 mark the time two moderate earthquakes occurred on the Calaveras fault in this region. Delta (δ) indicates the distance from the epicenter to the nearest station used in the difference. No significant changes >0.75 nT are observed in these data from magnetometer stations along the Calaveras fault after the Morgan Hill earthquake compared to data 16 months prior. In addition to these data, comparison of the averaged magnetic field differences for C1Y-COY in August, 1979 with April, 1984 indicate only a -0.16 ± 0.25 nT change for the 56 month period.

Figure 3 shows hourly averages of 10-minute differenced magnetic field data for stations along the Calaveras fault during the 12 days after the Morgan Hill earthquake. Tick marks at the bottom of the figure represent the logarithm of hourly averaged moment where:

$$\log M_0 = 1.5 M_L + 16 \quad \text{(Thatcher and Hanks, 1973)}$$

and is intended to indicate the seismic energy released during the aftershock period. To complicate interpretation of these differenced magnetic field data, storm level conditions existed in the geomagnetic field beginning at 1200 UT on April 25 and continuing to the end of April 26. The geomagnetic field storm conditions are suspected to be responsible for the 3 nT positive spike on April 26 shown on difference plot EMT-MTH and the changes at the beginning of difference plots EMT-COY and C1Y-COY (Figure 3). The increased noise level of differenced data for EMT-COY (σ=0.92 nT) is due to a greater station separation distance of 34 km versus station separation distances ~ 8 km for EMT-MTH (σ=0.60 nT) and C1Y-COY (σ=0.25 nT). No significant changes >1-2 nT are observed in these magnetic field data that relate to seismicity during the 12 day period following the Morgan Hill earthquake.

DISCUSSION

Local magnetic field perturbations are expected to result from stress drops occurring prior to and during moderate to large earthquakes. These seismomagnetic effects (Stacey, 1964) are derived from the stress dependence of the magnetic properties of crustal rocks near active faults. Models used to calculate the form and amplitude of magnetic field changes on the Calaveras fault for the August, 1979 Coyote Lake earthquake (Johnston et al., 1981) can be applied to the Morgan Hill earthquake. These models calculate the seismomagnetic anomaly on the earth's surface as a function of fault geometry, the distribution of magnetic material, and the stress change in the region.

Figure 4 illustrates the calculation of the seismomagnetic effect using a vertical finite slip patch 1 to 11 km deep, 21 km in length, with 10 cm of fault slip. A unform magnetization on both sides of the fault of 1 A/m is assumed. This solution indicates the three magnetometer stations near the Calaveras fault are poorly located for detection of local magnetic field changes and the amount of slip would have to triple in order to produce a change >1 nT at any of the stations.

Aeromagnetic surveys (U.S. Geological Survey, 1974) indicate more magnetic material is located on the western side of the Calaveras fault in this region. Figure 5 illustrates the calculation of the seismomagnetic effect using the same fault geometry as Figure 4, but uses a magnetization of 1 A/m only on the west side and a magnetization of 0.1 A/m on the east side of the fault. For this solution, station C1Y is best located to detect magnetic field changes for the Morgan Hill earthquake. The differenced data for C1Y-COY (Figure 3) indicate no significant magnetic field changes >1 nT during the aftershock period from April 26 to May 6. For this solution, if the signal were at the level of the noise, these data require a stress change $\leq$1.2 MPa for the period April 26 to May 6.

The two solutions using the seismomagnetic model indicate the optimum array of magnetometers for this magnitude earthquake would consist of pairs of stations located ~1-2 km on either side of the fault and having these pairs of stations at ~5 km intervals along the fault.

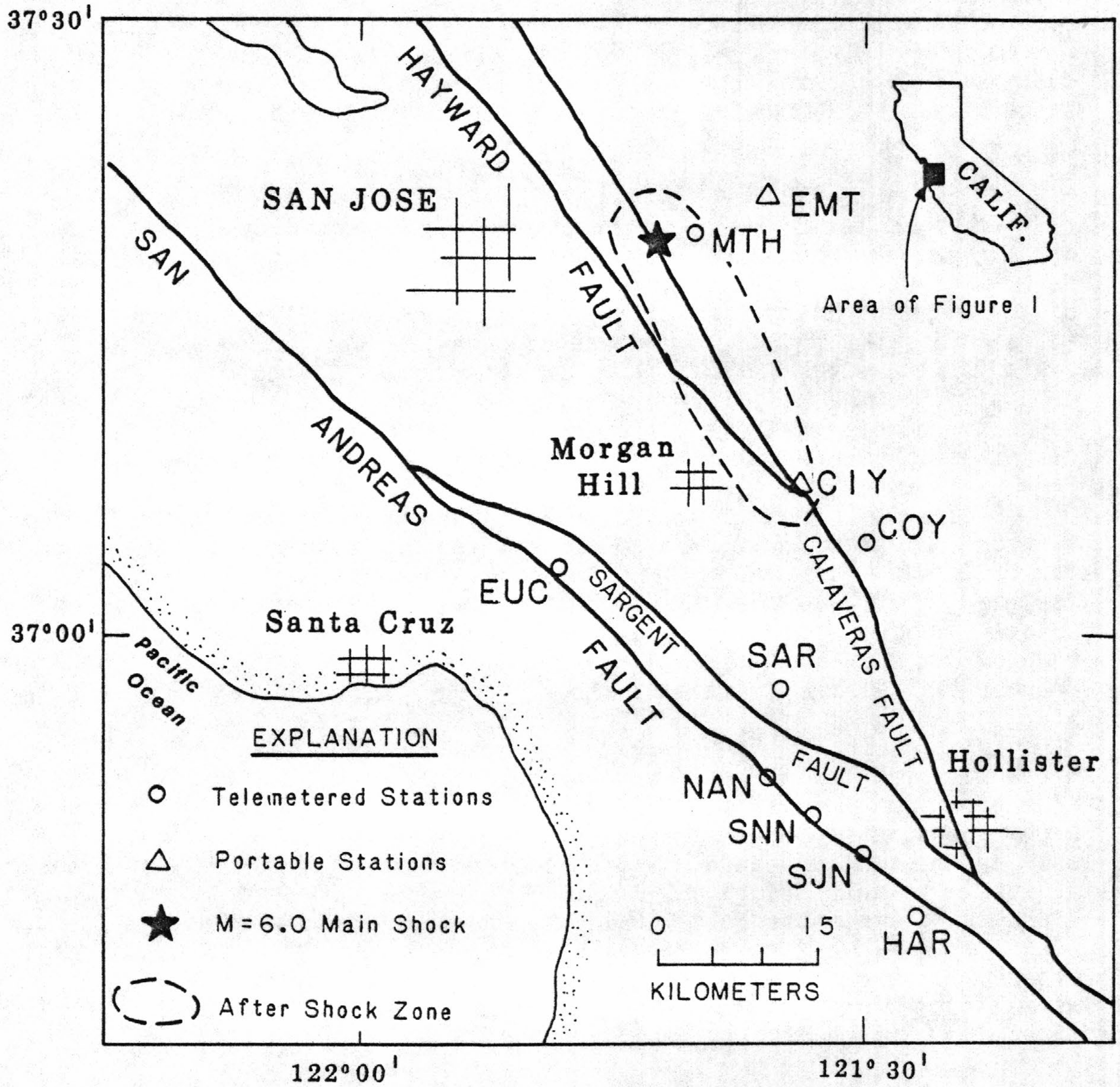

Figure 1. Map showing the location of magnetometer stations in central California relative to the April 24, 1984 Morgan Hill earthquake (star). The dashed area represents the aftershock zone.

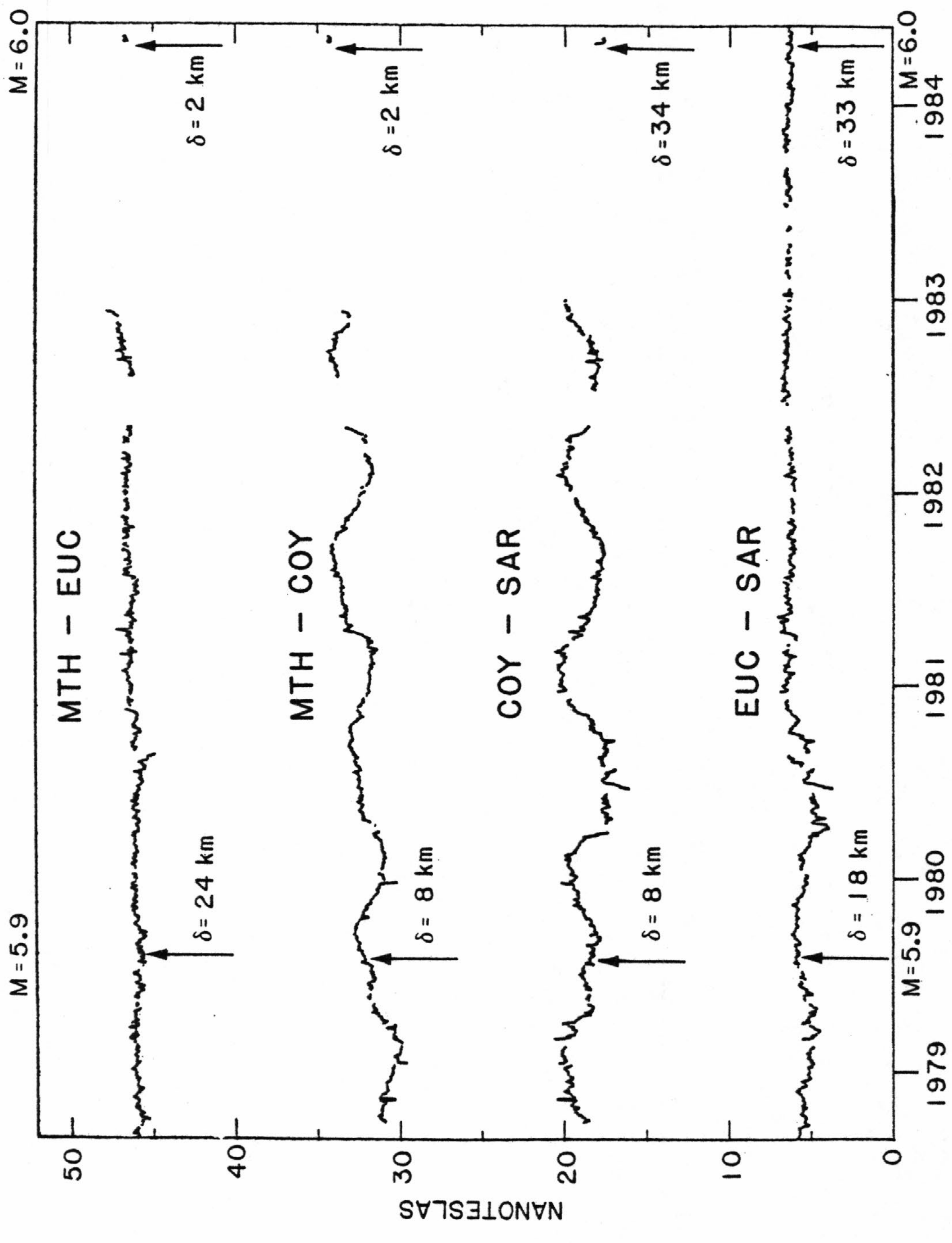

Figure 2. Three-day averages of differenced magnetic field data between 1978 and 1984. The three upper plots include data from stations located along the Calaveras fault. Arrows mark the time of two moderate earthquakes occurring on the Calaveras fault during this time period.

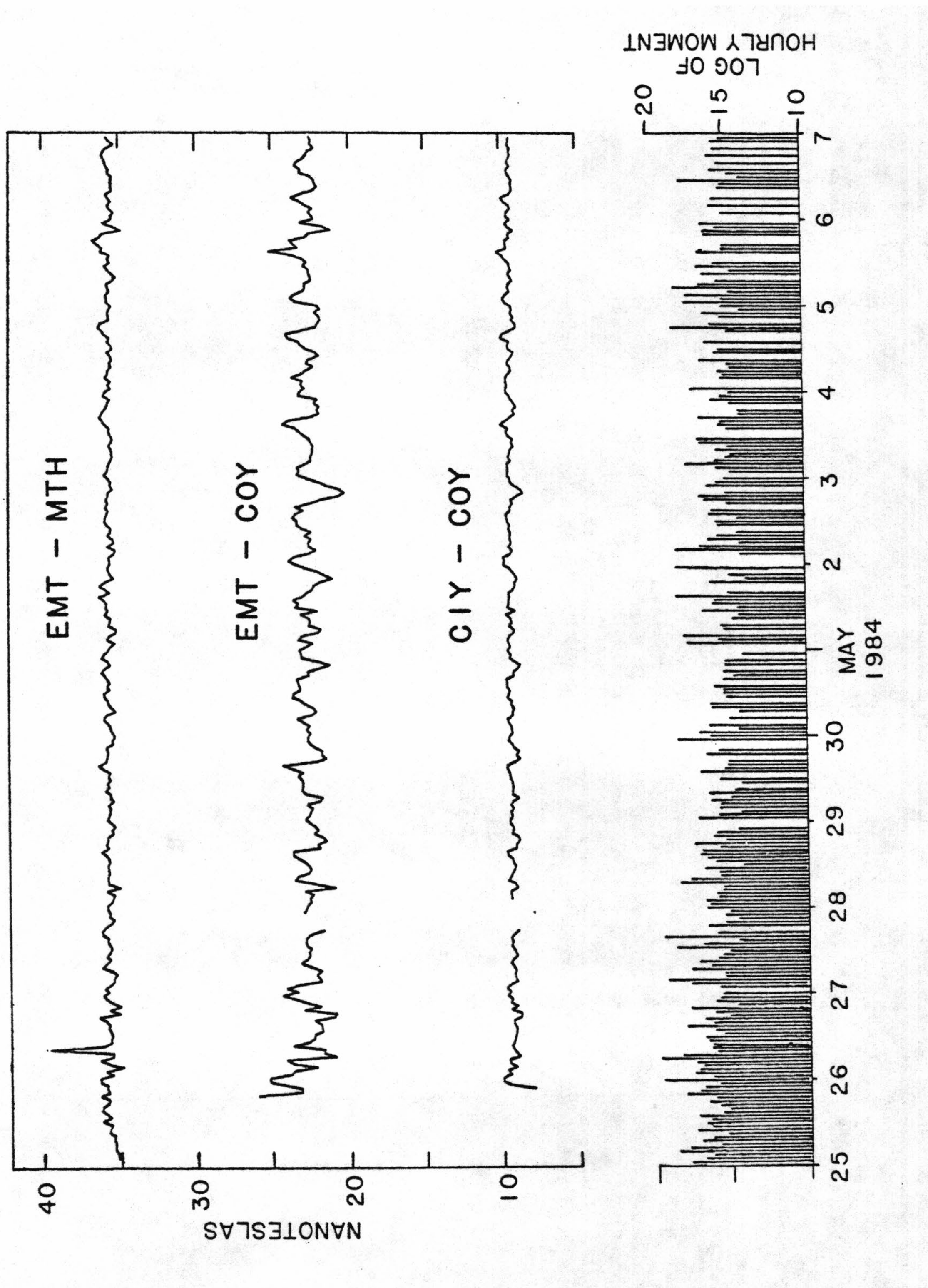

Figure 3. Hourly averages of differenced magnetic field data from stations along the Calaveras fault, during the 12 day period following the Morgan Hill earthquake. Tick marks represent logarithms of hourly averaged seismic moment ($\log M_0 = 1.5 M_L + 16$).

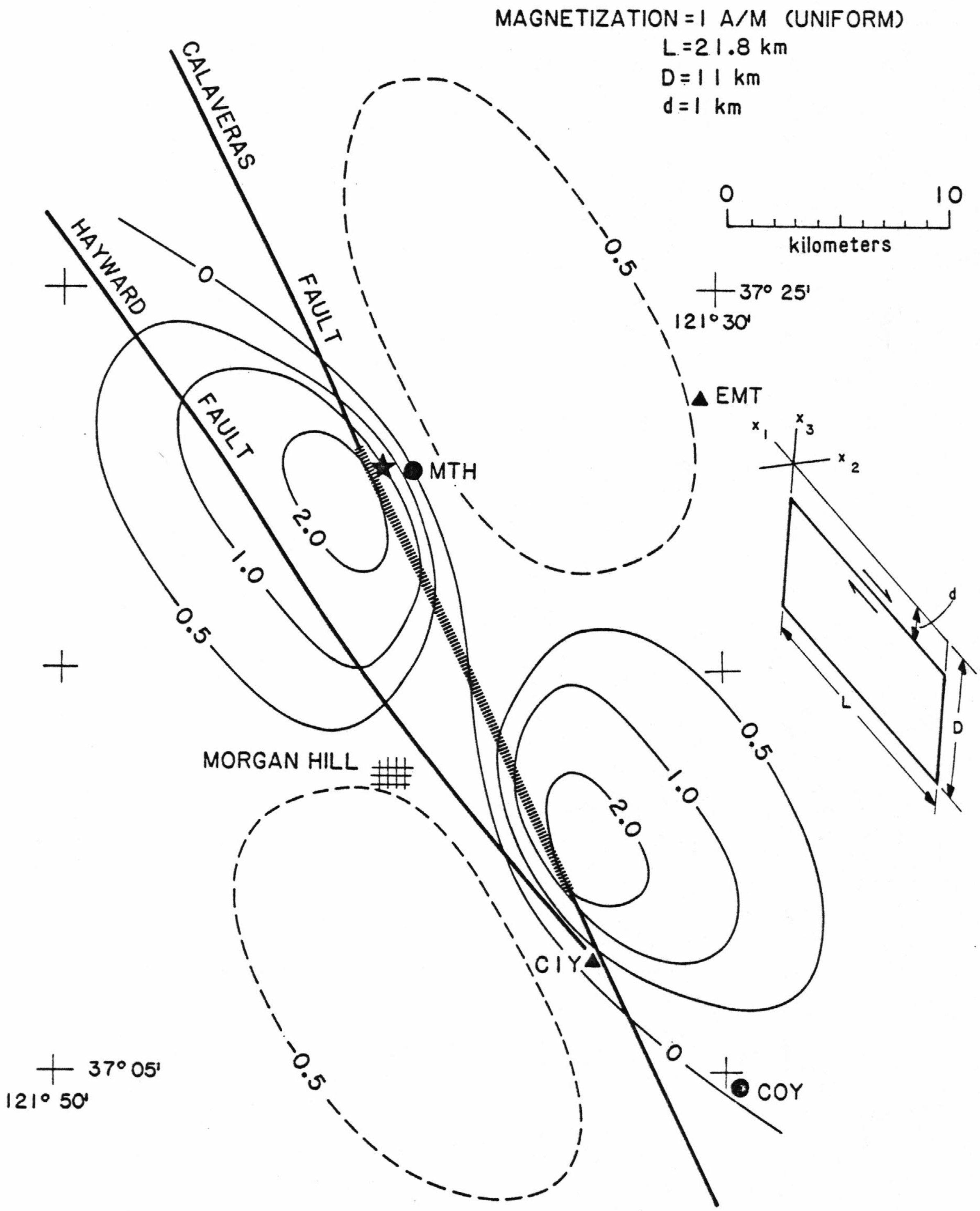

Figure 4. The location of magnetometer stations and the epicenter of the Morgan Hill earthquake (star) are shown in relation to magnetic anomaly contours (in nanoteslas). The magnetic anomaly contours represent 10 cm of slip on a fault plane 10 km by 21 km, with uniform magnetization of 1 A/m.

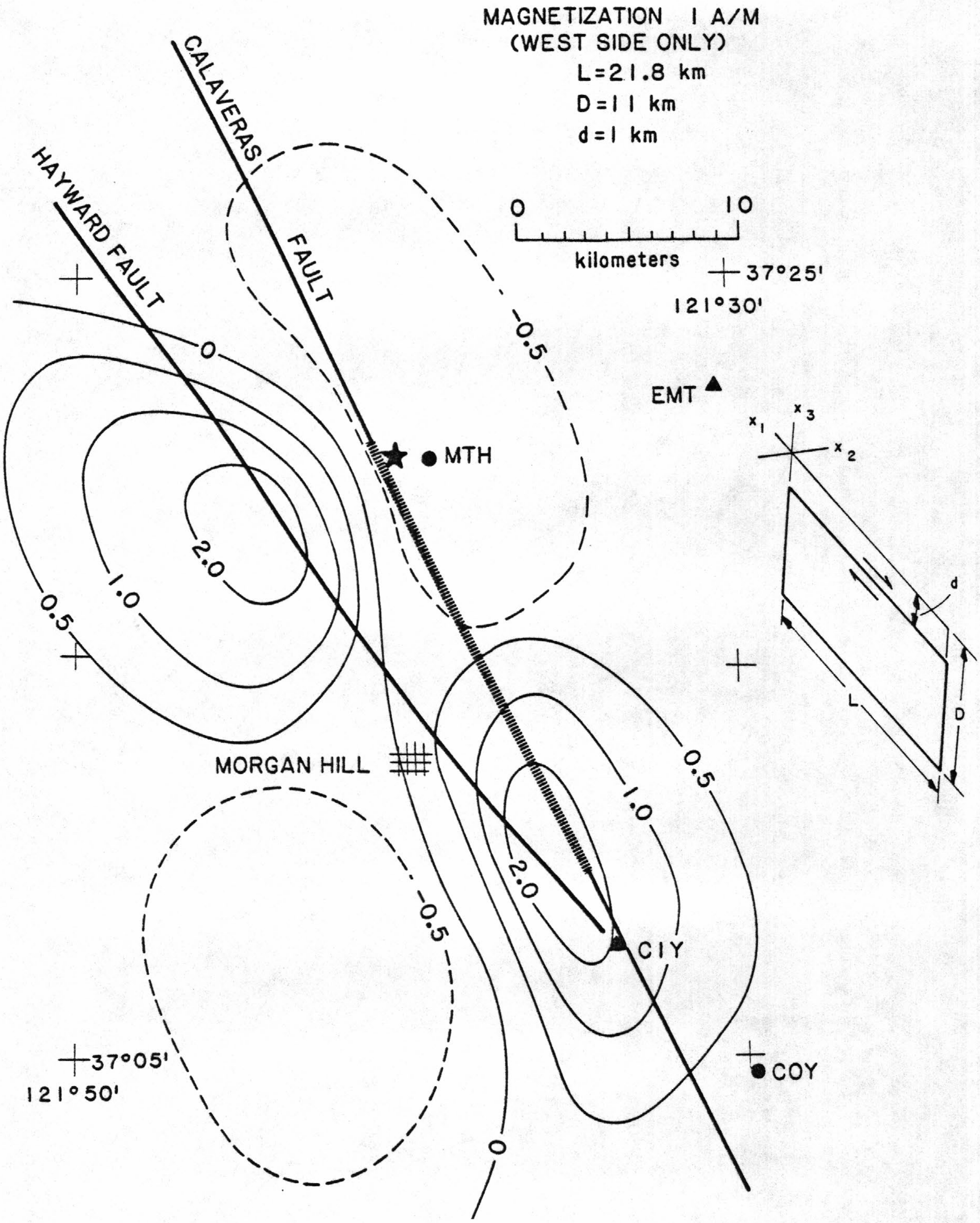

Figure 5. Magnetic anomaly contours (in nanoteslas) using the same model as Figure 4, but having magnetic material only on the west side of the fault.

CONCLUSIONS

Analysis of magnetic field data from stations located near Morgan Hill indicate no anomalous preseismic variations >0.75 nT with periods >16 months. For the 12 days following the earthquake, no magnetic field variations >1.0 nT are associated with the postseismic activity. Seismomagnetic models indicate either the magnetometer stations are poorly located for this earthquake or any stress changes during the 12 day period after the earthquake are $\leq$1.2 MPa. The lack of data at the time of and for the 16 month period prior to the Morgan Hill earthquake preclude the identification of magnetic field perturbations during this period.

REFERENCES

Johnston, M.J.S., R.J. Mueller, and V. Keller, 1981. Preseismic and Coseismic Magnetic Field Measurements Near The Coyote Lake, California, Earthquake of August 6, 1979, *Journal Geophysical Research*, v. 86, p. 921-926.

Mueller, R.J., M.J.S. Johnston, B.E. Smith, and V. Keller, 1981, U.S. Geological Survey Magnetometer Network and Measurement Techniques in Western U.S.A., *U.S. Geological Survey Open-File Report 81-1346*.

Smith, B.E., and M.J.S. Johnston, 1976, A Tectonomagnetic Effect Observed Before a Magnitude 5.2 Earthquake Near Hollister, California, *Journal Geophysical Research*, v. 81, p. 3556-3560.

Stacey, F.D., 1964, The Seismomagnetic Effect, *Pure and Applied Geophysics*, v. 58, 5-22.

Thatcher, W. and T.C. Hanks, 1973, Source Parameters of Southern California Earthquakes, *Journal Geophysical Research*, v. 78, 8547-8576.

U.S. Geological Survey, 1974, Aeromagnetic Map of Parts of San Jose, Santa Clara, and San Francisco 1° by 2° Quadrangle, *U.S. Geological Survey Open-File Report 74-79*.

SOUTHEASTERN LIMIT OF SURFACE DISPLACEMENT ON THE CALAVERAS FAULT ASSOCIATED WITH THE 24 APRIL 1984 MORGAN HILL EARTHQUAKE

Jon S. Galehouse
San Francisco State University

and

Beth D. Brown
U.S. Geological Survey

During the late afternoon of 25 April 1984, we made field observations along five roads crossing the Calaveras fault north of Hollister (see Figure 1) in order to determine if there were any signs of recent surface displacement that may have been associated with the Morgan Hill earthquake that occurred on the preceding day. Our observations and interpretations of the five sites, progressing from Wright Road near Hollister northward to Highway 152 about 15 km northwest of Hollister, are as follows:

1. Wright Road - We observed left-stepping en echelon cracks crossing Wright Road about 1.5 km north of Hollister at the approximate location of the fault as shown by Radbruch-Hall (1974). However, we had observed these cracks three months previously, and there did not appear to be any significant changes. No cracks or mole tracks were seen in the fields to the north and south of the site. In addition, theodolite measurements on 25 April 1984 compared with measurements made on 28 January 1984 also indicated no displacement associated with the earthquake at this site (see Galehouse, 1984).

2. McConnell Road - We found no evidence of recent displacement along McConnell Road about 4 km northwest of Hollister or in the recently-plowed and smoothed fields to the north and south.

3. Highway 25 - Two traces of the Calaveras fault (about 6.5 meters from one another) are evident in the asphalt of Highway 25 about 4.2 km northwest of Hollister. Both traces show well-developed left-stepping en echelon cracks. The more westerly trace only extended across the northern half of the road whereas the more easterly trace extended completely across. Neither set of cracks showed unequivocal evidence of recent displacement and no related cracking or mole tracks were found in the soil or fields adjacent to the road.

4. Shore Road - We found definite evidence of recent displacement along the trace of the Calaveras fault that crosses Shore Road about 5.8 kilometers north of Highway 25 and about 48 km southeast of the Morgan Hill epicenter determined by Bakun and others (1984). The well-developed left-stepping en echelon cracks in the asphalt could be traced into fresh well-developed cracks in the soil on either side of the road (Figure 2). The fault trend measured from the cracks in the soil on the south side of the road to the cracks in the soil on the north side was N17°W. A U.S. Geological Survey creepmeter (see Schulz, 1984) showed more than a centimeter of right-lateral displacement at this site associated with the Morgan Hill earthquake.

5. Highway 152 (Pacheco Pass Road) - We found evidence of recent cracking at three different locations near San Felipe Lake about 40 km southeast of the Morgan Hill earthquake epicenter. The trace mapped by Radbruch-Hall (1974) that continues south of Highway 152 (see Figure 1) showed well-developed cracks in the asphalt that could be traced into poorly-developed but fresh hair-line cracks in the soil on both sides of the road. The fault trend measured from the cracks in the soil on the south side to those in the soil on the north side was N18°W. The curb on the north side of the road was offset about one centimeter in a right-lateral sense (see Figure 3). This offset could also be seen in the soil and is almost certainly associated with the preceding day's earthquake. There is no unequivocal way to tell if displacement occurred shortly before, during, or shortly after the earthquake. It is likely, however, that offset occurred shortly after the earthquake, similarly to the offset determined by the creepmeter at Shore Road, about 5 km to the southeast (see Schulz, 1984). We also found two additional sets of cracks located about 4.6 meters from one another and located about midway between the two traces of the Calaveras fault that Radbruch-Hall (1974) shows northwest of Highway 152 (see Figure 1). The more easterly of these unmapped sets of cracks trends about N35°W across the road (see Figure 4) and the more westerly set trends about N40°W. Both sets show hair-line cracks that extend from the asphalt into the soil on both sides of the road. Several other sets of northwest-trending cracks also cross Highway 152 in this area. None showed associated cracks in the soil bordering the Highway.

In summary, on 25 April 1984, one day after the Morgan Hill earthquake, the two northernmost of five roads crossing the Calaveras fault north of Hollister showed strong evidence of recent displacement. The three southernmost roads showed no unequivocal evidence of recent displacement. Consequently, the southeastern limit of surface displacement along the Calaveras fault associated with the 24 April 1984 Morgan Hill earthquake appears to be along a 5.8 kilometer segment of the fault between Shore Road and Highway 25, about 48 to 54 kilometers southeast of the epicenter.

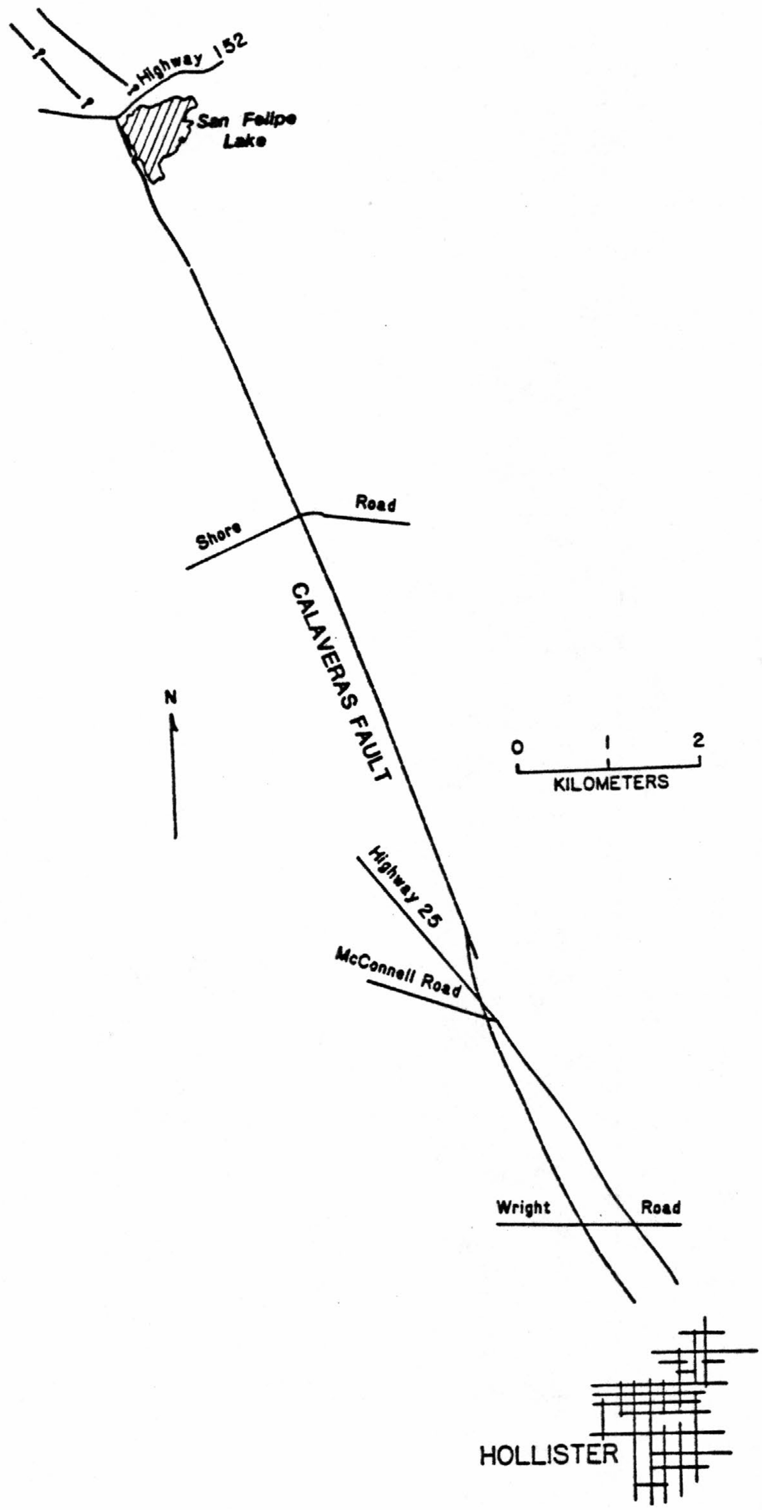

Figure 1. Location map of roads crossing the Calaveras fault from Hollister northward to Highway 152. Fault traces from Radbruch-Hall (1974).

Figure 2. Calaveras fault at Shore Road on 25 April 1984. The left-stepping en echelon cracks appear in the asphalt and also in the dirt (pen for scale).

Figure 3. Calaveras fault at Highway 152 (Pacheco Pass Road) on 25 April 1984. Crack in darker upper part of photo is in asphalt of the road. Crack in lighter middle part of photo above the knife is in road curb which is offset about one centimeter in a right-lateral sense. Crack beneath knife and in lower part of photo is in dirt alongside the road and also shows right-lateral offset.

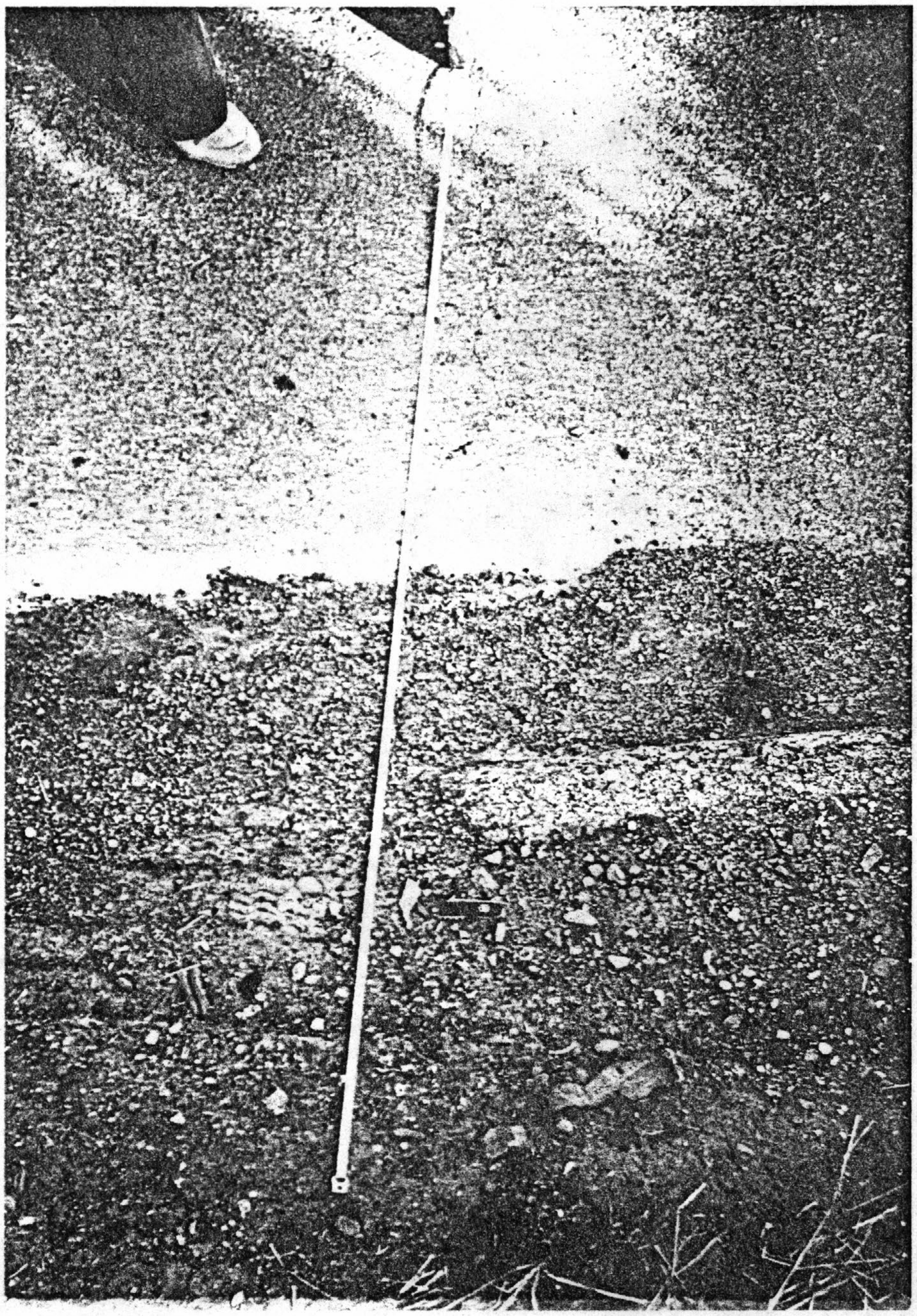

Figure 4. Calaveras fault at Highway 152 (Pacheco Pass Road) on 25 April 1984. This crack is northeast of the one shown in Figure 3. Crack in lighter upper part of the photo to the right of the tape is in asphalt. Crack in darker lower part of the photo is in dirt and runs from underneath the knife downward and underneath the tape about 1.5 knife lengths from the end of the tape.

REFERENCES

Bakun, W. H., Clark, M. M., Cockerham, R., Ellsworth, W. L., Lindh, A. G., Prescott, W. H., Shakal, A. F., and Spudich, P., 1984, The 1984 Morgan Hill, California earthquake: a preliminary report: in *U.S. Geological Survey Open-File Report 84-498*, p. 1-9.

Galehouse, J. S., 1984, Theodolite measurements following the 24 April 1984 Morgan Hill earthquake: in *U.S. Geological Survey Open-File Report 84-498*, p. 72-75.

Radbruch-Hall, D. H., 1974, Map showing recently active breaks along the Hayward fault zone and the southern part of the Calaveras fault zone, California: *U.S. Geological Survey Miscellaneous Investigations Series Map I-813, 2 sheets*, scale: 1:24,000.

Schulz, S. S., 1984, Response of USGS creepmeters near Hollister to the April 24, 1984, Morgan Hill earthquake: in *U.S. Geological Survey Open-File Report 84-498*, p. 64-71.

THE APRIL 24, 1984 MORGAN HILL, CALIFORNIA EARTHQUAKE: THE SEARCH FOR SURFACE FAULTING

Katherine K. Harms, Malcolm M. Clark, Michael J. Rymer, Manuel G. Bonilla, Edwin L. Harp, Darrell G. Herd, Kenneth R. Lajoie, James J. Lienkaemper, Scott A. Mathieson, James A. Perkins, Robert E. Wallace and Joseph I. Ziony

U.S. Geological Survey
345 Middlefield Road, MS-977
Menlo Park, CA 94025

INTRODUCTION

This report summarizes our investigations to determine if surface faulting accompanied the April 24, 1984, Morgan Hill earthquakes. One of the main objectives of the report is to record detailed information, in summarized field notes, about our initial search for surface faulting. We think this information may be very important to investigaters of future earthquakes in this area. Thus we supply more than customary detail of routes and observations, and we include some descriptions of the same sites by different observers. We also include, rather than eliminate, observations of marginal or uncertain value to future investigators.

Our investigation started the day of the earthquake, and continued through April 27 as we inspected traces of the Calaveras fault (Radbruch-Hall, 1974; Dibblee, 1973) as well as nearby traces of the Hayward fault (see Plate 1 and Figure 1). After getting D. G. Herd's unpublished maps of recent traces of the Calaveras fault, on May 2-4 we rechecked all of his mapped traces in the epicentral and aftershock zone. We investigated in detail the region at the southeast end of Anderson Reservoir again on May 11 and 16.

Most of the abundant earthquake-associated cracks in the epicentral region are related to downslope movement, lurching, differential settling, or other near surface movement of young alluvium or artificial fill. However, origin of cracks in two areas of San Felipe Valley and near the southeast end of Anderson Reservoir is less certain, and we carefully investigated these cracks and monitored some of them with quadrilaterals, alignment arrays, and detailed mapping.

We used two characteristics to distinguish tectonic cracks (the surface expression of deep-seated faults) from non-tectonic cracks: (1) tectonic cracks should have net slip in the plane of the crack, and (2) net slip (as well as trend for strike-slip faults) should show broad consistency or regularity along strike for tectonic cracks or zones of tectonic cracks. We accept that the origin of cracks that meet both these criteria, but which also can be reasonably created by non-tectonic processes, may remain uncertain.

The northern of two sites of possible tectonic breaks in San Felipe Valley, site 25 (Pl. 1) included cracks that were distinct from the surrounding desiccation and differential settling cracks, but showed no recognizable tectonic displacement. However, these fractures were aligned with clearly defined fault scarps to the southeast and the northwest. We installed a quadrilateral across the cracks on April 25 to help determine if they were of tectonic origin. After four remeasurements we detected no afterslip across this quadrilateral.

Farther south in San Felipe Valley, at site 36, north-northwest-trending cracks extended for approximately 10 m along the east shoulder of the paved portion of San Felipe Road, and about 40 m along the unpaved portion of the road. The unpaved portion of the road was scraped into alluvium, with no fill added. At the northern end the cracks were most abundant in the coarse-grained deposits of the alluvium (granule to pebble gravel) and ended at the northern contact of this gravel with a finer-grained deposit. We installed a quadrilateral at site 36 on April 25. It also showed no movement after four remeasurements.

Site 64, about 1/2 km west of Cochrane Bridge at the southeast end of Anderson Lake, also exhibited cracks and offset of equivocal tectonic origin. These cracks showed approximately 15 cm of right-lateral displacement across five fractures in a zone about 30 m wide. These breaks crossed Dunne Road along a ridge crest, and showed generally increasing azimuth from east to west. South of the road (towards the shore), the fractures did not continue in a consistent manner, but became indiscernible from other randomly oriented cracks. These shore-zone breaks seemed to represent slumping or lateral spreading, and were dominantly extensional, with both minor left-lateral and right-lateral components of slip. North of the road, the cracks merged with west-trending cracks related to slumping. There was no clear evidence for a continuing right-lateral component of displacement north of the road, though a set of right-stepping extensional cracks lay on trend with those at site 64. Although locally or individually these breaks appeared to be tectonic, they occurred within a broad zone of active landslides and slumps, and showed little continuity of trend or displacement within, and none beyond, the landslide-slump region.

Southwest of Cochrane Bridge, on trend with the above cracks, fractures extended about 50 m southeast from Dunne Road (just west of the Martin driveway) up and beyond a steep embankment. These fractures exhibited dominantly right-lateral displacement with minor extension. The cracks did not clearly relate to landsliding. Two fractures, each with more than 100 mm of right-lateral displacement, crossed Dunne Road (site 65) on trend with these cracks and may be related to them. However, these fractures in Dunne Road may be related to local failure of the road fill. No cracks crossed the unvegetated shore-zone farther northwest of this site where they would have been very easy to detect. Farther to the southeast, the cracks entered a dense patch of poison oak 20-30 m long, but were not present on the other side of the patch, nor could we find them on benches and slopes farther to the southeast.

From the evidence, the question of whether or not surface faulting accompanied the April 24 earthquakes is now and may remain unanswered. Clearly, if they are present, tectonic ruptures were short, scattered, and showed small offset. Evidence in favor of a tectonic origin for the surface breaks in San Felipe Valley and near the southeast end of Anderson Reservoir included their northwest-southeast orientation and position along mapped or suspected late Quaternary traces in the fault zone and their component of right-slip. Evidence against a tectonic origin for these cracks is (1) those in San Felipe Valley displayed no or equivocal lateral displacement and those at Anderson Reservoir lay in zones of active landslides or slope failure, (2) all four zones (sites 25, 36, 64, and 65) were short and were both internally discontinuous and had clear boundaries on strike that were definitely not faulted, and individual cracks lacked continuity of displacement and trend found elsewhere with tectonic ruptures of small displacement (for example, Clark and others, 1976; Allen and others, 1972; Fuis, 1982; Sieh, 1982).

The following are summaries of field observations, arranged chronologically and approximately north to south. Time is Pacific Daylight Time. Plate 1 is a strip map of the Calaveras fault in the Lick Observatory, Morgan Hill, and Mt. Sizer 7-1/2 minute quadrangles. This map includes a compilation of fault trace interpretations (D. G. Herd, unpublished map; Radbruch-Hall, 1974; Dibblee, 1972, 1973), the routes traveled during this investigation (by vehicle and on foot), as well as sites of primary interest. Figure 1 includes the significant localities and routes traveled outside of these three 7-1/2 quadrangles. Numbered sites used in the text refer to localities shown in Plate 1, and sites designated by letters are located on Figure 1.

April 24, 1984
Rymer and M. E. Schiltz, near Cherry Flat Reservoir
3:00-5:00 p.m. Drove along Alum Rock Falls Road, east of San Jose and Alum Rock Park, near Cherry Flat Reservoir. No fresh cracks of tectonic origin were noticed along the paved road or in packed dirt shoulders to the road where the mapped fault crosses the road.

April 24, 1984
Lajoie and Mathieson, Halls Valley

We drove to Halls Valley in Santa Clara County to check for surface ruptures along mapped strands of the Calaveras fault. (3:30-7:10 p.m.)
Observations:

Mount Hamilton Road from Alum Rock Park to Halls Valley. No observed damage to nearby structures or to roadway. No minor failures in numerous road cuts.

Regional Park in Halls Valley. Drove and walked on freshly graded horse and hiking trails in park (see Plate 1). Found no evidence of ground rupture along linear topographic scarps that delineate most active trace. No ground breakage on trails that cross scarps. (11) One redwood water tank slightly damaged (hoops dropped). A few dead branches down. (9) No visible damage to hay barn built with only minor lateral bracing.

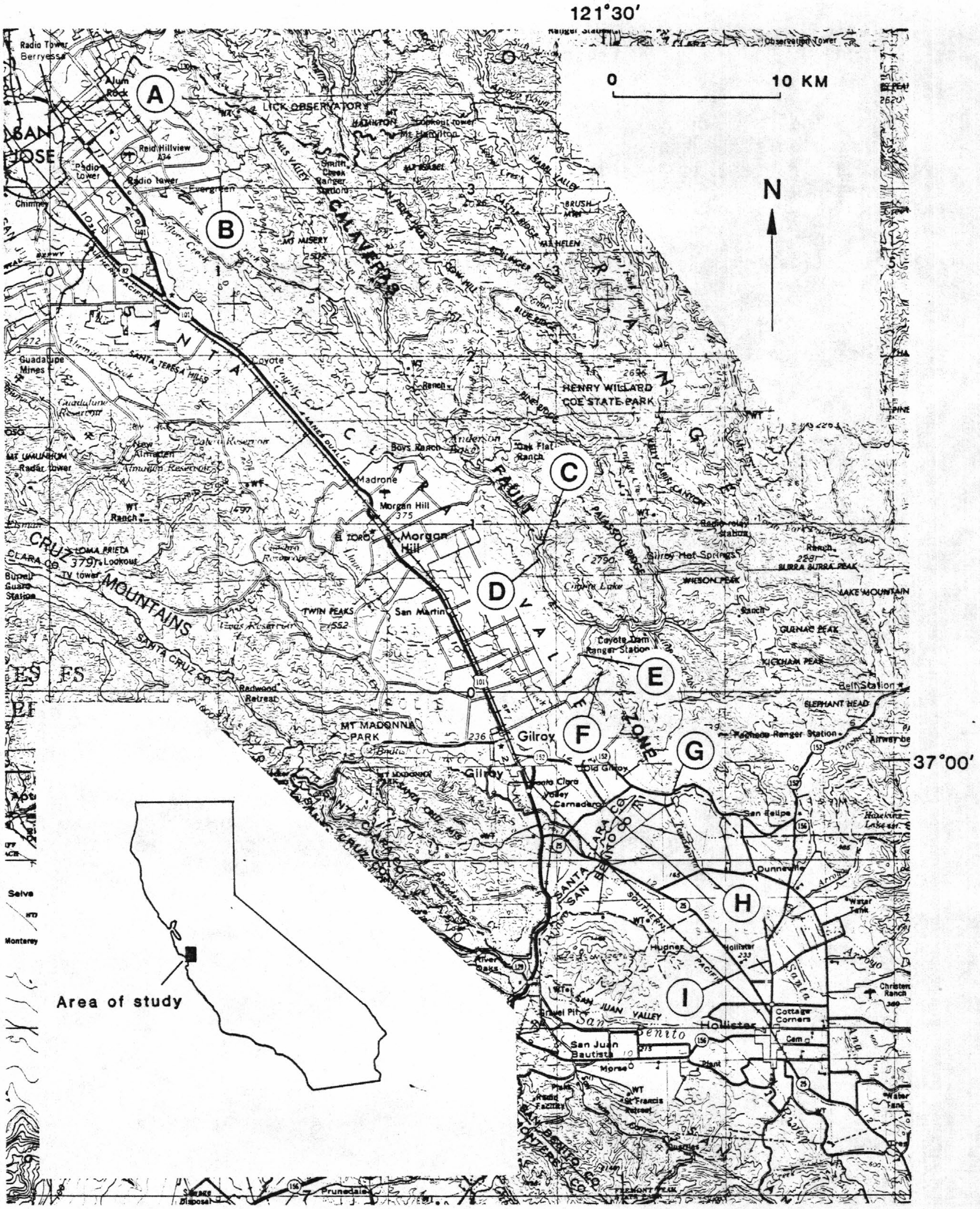

Figure 1. Map showing sites investigated in Calaveras and Hayward fault zones that lie beyond the aftershock zone of the Morgan Hill earthquakes.

April 24, 1984

Mathieson and Lajoie, Halls Valley

Area of epicenter:

(11) Hoops shifted on water tank, dropping 15-30 cm in a systematic fashion (down on the west); no shifting of tank on timber footings. Staves were forcibly shifted, both in and out--tank was full, but not leaking, and therefore has a liner. This was the only example of quake-related disruption that we saw. Another water tank (at Quimby and Mt. Hamilton Roads) was undamaged.

(12, 13) Walked due east of road to bench produced by the Calaveras fault. No cracks. Road was especially good for showing fractures; it was very recently graded, damp but firm, and had a muddy film. A nearby offset stream constrained the location of the fault to within a few meters. Partly rotted (up to 90% of cross section) branches to 4" diameter had been broken from oaks.

(15) Apparently tectonic swale on Coe property: no cracks.

(9) Barn apparently unaffected.

(10) No cracks in roads, aside from minor desiccation.

(7) Same.

(4) Quimby Road (paved): no evidence of displacement. Fault and/or lithologic boundary present. Large landslide complex extends to south approximately 1.5 km, no movement observed.

(2) Dirt road: no cracks.

(1) Landslide with deep (2') crevasses beside unpaved road. No unequivocal movement of slide, no other fresh features seen.

April 24, 1984

Lienkaemper and Perkins, San Felipe Valley, NW end of Anderson Reservoir

(36) End of San Felipe Valley Road pavement, no important cracks on roads seen so far. We met Winifred Coe leaving her residence, #8824 San Felipe Road.

(37) Visit Henry Coe residence for permission to inspect Coe land. Much damage of fragile contents. Coe house damaged ca. $38,000 in 1955, according to Henry Coe.

(35) Drove out road to Hewlett and Packard ranch, managed by Mr. and Mrs. Reese. Many extensional cracks in vicinity of San Felipe Creek, particularly on eastern bank at fill for bridge abutment.

(37) Met Herd and Ziony. Herd found cracks along roadside. Perkins and I judged these cracks to be nontectonic.

(33) HP Ranch. Norma Reese, Randy and others spoke with us. Road was being graded the day of the earthquake. Randy claimed a hump greater than one inch formed in the road at (35), not seen until after the earthquake. We returned to the location Randy remembered, about 100 m from the creek (site 35) The hump showed no cracks. No cracks or hump were seen near the edge of the road. Abundant large desiccation cracks could have easily obscured 1 cm of displacement.

(22) Road shown on topographic map ends near dam. No cracks seen on hard-packed dirt road to dam. Good visibility on hard-packed cattle trails around pond.

(25) No tectonic ruptures seen.

(38) Herd and Ziony saw no cracks in pavement here.

(42) Enroute to O'Connell's ranch via Las Animas Road, we met Tim Hall and Pat McClellan inspecting cracks crossing the pavement. Tim showed us,

on a map of geologic units and faults he compiled, that we were near the Las Animas fault. We judged them to be slumping of the road fill. Extensional cracks had no significant vertical displacement, and a few lateral offsets of up to ± 1 mm, changing along the crack.

(43) Received permission at Tony Pierce house to enter the O'Connell ranch. We drove SE from the Pierce house, carefully looking for breaks in the hard-packed dirt road and saw none.

(45) On foot we inspected an especially clean outcrop of fault gouge and sheared rock, and saw no throughgoing cracks up the outcrop. Below the fault outcrop, the hard-pack surface of the dirt road showed many short hairline extension cracks parallel to the fault strike. No measurable displacements (i.e., $\geq$1 mm all components).

7:00 p.m., return via Metcalf Road.

April 24, 1984

Ziony and Herd, San Felipe Valley

We drove to San Felipe Valley via Metcalfe Road late the afternoon of the earthquake. We carefully checked for new breaks in the pavement along the road that extends northward from the Highland School site and crosses the major mapped strands of the Calaveras fault. Our results were negative, except near the end of the public highway at locality 36. There, a narrow north-northwest-trending zone of freshly opened discontinuous cracks was observed along and generally parallel to the northeast margin of the paved road and its gravelled northern extension. The zone could be traced for about 40 meters and crossed the dusty dirt road that leads from the pavement northeastward to the nearby Hewlett and Packard ranch house.

When observed at about 4:30 p.m., individual cracks were as long as about 1.5 meters and opened from one to three millimeters. We took several photographs of the cracks. We attempted to trace the cracks northward from the road intersection but were unable to identify the zone beyond about 30 meters from the ranch-house road. The soil of the adjacent fields contained a maze of desiccation(?) cracks with no obvious trends.

Herd was strongly convinced that the zone of aligned cracks was tectonic because it is near the main trace of the Calaveras fault that he previously had mapped at the foot of a north-northwest-trending scarp just east of the paved road. He thought he saw possible right-lateral separation of about one millimeter across a zig-zag along one of the cracks. However, Ziony thought that differential settlement due to strong shaking could not be precluded because the zone of cracking also is coincident with the filled or bladed shoulder of the paved road.

We were surprised by the apparent lack of significant earthquake-triggered slope failures in the steep, friable roadcuts along Metcalfe Road. Only small piles of pebble/cobble-sized debris, which could have resulted from rainfall of the previous week, were evident locally. However, freshly broken small pieces of tree limbs were strewn across the road in places near San Felipe Creek, possibly due to strong shaking.

April 24, 1984

Clark and Harms, Southeast end of Anderson Reservoir

4:00 p.m.

Between site 65 and just north of Cochrane Bridge, are many slope failures of road fill.

(66) Rockfall onto road.
(70) Notch--no rupture on road (2-4 mm detection limit; 5-15 mm detection limit in adjacent grass).
(71) No rupture in grassy valley and notch (5-15 mm detection limit).
(72) No rupture in notch (5-15 mm detection in grass, limit, 2-4 mm in road).
(73) No ruptures on road (5-10 mm detection limit) or fields (5-15 mm limit).
(74) No rupture on small linear flat.
(63) Abundant cracks across road and below road; many appear to be related to lateral spreading or slope movement. Stop inspection at 1900.

April 24, 25, 1984
Bonilla, Aerial inspection of fault (4/24), San Felipe Valley (4/25)

The afternoon of the earthquake, Alan Bartow and I looked at the Calaveras fault from a low wing aircraft, between Calaveras Dam and Highway 152. (San Felipe Lake).

We saw no new faulting and only one landslide--the debris slide just north of the Cochrane bridge across the south arm of Anderson Reservoir.
(25) Small quadrilateral installed by Wallace and Bonilla at 1:00 p.m., 4/25/84.

April 25, 1984
Wallace and Bonilla, San Felipe Valley
(39) No cracks.
(40) Scarp, probably stream cut; no cracks.
(41) No tectonic cracks.
(25) Swale along fault. Hairline cracks.
(21) Linear scarp.
(22) No cracks in dam.
(23) Slump cracks.
(26) Well-defined fault topography.
(32) Cracks present, but not tectonic.

April 25, 1984
Lienkaemper, Perkins, Bonilla
ca 9:30 a.m., Lienkaemper, with Bonilla and Perkins, checking cracks seen by Herd in San Felipe Valley.
(36) We crossed the north gate onto the HP property and tried to find Herd's cracks. A few cracks (~ 50 cm long, no displacement) were observed in the road for ~ 60 m north of the gate. All cracks occurred in deposits that contain a significant amount of pebble and cobble size clasts. No cracks occurred within the finer grained deposits. Cracks were most probably a result of shaking and are concentrated in the coarse grained deposits. We saw none with displacement, nor any with en echelon pattern.
(31) We turned around here in careful search, walking southward also.
(36) We installed a temporary quadrilateral around Herd's cracks at the end of San Felipe Road. The quadrilateral consists of two PK-nails in the road, and two redwood stakes above the shoulder. Perkins and I measured the quadrilateral twice. 12 noon, return to Menlo Park.

April 25, 1984
Clark, Southeast end of Anderson Reservoir
07:30-10:30 a.m.

(62) Six cracks across road in zone 20-25 m wide, average azimuth of cracks, 120°; azimuth of slip about 075°. Max. net slip about 20 mm. on largest crack.

(58) No cracks in line with linear valley to southeast (which lies west of Unger Ranch driveway).

(57) Two NW-SE cracks ~ 5 m apart across road, 5 mm slip at 085° on each. Location is about 100 m E of Unger Ranch driveway.

(64) Series of large cracks across road. NW-most pair are 8 m apart, trend 170°. Easternmost of this pair shows net right-lateral slip of 70 mm, az. 115°. Westernmost shows some thrusting. Six more cracks further east in a 30 m-wide zone.

April 25, 1984
Clark, San Felipe Valley
11:00 a.m.-12:30 p.m.

(36) A few ~ 1 mm cracks have survived along E shoulder of N-S road, north and south of intersection.

(29) No cracks in E-W road.

(34) No cracks in H P road.

(35) Estimate 2-5 mm open cracks across road parallel to San Felipe Creek; have been degraded by traffic and grading. Roads at sites 29 and 34 would show 2-3 mm cracks, if present.

(38) Inspection of road from car at 5 mph; no cracks in fault zone here.

April 25, 1984
Harms and Rymer, Southeast end of Anderson Reservoir, San Felipe Valley
9:00-12:00 a.m. Recheck of cracks at location 64 to more carefully document displacement. Cracks trend 130°-160°, with generally increasing azimuth from east to west. Cracks are located on a ridge crest and are parallel to the ridge.

To the SW of the road, along the shoreline, there are abundant cracks with no dominant trend or sense of displacement. Cracks at this site range from those dominantly extensional with some vertical component, to those showing minor right-lateral or left-lateral slip. The cracks here seem to be related to slumping. Liquefaction occurred between the lake and a closed depression. This closed depression could be fault related, but is more likely caused by slumping. The liquefaction apparently occurred along the edge of this slump block.

To the NE of the road at this site the cracks continue for 10-15 m before they are dominated by more westerly-trending cracks. These cracks define several small slump blocks, but no lateral cracks were found at the western ends of these slump blocks.

We continued up the road to determine whether there was any tectonic cracking associated with the linear ridge or valley in the area of locality 58; no cracks were found.

1:00-2:30 p.m. Drove to San Felipe Valley via Metcalf Road. We weren't convinced that the cracks at site 36 were tectonic, though they had been quite degraded since the previous day. We walked eastward up the driveway and saw no fresh tectonic cracks. We walked west up the driveway to the H P Ranch and again saw nothing convincingly tectonic.

2:30-4:30 p.m. Drove west on San Felipe Road to Quimby Road. Drove slowly (~10 mph) up Quimby Road to site A (figure 1) to determine if any tectonic cracking had occurred on the Hayward fault; no fresh cracks. Drove east on Yerba Buena Road, but stopped at the edge of Kuhn property (west of site B, figure 1), because we had no permission to enter.

April 25, 1984

Mathieson, Jackson Oaks

(69) (12:00-1:30 p.m.) Jackson Oaks Tract--Oak Ridge Court and Lane traversed on foot. Five houses evacuated and condemned; a prominent crack beginning at the ridge crest was noted (see figure 2). I felt that it was associated with land failure, but its geometry was not clear to me in the short time I was there. No one knew if the crack was co- or post-seismic, but the damage to the homes implied high rates of lateral ground acceleration to the south.

Inspection of roads in Holiday Lake Estates (northwest of Jackson Oaks, see Plate 1) no breaks were noted.

April 26, 1984

Lienkaemper, B. D. Brown, K. Breckenridge, and Mathieson, San Felipe Valley

1:00 p.m.

(36) Remeasure quadrilateral at #8824 San Felipe Road, i.e., the end of the pavement. No change noted above noise since 4/25/84.

2:00 p.m.

(25) Remeasure quadrilateral at site 25, 300 ft. north of barn. Installed yesterday by Bonilla and Wallace. No changes discernable.

3:00 p.m.

Mathieson and I returned via Yerba Buena Road (site B, figure 1), a site on Hayward fault zone, and saw no cracks in the road at the distinctive scarp there.

April 26, 1984

Mathieson, Lienkemper, K. Breckenridge, B. D. Brown

To San Felipe Valley to inspect "surface rupture" and measure quadrilaterals

(36) A riser next to the flume suggests a fault scarp, perhaps accentuated (height) by the flume. This riser is straight, 2.5 m high, crosses San Felipe Road 450 m southeast of site 36--where a dip in the road sited to north scarp(?) ends abruptly.

(28) Fence lines offset left- and right-lateral, equivocal. Fence lines may have been built crooked.

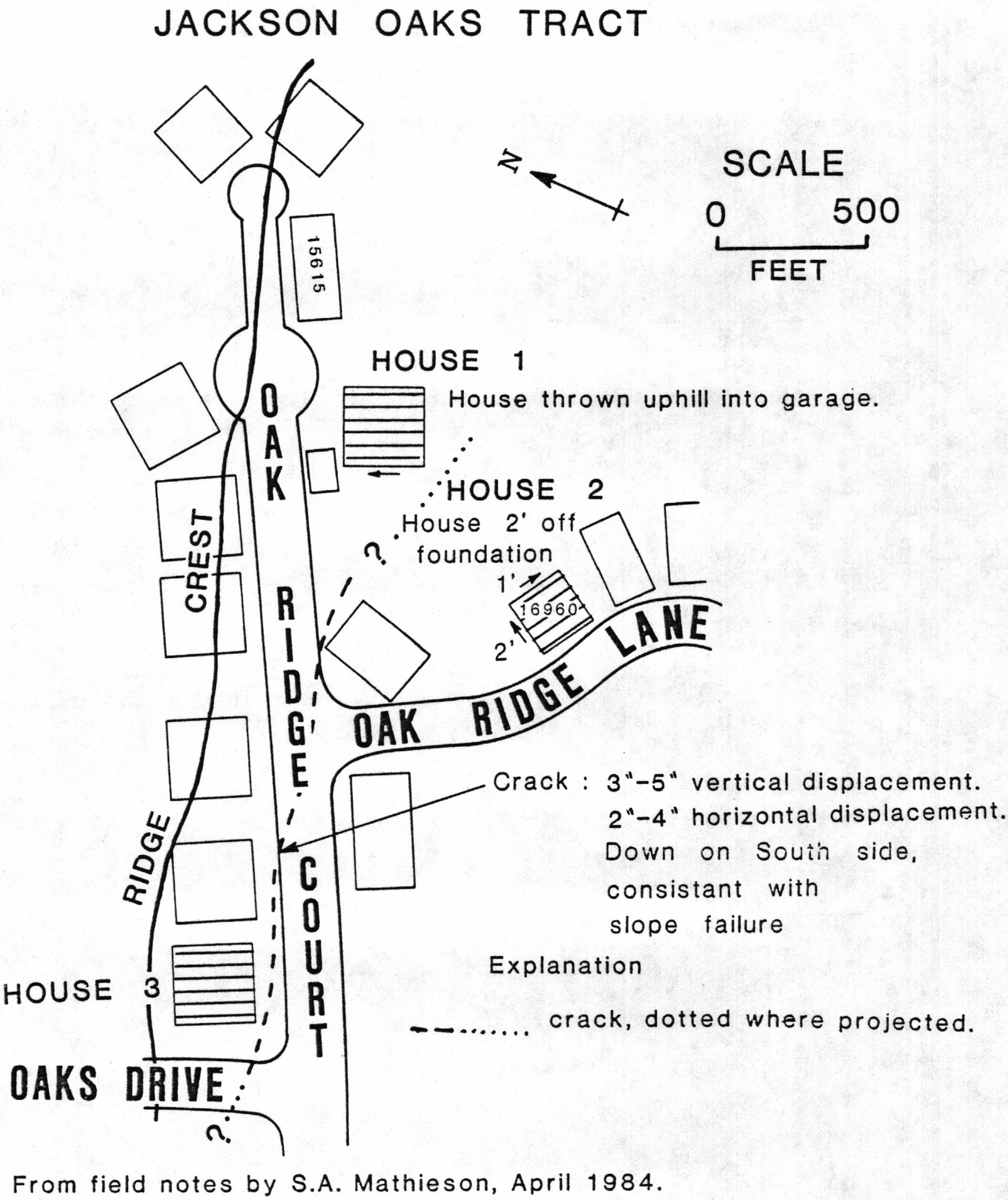

Figure 2. Sketch-map showing crack through part of the Jackson Oaks subdivision and some damage to houses.

April 26, 1984

Harms, Southeastern end of Anderson Reservoir

(62) Set of fresh cracks: SE crack is purely extensional, pre-existing crack with fresh opening. Second crack is 3-5 cm left-lateral. Overall trend of cracks is 130°, not linear.

(61) Set of cracks, zone ~ 6 m wide. Was patched on April 24, in the morning. Overall trend of cracks is 175°, extensional with minor component of left-lateral slip.

(60) A wide zone of cracking at the northern end of a slump block. Cracks are arcuate, concave towards the lake.

(59) A single crack, up to 2 cm right-lateral, 3-4 cm extensional, with an E-W orientation.

(54) Two cracks, aligned with mapped fault traces. Az. of western crack is 320°, slip vector is 4 cm long at 280°. Left-stepping en echelon cracks at northern side of road. The second crack, ~ 5 m E has an orientation of 345° with pure extension of 4 cm. This crack continues up the free face to the north of the road ~ 10-15 m, but is not apparent to the south where 2 cm displacement is the minimum visible in the surrounding vegetation.

(55) Very small fresh cracks with a series of left stepovers. Trend of cracks 011°. North to south vector azimuths and displacements are 097°, 12 mm; 078°, 7 mm; and 095°, 7.5 mm. This set of cracks continues for ~ 10 m north of the road, but is not discernable south of the road.

(56) Small extensional cracks with trend of 325°; significant only because no other cracks are present on the driveway and because it seems on trend with the linear valley to the southeast.

(64) Set of cracks, from East to West:

trend	displacement vector
325°	275°, 7 cm
307°	260°, 3 cm
320°	295°, 5 cm
342°	294°, 6 cm

April 27, 1984

Lienkaemper and L. M. Gilpin, San Felipe Valley

1:40 p.m.

(36) Remeasure #8824 San Felipe Road quadrilateral. No change.

2:15 p.m.

(25) Remeasure Bonilla-Wallace quadrilateral. This line is grassy and the grass gets flatter every remeasuring, thus all lines have shortened. Noise level is about 0.5 cm. Nails used are not very firmly planted, so this line will probably continue to be noisy. No change above noise.

3:00 p.m., after searching for faulting at (22) and (25) without finding any, we returned via Silver Creek Road.

April 27, 1984

Perkins, Radbruch-Hall fault traces between San Felipe Creek and Anderson Reservoir. All sites were investigated on foot. No primary tectonic rupture related to surface faulting was found.

(44) (1:00 p.m.) Road and stream cut along San Felipe Creek. Good exposure of the fault zone in bedrock and Holocene terrace deposits. The bedrock and related gouge contained many recently formed cracks. Some cracks were oriented subparallel to the trend of the fault. The cracks were ~30 cm in length and exhibited no offset. The cracks were within a zone ~5 m wide and coincident with the fault. In vertical exposures the cracks penetrated the ground less than 50 cm. The Holocene terrace and flood plane deposits locally contained cracks subparallel to the trend of the fault. These cracks exhibited no offset. Detection level > 2-5 mm.

(45) (1:30 p.m.) Dirt road coincided with the fault for ~ 50 m, and the fault continues on into a small vegetated valley that contains a small sag pond. The hard-packed dirt road contained abundant fresh cracks, most of which were randomly oriented. There is a tendency for some cracks to be subparallel to the trend of the fault in a ~ 5 m-wide zone. Most cracks were less than 50 cm long and exhibited no offset. No cracks were observed in the valley or in the mud surrounding the sag pond. Detection level on the road was > 2 mm, in the valley > 5 mm.

(47) (2:00 p.m.) Fault located in saddle east of the road, for ~40 m. Poor exposure of trace owing to soil and thick vegetation. No cracks were observed. Detection level > 10 mm.

(48) (2:30 p.m.) Fault is adjacent to, or coincident with, the dirt road for 500 m. On the road, good surface exposure; off the road, fair to poor exposure. Abundant desiccation cracks on and off the road. Some small (~30 cm) cracks on the road are subparallel to the fault and exhibit no offset. Detection level on the road > 2 mm, off the road 2-10 mm.

(49) (3:15 p.m.) Investigate road between the 2 strands of the fault. Walked road for ~700 m. Abundant desiccation cracks in fine-grained portion of the road. No cracks with consistent trends observed. Detection level > 2 mm.

(50) (4:00 p.m.) Fault is coincident with the road for ~ 250 m. Abundant desiccation cracks in the clay-rich portions of the road. No cracks consistently oriented subparallel to the trend of the fault. Detection level > 2 mm.

(52) (4:45 p.m.) Fault adjacent to and coincident with dirt road for 200 m. Abundant desiccation cracks on and off the road. No cracks consistently oriented subparallel to the fault. Detection level on the road > 2 mm, off the road 5-10 mm.

April 27, 1984

Harms, SE end Anderson Reservoir and southern end of San Felipe Valley

Rechecked the cracks at the southeastern end of Anderson Reservoir. E. Hart (CDMG) and others had painted the cracks at site 64; no change there.

Drove to San Felipe Creek, via Metcalf Road. Walked two traverses (east of San Felipe Road, between sites 42 and 43) that cross the mapped fault, searching for breaks. No cracks were present on these roads. (Refer to Plate 1 for location).

April 27, 1984

Rymer, Inspect surface rupture associated with 1979 Coyote Lake earthquake. Locations are on Figure 1.

(H) 9:30 a.m. Shore Road, adjacent to creepmeter, 4.8 km SE of Highway 152 and San Felipe Lake. The creepmeter showed 13 mm of coseismic slip (see Schulz, this report). Fresh cracks on the SE side of the road, within 2 m of the creepmeter have a net offset of only 3-1/2 mm. This fresh crack is en echelon with older cracks in the pavement, which also have fresh crack extensions. The fresh crack on the SE side of the road is 110 cm long. On the NW side of the road, new fresh cracks are less well-developed and have only as much as 2 mm of right-lateral slip parallel with the fault.

Azimuth of fault = 350°; offset is 5 mm at 304°.

(I) No fresh tectonic cracks were observed in this region.

(G) 10:30 a.m. On Highway 152, north of San Felipe Lake, at site of 1979 surface rupture. Slight fresh cracking on north side of road, but still in pavement. The new cracks extend from older cracks and are in a set that crosses the road parallel with the fault.

Azimuth of fault = 146°, offset is 1 mm at 128°.

May 2, 1984

Lienkaemper and Mathieson, Halls Valley, San Felipe Valley, Coyote Lake

09:30 a.m., Arrived at Halls Valley, via Mt. Hamilton Rd.

Search pavement for breaks at faults on Herd's maps. No breaks seen in pavement at (5), (6), and (8). Turn back at Smith Creek Ranger Station. We walked across mapped fault lineaments on east side of Grant Lake; nothing noted.

10:45 a.m., Leave Grant Lake, Halls Valley via Quimby Road, enroute to San Felipe Valley.

(38) No breaks seen while driving by.

(36) 11:40 a.m. Remeasured quadrilateral. No changes above noise.

(22) to (14) 12:40 p.m. On foot to Panochita Hill. This closes the gap with checking by Lajoie and Mathieson.

(19) Stream deeply incised (ca. 2-2.5 m) with ~ 90° walls along the channel; indicates possible rapid uplift here.

(16) Opportunity for spotting any ruptures was good in here. About a millimeter of consistent lateral offset would show here, but did not. This part of the fault did not rupture.

2:30 p.m.

(25) Bonilla-Wallace quadrilateral remeasured. No change since 4/26/84.

(24) No breaks found. Conditions poor, a few cm of lateral offset, might not be visible.

(C) (Figure 1) Walked across Coyote Lake dam. Good for seeing ~ 1 cm offsets, but none seen. Concrete in floor of spillway is clearly unbroken. East wall of spillway is full of breaks from continuing slumping in that abutment.

(D) (Figure 1) 4:30 p.m. Check lineament on Herd's map. Minimum detection of 3 mm of lateral displacement in the ~ 1 cm desiccation cracks. probably no tectonic breaks here.

(E) (Figure 1) 5:00 p.m. Look at en echelon, left-stepping cracks across Roop Road. They are very old and have been spray painted.

Drove back to highway via Ruby Canyon (Leavesley Road); nothing noted.

May 2, 1984

Mathieson and Lienkaemper, Halls Valley, San Felipe Valley, Coyote Dam

(30) 12:30 p.m.--Drove along westernmost of two roads north of Hewlett-Packard Ranch; supposed to be directly astride one of Herd's solid traces, nothing noted. Trace 20-30' west of road at subtle break in slope.

12:45 p.m.--Began traverse to Panochete Hill to end of Mathieson-Lajoie traverse. Cracks along the long stretch of road farthest from Herd trace (Site 17) appear to result from clay concentration in the road surface and desiccation.

(18) West branch of San Felipe Creek is freshly incised from 1 to 2.5 m.

(20) Side creek incised to 0.75 m. Incision up to .5 meters is common along west branch of Las Animas Creek, along San Felipe Road near United Technology property.

(44) 5:10 p.m.--0.4 miles south of dam where Herd shows solid line trace of fault, nothing noted aside from many desiccation cracks.

May 3, 1984

Lienkaemper, Mathieson, and B. D. Brown

A M_L 4.5 aftershock in San Felipe Valley occurred ~ 6:00 a.m.

(36) (10:45 a.m.) No change in quadrilateral since 04/25/84.

(25) Bonilla-Wallace quadrilateral (11:20 a.m.). No change since 04/26/84.

May 3, 1984

Harms and Rymer, SE end of Anderson Reservoir

(53) Two cracks, not previously noticed, extend into the shoulder of the road. Orientation of the southern crack is 016°, with a 5 mm of slip at 085°. Orientation of the northern crack is 018°, with 5 mm of displacement at 091°.

Cracks along shoreline adjacent to site 64 demonstrate no consistent sense of right-lateral movement. Left-lateral displacement and pure extension dominate. The cracks seem to be related to slumping.

(78) Fresh cracks along the SW shoreline of Anderson Reservoir show 3.5 cm left-lateral displacement and 3 cm extension. This is a slump toward the lake, on the NW side of a young fan deposit.

(75) Cracks lie on trend with the cracks across the lake at site 64. These trend 165° and have 11 cm of extension; no lateral component of slip is present. At the southern end these cracks curve downhill. Distinctive cracks at site 65, extend approximately 50 m SE of the road. These cracks trend 300-310°, with 2.5-5 cm of displacement at 255°.

May 4, 1984

Clark, SE End Anderson Reservoir

(65) Two cracks across Dunne Road west of Martin driveway, 2-3 m apart. Northernmost has 120-mm right-slip at 095° azimuth; southernmost has 100 mm of right slip at 105°. One-half to two m long, left-stepping en echelon cracks lie on trend to the SE at top of road cut. They enter heavy brush ~ 30 m SE of top of cut. No cracks seen along zig-zag route followed along trend 50-60 m from cut SE of heaviest poison oak.

(68) No cracks from (13) to corral NW of barn, which has many dilation cracks with up to 50 mm open and 50 mm N-E side down. Cracks trend 90°-205°. They appear to relate to free faces to the N and E. Cracks do

not cross cleared ground to SE and NW. No cracks along scraped E and N boundaries of housing (Jackson Oaks).

(67) Walk path along scarp and notch SE of Cochrane Bridge. Has small depression, but no sign of cracks. Cracks > 5 mm open would be visible if present.

May 11, 1984

Harms, Anderson Reservoir

Checked Steeley Rd., as is shown on Plate 1, for tectonic fractures, especially in the linear bedding at the NE end near Finley Ridge. No cracks were found.

May 16, 1984

Harp, Jackson Oaks

On 5/16/84, I investigated the fissure that extends through the street and driveways along Oak Ridge Court in Jackson Oaks (site 69) in approximately an E-W orientation in an attempt to determine whether the crack is of fault origin or related to the movement of a preexisting landslide during the earthquake. In my inspection, I used the sketch map prepared by Mathieson (Figure 2) to take advantage of earlier observation of the feature.

The present state of the fissure is as Mathieson has sketched it, (figure 2) except that, at its east end where he has dashed it with question marks between house #1 and the house on the corner of Oak Ridge Court and Oak Ridge Lane, I cannot find it. I can trace it eastward through the driveway of the corner house, but it disappears there. If present beyond there, it should show well in the lawn south of house #1, but it does not. I continued to search for any eastward extension of the fissure for approximately 300-400 m from house #1, but could find none.

In my opinion, there is nothing about the fissure that suggests definite affinity with any preexisting landslide mass. The terrain east of Jackson Oaks certainly has the morphology of old, greatly modified slump/earthflow topography; however the crack in question does not appear to me to be related to the movement of an old landslide. In fact, I could find no evidence of any landslide movement in the immediate area due to the earthquake with the exception of some rocks dislodged by shaking just east of the end of Oak Ridge Court.

I suspect the fissure may owe its origin to shaking-induced settlement of fill placed in a water-line or some other type of trench, or to settlement of fill along a grading contact created during development of the subdivision. Without further investigation such as trenching or inspection of maps of utility lines and fill limits, the relationship of the fissure to fill emplacement and settlement cannot be definitely established.

May 16, 1984

Harms, Southeastern End of Anderson Reservoir

Mapped the northward extension of the cracks at site 64. These cracks curve to the west and step right for about 75-100 m. The overall trend is more northerly ($\sim 350°$) than for the cracks visible in the road. The cracks apparently have no lateral component, though recognition would be difficult in that vegetation. Extension across these cracks was up to 5 cm.

(76) A long, continuous crack follows the well-defined linear valley just south of the Unger Ranch house. It has ~ 1-2 cm extension, is oriented at 160° and continues for ~ 50 m. This crack has no lateral displacement.

(77) A crack parallels the road, with an azimuth of ~ 145°. It has ~ 1 cm extension, no lateral displacement and continues for 30-35 m.

REFERENCES

Allen, C. R., Wyss, Max, Brune, J. N., Grantz, Arthur, and Wallace, R. E., 1972, Displacements on the Imperial, Superstition Hills, and San Andreas faults triggered by the Borrego Mountain earthquake, in The Borrego Mountain earthquake of April 9, 1968: *U.S. Geological Survey Professional Paper 787*, p. 87-104.

Clark, M. M., Sharp, R. N., Castle, R. O., and Harsh, P. W., 1976, Surface faulting near Lake Oroville, California, in August. 1975: *Bulletin, of the Seismological Society of America*, v. 66, p. 1101-1110.

Dibblee, T. W., 1972, Preliminary Geologic Maps of three quadrangles, Santa Clara County, CA: *U.S. Geological Survey Open-File Report 72-90*.

---1973, Preliminary geologic maps of the Gilroy Hot Springs, Gilroy, Mt. Sizer, Mt. Madonna, and Morgan Hill quadrangles, Santa Clara and Santa Cruz Counties., CA: *U.S. Geological Survey Open-File Report 73-59*.

Fuis, G. S., 1982, Displacement on the Superstition Hills fault triggered by the earthquake, in The Imperial Valley, California, earthquake of October 15, 1979: *U.S. Geological Survey Professional Paper 1254, p. 145-154*.

Radbruch-Hall, D. H., 1974, Map showing recently active breaks along the Hayward fault zone and the southern part of the Calaveras fault zone, California: *U.S. Geological Survey Miscellaneous Investigations Series, Map I-813*.

Sieh, K. E., 1982, Slip along the San Andreas fault associated with the earthquake, in The Imperial Valley, California, earthquake of October 15, 1979: *U.S. Geological Survey Professional Paper 1254, p. 155-160*.

LANDSLIDE AT LA HONDA, CALIFORNIA PROBABLY TRIGGERED BY THE APRIL 24, 1984, MORGAN HILL EARTHQUAKE

Gerald F. Wieczorek and David K. Keefer

U.S. Geological Survey
345 Middlefield Rd. ms-998
Menlo Park, CA 94025

INTRODUCTION

The April 24, 1984 Morgan Hill earthquake was felt strongly throughout the San Francisco Peninsula and the Santa Cruz Mountains (Fig. 1). A large landslide near La Honda, California was observed soon after the earthquake and was probably triggered by the earthquake. This landslide of approximately 6.5 hectares (16 acres) was first noticed by Mr. Henry Cunha on April 25, the day after the earthquake, when he made a survey of his ranch. He observed fresh ground cracks, crevices, grabens and other evidence of landslide movement. These landslide features had not been present when Cunha had previously traversed the area on April 20. Although no nearby strong-motion records are available, the shaking intensity near the landslide was so strong that one resident ran from a house; this suggests an intensity of Modified Mercalli (MMI) VI.

Description of the landslide

The landslide is approximately 200 m (660 ft) wide by 280 m (920 ft) long. The surface is gently rolling and covered with grass and oaks (Fig. 2a). The average surface slope from the head of the landslide to the toe is between 7 and 11 degrees (12 to 19 percent). The morphology and predominantly translational movement of the landslide indicate that it is a block slide according to the landslide classification of Varnes (1978). At the head of the landslide is a prominent graben. Preliminary measurements in the horizontal plane across the graben indicate displacements of 1.2 to 1.5 m (4 to 5 ft) to the southwest (Fig. 2b). The lateral margins of the landslide are marked by jagged lateral shear surfaces. The toe of the landslide is marked by a low ridge, a few tens of centimeters high. This contains an underthrust shear surface, where the landslide toe has been thrust 25 cm under the ground surface immediately downslope. The landslide exhibits one zone of internal cracking; however, most of the ground surface on the landslide is intact, and trees on the surface are not tilted. The landslide thus moved largely as a single, intact translational block. Amounts and directions of displacements are shown in Figure 3.

The graben, the cracks along the lateral margins of the landslide, and most internal cracks do not comform the topography, but rather trend across topographic lows and highs. This and the lack of surface disruption suggest that the landslide is deep-seated. Along the southeastern margin of the landslide, cracks up to 5 m (16 ft) deep disrupt the surface of the ground at Pt. A (Fig. 3), which is 20 m (65 ft) lower in altitude than the top of the adjacent rise (Pt. B, Fig. 3). This relationship suggests the depth of the landslide is at least 25 m (80 ft). The landslide occurred in an area of prehistoric deep-seated landsliding estimated to be between 15 and 60 m deep (Wieczorek, 1982). The sliding surface may have occurred on a deep plane of low resistance formed by previous episodes of landsliding.

Climatologic and Hydrologic Conditions

Although landslides are common in this part of the Santa Cruz Mountains, most are triggered by intense storm rainfall in December, January or February or by ground-water levels that gradually rise during the rainy winter season, which usually extends from October through April (Wieczorek, 1982). During the 1983-84 winter, the intense storms terminated in late December of 1983, and less frequent showers of more moderate intensity continued until March. Total 1983-1984 seasonal precipitation prior to the earthquake was approximately 20 percent less than normal. Some deep-seated landslides in the La Honda area moved during the very wet winters of 1981-82 and 1982-83 and showed signs of renewed activity in November and December, 1983 and(or) January 1984. However, because of fewer late-winter storms and below-average annual rainfall, landslide movements ceased in January of 1984 as ground-water levels in the hillside materials began to decline (G. F. Wieczorek, unpublished data). Mr. Cunha observed no landslide movements on his ranch this winter prior to the April 24 earthquake.

When we inspected the landslide on May 15 and May 18, 1984, we observed no water standing in cracks and noted that soil exposed in scarps and cracks was dry or only slightly moist. Thus, the ground-water level was at least 5m below the ground surface at that time. The bowl-shaped topography of the area upslope from the landslide (Fig. 3) suggests that water may infiltrate into the slopes above the landslide and flow towards the flatter-lying area of the landslide, thus creating a body of perched ground water in the landslide. From measurements of ground-water levels on other slopes of similar gradient and material composition in this vicinity, ground-water levels in April and May are generally between 10 and 25 m (30 and 80 ft) deep (Wieczorek, 1981).

Earthquake Magnitude and Distance of Earthquake Epicenter From the Landslide

This landslide is 53 km (33 miles) from the preliminary epicenter (Eaton, this volume) of the April 24, 1984 Morgan Hill earthquake ($M_S = 6.1$) (Fig. 1). According to a worldwide historical review of relations between earthquake magnitude and epicentral distance for different types of landslides (Keefer, 1984), this landslide is approximately at the maximum distance from the epicenter that a $M_S = 6.1$ event is likely to cause a block slide in a highly susceptible material. The distance of the block slide at La Honda from the epicenter (53 km) is plotted as point A on the magnitude-distance diagram in Figure 4. Most or all other landslides presumed to have been caused by this earthquake, however, are within about 30 km (20 miles) of the epicenter (E. L. Harp, D. K. Keefer, and R. C. Wilson, unpublished data). Thus, if the La Honda landslide were seismically triggered, it probably involved one or more rather unusual conditions, such as significant focusing of seismic energy at the site, anomalous pertubations of the ground-water level by the shaking, or a very marginal stability of the hillside before shaking began.

Conclusions

The lack of rainfall during the time preceding the landslide, the lack of other landslide activity in the La Honda area during the previous several months, and observations that conclusively bracket the landslide occurrence in a 5-day-long period that included the Morgan Hill earthquake suggest that the

La Honda landslide was probably seismically triggered. The landslide is located at approximately the greatest epicentral distance that a M_S 6.1 event is likely to trigger a landslide of this type, based on worldwide historical evidence. However, most or all other landslides from this earthquake were much closer to the epicenter, suggesting either that the timing of the landslide was coincidental to the earthquake or that some unusual conditions that aided seismic triggering were present at the La Honda site. We are currently conducting studies of this landslide to determine the surface and subsurface conditions in more detail.

References

Keefer, D. K., 1984, Landslides caused by earthquakes: *Geological Society of America Bulletin*, v. 95, no. 4, p. 406-421.

Varnes, D. J., 1978, Slope movement types and processes, in Schuster, R. L. and Krizek, R. J., eds., Landslides: analysis and control: *National Academy of Sciences, Transportation Research Board Special Report 176*, p. 12-33.

Wieczorek, G. F., 1981, Ground-water level and precipitation data for slopes near La Honda, California: *U.S. Geological Survey Open-File Report 81-367*, 25 p.

Wieczorek, G. F., 1982, Map showing recently active and dormant landslides near La Honda, central Santa Cruz Mountains, California: *U.S. Geological Survey Miscellaneous Field Studies Map 1422*, scale 1:4,800.

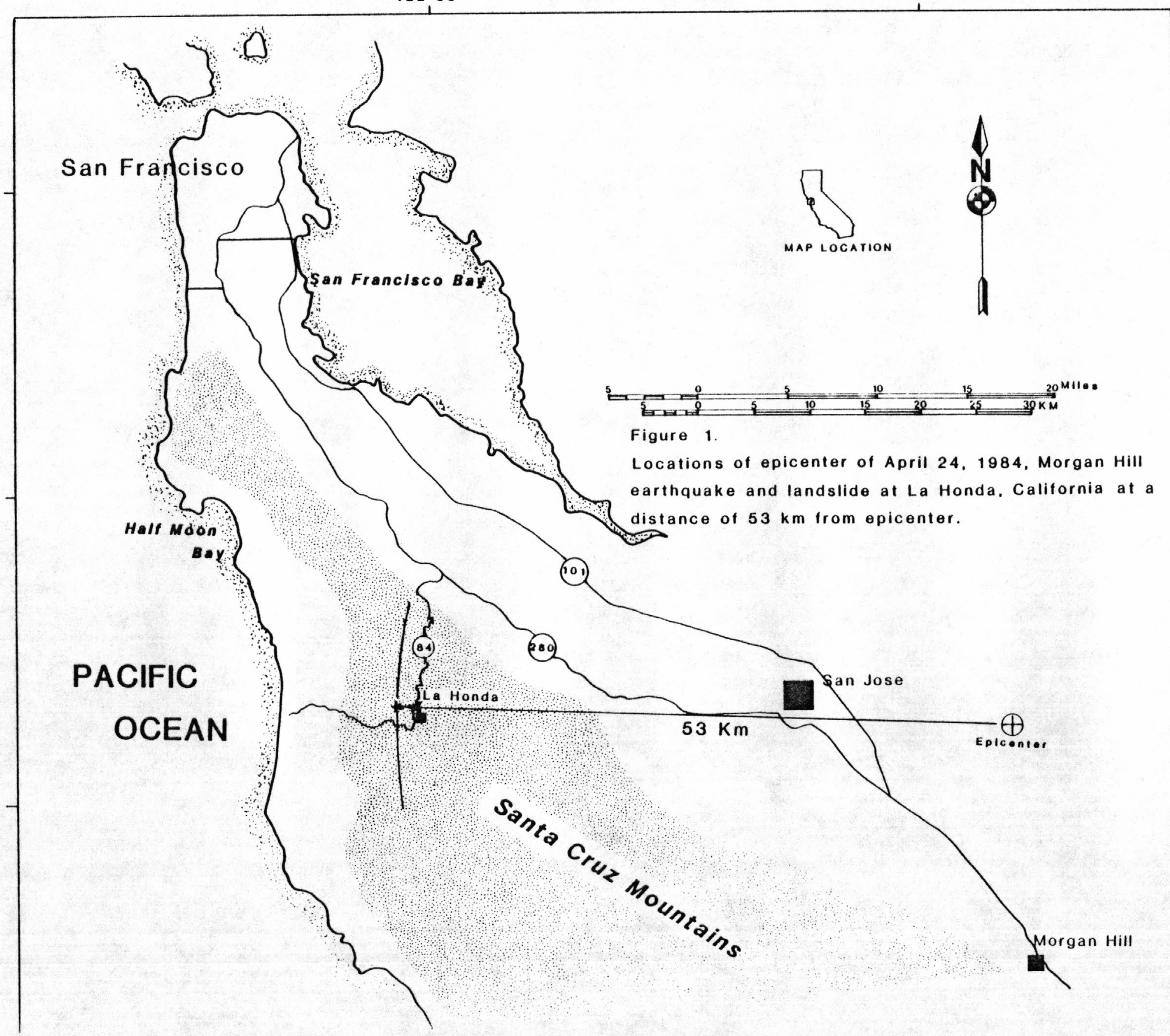

Figure 1.
Locations of epicenter of April 24, 1984, Morgan Hill earthquake and landslide at La Honda, California at a distance of 53 km from epicenter.

Figure 1. Locations of epicenter of April 24, 1984, Morgan Hill earthquake and landslide at La Honda, California at a distance of 53 km from epicenter.

a)

b)

Figure 2. Landslide at La Honda, California probably triggered by the April 24, 1984, Morgan Hill earthquake. a) Scarp along northeastern portion of landslide. View north. b) Graben at head of landslide, measurements across graben show 1.2 m (4 ft) of displacement toward the southwest.

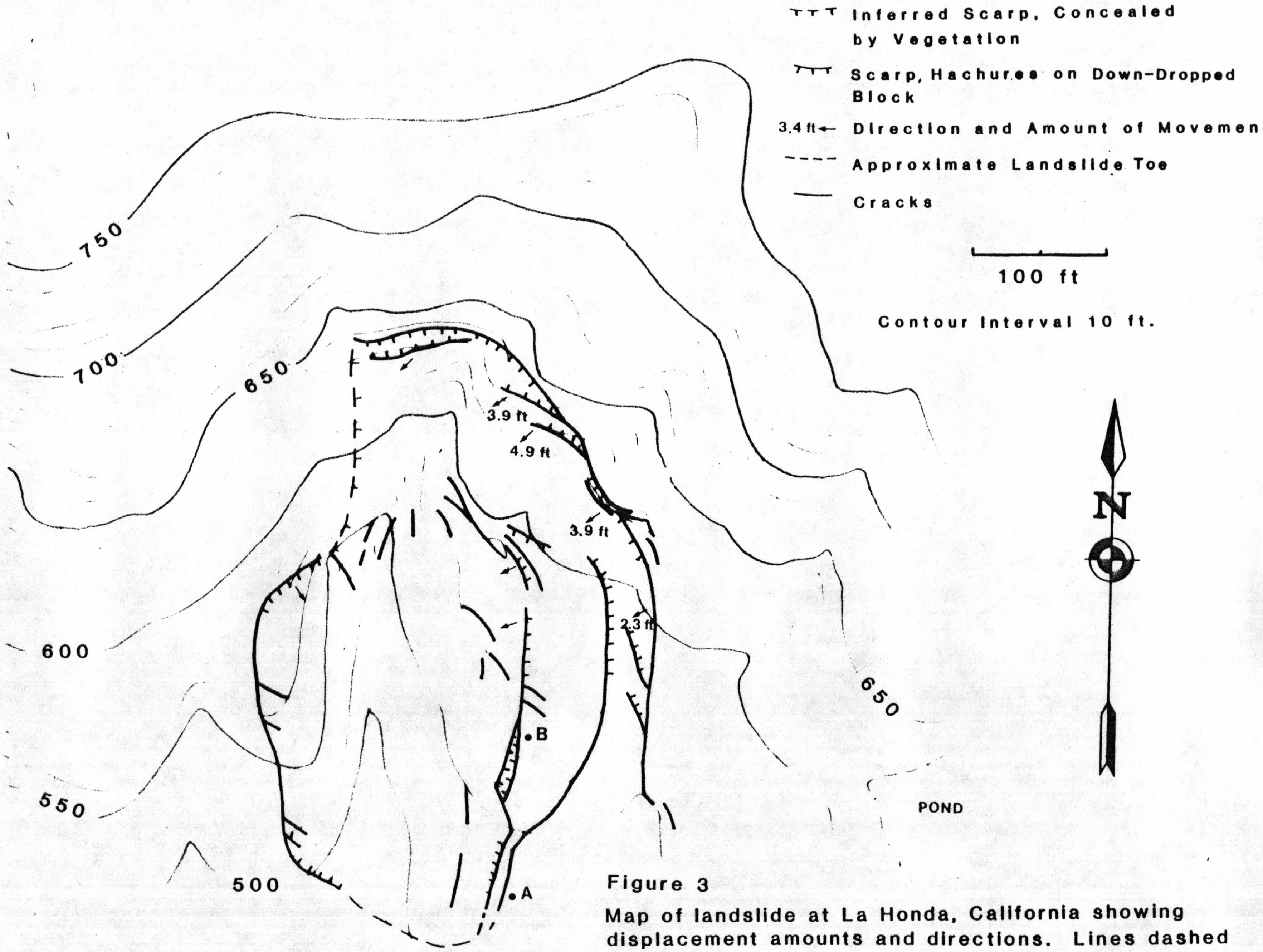

Figure 3

Map of landslide at La Honda, California showing displacement amounts and directions. Lines dashed where locations approximate. Points A and B discussed in text.

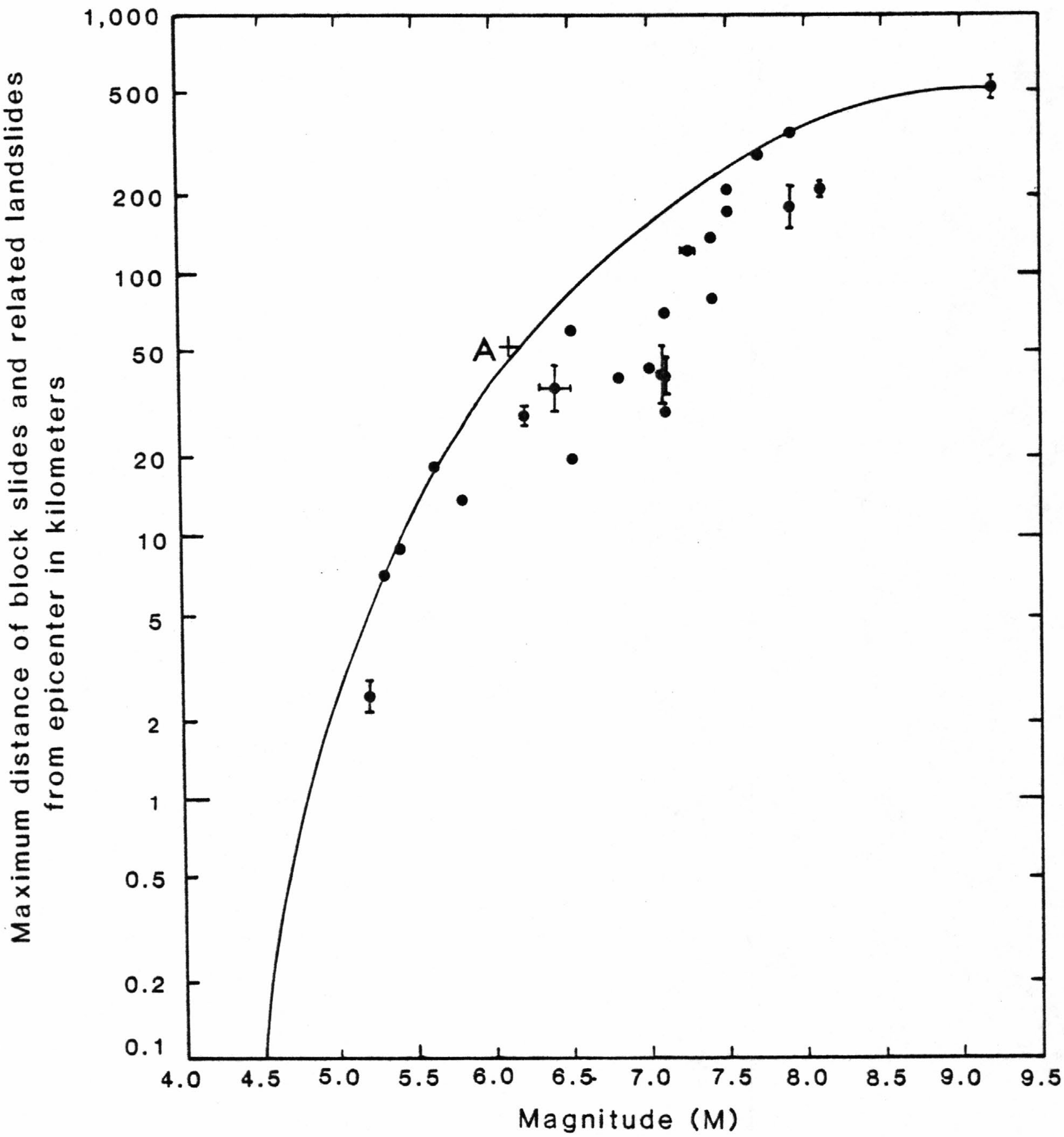

Figure 4.

Plot of maximum epicentral distance for block slides and related landslides as a function of earthquake magnitude for historical earthquakes. Dots are historical earthquakes referenced in Keefer (1984). Solid line is approximate upper bound enclosing all historical data as determined by Keefer (1984). Point A represents the epicentral distance of the landslide at La Honda from the April 24, 1984 Morgan Hill earthquake (M_S = 6.1).

GROUND FAILURE DAMAGE AND LIQUEFACTION DURING THE 1984 MORGAN HILL, CALIFORNIA, EARTHQUAKE

T. Leslie Youd

U. S. Geological Survey
345 Middlefield Rd. MS-977
Menlo Park, California

The April 24, 1984 Morgan Hill, California earthquake caused severe damage to several houses and and a bridge in the Morgan Hill area and generated a few minor liquefaction effects. This study investigated the influence of ground failure on earthquake damage and the extent of the liquefaction effects.

Initial news reports from the Morgan Hill area noted that several houses were "off their foundations" in the Jackson Oaks subdivision (Fig. 1). I inspected the more severely damaged of these homes and found that the perimeter and interior footings were not damaged by the earthquake. The severe damage to the structures was due to shear deformation within the wall immediately above the foundation. In most instances, the exterior sheeting, either plywood or fiberboard, provided the shear resistance for these structures. This sheeting fractured or pulled away from the wall during the earthquake, allowing the walls to distort in shear. It was these distortions that caused the houses to shift "off" their foundations (Fig. 2).

A prominant fissure cracked driveways and the street near the crest of the hill upslope from the damaged houses described above (Fig. 3). This fissure which was as wide as as 50 mm and contained scarps as high as 150 mm probably was caused by local ground failure and probably marked the head of an incipient slope failure. The fissure and accompanying minor downslope movement, however, had no detectable influence on damage to the houses. One or more pipeline breaks, however, occurred along the fissure.

A bent[1] supporting the south end of the Cochrane bridge (Steeley Road) was tilted and fractured by the earthquake (Fig. 4). The cause of the damage to the bent may have been downslope movement of a deep landslide that pushed or carried the pier supporting the bent toward the reservoir.

Fissures caused by landslide movements fractured the pavement of Steeley road on both sides of Anderson Reservor. Many of the fractures broke through recent patches in the road pavement. Interviews with local residents confirmed that landslides had caused considerable disruption to the road during the previous winter and that repairs had been made prior to the earthquake. Many of these landslides were reactivated by the earthquake. More detailed descriptions and delineations of fissures and landslides in these areas are given by Harms and others in the section entitled, "The Search for Ground Rupture".

----

[1]A bent is a structural frame, usually trapezoidal in shape, that provides vertical and lateral support to a bridge, building, or other structure.

A search was made for liquefaction effects in the area surrounding Anderson Reservoir and in San Felipe Valley. The only sand boils discovered were at a single locality near the east shore of Anderson Reservoir (Fig. 1). Most of these these sand boils erupted through earthquake-generated fissures and deposited thin veneers of sand in generally circular-shaped areas surounding each vent (Fig. 5). Sand boil deposits were up to one meter in diameter but only a few centimenters thick. The arcuate-shaped fissures were as wide as a few centimetes and evidently were caused by minor lateral spreading as a consequence of liquefaction.

With the help of M. J. Bennett, I searched several other areas where geologic conditions appeared favorable for liquefaction to occur. In particular, I searched the flood plain and nearby area along Coyote Creek west of Anderson Reservoir (Fig. 1) and the lowlands along San Felipe Creek in San Felipe Valley. I found no sand boils or fissures along Coyote Creek and only a few millimeter-wide cracks along San Felipe Creek. The north and south ends of Anderson Reservoir could contain sediment layers susceptible to liquefaction, but because of their inaccessibilities, we did not search these deltas on foot, but did I did view the delta at the south end from a hill about 1 km away with the aid of binoculars. I could not discern any fissures or sand boils on that delta. Also I did not hear any reports of fissures or sand boils from others who visited or flew over the deltas and other areas in the region.

The sediment in Along Coyote and San Felipe creeks is coarse, containing large fractions of gravel and cobbles. This coarseness may render this sediment too permeable for build up of pore-water pressure and the onset of liquefaction.

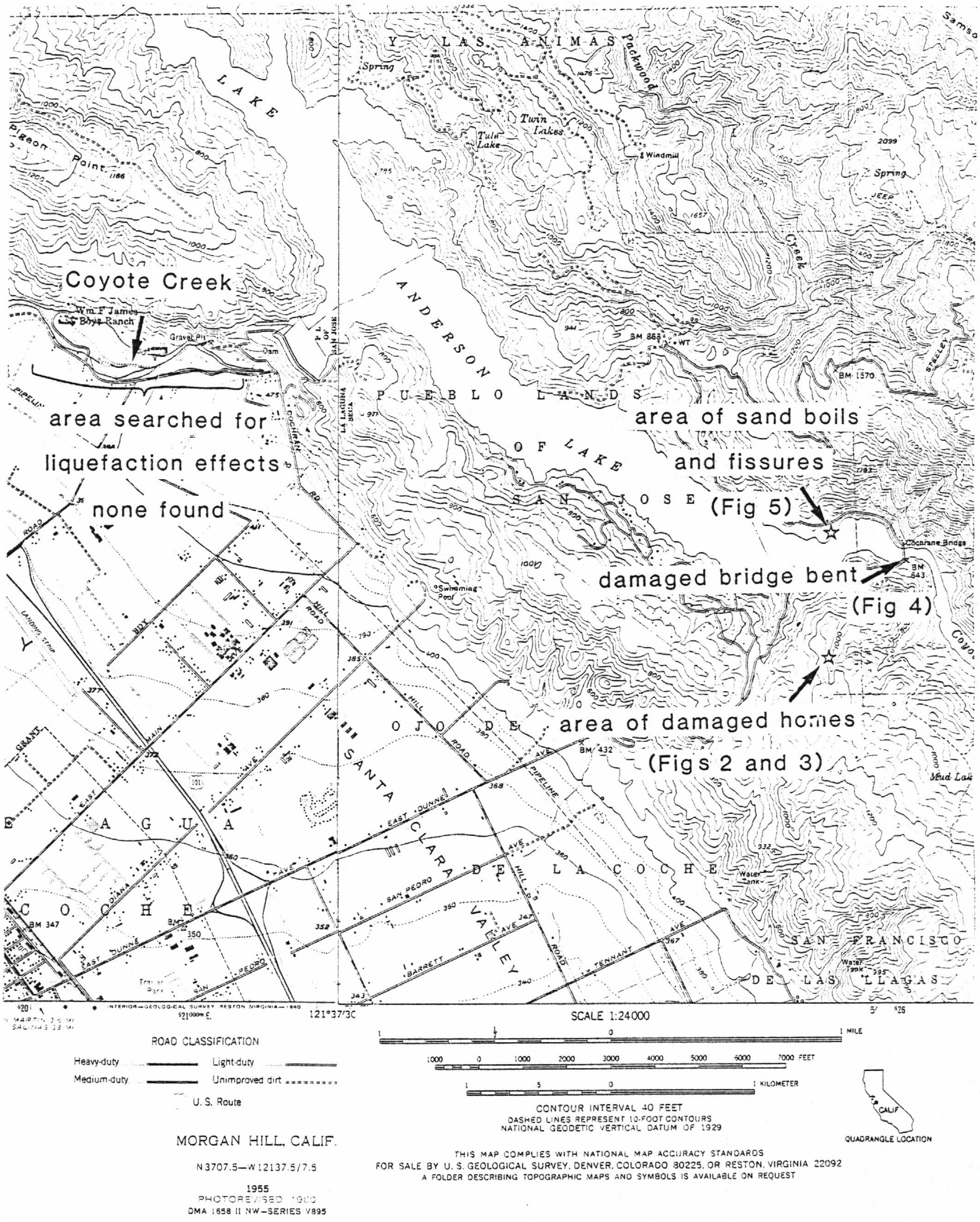

Figure 1. Map the area near Anderson Reservoir showing localities of earthquake effects described in this report.

a)

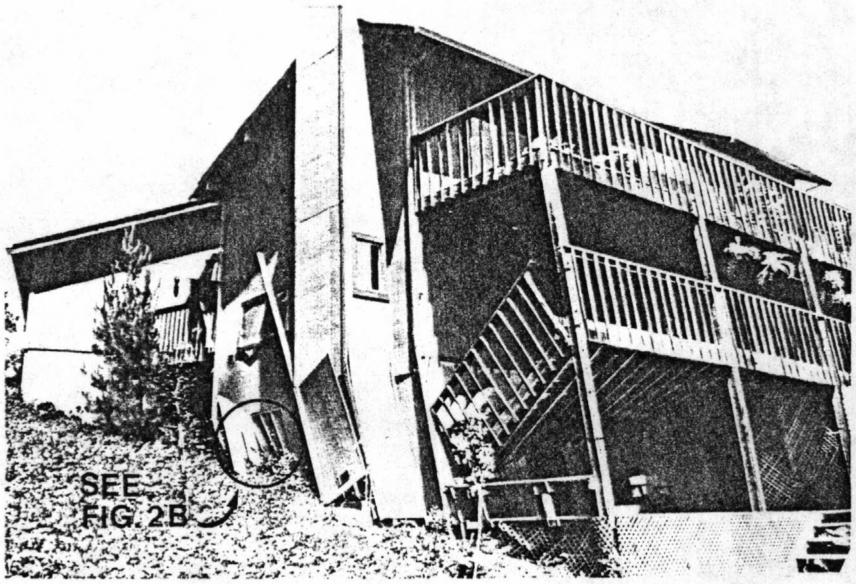

b)

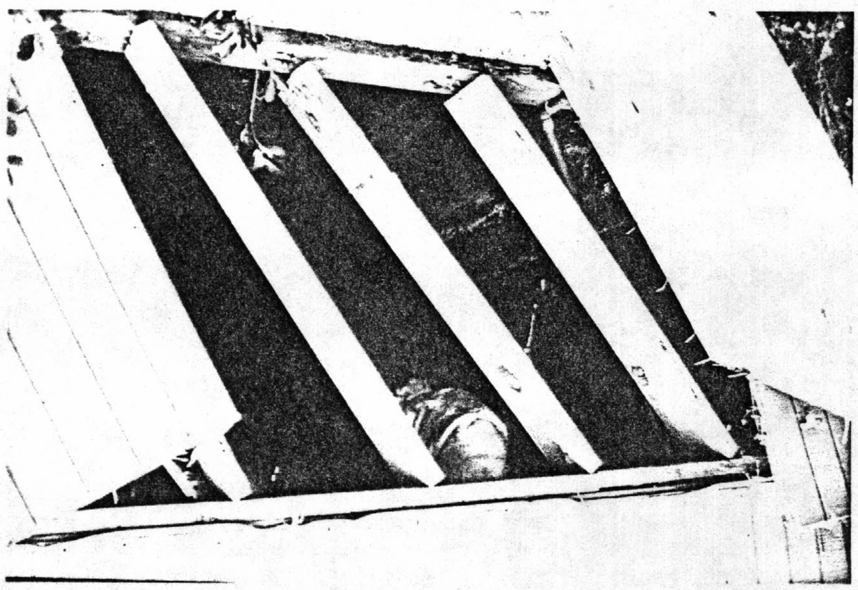

Figure 2. A house reported as "off its foundation" in Morgan Hill. The perimeter and interior footings of the house are intact and undamaged by the earthquake. The lateral displacement of the house and consequent damage was due to shear deformation within the wall immediately above the foundation. a) View of house from a distance showing damage and distortion to the sturcture. b) Close-up view skewed studs and siding that pulled off from the wall as the structure deformed.

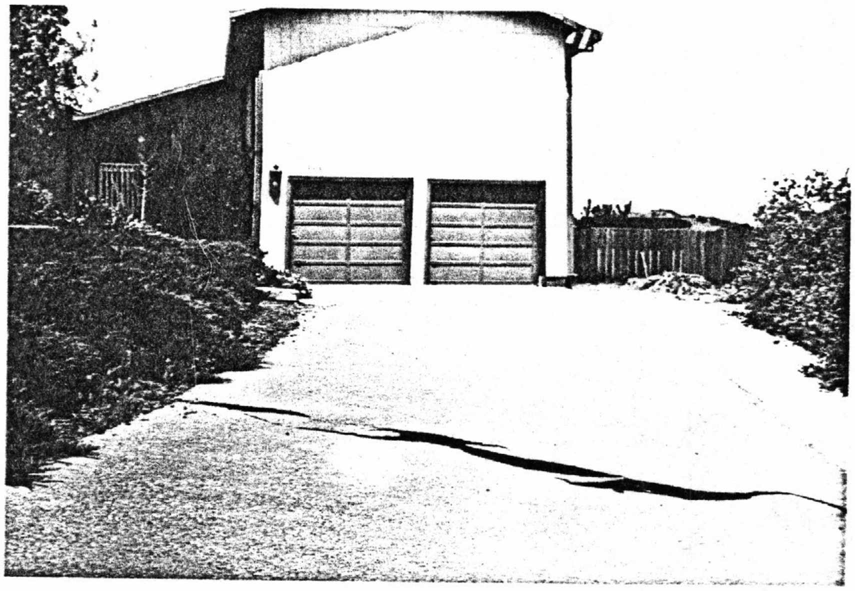

Figure 3. Prominent fissure in a driveway near the crest of the hill above the house shown in Fig. 1. The fissure was caused by local ground displacemnt, probably an incipient slope failure, but had no significant influence on damage to the houses in the area.

Figure 4. Tilted and fractured bent[1] of Cochrane bridge. The tilting and fracturing of the bent were possibly caused by deep-seated movement of a landslide that pushed or carried the pier supporting the bent toward Anderson Reservoir.

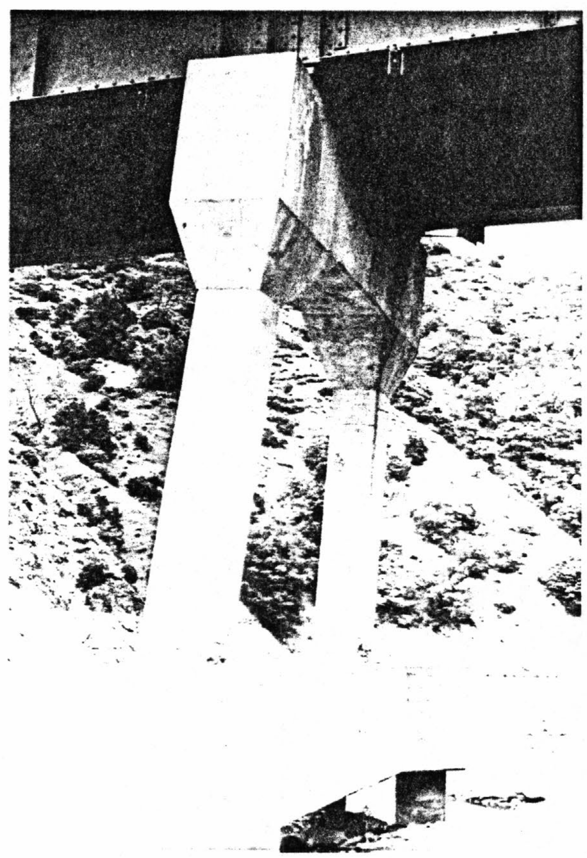

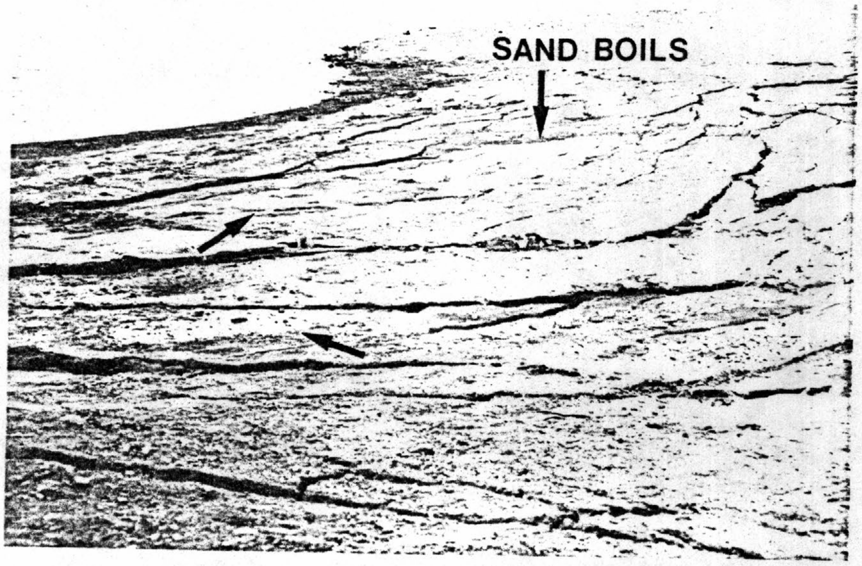

Figure 5. Sand boils and fissures near the shoreline on the east side of Anderson reservoir. Liquefaction and minor lateral spreading caused these features.

GROUND-WATER CHANGES BEFORE THE MORGAN HILL EARTHQUAKE

Chi-Yu King and David Basler

U.S. Geological Survey
345 Middlefield Road
Menlo Park, CA 94025

This report presents some preliminary data recorded at two springs and two shallow wells situated along the Hayward fault, where the ground water seems to have shown some anomalous changes in quality beginning two years before the magnitude 6 Morgan Hill earthquake on April 24, 1984. Temperature, salinity and conductivity of ground water have been measured with a portable instrument (Yellow Springs Instrument Co., Model 33) about once a month since late 1975 at two springs in Alum Rock park east of San Jose and approximately 15 kilometers from the epicenter of the Morgan Hill earthquake (fig. 1). Water flow rate has also been recorded at the orifice of one of the springs (Sulfur Spring #11). Both springs are located within the middle member of the Monterey formation which consists of thin bedded opaline chert and cherty shale (Crittenden, 1951).

The measured conductivity and salinity values show a gradual decline of 40% from about the end of 1981 to April 9, 1984 (fig. 2). This result is corroborated by an independent study of William C. Evan (USGS Water Resources Division) who has been regularly collecting water samples from one of the springs, Sulfur Spring #4, for chemical analysis. Evans' data show a similar decline in HCO_3^- content in the water. Our post-earthquake measurements taken on May 9 and June 8, 1984 show a small recovery of conductivity (and salinity) at both springs (fig. 2).

One of us (D.B.) visited the springs on April 25, the day after the earthquake, and observed an appreciable increase of flow at Sulfur Spring #4 and recorded a large increase in flow rate at Sulfur Spring #11 (more than twice as high as measured on April 9 and highest since our study began in 1975). The flow increase cannot be attributed to rainfall, which has been extremely small for the 1983-84 winter season, but may be induced by the stress-field changes associated with the earthquake because the springs are situated in a compressional quadrant of the earthquake (Wakita, 1975). Also the color of the water in the springs changed from whitish to greyish-brown because of the large amount of sediments in the water. The flow rate at Sulfur Spring #11 was measured again on May 9 and June 8, and was found to have dropped back considerably but was still higher than normal (fig. 2a). The water color had returned to normal (whitish) by May 9.

Measurements have also been made at two shallow wells in east Oakland near the Hayward fault (Oakland and Chabot, fig. 1). A gradual decline in conductivity and temperature during the past two years (1982-83) is noticeable in the data, although it is dominated by seasonal variations (fig. 3).

It is not clear at the present whether the observed ground-water changes are due to tectonic or climatic effects (the 1981-82 and 1982-83 winter seasons had an above normal amount of rainfall). Radon content of ground water has been continuously monitored for several years at an artesian well south of

San Juan Bautista near the San Andreas fault (fig. 1). The radon data show no significant changes.

REFERENCES

Crittenden, M. D., Jr., 1951, Geology of the San Jose-Mount Hamilton area: *California Division of Mines Bulletin 157*.

Wakita, H., 1975, Water wells as possible indicators of tectonic strain: *Science*, vol. 189, p. 553.

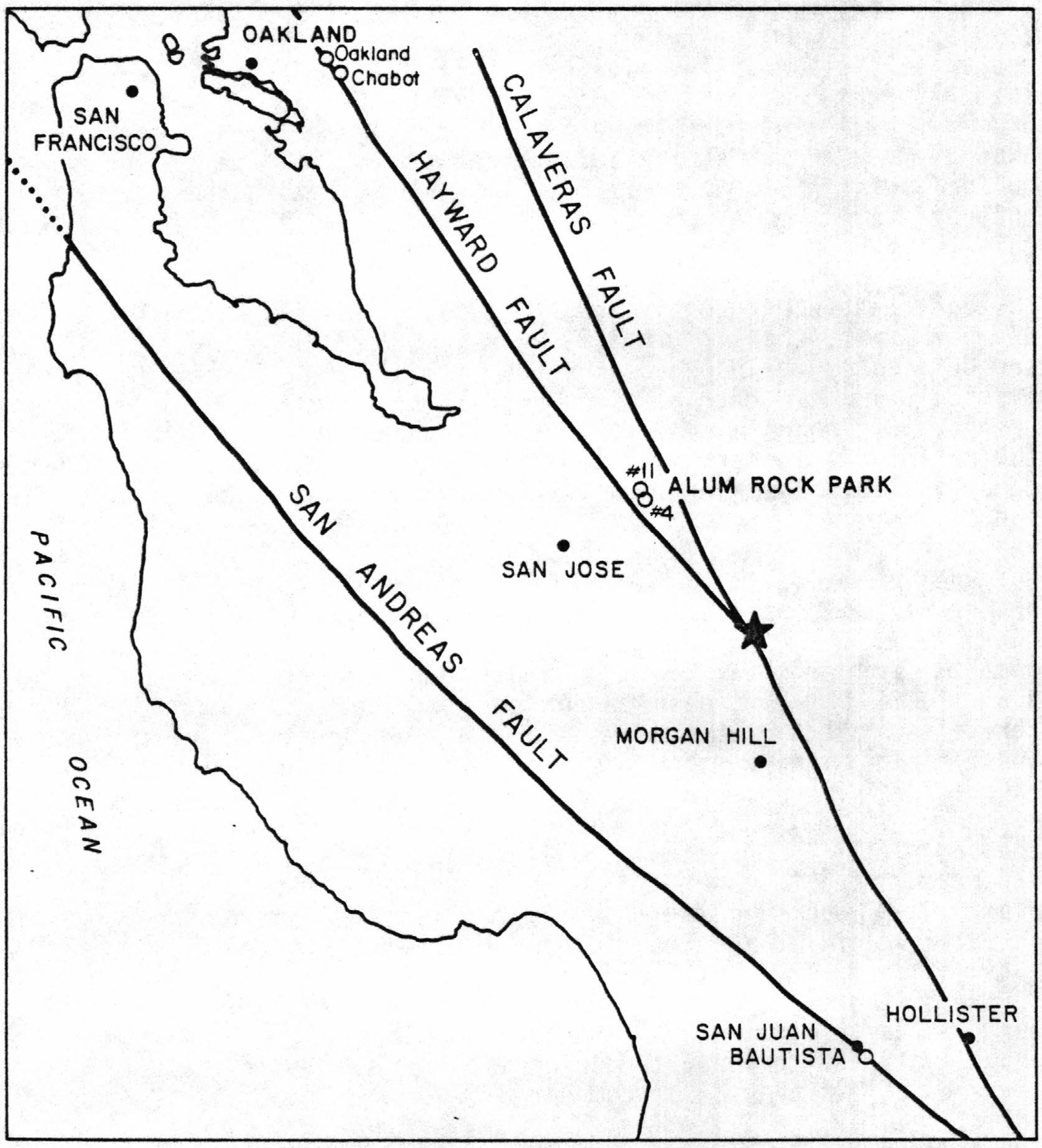

Figure 1. Location of ground water measurement sites (circles) and epicenter of the Morgan Hill earthquake (star).

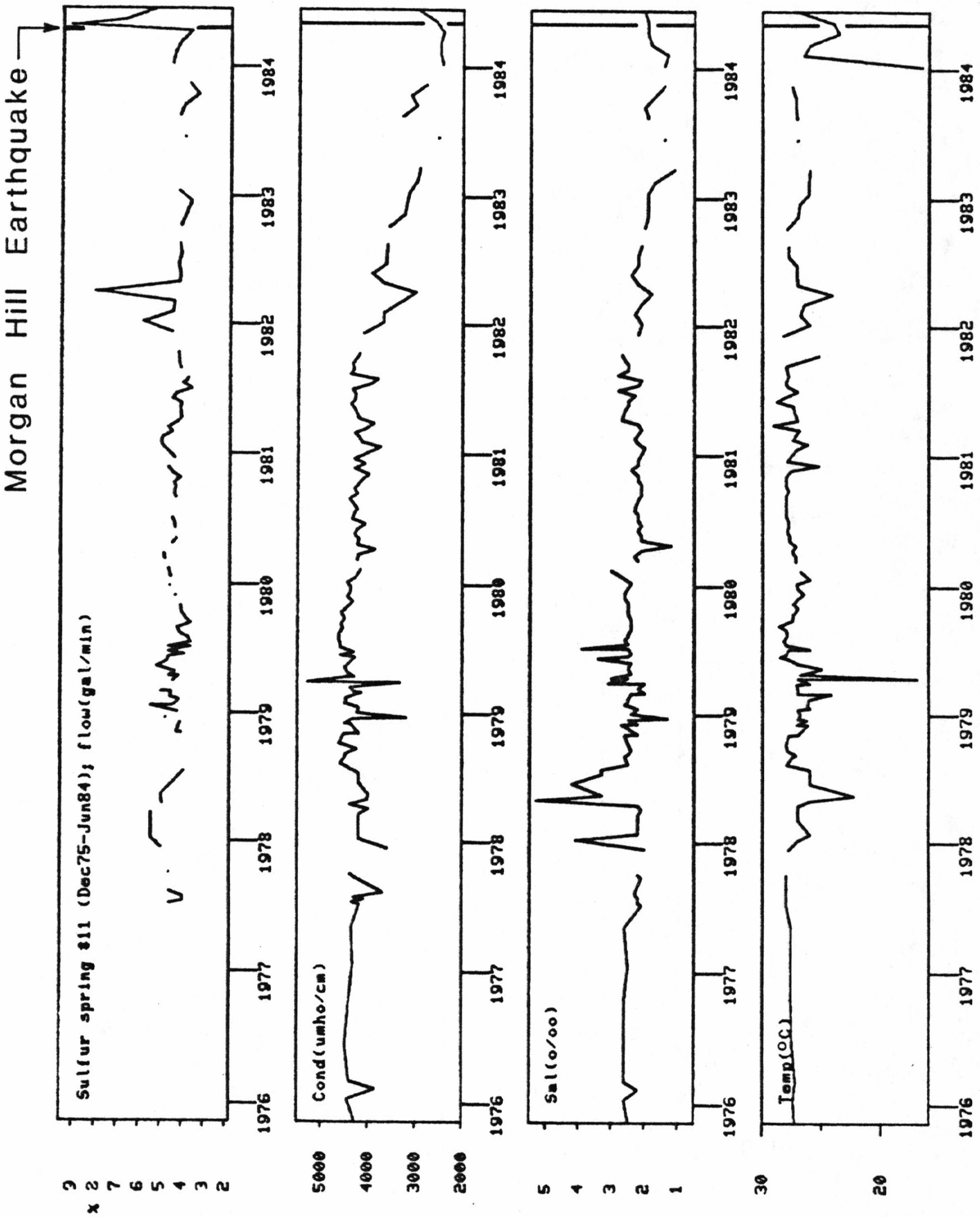

Fig.2 (a)

Figure 2. Flow rate, conductivity, salinity and temperature data from two springs in Alum Rock park. (a) North; (b) South.

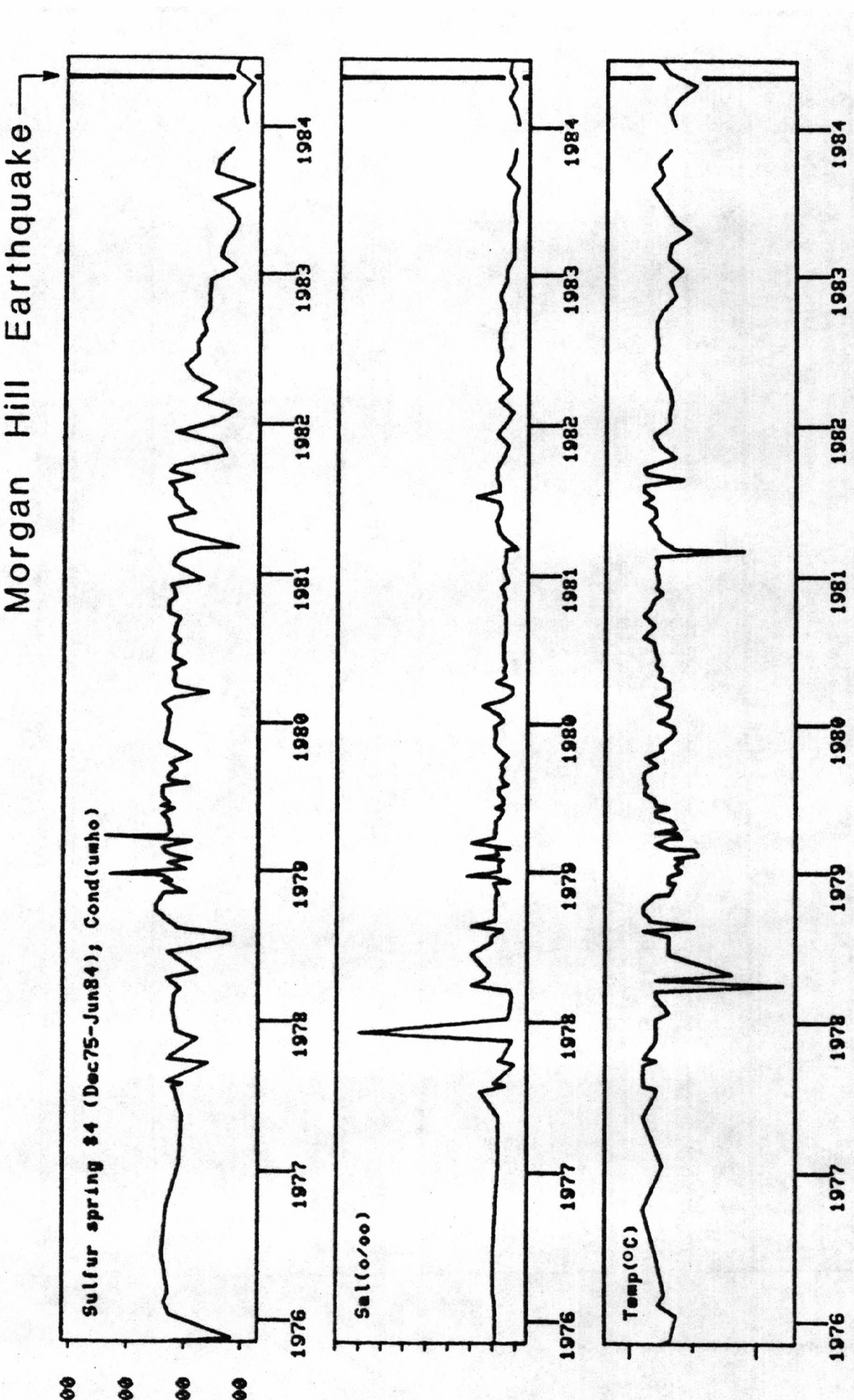

Morgan Hill Earthquake
Sulfur spring $4 (Dec75-Jun84); Cond(umho)
Sal(o/oo)
Temp(°C)
5000
4000
3000
2000
x
9
8
7
6
5
4
3
2
1
30
20
1976
1977
1978
1979
1980
1981
1982
1983
1984

Fig.2 (b)

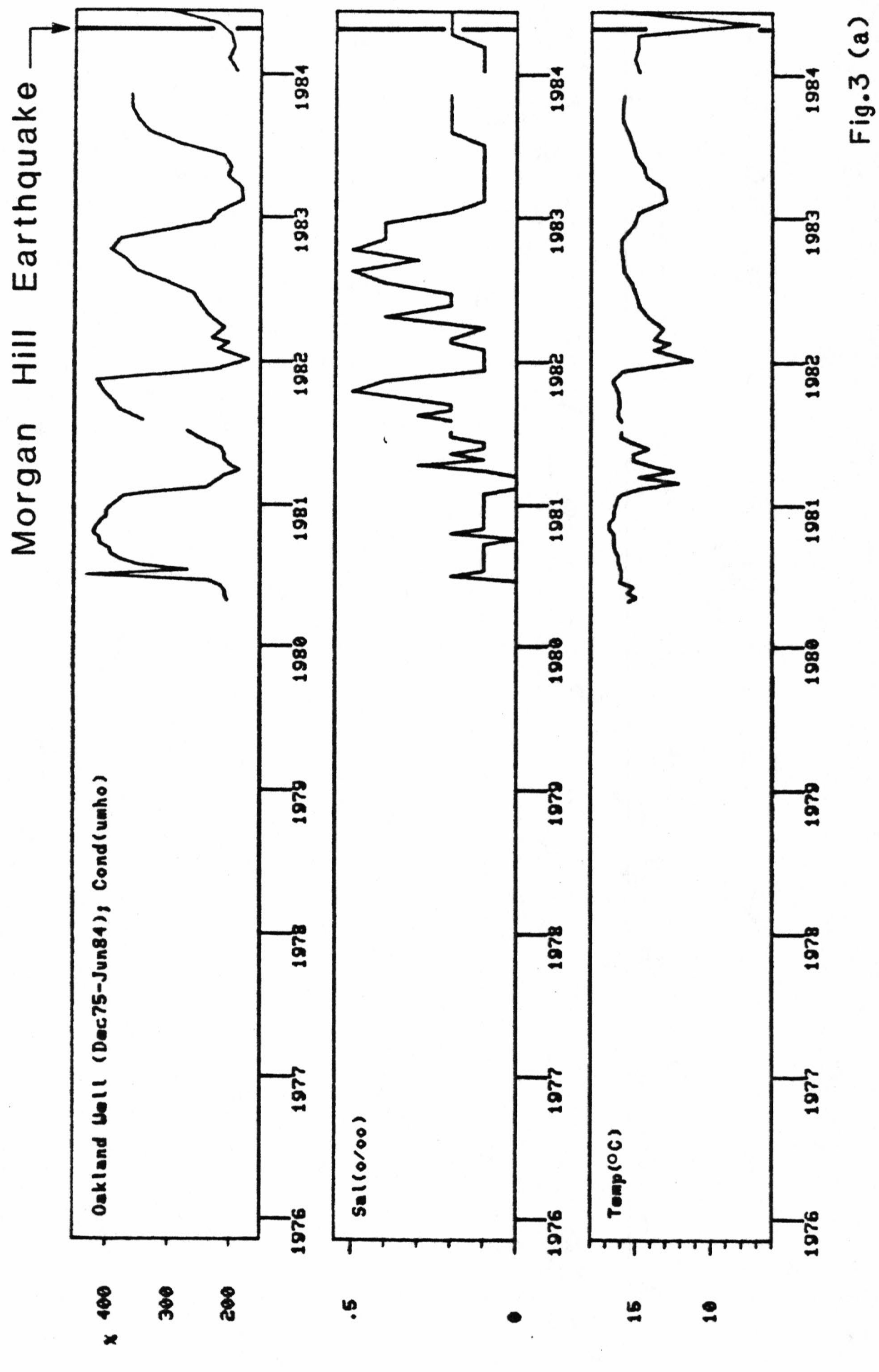

Figure 3. Conductivity, salinity and temperature data from two wells in east Oakland. (a) Oakland; (b) Chabot.

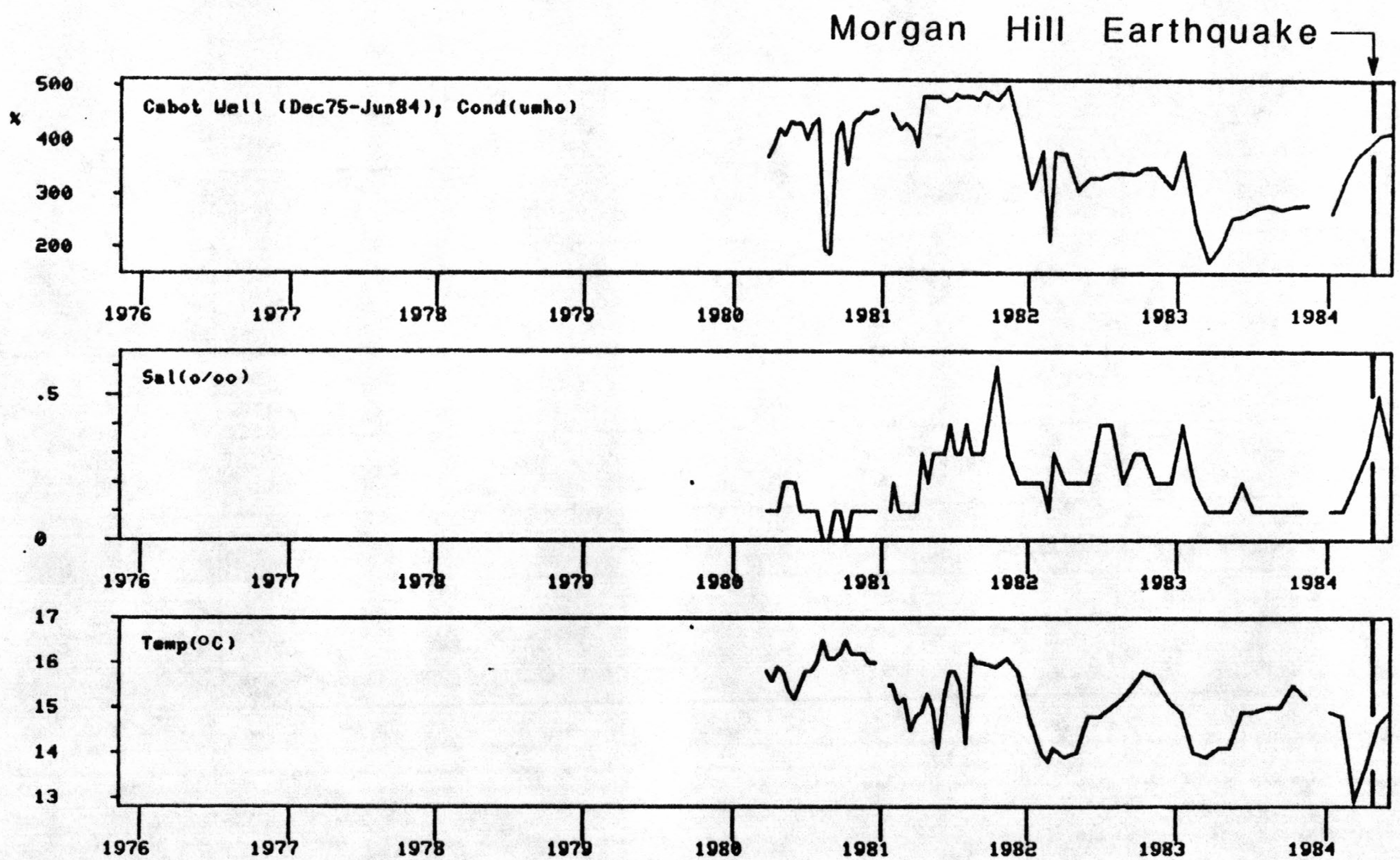
Morgan Hill Earthquake
Cabot Well (Dec75-Jun84); Cond(umho)
x
500
400
300
200
1976
1977
1978
1979
1980
1981
1982
1983
1984
Sal(o/oo)
.5
0
Temp(°C)
17
16
15
14
13

Fig.3 (b)

DAMAGE TO ENGINEERED STRUCTURES ASSOCIATED WITH THE APRIL 24, 1984 MORGAN HILL EARTHQUAKE, SANTA CLARA COUNTY, CALIFORNIA

Scott A. Mathieson

ABSTRACT

The earthquake of 24 April 1984 produced widespread damage to engineered structures in Morgan Hill and the surrounding region. A partial catalog of that damage, based upon approximately 2.5 man days, is included here. The types and distribution of damage reported here should provide a data base for assessing the probable damage to similar structures during earthquakes in the future.

INTRODUCTION

This report represents a catalog of damage to engineered structures resulting from the Morgan Hill earthquake of 24 April 1984 (Figure 1). This in not a comprehensive catalog, but represents the results of approximately 2.5 days of field investigations and encompasses the full range of structure damage that followed this earthquake and its aftershocks.

All of the localities included here represent the most dramatic effects of this earthquake, that is, those effects that were reported by the various news media. Sequentially numbered localities throughout the downtown area of Morgan Hill (Figure 2) represent a part of the path followed during the investigation on 25 April 1984. Location numbers shown in parenthesis are outside of the downtown area and itemize structure damage associated with this earthquake in Halls Valley, San Felipe Valley, and the Jackson Oaks subdivision (located adjacent to Anderson Reservoir, Figure 3). The locations with parenthesis can be found on Plate 1 of Harms and others (this volume).

Much site-specific geotechnical investigation is presently underway in the consulting community and will hopefully reveal the many reasons for the instances of damage reported here. The origin of much of the damage will not be addressed in great detail in this report.

STRUCTURE AND DAMAGE SUMMARY

Four general catagories of structures were damaged as a result of the Morgan Hill earthquake. These include one unreinforced masonary commercial building (the 1905 Building), neoclassic vintage homes (in the San Felipe Valley), conventionally founded mobile homes (such as those at Madrone Mobile Estates), and post-World War II homes (represented by the Jackson Oaks subdivision). Aside from these structures, one bridge, numerous paved roads, and one dam exhibited damage associated with the moderate to severe shaking that accompanied this earthquake.

There are many masonary structures within the downtown area of Morgan Hill. Only one, the two story 1905 Building, was damaged more than superfically. The 1905 or Coast Reality Building on Second and Monterey Streets actually held up well as no one was injured or killed but cracks within and between bricks are evident. Antiquity of the gas pipes or settlement of the building upon the gas pipes apparently led to the disruption of gas service immediately following the mainshock event.

The only intermediate aged residences visited were located in San Felipe Valley. These consisted of both wood frame houses constructed in approximately 1914 and 1930 and one masonary house constructed in approximately 1930. The only pervasive damage noted in the wood frame structures was the cracking of foundation stem walls (and footings?) near building corners. Much of this damage appears related to settlement of Holocene and Pleistocene valley fill and stream terrace deposits. The masonary home sustained no external damage but some damage to contents was reported.

Mobile homes suffered surprisingly little damage. Every trailer investigated in three separate parks had identical foundation system consisting of concrete, steel, or ureinforced cinder block footings. None of these homes had any discernible shear protection. The focus of the most concentrated trailer damage was located on the western third of the Madrone Mobile Estates. Partial or total collapse and popping of skirting panels was common here while no damage was noted only 0.1 km (1/4 mile) closer to the epicenter at Hacienda Mobile Estates. No other mobile home park investigated sustained the degree of damage that the western part of Madrone Mobile Estates did. The concentrated damage to Madrone Mobile Estates suggests a localized subsurface problem perhaps related to expansive or liquefiable materials or to settlement. An eighty year old home due south of the west end of Madrone Mobile Estates, on Pebbles Avenue, has apparently been subjected to considerable long-term stress, presumably associated with expansive soils. This house has no foundation other than a mud sill and is settling differentially.

The Jackson Oaks residences appear to have failed as a result of high horizontal ground accelerations (a downhill home was thrust uphill into its detached garage) and inadequate shear wall protection.

Damage to engineered structures, other than buildings, that showed the effects of this earthquake seems most often related to settlement of fill masses. Fill settlement seems to have been the single most important process resulting in both road bed failure, and the longitudinal cracks that developed along the crest of the Anderson Lake Dam. The second leading cause of road closures was rockfalls from roadcuts in bedrock.

LOG OF OBSERVED EARTHQUAKE EFFECTS

From notes taken 24 April 1984, 3:31-7:11 p.m., w/ K. R. Lajoie:

(11). Water tank hoops shifted downward and diagonally 15-30 cm (6-12 inches) in a systematic fashion (down on the west) (Figure 4); no shifting of tank on timber footings noted. Staves were forcibly shifted, both in and out--tank was full, but not leaking, and therefore has a liner. Hoops had been reset recently, perhaps to insert liner. This was the only bona fide example of quake-related disruption in the epicentral area.

A water tank (at Quimby and Mt. Hamilton Roads) was undamaged.

(9). Old barn unaffected--appears straight and level form a distance.

(4). Quimby Road--paved--no evidence of displacement or cracking. Fault and/or lithologic boundary was noted. Large landslide complex extends to south approximately 1.6 km (1 mile), no movement discernible.

From notes taken 25 April 1984:

1. Madrone Mobile Estates, 200 Burnett Avenue. Only those homes west of the west side of Greenwood Circle were affected by the earthquake. This may reflect a Qal problem, or perhaps is evidence for artifical fill. Three degrees of damage were noted: 1) Skirt panels popped off but there was no permanent tilting. (Tr. #26 and others.), 2) partial collapse, skirt panels popped and/or rotated. Footings tilted but house did not fall (Figure 5), and 3) total collapse of footings, some jack posts penetrated the floors of some of these homes (figure 6). None of the footings in any of the three cases was attached at the top or bottom. One trailer was destroyed by fire due possibly to disruption of gas or electrical service during the shaking. All of the homes west of Greenwood sustained considerable damage to contents. Those east may also have sustained internal damage, but because of the lack of external damage, no activity was noted and no further investigation was made. The only structure with a conventional foundation is the community center with pool, laundry, game rooms, etc. No damage was noted. No one was available to inquire about a seich in the pool. Of 172 total trailers, approximately 60 are located west of Greenwood, and of those 60 approximately 20, experienced partial or complete collapse. One redwood-potted Juniper toppled. Met Office of Emergency Services inspector assessing damage from here to Gilroy. All trailers tipped or collapsed to the north.

2. Hacienda Valley Mobile Estates, 275 Burnett Avenue, 0.2 km (1/8 mile) east, across road. Noted only one horizontal siding-type skirt panel popped out at one end, this trailer is oriented with its long axis east-west along the main road to this park.

3. Baumann Court. No damage, even though ranch style homes are quite large and rambling. Much glass utilized in construction but no broken panes or apparent distress. An old farmhouse with palm tree is adjacent to the Baumann Court homes, no damage or distress was noted.

4. Water tank on ground toppled from loose timber footings.

5. Along Vista de Lomas east of 101, water tank on corner; hoops shifted, filling pipe pulled away. Of 7 hoops, 4 slipped down, and are within a 15 cm (6 inch) span of the tank. Hoops bunched on the west side of the tank. Tank dry, so perhaps the house now has piped water. Camper shell on 1.2 m (4 foot) tall sawhorses was unaffected.

6. Quinn Court (off Vista de Lomas). Solar panel on roof of residence damaged. Not known if from roof deformation or something else--no one at home.

7. Freeway Vista--60 m (200 feet) south of Burnett Avenue, (west of 101). Sheet steel tank atop old water tower--not centered, or perhaps shifted. Does not appear attached to tower, but is over near its fill pipe, shifting doubtful.

8. Peebles Avenue. Trailer adjacent to greenhouses toppled.

9. Old house across from greenhouses, sagging badly, no apparent recent damage, but the house is in line with west end of trailer park. Perhaps expansive soils have resulted in the overall strained appearence of this home.

10. 18000 block of Monterey Street. Unnamed new trailer park. All of these trailers are going in at one time. Many without skirts, many on cedar shims and concrete footings or unreinforced cinder blocks, but none shifted, toppled, etc. Certainly no reason for these not to have fallen, so a minimum of shaking must have occurred here.

11. The Adelaide Sharp Walgren home. Historic landmark; no damage noted. Workers in process of constructing masonry wall around, or at least in front of the property. No shifting, settling or cracking of the mortar.

12. 1905 building (Figure 7). South Coast Realty Building, 2nd and Monterey Streets. Building has a skirt or cornice around roof perimeter (Figure 8). The cornice on south side toppled north. The bottoms of the cornice blocks are hollow or partially filled with mortar or concrete. The cornice and perhaps the rest of this building appear unreinforced. (KCBS indicated that gas service was disrupted during the quake). Cinder block or something else fell to the south and hit the awning above front door to South Coast Realty (southwest corner of building). Channel 7 news, 30 April, indicated building is to be torn down. Corner Drugstore at southwest corner 2nd and Monterey Streets. Plate glass window shattered and opening boarded up. Corner Drugstore the only glass damage noted, or that had not yet been repaired in Morgan Hill's downtown.

13. United Methodist Church, 4th and Monterey Streets, no damage noted. Drove down to Barnett and returned to 5th, turned right to the corner of 5th and Depot Avenue.

14. Hammond Bros. Wholesale Lumber, Depot Avenue. E-W piles to 4 bundles high (4.5 m, 16 feet), not disturbed. N-S piles to 3 bundles high (3.5 m, 12 feet) not disturbed.

15. Pearson's Hardware and Supply--2nd and Depot. Items outside: roll roofing, fertilizer all toppled to north. Items inside, on north-facing shelves, toppled into the aisles; paint ankle-deep on floors (Figure 9). On south-facing shelves, items stayed in place. Farmers Insurance man saw Dunne Bridge damage; Jackson Oaks damage.

16. House 150 m (500 feet) west if 101, north side of Main (no address seen), windows boarded, siding shattered and missing. Chimney down, may well be unrelated to quake, building in general state of disrepair.

17. Main at Laurel, water tank unaffected.

18. Emilio Guglielmo Winery, since 1925, 1480 Main Street (across from Live Oak High School). Some barrels (100-200 gallon capacity) were toppled (1) from racks bolted to cinder block walls, and (2) from cannonball-like piles. 643 gallon barrel tilted 25° east (this barrel and supports were constrained from N or S movement by larger barrels). Support consisted of 6 x 6 timbers in a horizontal plane held up by 6 x 6 timbers without any shear support. Many 8,000 gallon wooden barrels that stand on end normally shifted on timber supports and concrete footings 23 cm (10 inches) high, many were leaking from the bottom to a minor extent. 3 cases in which 10,250 gallon stainless steel tanks (also standing on end normally) were damaged: 1) tank empty--moved 8 cm (3 inches) south, 2) tank empty, but welded to vertical catwalk support--rotated 2.5 cm (1 inch) counterclockwise (Figure 10), 3) tank full--moved 2.5 cm (1 inch) south and bottoms buckled (elephant toes) within 5.5 cm (6 inches) of tank bottom and over an arc of 150° to 210° azimuth. None of these tanks was bolted to its concrete slab. These tanks buckled both inward and outward; one of the tanks was buckled out then in then out over a continous section ranging 120° of azmuith. Approximately 30 m^2 (400 ft^2) of sheetrock fell (Figure 11) from ceiling of storage warehouse. Sheetrock-gypsum still around nails in ceiling rafters. Sheetrock sections that fell were adjacent to westernmost cinderblock wall, room 8 m (25± feet) high. One fluorescent light fixture on chain fell and broke.

19. Main Street at Walizer Court; water tank toppled from footing to the E-SE.

(51). Anderson (Reservoir) Dam--2 sets of lateral cracks, each about 2 m (6 feet) inboard of front slope-crest and back slope-crest intersections (Figure 12). Cracks extend throughout 75% of dam crest. One longitudinal soil-type backhoe pit through the upstream crack had been excavated shortly before I arrived (Figure 13). Cracks extend a minimum of 2.5 m (7 feet) into dam, possible curvature at 2-2.5 m (6-7 feet) depth was noted. Blockhouse for control of gates rotated 3.5 cm (1-1/2 inches) toward reservoir. A second trench transverse to the dam axis was begun as I was leaving the area. Bob Tepal of the Santa Clara Water District was supervising the operation.

(69). Jackson Oaks Tract--Five houses evacuated and condemned; a prominent crack begining at the ridge crest was noted (Figure 14). It is associated with land failure, but its geometry was not decernable in the short time I was there. No one knew if the crack was co- or post-seismic but the damage to the homes implied high rates of lateral ground acceleration to the south. Construction in this tract is generally average to poor; no provision for adequate shear protection was evident. Downhill home thrown up and north into its detached garage therefore, the soil was thrust to the south very quickly. This particular house (house #1 on Figure 3)) had inadequate shear protection with few (4?) nails per panel. Panels popped off, leaving 2-3 m (6-10 foot) studs below main-level joists unsupported. House on

Oak Ridge Lane ripped from foundation (Figure 16), thrown 0.6 m (2 feet) NE, 0.3 m (1 foot) SE, sill still very adequately attached to concrete stem walls (house #2 on Figure 3). Plant pots and a front-yard water fountain (the house with toppled fountain is shown in Figure 17 and is not on sketch map, Figure 3) were toppled. Various cracks in stucco around garage doors and windows. House #3 (Figure 3) rocked out of plumb but still on foundation.

Oak Ridge Court and Lane traversed on foot. Trench to locate pipes in deformed pavement excavated. Found very badly weathered plastic, clayey decomposed Santa Clara Formation.

Cotton and Associates are the consultants to the city through city manager's office. Peter Anderson and Bill Fowler in attendance.

Dunne Avenue foot traverse from junction of Holiday Lake Estates and Dunne Avenue to 0.1 km (1/4 mile) beyond Cochrane bridge. Numerous moderate slope failures of fill parallel to road alignment (Figure 18). Pavement heaved at one point into tent-like configuration. Many rockfalls from roadcuts within 0.8 km (1/2 mile) of bridge. Large landslide that obscures the trace of the Calaveras fault moved 20-30 cm (8-12 inches) along old repaved fractures (Figure 19). Cochrane Bridge (Figure 20) pushed 7-10 cm (3-4 inches) to south (all I-beams above and transverse to main north-south I-beams crossing reservoir rotated in a vertical plane 5 cm (2 inches) (Figure 21), rivets were torn out in the process, the two westermost concrete posts spalled at base; resultant concrete flakes adjacent to post bases (Figure 22). The Cochrane Bridge was shortened 5-7 cm (2-3 inches), in a telescoping fashion, along the timbers supporting the planks which in turn support the asphalt roadbed. There was a possible rotation of bridge 5-7 cm (2-3 inches) counterclockwise in horizontal plane. A 15-30 m^3 (20-40 yd^3) rockslide fell east of the bridge blocking access (Figure 20). The 0.6-1.0 m (2-3 feet) of Dunne Avenue roadbed adjacent to and on both sides of the reservoir dropped 20-25 cm (8-10 inches) towards the reservoir (vertical components are larger to the east of the bridge.

Holiday Lake Estates (northwest of Jackson Oaks)--Inspected many roads and homes in this housing tract. The area is famous for instability in regard to landsliding--no damage was noted.

From notes 26 April 1984, 1:00-3:00 p.m.

(36). In area of flume, there is a compelling tendency to think that this riser is a fault scarp, perhaps accentuated (in height) by the flume. The riser is arrow-straight, 2.5 m (7 feet) high and crosses San Felipe Road 450 m (1500 feet) south of road's end. There is a dip in road to the south that coincides with the riser. To the north the riser ends abruptly and appears offset from the ridge farther north and west. The pavement driveway up to masonry house exhibits an arrow-straight break, patch, or joint at the base of the riser--no lateral offset was noted.

(33). San Felipe Ranch (a division of San Felipe Rancho--The Hewlett-Packard Ranch)--8025 San Felipe Road--Norma Reese led me around main house, guest houses, pool area; fallen chimney on main house (built 1914, Figure 23), foundation cracks, pool apron settling differentially (Figure 24)--old pool site experienced settlement as well. Mrs. Reese indicated major component of motion within the valley east-west; dishes in eastern cabinets fell west. Cracks in parking area assumed lateral spreading and settlement of Holocene and Late Quaternary valley fill towards San Felipe Creek 50 to 100m (160-300 feet) to the east. Concrete patio at rear of first guest house, built in 1957, north of main house, experienced severe cracking and settlement 5 cm (2 inches) lower adjacent to the house, 10-15 cm (4-6 inches) lower at outside edge (2 m, 6 feet away from house). Two other guesthouses, built before 1937, suffered mild foundation cracks at east-side corners.

(28). Fence lines offset left- and right-lateral but this is equivocal evidence at very best. Fence lines may well have been built crooked.

Notes from 2 May, 1984, Mathieson and Lienkaemper, 9:40 a.m.-5:10 p.m.

Checked portion of Mt. Hamilton Road from Mathieson-Lajoie stopping point to Smith Creek Ranger Station. Nothing, aside from minor slope and fill failures. 9:40-10:15 a.m.

To Grant Ranch Visitors Center to obtain key or combination to Grant Lake trails. No one there. No damage to Victorian house or 8 m (25 foot) tall water tower (tallest thus far seen in this region). 10:25 a.m.

(43). Coyote Dam and spillway. Nothing noted in the slides in, around, and under the concrete lined spillway. 4:45 p.m.

Finished observations at 5:10 p.m.

ACKNOWLEDGEMENTS

Thanks to Ray Eis for drafting figures 1 and 3, to Alice Olsen for typing parts of this manuscript, and to Dan Ponti and Jim Perkins for their review comments.

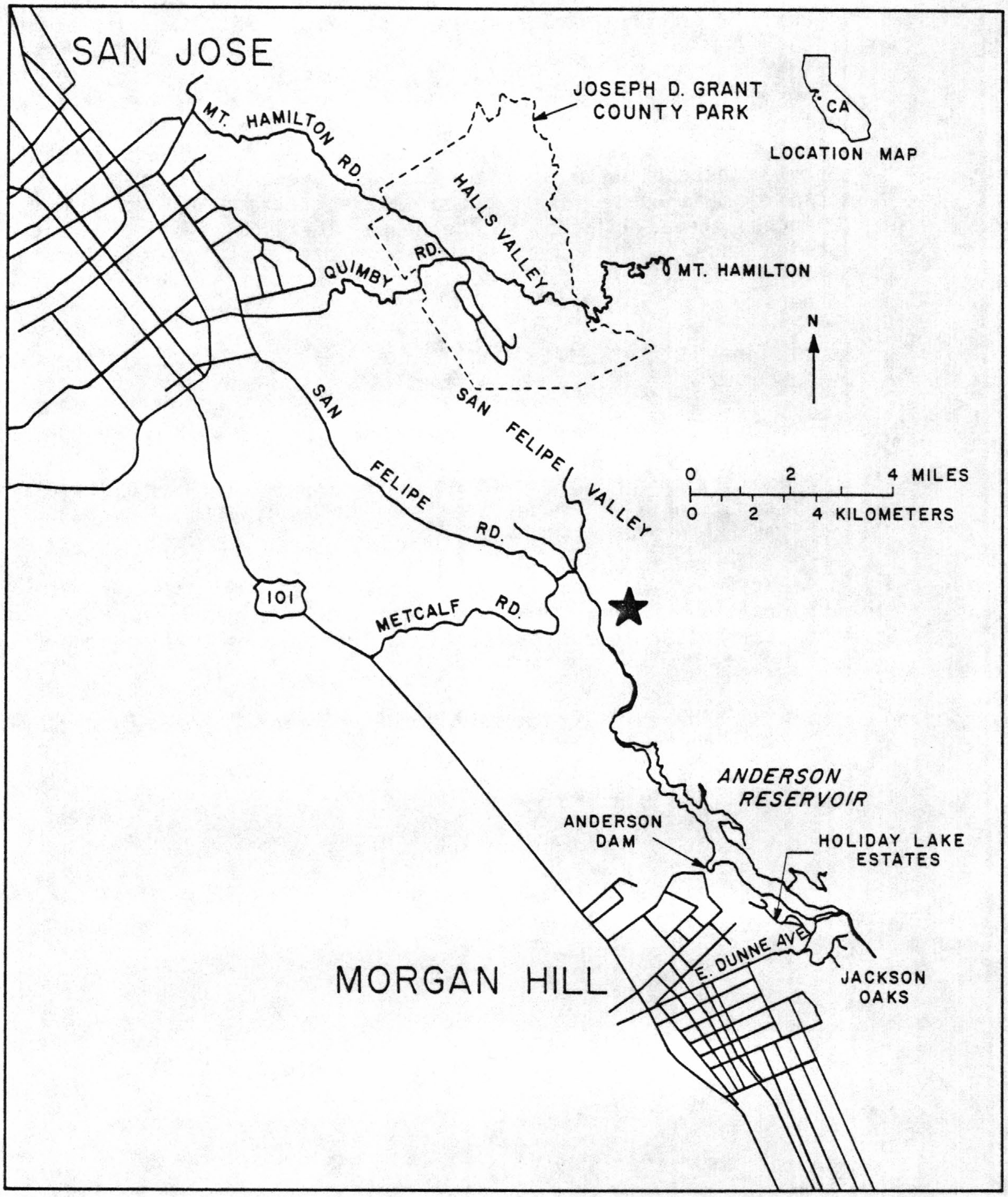

Figure 1. Regional location diagram showing Halls Valley, San Felipe Valley, Jackson Oaks, and regional access routes. Also show is the epicenter of the 24 April 1984 mainshock from King (personnal communication 1984).

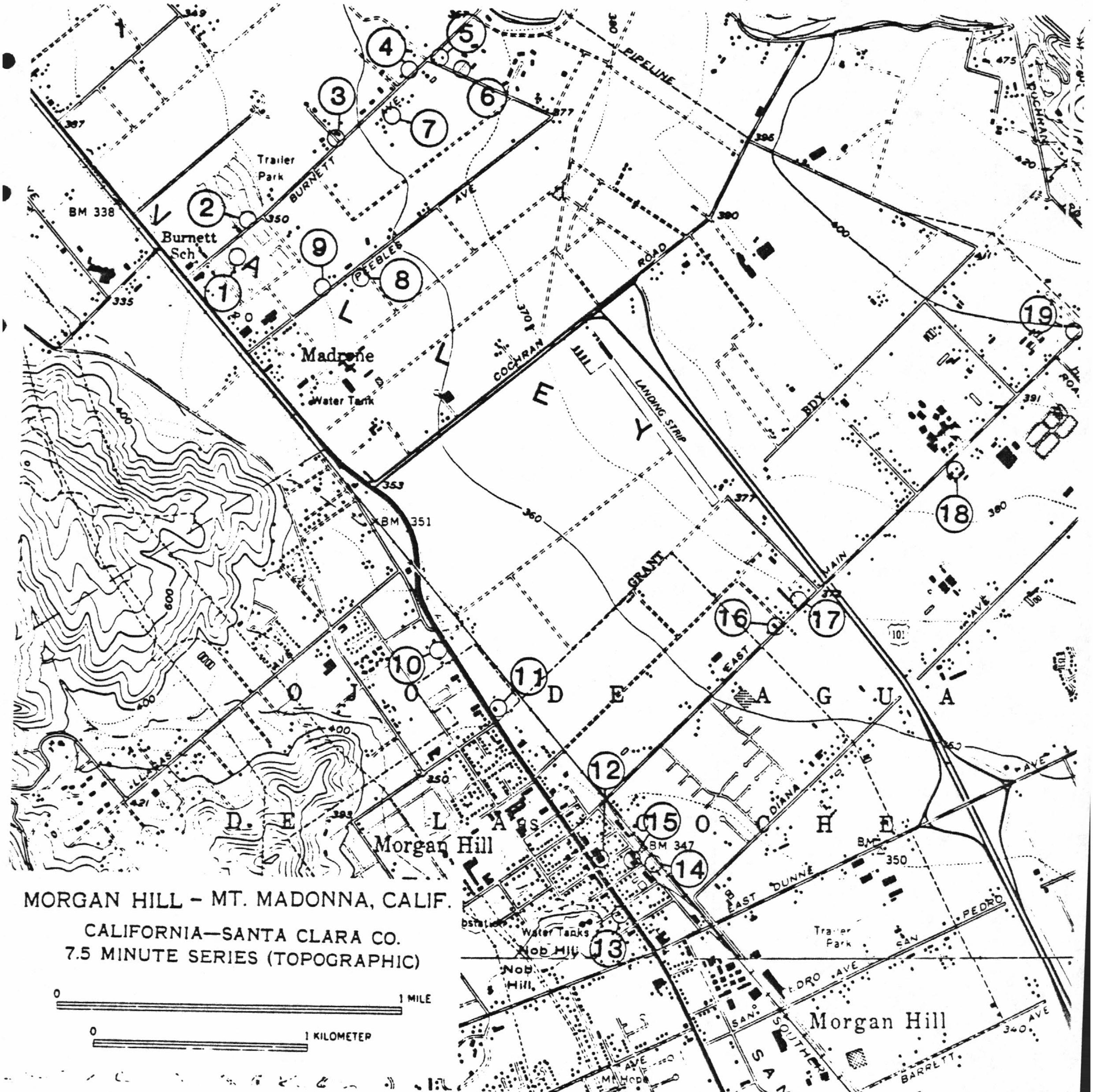

Figure 2. Downtown Morgan Hill with numbered localities. These localities are keyed to descriptions in the text.

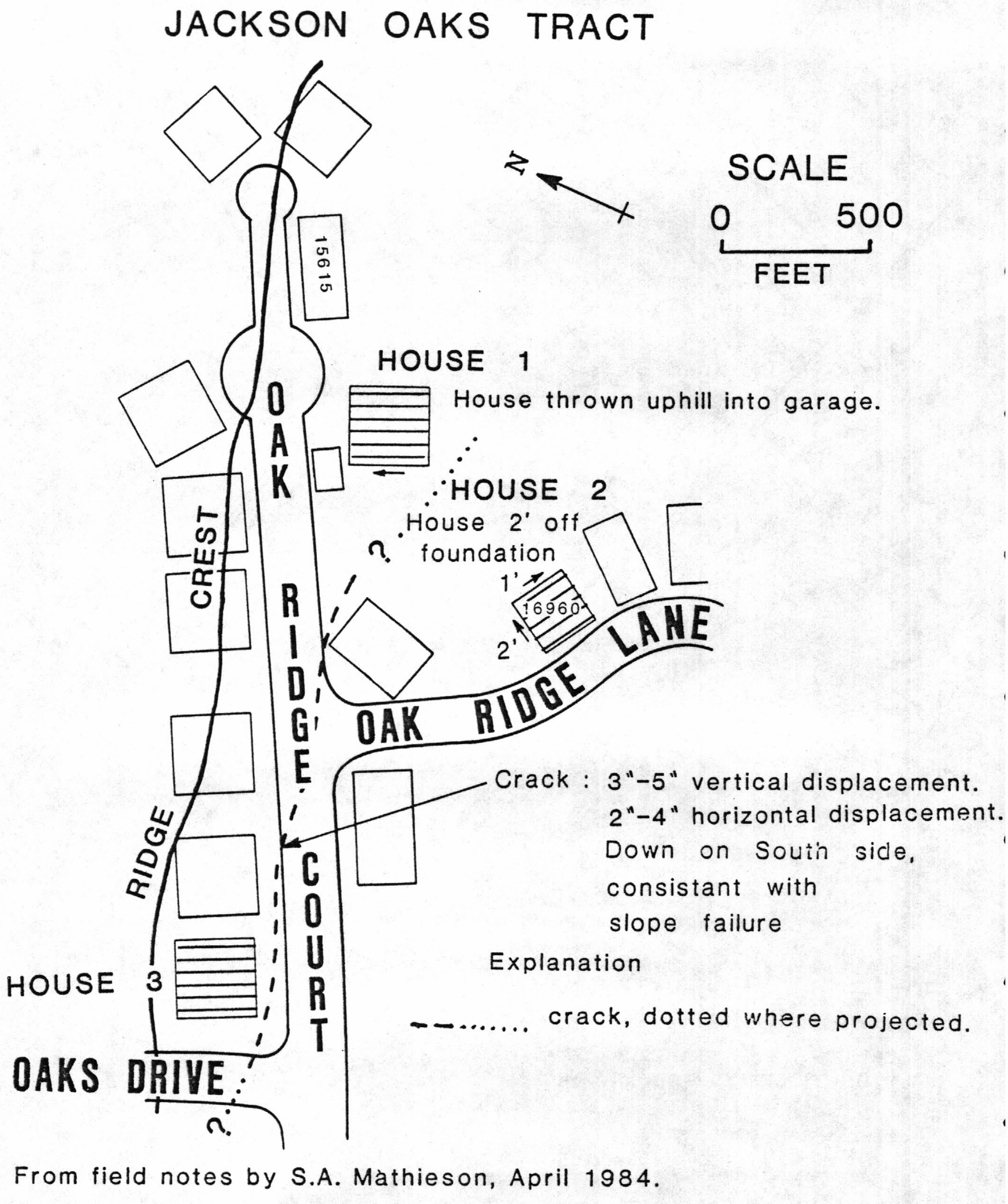

Figure 3. Rough sketch map of a portion of the Jackson Oaks housing tract (location (69)). The occasional five digit numbers are house addresses where they were noted. Houses #1, #2, and #3 are referred to in the text.

Figure 4. Photo of location (11) showing shifted water tank hoops in Halls Valley. Hoops are down to the west.

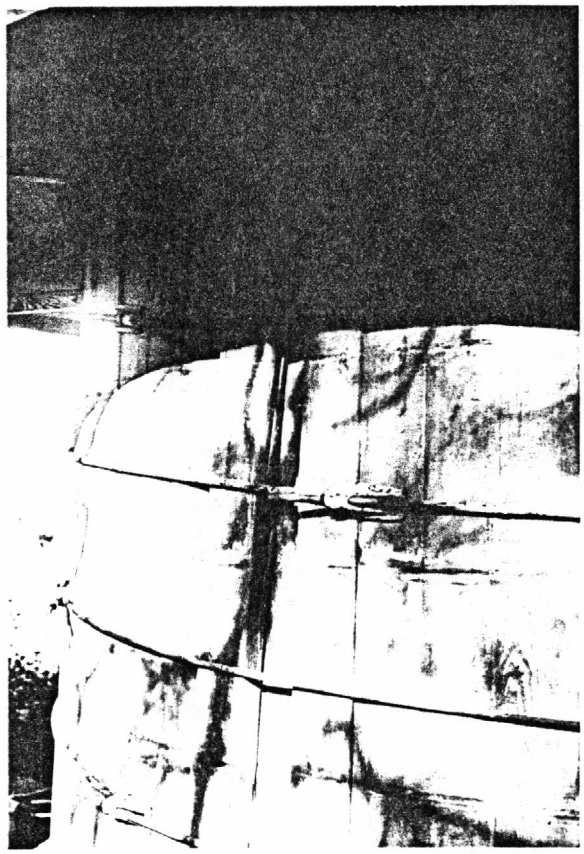

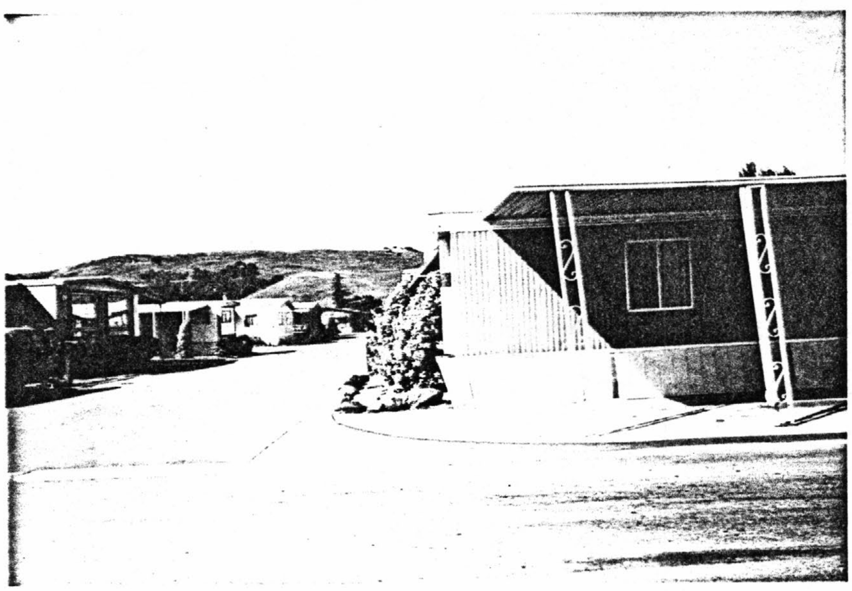

Figure 5. Partially collapsed mobile home at location 1 in Madrone Mobile Home Estates. North is to the right.

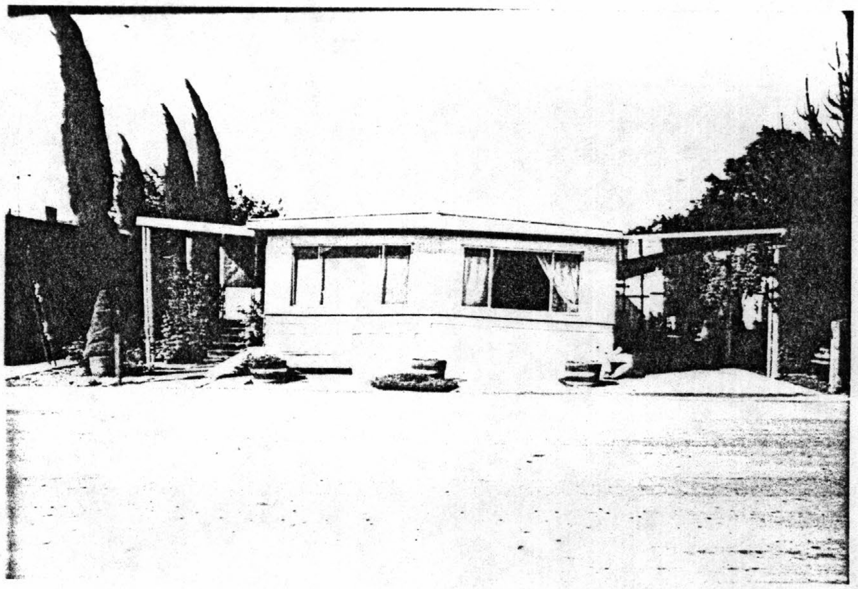

Figure 6. Completely collapsed mobile home at location 1 in Madrone Mobile Home Estates.

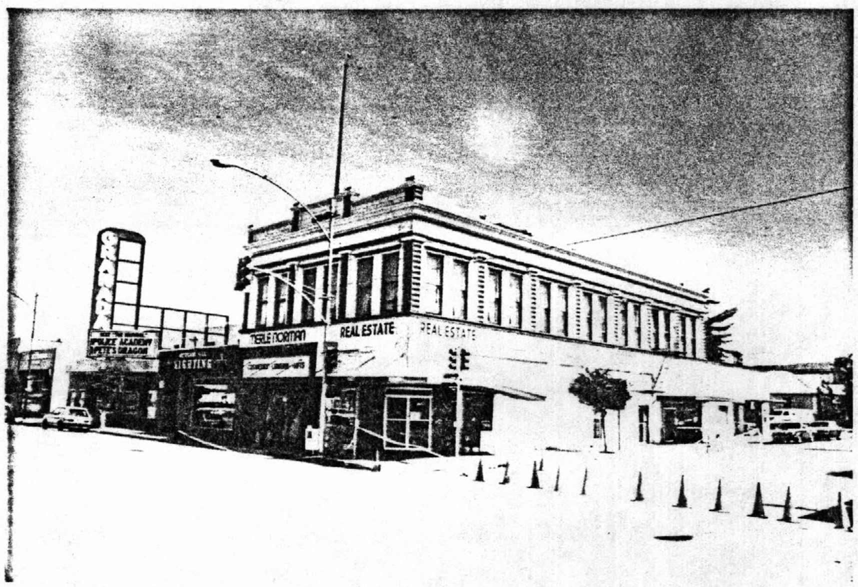

Figure 7. The 1905 building at location 12. Photo taken from Monterey Road at the corner of 2nd and Monterey.

Figure 8. Closer view of the 1905 building at location 12. Photo taken from Monterey Road at the corner of 2nd and Monterey. Note arrow pointing to the tumbled portion of the roof cornice; cornice fell to the north. Also note partially collapsed awning at the side left corner of the building that was struck by a heavy object, perhaps a block from the cornice.

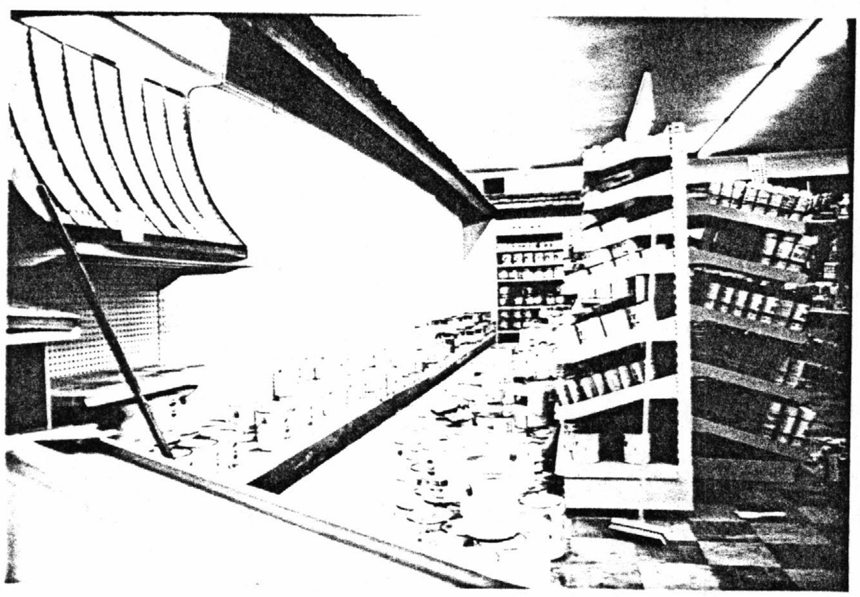

Figure 9. Pearson's Hardware at the corner of 2nd and Depot at location 15. Photograph inside of store shows that paint cans on north-facing shelves were throw into aisles, cans on south-facing shelves remained on the shelves. Paint in this area of the store was ankle deep.

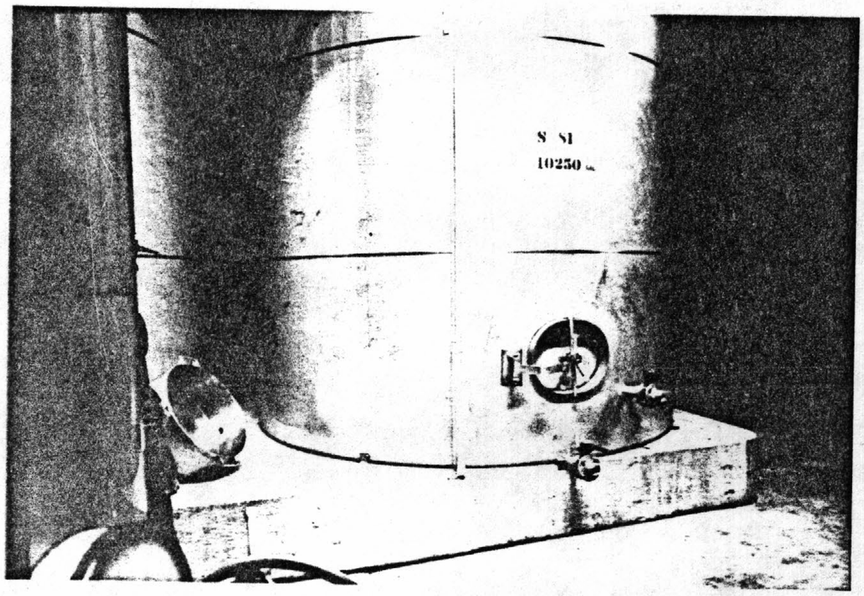

Figure 10. Photograph inside the Emilio Guglielmo Winery, 1480 Main Street (location 18). Photograph shows 10,250 gallon storage tank that was welded to catwalk support which in turn was bolted into the concrete pad. This stainless steel tank rotated 2.5 cm (1 inch) counterclockwise (to the right), the catwalk was mildly wrenched. This tank was empty. Other tanks that were filled to capacity and developed elephant toe bulges over consistent azmuthal arcs while shifting on the same concrete pad.

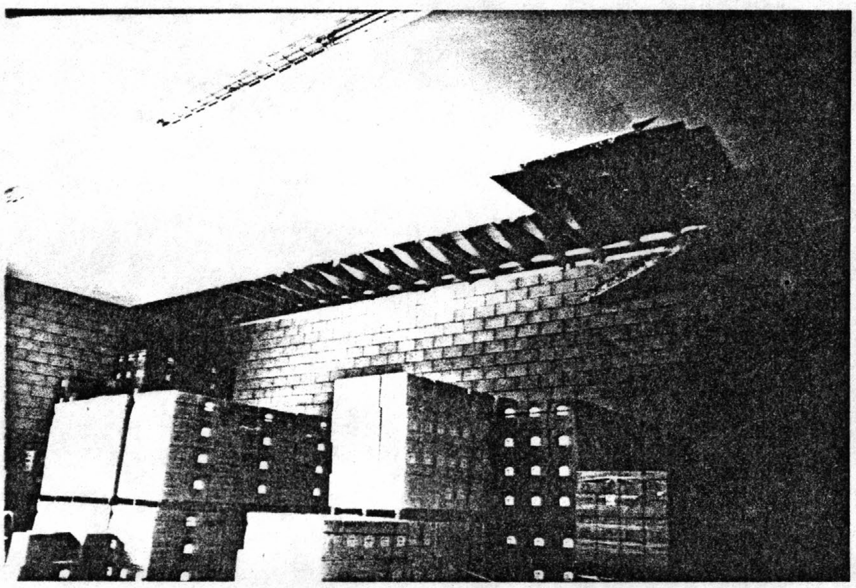

Figure 11. Sheetrock that fell from ceiling adjacent to western-most cinder block wall at the Emilio Guglielmo Winery (location 18).

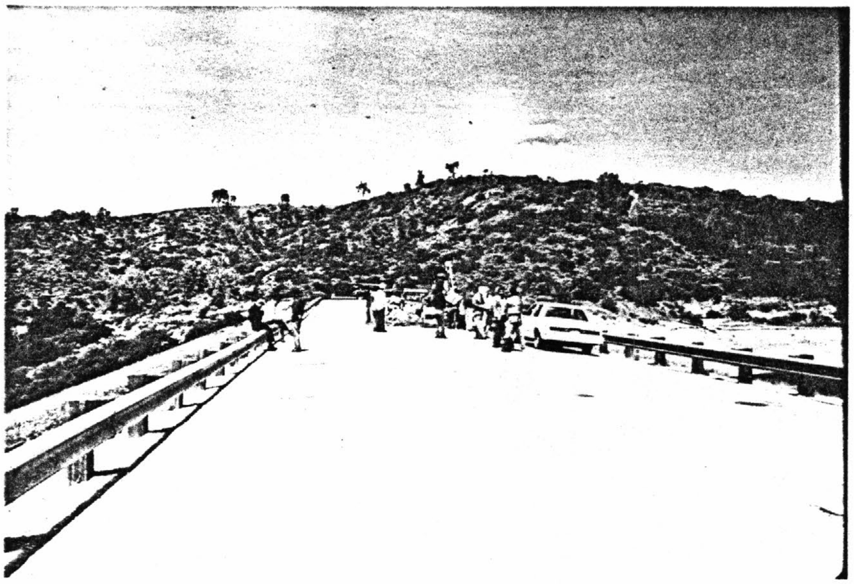

Figure 12. Longitudinal cracks that developed along the crest of the Anderson Dam (location (51)). The location of trench parallel to the longitudinal upstream crack is in the right center.

Figure 13. Soil-pit type trench through the crest of Anderson Dam (location (51). Crack in pavement can be seen in northern vertical trench wall and appears curve outwards toward the upstream face of the dam, to the right near the bottom of the excavation.

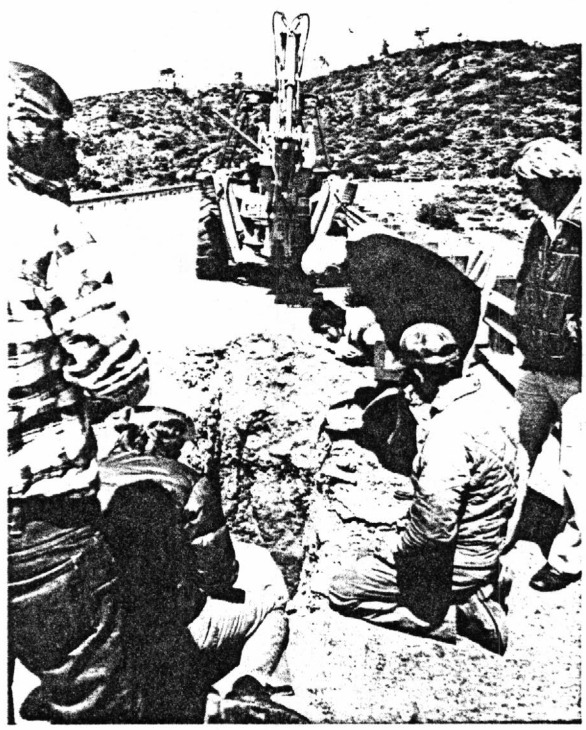

Figure 14. Racked house (house #3, in Figure 3) along Oak Ridge Court in Jackson Oaks tract (location (69)) with crack propagating east-west through its driveway. Crack has both extensional and vertical components (down on the south). View is to the north.

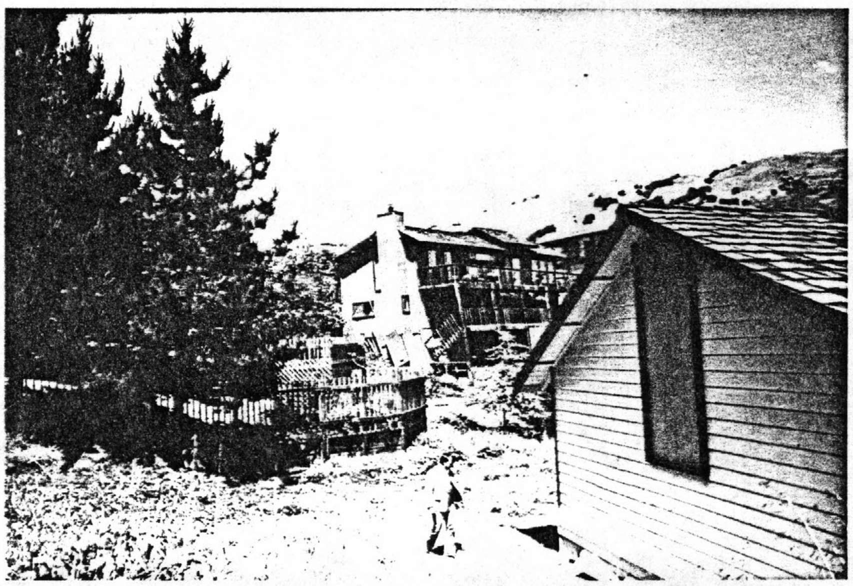

Figure 15. Jackson Oaks housing tract (location (69)). House #1 from next to house #2 (house numbers from Figure 3). Note unshattered and rotated shear panels on house #1 which appear to have provided little shear protection.

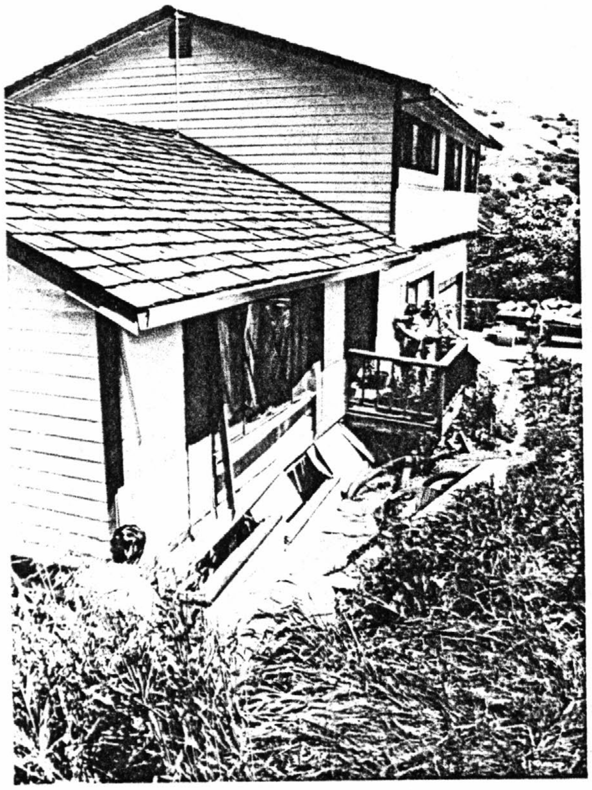

Figure 16. House #2 along Oak Ridge Lane (location (69)). Note sill plate still secured to the concrete perimeter foundation. This instance of a house ripped from its foundation suggests high lateral ground accelerations.

Figure 17. House in the Jackson Oaks subdivision west of area shown in Figure 3 sketch map (location (69)). Note toppled front yard fountain.

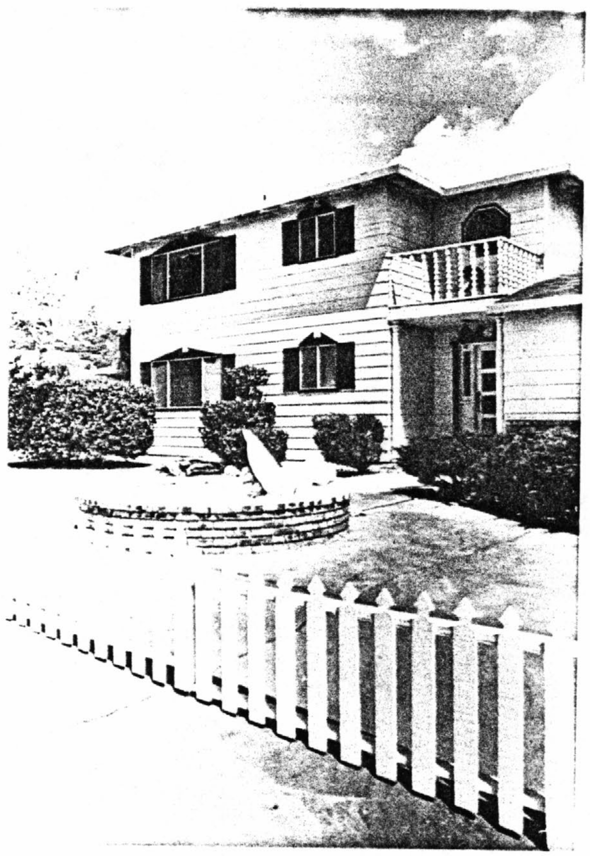

Figure 18. One of many fill failures along East Dunne Avenue within 0.8 km (0.5 miles) of the Cochrane Bridge. These failures were typically down toward the reservoir which is to the right of the photo.

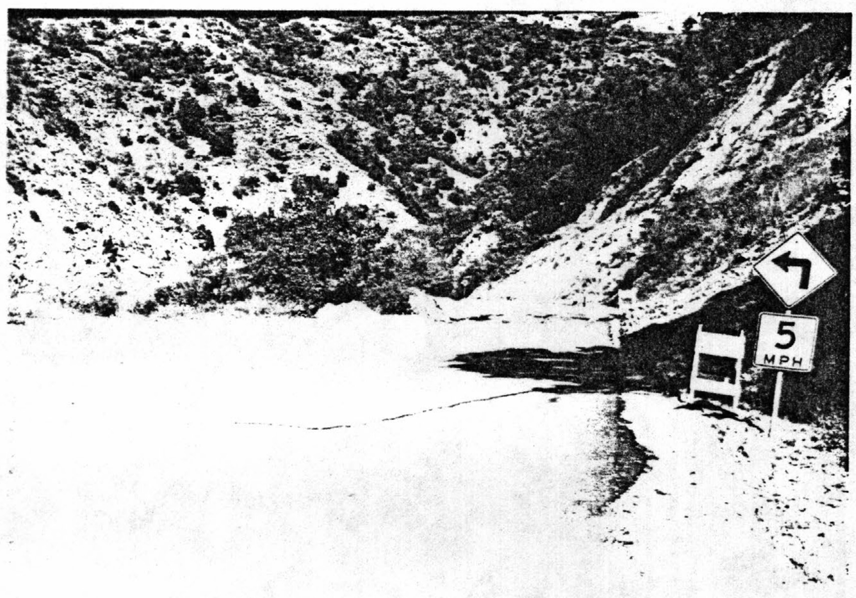

Figure 19. Large complex landslide within 0.2 km (1/8 mile) of the Cochrane Bridge disrupts the East Dunne Avenue right-of-way (near location (69)). This landslide obscures the trace of the Calaveras Fault. Note repeated patching of pavement along this stretch of the road.

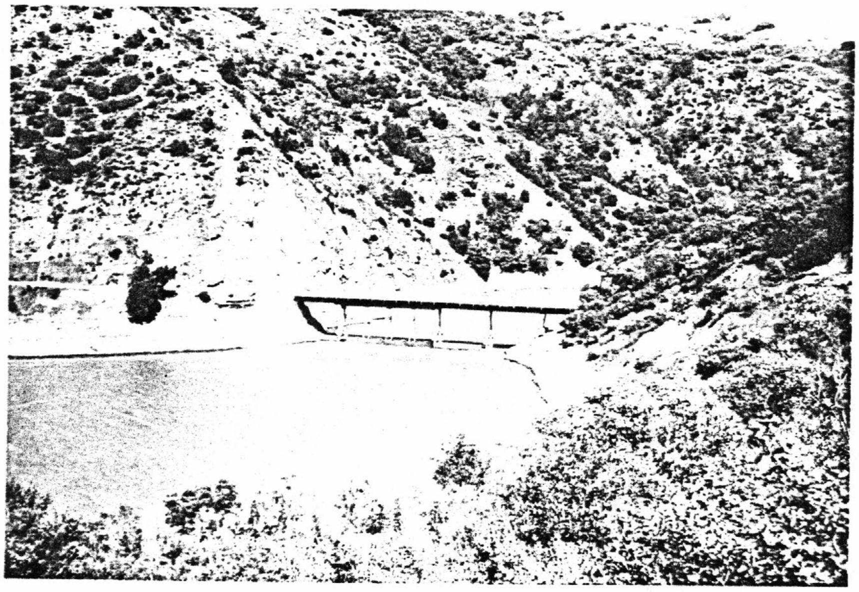

Figure 20. Cochrane Bridge over Anderson Reservoir. Bridge has been shortened by the telescoping of the timbers which support the pavement roadbed. Note the rockfall which covers East Dunne Avenue east of the Cochrane Bridge (near location (69)).

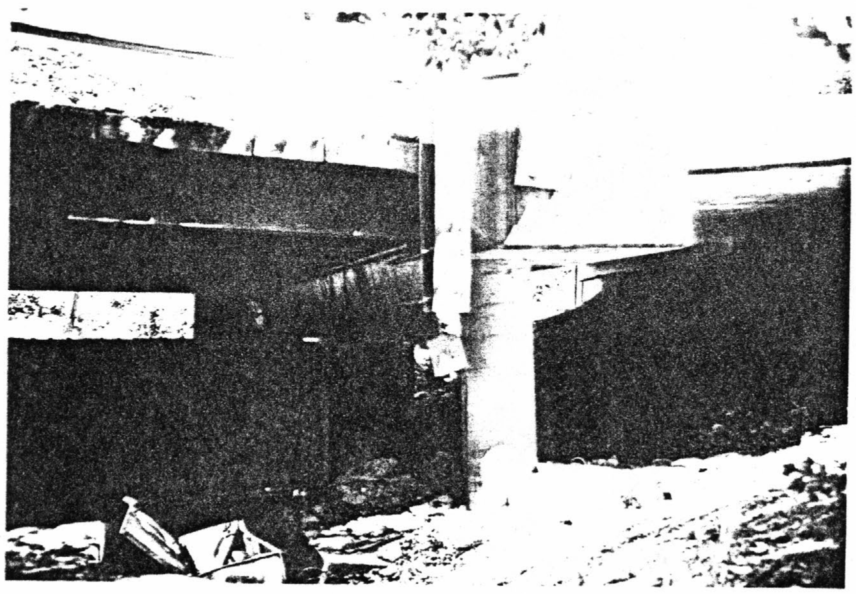

Figure 21. Rotated I-beam beneath Cochrane bridge (near location (69)) and bridge support timbers. Rivets have been torn out at a number of locations.

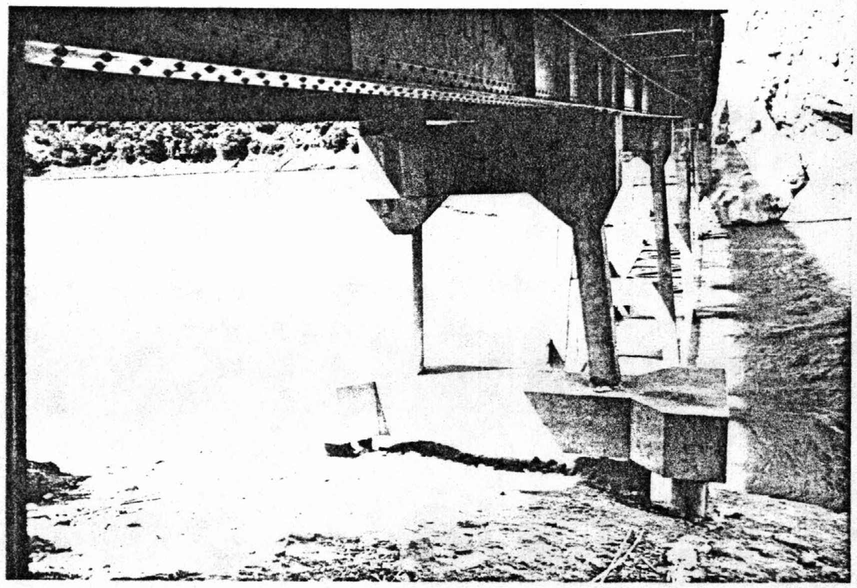

Figure 22. Spalled post added to strengthen the Cochrane Bridge (near location (69)) after a creeping segment of the Calaveras was discovered to be twisting the bridge.

Figure 23. Circa 1914 wood frame house in San Felipe Valley at location (33) with fallen chimney and stem wall cracks in its perimeter foundation. View to the ESE.

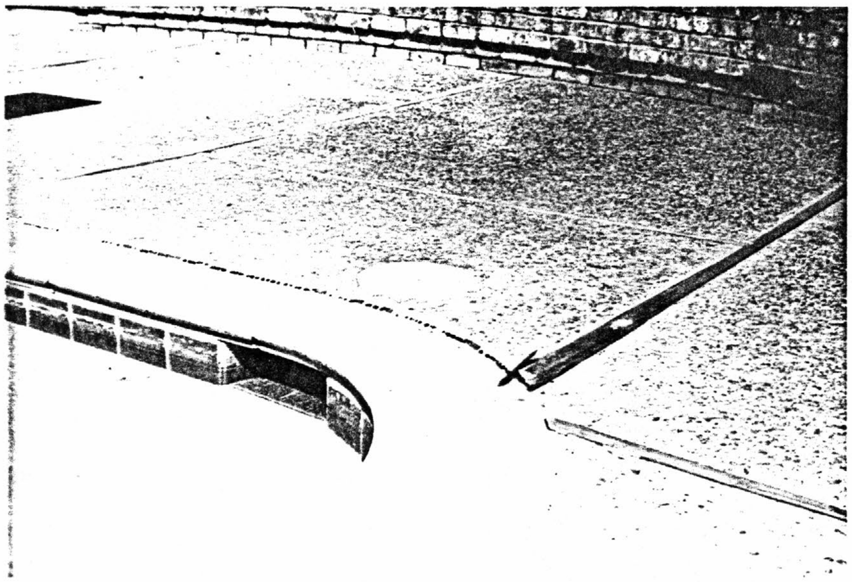

Figure 24. Concrete pool apron in the San Felipe Valley at location (33) that has settled differentially due to minor lateral spreading of Holocene and Late Pleistocene stream deposits.